From:	Bonnie Rippingille Chair Special Committee for Turkey Point Issues Ocean Reef Community Association (ORCA) Key Largo, Florida
To:	Rulemaking Comments Resources
Subject:	Comments re: NUREG-1437, Generic Environmental Impact Statement for License Renewal of Nuclear Plants (SLR)
Date:	May 2nd, 2023

Please accept these comments on the proposed changes to NRC regulations, draft Revision 2 to NUREG-1437 prepared by the Ocean Reef Community Association Special Committee (ORCA) for the FPL Turkey Point Power Plant, a 4000-acre community of approximately 2100 residential homes in North Key Largo, Monroe County, Florida located 5.5 miles across Card Sound from the coastal FPL Turkey Point Power Plant.

Our comments relate to proposed environmental review rule and category changes in Document ID NRC -2018-0296-0017, Article II, Section D Proposed Actions and Basis for Changes to 10 CFR Part 51, Appendix B to Subpart A of 10 CFR Part 51:

Historical Information on the Cooling Canal System at Turkey Point Applicable to All Comments

The Applicant uses a unique, open, shallow, and unlined seawater cooling canal system (CCS) constructed in 1976 to cool water used to operate two nuclear reactors at Turkey Point. After more than 45 years of operation, the CCS is still not used in any other nuclear facility in the United States.

The CCS network comprises 168 miles of serpentine canals and 5,900 acres of coastal land. The Applicant has an industrial wastewater facility permit from the State of Florida FDEP to operate the CCS and the permit is reevaluated and renewed every five years. The CCS is excavated into the native porous limestone and within the underlying surficial Biscayne aquifer (BA) which is the federally designated "sole source drinking water aquifer" for the Florida Keys and South Florida. The CCS berms, which are essentially at mean sea level elevation on the coast, was not designed as a closed loop cooling water system. It experiences a daily high/low tidal seawater exchange from Card Sound which is part of Biscayne Bay. Its performance is significantly weather dependent, relying on sufficient and regular rainfall to dilute the salty sea water in the canals and make up for the water lost through evaporation and seepage from the canals. The evaporative cooling method which is used in the CCS causes the heavier salt to settle and concentrate at the bottom of the canals, making the water leaking from the CCS into the Biscayne Aquifer much saltier than seawater unless the salt is dredged

from the canals regularly as the designer intended. Over time, because of increasing ambient temperatures, increased evaporation and poor operation & maintenance practices by the Florida Power and Light, salt and decayed organic matter from trees and other vegetation on the berms flanking the CCS were allowed to accumulate in the canals causing a hypersaline and nutrient-polluted water quality condition in the CCS. By 2014, a massive hypersaline, polluted-water plume created by the leakage from the CCS was identified to extend 2-4 miles to the north, south and west beyond the Turkey Point Plant property line in the Biscayne Aquifer. The plume had been moving in all directions out from the TP plant site and towards Biscayne National Park, FKAA and the Miami Dade County wellfields in Florida City, which supply drinking water for Monroe County and South Miami-Dade County.

In 2011, because the CCS design made its performance as a cooling water system subject to the varying weather and extensive maintenance, which was not being performed, the Applicant began pumping millions of gallons a day of supplemental cooler surface water and ground water into the CCS. The first source used was the SFWMD L31E freshwater Canal adjacent to the west property line. When that surface water source was disallowed in 2014 by the SFWMD, the Applicant was allowed by FDEP to pump millions of gallons of cooler dilution water from the brackish Floridan Aquifer to attempt to reduce the hypersaline condition in the CCS and to reduce the CCS water temperature and replace evaporating canal water to increase cooling capacity of the CCS to meet NRC permit thermal efficiency requirements.

In 2016, before the initial license renewal (LR) and the subsequent license renewal (SLR) for Turkey Point in 2019 to year 2052, the Florida Department of Environmental Protection (FDEP) finally acted on these serious environmental pollution violations and entered a Consent Order (CO) with the Applicant in 2015 to mitigate the impact and eliminate the cause of the water quality violations. In 2016, Miami Dade County also acted on the water environment pollution and entered into a Consent Agreement (CA) with Applicant to remediate the groundwater pollution caused by poor operation and maintenance of the CCS. The FDEP CO required FPL to:

- to halt the westward migration of the massive hypersaline plume from the TPPP canal system (CCS) into the Biscayne Aquifer within three years from the start of the agreed remediation plan activities, and
- to withdraw the entire defined volume of hypersaline plume leaked from the CCS back to east side of the SFWMD L-31E canal within 10 years from the start of the agreed remediation plan activities.

The 2016 Miami-Dade Consent Agreement (MDC CA) required the Applicant to demonstrate over a ten (10) year period ending in May 2028, valid reductions in the salt mass and volume of hypersaline water in groundwater west and north of FPL's property without lowering the groundwater table and creating adverse environmental impacts. Hypersaline groundwater is defined in both the FDEP CO and MDC CA as groundwater with a chloride concentration greater than that of seawater (19,000 milligrams per liter (mg/L)

To accomplish the requirements of the CO and CA, the Applicant constructed a Recovery Well System (RWS) comprised of ten (10) groundwater extraction wells along the western edge of the CCS which capture and extract the hypersaline water from the Biscayne Aquifer after it flows out of the CCS and then pumps it through a conveyance pipeline system to a permitted Deep Injection Well (DIW) located near the center of the CCS for disposal into the Boulder Zone located 3,000 ft below the ground surface of the Biscayne Aquifer.

The RWS became operational on May 15th, 2018, and May 16th, 2018, became the start date for the applicable 5 year and 10 year compliance deadlines in the CO and the CA. FPL is required by FDEP and MDC to prepare and file a Remedial Action Annual Status Report on the Recovery Well System (RAASR) with FDEP and MDC. The fourth year RAASR was filed with FDEP and MDC in November 2022.

Neither FDEP nor MDC have completed their review of the RAASR as of May 2nd, 2023, and submitted written comments on this document. We will submit an amendment to these comments to include FDEP and MDC comments once they are provided.

The CO and the CA provide that the Applicant can continue to recalibrate its model in year 5 to achieve compliance with the CO and CA by 2028. In the fifth year which ends on May 16th, the Applicant is required to file a report analyzing the effectiveness of the RWS within 60 days of filing the 5th year RAASR. We reserve the right to comment on this document.

Of major concern is that both the 3rd year and the 4th year RAASR modeling results predict that FPL cannot completely comply with the CA and the CO mandates. The RWS will not be able achieve full retraction/removal of the hypersaline water plume in the "State of FL designated compliance area" in the middle and lower modeled layers of the Biscayne Aquifer by 2028, the date for the 10 year compliance under the CO and CA. Partial, not complete, retraction of the hypersaline water plume edge within the compliance area" by 2028 fails to meet the FDEP Consent Order requirement. There is also no decreasing trend in total phosphorus and chlorophyll and tritium concentrations reported in the 4th year RAASR.

The operation and maintenance of the CCS, a major component of the nuclear reactor system, is a significant site-specific environmental issue that affects the safe and efficient operation of the Turkey Point Power Plant and our primary and secondary sources of drinking and agriculture water in South Florida and Monroe County. The NRC must consider requiring the Applicant to replace the archaic non-closed loop cooling canal system which is subject to sea level rise with the non-weather dependent, industry standard method of cooling towers as a key part of its review of aging nuclear reactor system in determining whether to renew the FPL license for Turkey Point Power Plant from 2033 to 2053. The continued CCS operation will have an impact on all generic environmental and site specific environmental category issues and they should all be moved to site specific review. The following exhibits support our comments on proposed NRC environmental review rules changes:

Exhibit 1 - *4th Remedial Action Annual Status Report by FPL*, filed in November 2022

Exhibit 2 - *Letter from Stan Austin, Regional Director, National Park Service to Frank Astulewicz , Director New Reactor Licensing* , December 19th , 2016 .

Exhibit 3 - *Evidence of salt plume under Turkey Point nuclear plant goes back years*, J. Staletovich, Miami Herald, April 21, 2016.

Exhibit 4- *Report on Recent Biscayne Bay Water Quality Observations*, Lee Hefty, Assistant Director, Division of Environmental Resource Management, December 15, 2015

Section 51.53 (C)(3)(ii)(D): Post–Construction Environmental Reports

We support the proposed language changes and consolidation of the groundwater quality degradation issues into a single consolidated Category 2 level. The revised LR. GEIS in 2013 "based on new information" was correct in its finding that cooling ponds or cooling canals at both inland and coastal plant sites can and have impacted groundwater and surface water quality because of the migration of contaminants discharged from the cooling ponds or cooling canals. The contaminants, through the negligent operation and maintenance of the cooling ponds or canals, can be created in said cooling ponds and canals and, through migration in the aquifer and surrounding groundwater, and can result in an adverse impact to the groundwater and surface water in the environment around the nuclear power plant site. The impact at Turkey Point and surrounding areas is large and includes Biscayne National Park, the surrounding wetlands, and the Everglades .

We support the 2013 LR GEIS finding and Category 2 designation as an environmental site-specific issue.

For example, in 2014, the cooling canals at the FPL Turkey Point Power Plant, drought conditions and extremely high ambient temperatures coupled with Applicant's poor operation & maintenance practices of the CCS caused reactor intake water temperatures to reach 104 degrees F, This exceeded the design limit by 8 degrees F and the Applicant had to apply for and was granted an emergency increase from the NRC which was unprecedented and the highest input temperatures of any nuclear plant in the nation. This caused the NRC to require FLPL to temporarily ramp down the operating capacity of the 2 nuclear reactors. FPL obtained an emergency permit from SFWMD to withdraw millions of gallons of L31E canal water (freshwater) to pump into the CCS to reduce the temperature of the CCS.

Turkey Point is an example of what can occur when the State and County do not monitor the performance of all critical plant components post construction. It was not until 2015 and 2016, that the State and County finally issued groundwater quality violations caused by polluted, hypersaline water which had been migrating from the cooling canal system over decades after completion of construction of the CCS and required FPL to clean it up. The 4th RAASR indicates that improvements CCS have been made but that there is still more to be done to clean it up. The NRC relied upon

the projected success of the RWS to issue the LR and SLR in 2019 but FPL now predicts that it will not be able to achieve compliance by 2028. The cooling canal system is an integral nuclear power plant component under the NRC license and the performance as designed is vital to the safe and efficient operation of the nuclear reactors, not just an industrial wastewater basin.

Subsection vii Groundwater Resources- (22) Groundwater Use Conflicts for Plants Withdrawing More than 100 gpm of Make-up Water from a River:

This proposed rule should be modified/ expanded to include those plants that withdraw more than 100 gpm of make-up water from a state identified drinking water aquifer for a closed-loop or non-closed loop cooling water system. Alternatively, the NRC could create a new Sub-Section vii Category (26) for those nuclear power plants that withdraw more than 100 gpm of make-up water from an aquifer for a closed-loop or non-closed loop cooling water system.

As a site-specific example, The Turkey Point Plant has pumped 15 mgd – 30 mgd first from the L31 and then from the Floridan since 2011. FPL is one of the largest users of water in Florida where the diminishing trend in drinking and irrigation water supply is alarming.

The Floridan, which is Florida's largest aquifer, lies beneath most of Florida and underpins life in Florida by providing most of the drinking water and water for other uses in the state except in South Florida and Monroe County which relies on the Biscayne Aquifer for drinking water. The L31 is used for agricultural and it has become increasingly salty due to the operation of the CCS and saline intrusion. Florida's demand for water is increasing and water levels in the Floridan are dropping caused by overextraction due to dramatic population growth and development which diminish recharge as lands that recharge the aquifer are drained and covered with concrete. The Floridan Aquifer is not unlimited and in recent years the water levels in the Floridan have been dropping due to population growth and development, contamination , over extraction, saltwater intrusion, and the effects of climate change. The brackish Floridan is also exhibiting an increasing saline concentration. A source other than Floridan must be located for use by FPL at Turkey Point because of groundwater use conflicts. This proposed rule should be modified, or a new rule proposed which should also include the following requirements:

For an initial or subsequent term renewal application for a nuclear power plant planning to withdraw over 100 gpm (140,000 gpd) make-up water from a State-identified irrigation water and/or drinking water aquifer for any on-site purpose, the Applicant must be required to provide in its site-specific environmental report to the NRC a comprehensive review of all other known available water supply resources in the surrounding environment, including, but not limited to, advanced- treated municipal or industrial waste water effluent sources. The applicant shall also be required to include in the site-specific environmental report a complete qualitative and quantitative analysis of

the water demand for the entire nuclear power plant. This analysis shall include, but not be limited to, the ultimate destination of all used water discharges.

Exhibit 5 : *Recharging the Floridan Aquifer: Threats to the Floridan Aquifer*, August 22, 2022, www.nflt.org
Exhibit 6: *The Floridan Aquifer: Why one of our rainiest states is running out of water*, National Geographic.com, July 29th, 2020 .
Exhibit 7- *Protecting Fresh Water We're working to ensure clean water for Florida's people and nature.* The Nature Conservancy July 14, 2020 , *updated July 28, 2022*

Subsection xvii (74)- Climate Change Impacts on Environmental Resources:

This proposed rule is lacking in that as written it only requires evaluation of impacts of climate change on environmental resources that are affected by the continued nuclear power plant operation and refurbishments during the license renewal term (initial LR or SLR). The proposed rule should be modified/ expanded to require thorough evaluation of impacts of climate change on the continued safe nuclear power plant operation and refurbishment itself during the license renewal term. The evaluation of climate change impacts on safety and performance of nuclear power plants located directly along a coast, such as the Turkey Point in Miami-Dade County which is located just above mean sea level on the coast and between Biscayne Bay National Park and the Atlantic Ocean and Everglades National Park and adjacent to coastal wetlands is a critical issue which deserves the minimum Category 2, and probably a Category 3 classification and affects many of the generic issues related to the environment.

Existing aging nuclear plants are extremely vulnerable to climate change impacts which can decrease the efficiency of nuclear reactors, require operators to cut back or shut off reactors, increase the cost of nuclear power, and increase safety and environmental risks. Rising temperatures can warm the power plant's source of cooling water, relied upon to ensure safety within the core and in spent fuel storage areas. Recently warming waters have already caused many global nuclear power plants to scale back generation or shut down temporarily. The IPCC has just announced that the world is likely to surpass its most ambitious climate target _limiting warming to 1.5 Celsius (2.7 degrees F) above preindustrial temperatures by the early 2030's. Scientists predict that beyond that threshold, climate disasters will be extreme and cause irreversible damage to communities and ecosystems unless carbon emissions are reduced. Higher temperatures resulting will make storms more powerful and sea level rise makes flooding from these storms more intense.

Increasing temperatures and decreasing rainfall can and do impact the performance of nuclear power plant reactors and support systems such as the cooling canal system, which can adversely affect the capacity and thermal efficiency of the reactor(s) water cooling system if ponds or canals on / adjacent to the nuclear plant site are utilized. The inability of the weather/ climate dependent cooling ponds or canals to reliably return

water to the nuclear reactors which is cooled to the design influent temperature can cause a reduction or shut down in the electrical power generating capacity of the nuclear power plant .

Increasingly severe hurricanes and flooding as a result of global warming can damage nuclear power plants and cut off access to cooling water, like the events of the Fukushima Daiichi nuclear accident. The risks to both operational and decommissioned nuclear plants that store nuclear waste on-site are increasing and climate Impacts to nuclear power plants can lead to catastrophic accidents with irreversible and widespread health and environmental effects.

Recent sea level rise studies by renown climate scientists, Jianjun Yin and Sonke Dangendorf have concluded that a quickly warming Gulf of Mexico is driving a faster than expected rise in sea levels along the Gulf and across the east coast of Florida that is "unprecedented in at least 120 years". The findings by these scientists are incorporated in the recent Washington Post article, in the UN Intergovernmental Panel on Climate Change report. (IPCC) and in July last, the Southeast Florida Regional Climate Change Compact projected that by 2040, seas would rise between 10 to 17 inches over 2000 levels, based on predictions from NOAA and the Intergovernmental Panel on Climate Change, the United Nations body that has studied the issue since the 1980s.

Sea level rise and resulting saline intrusion will cause contamination of aquifers in Florida and will flood the CCS and prevent it from serving the purpose for which it was intended as well as cause saline intrusion into Florida's aquifer system. It will also severely restrict access to access for the proper operation and maintenance of the 168 miles of canals comprising the CCS as well as transportation corridors around the Turkey Point property.

NRC should also require the applicant to address in the site -specific environmental report for a nuclear power plant located on US Atlantic, Pacific and Gulf Coast that proposes to continue to use ponds and canals as the cooling water system based upon the actual predicted level of sea level rise, projected rise in ambient temperatures ,storm surge and King Tides instead of the historic levels which FPL used in its EIS in support of its SLR application in 2019 . All these factors will adversely impact the operational integrity and the thermal efficiency of the cooling canals or ponds in the next 30 years if the NRC extends the life of the reactors to 2052 which exceeds design specifications for nuclear reactors. The applicant must be required to demonstrate how these adverse impacts can be prevented by a proven refurbishment to the pond or canal system or by complete replacement of the CCS with new industry-standard cooling towers constructed well above sea level rise and hurricane storm surge. If replacement is the only viable option, then the renewal permit should stipulate immediate termination of water use from the canals and ponds and, if on-site, immediate decommissioning of the canals or ponds after the cooling towers are completed, tested, and put online.

Exhibit 8- *Seas have drastically risen along southern U.S. coast in past decade,* The Washington Post, April 10, 2023.

Exhibit 9-*Unified Sea Level Rise Projection for Southeast Florida,* prepared by the Florida Regional Climate Change Compact's Sea Level Rise Ad Hoc Work Group, pp 9-23.

Exhibit 10- *World is on brink of catastrophic warming, UN Climate Change Report says,* Sarah Kaplan, March 20th, 2023.

Subsection ix, Aquatic Resources (35), Impingement Mortality and Entrainment of Aquatic Organisms:

We agree that this proposed new rule must be a Category 2 site specific for nuclear power plants where the environment around the plant site contains "aquatic resources". This rule should contain a specific definition of and examples of "aquatic resources" covered by the rule, i.e., wetlands, coastal estuaries, streams, lakes, rivers, springs, seeps, ponds, groundwater. The scope of the rule should be modified / expanded to include "cooling canals". This following additional text should be added to this proposed rule.

- *An Applicant seeking a LR or SLR for a nuclear power plant located next to a coastal bay or ocean waters and which expects to continue using non-closed loop (unlined) cooling ponds or canals that utilize seawater for make-up and (1) leak into the groundwater and /or (2) experiences a daily tidal exchange of seawater with said coastal bay or ocean waters must include in its Site Specific Environmental Report a qualitative and quantitative evaluation of the impacts on the aquatic resources contained within the environment around the plant site during the SLR term.*
- *Furthermore, the Site- Specific Environmental report must describe how the Applicant intends to mitigate any predicted adverse impacts and how it will monitor the status of the health of the aquatic resources during the renewal term to determine the level of success of the mitigation measures. The Applicant shall also be required to include this information in the annual plant report to the NRC.*

Subsection xvii (73)- Greenhouse Emissions and Climate Change:
We agree with the comments filed by the U.S Department of Environmental Protection's comments filed in these proceedings and that this new category should be added but not as a Category 1 issue; it should be added as a Category 2 issue for site specific analyses. The draft GEIS has assigned Category 2 to climate change impacts and adaptions and should also assign Category 2 to Greenhouse upstream and downstream emissions. Although the NRC evaluation of nuclear power plants' operations concludes that GHG emissions are inherently low and impact on climate change would be "SMALL", there is strong evidence that GHG emissions coming from transmission facilities conveying electrical power from the nuclear power plant is

"MODERATE to LARGE". Therefore, this issue during environmental review should justify a Category 2 classification and we attach the following as further support.

Exhibit 11 - *US Emissions of the World's Most Potent Greenhouse Gas are 56 percent higher Than EPA Estimates, a New Study Shows*. Inside Climate News, January 31, 2023.

Subsection xx (80)- Termination of Nuclear Power Plant Operations and Decommissioning

This issue must be elevated to a Category 2 or 3 level. It is imperative that every nuclear power plant seeking a license renewal term must resubmit to the NRC for approval as part the application and environmental review an updated plant and plant site "Termination and Decommissioning Plan " based on the current integrity and age of the plant components and systems, feasible refurbishments to same, conditions of environmental resources affected by past and continued plant operations and foreseeable impacts of changes in climate during the proposed renewal term. It takes decades to decommission a nuclear plant and sea level rise and resultant flooding during the SLR and beyond needs to be considered and decommissioning timed correctly so that projected sea level rise does not interfere with the successful decommissioning of the nuclear plant.

The applicant, based on all the above considerations, must include a re-assessment of the service life of the major components of nuclear power plant, storage of spent fuel, feasibility of refurbishment and an updated schedule for decommissioning and termination. The plan shall state a primary federally approved site and a secondary federally- approved site for the disposal of the spent fuel stored on-site once decommissioning has commenced. Public safety demands the classification of the Applicant's submittal and the NRC review of an updated site-specific termination and decommissioning plan as a Category 2 or 3 issue.

Respectfully submitted,

Bonnie Rippingille

Bonnie Rippingille
Chair
Special Committee for Turkey Point Issues
Ocean Reef Community Association
Key Largo, Florida

Resources:

Exhibit 1 - *4th Remedial Action Annual Status Report by FPL*, filed in November 2022

Exhibit 2 -- *Letter from Stan Austin, Regional Director, National Park Service to Frank Astulewicz , Director New Reactor Licensing* , December 19th , 2016 .

Exhibit 3- *Evidence of salt plume under Turkey Point nuclear plant goes back years*, J. Staletovich, Miami Herald, April 21, 2016.

Exhibit 4-*Report on Recent Biscayne Bay Water Quality Observations*, Lee N. Hefty, Assistant Director, Division of Environmental Resource Management, December 15, 2015

Exhibit 5 : *Recharging the Floridan Aquifer: Threats to the Floridan Aquifer*, August 22, 2022, www.nflt.org

Exhibit 6: *The Floridan Aquifer: Why one of our rainiest states is running out of water*, National Geographic.com, July 29th, 2020 .

Exhibit 7- *Protecting Fresh Water We're working to ensure clean water for Florida's people and nature.* The Nature Conservancy July 14, 2020 , *updated July 28, 2022*

Exhibit 8- *Seas have drastically risen along southern U.S. coast in past decade*, The Washington Post, April 10, 2023.

Exhibit9 -*Unified Sea Level Rise Projection for Southeast Florida*, prepared by the Florida Regional Climate Change Compact's Sea Level Rise Ad Hoc Work Group, pp 9-23 .

Exhibit 10- *World is on brink of catastrophic warming, UN Climate Change Report says*, Sarah Kaplan, March 20th, 2023.

Exhibit 11 - *US Emissions of the World's Most Potent Greenhouse Gas are 56 percent higher Than EPA Estimates, a New Study Shows.* Inside Climate News, January 31, 2023.

TURKEY POINT CLEAN ENERGY CENTER

Remedial Action Annual Status Report

Year 4

November 15, 2022

TABLE OF CONTENTS

<u>Appendices</u>

LIST OF TABLES

LIST OF FIGURES

ACRONYMS AND ABBREVIATIONS

°C	degrees Celsius
°F	degrees Fahrenheit
2D/3D	2-dimensional/3-dimensional
AEM	aerial electromagnetic
AGF	Aqua Geo Frameworks
APT	aquifer performance test
Arcadis	Arcadis U.S., Inc.
CA	Consent Agreement
CCS	cooling canal system
CO	Consent Order
CSEM	continuous surface electromagnetic mapping
DERM	Department of Environmental Resources Management
DIW	deep injection well
DUS	data usability summary
EDMS	Electronic Data Monitoring System
EM	electromagnetic
EPU	extended power uprate
ET	evapotranspiration
ET_o	reference evapotranspiration
FDEP	Florida Department of Environmental Protection
FPL	Florida Power & Light Company
ft	foot/feet
GTI	Groundwater Tek Inc.
GPS	global positioning system
HEM	helicopter electromagnetic
HFZ	high-flow zone
HSI	saline-hypersaline interface
ID	interceptor ditch
LCI	laterally constrained inversion
m	meter/meters
MDC	Miami-Dade County
mg/L	milligrams per liter
mgd	million gallons per day
mL	milliliter
NMP	Nutrient Management Plan
ohm-m	ohm meter
PEST	parameter estimation
PFC	primary field compensation
pCi/L	picocuries per liter
ppt	parts per thousand
PSU	practical salinity unit

QAPP	Quality Assurance Project Plan
RAASR	Remedial Action Annual Status Report
RAP	Remedial Action Plan
RWS	recovery well system
SCADA	Supervisory Control and Data Acquisition
SCI	spatially-constrained inversion
SFWMD	South Florida Water Management District
SkyTEM	SkyTEM Canada Inc.
SSMP	Supplemental Salinity Management Plan
TDS	total dissolved solids
TEM	transient electromagnetic
TEP	thermal efficiency plan
TN	total nitrogen
TP	total phosphorus
TPGW	Turkey Point Groundwater
Turkey Point	Turkey Point Power Plant
UFA	Upper Floridan aquifer
UIC	underground injection control
UICPW	underground injection control production test well
US 1	U. S. Highway 1
USEPA	United States Environmental Protection Agency
USGS	United States Geologic Survey
V1,V2	Version 1, Version 2, etc.
VDF	variable density flow

EXECUTIVE SUMMARY

Analyses of data through Year 4 of remediation demonstrate that the net westward migration of the cooling canal system (CCS) hypersaline plume has been halted, and hypersaline groundwater from the CCS is being intercepted, captured, contained, and retracted by recovery well system (RWS) operations. The aerial electromagnetic (AEM) data shows that the volume of hypersaline water in the compliance area has been reduced by 67% since remediation began in 2018. In addition, many of the groundwater monitoring wells are showing declining trends in salinity, and there are notable improvements in CCS water quality, reductions in algae, and continued improvements in thermal efficiency. Evaluations to better align groundwater monitoring data, AEM surveys, and groundwater modeling results will continue in preparation for the Year 5 Remedial Action Annual Status Report.

The Florida Power & Light Company (FPL) has prepared this Remedial Action Annual Status Report (RAASR) to document the results of the Year 4 Recovery Well System (RWS) operation, in compliance with the monitoring and reporting objectives of the Miami-Dade County (MDC) Consent Agreement (CA) and Florida Department of Environmental Protection (FDEP) Consent Order (CO). The RWS groundwater remediation system is designed to intercept, capture, contain, and retract hypersaline groundwater located to the west and north of FPL's property without creating adverse environmental impacts. The RWS consists of 10 extraction wells that remove hypersaline water from the Biscayne aquifer and dispose of it in the Boulder Zone, more than 3,000 feet below the base of the aquifer, through an underground injection control (UIC) well system. FPL successfully initiated operations of the Turkey Point RWS on May 15, 2018.

FPL uses three primary tools to assess remediation progress: groundwater monitoring, continuous surface electromagnetic (CSEM) survey using aerial electromagnetic (AEM) methods, and groundwater modeling (i.e., variable density flow and salt transport model). Data collected from groundwater monitoring wells from 2018 through Year 4 (July 1, 2021, to June 30, 2022) of remediation, in conjunction with the comparative 2018–2022 AEM surveys and updated and recalibrated modeling results, were used collectively to assess changes in the volume and extent of the hypersaline plume. The groundwater model was also used to estimate future reductions to the hypersaline plume based on 4 years of remediation data. Data and modeling confirm the objectives of the CA and the CO through Year 4 are being met. The following is a summary of the major findings of this evaluation:

- After 4 years of remediation operations, the CA objectives to intercept, capture, contain and demonstrate statistically valid reductions in the salt mass and volumetric extent (retraction) of hypersaline groundwater from the CCS continue to be met. The CO requirement to halt the westward migration of hypersaline water from the CCS within 3 years was achieved and documented in the April 2021 Year 2 Part 2 RAASR; significant reductions continue to be demonstrated by analyses conducted in this report.

- Since inception of the remediation system, approximately 23.43 billion gallons of hypersaline groundwater and 9.24 billion pounds of salt have been extracted from the Biscayne aquifer. Approximately 6.18 billion gallons of hypersaline water and 2.37 billion pounds of salt were removed during this reporting period.

- In total, 21 of 26 monitoring wells west and north of the CCS used in the remediation assessment showed a statistically significant declining trend in one or more parameters (quarterly chloride, quarterly tritium, and weekly average automated salinity) and multiple wells had one or more parameters that were the lowest value on record this reporting period.

- The fact that the majority of the wells have a declining trend since the start of the RWS and a number of the wells, including intermediate and deep wells, continue to show lower chloride, salinity, and/or tritium concentrations each year indicates positive progress in meeting the objectives of the CA and CO.

- Greatest reductions in chloride levels are being measured in shallow monitoring wells next to the CCS where shallow fresher groundwater replaces hypersaline water along the top of the plume. The gradual reductions occurring in the middle and deep monitoring wells near the CCS are expected to increase as the continuing plume retraction reaches the narrow monitoring intervals of the deeper monitoring wells.

- The Year 4 AEM results, compared to the 2018 baseline survey results, indicate the volumetric extent of the hypersaline plume has been reduced by 67% after 4 years of RWS operation. The location of the leading edge of the CCS-sourced hypersaline plume west and north of the Plant site is shown to have retracted back to the CCS by as much as 1.25 miles.

- Based on AEM data, the greatest reduction in hypersalinity volume is occurring in the lower portion of the aquifer as the plume west of the L-31E canal is retracting eastward.

- The Year 4 recalibrated V7 model forecast simulations for Years 5 and 10 of remediation show improved hypersaline retraction results at all depths of the modeled aquifer. Complete retraction predominantly occurs in shallow and intermediate model layers. Retraction in the deepest model layers is focused in northern areas.

In addition to reductions in groundwater hypersalinity to the west and north of the CCS, FPL has successfully completed multiple restoration and remediation activities outlined in the MDC CA and the FDEP CO which have resulted in tangible improvements within the CCS:

- Reduction of the annual average salinity in the CCS to 36.1 PSU (June 1, 2021, to May 31, 2022) which is its lowest annual level since 1977. Reducing salinities in the CCS reduces the formation of hypersaline water and reduces the driving head on hypersaline groundwater beneath the CCS, aiding in the retraction of the hypersaline plume.

- CCS thermal efficiencies have exceeded the CO minimum value of 70% since 2016, with the annual average CCS thermal efficiency for the period from June 2021 through May 2022 being 86.2% (FPL 2022).

- There is a statistically significant declining trend in total nitrogen over the past three plus years, while the total phosphorus levels remain relatively low, ranging between 0.01 to 0.05 mg/L.

- Algae levels show dramatic declines during the reporting period, reaching their lowest levels since 2016. Reductions in turbidity and increases in water clarity have been coincident with the algae reduction.

During the reporting year, FPL implemented various actions to enhance the ongoing remediation and to further enhance the objectives of the CA and CO, including enhancing processes and procedures to improve resiliency of the RWS system, maximizing flow, expanding the groundwater network by adding TPGW-23, and increasing the Upper Floridan Aquifer allocation for CCS freshening.

Given the significant progress of remediation since initiation of the RWS, FPL does not propose any changes to the Agencies' approved remediation plan at this time. However, based on review of groundwater monitoring data, Year 4 AEM survey data, and the updated and recalibrated Year 4 (V7) forecast modeling, FPL plans to undertake the following recommended actions in preparation for the Year 5 RAASR:

- Conduct evaluations of the AEM results to further verify documented changes along the western edge of the plume, determine the nature of isolated lenses of hypersalinity, evaluate areas of lower salinity groundwater located along the base of the aquifer beneath AEM-identified hypersaline layers, and evaluate areas where AEM-estimated chloride values significantly differ from adjacent monitoring well values.

- Continue to refine and improve the model as a predictive and management tool by refining the technique for using inputs from the water and salt balance in the groundwater flow and saltwater transport model; explore alternative conceptual models of the near-RWS flow system to align the modeled hypersaline interface more closely with those characterized by AEM and monitor well data; continue to collect data reflective of long-term RWS operations and recalibrate the model to help inform the model and increase its accuracy in simulating the effect of the RWS; conduct additional analysis to understand the hypersaline plume development and retraction in the lower model layers; and verify the degree to which model-generated, non-CCS hypersaline groundwater impacts remediation objectives.

It is important to note that the aquifer system is complex and subject to many external factors beyond the CCS and RWS; therefore, continued monitoring, model updates, and scientific data analyses are performed to improve our understanding of the impact of RWS operations in concert with these other factors. FPL will continue to monitor and evaluate progress in meeting the requirements of the CA and CO and make recommendations for modifications as needed.

1   INTRODUCTION

> FPL is submitting the Year 4 Remedial Action Annual Status Report (July 1, 2021, through June 30, 2022) on the status of remediation and progress in meeting the objectives of the MDC CA and FDEP CO. The remediation efforts have resulted in significant reduction in salt mass and the volumetric extent of hypersaline groundwater west and north of the FPL property over the last 4 years. Additionally, multiple restoration and remediation activities outlined in the CA and CO have been completed and FPL and has made substantial progress in implementing and completing activities which have resulted in tangible improvements within the CCS.

1.1   BACKGROUND

Florida Power & Light Company (FPL) submits this Year 4 Remedial Action Annual Status Report (RAASR) pursuant to paragraphs 17.b.ii and 17.d.v of the Miami-Dade County (MDC) Department of Regulatory and Economic Resources (DERM) Consent Agreement (CA) and paragraphs 28, 29.c. and 33 of the Florida Department of Environmental Protection (FDEP) Consent Order (CO). FPL entered into the CA on October 7, 2015, and the CO on June 20, 2016. FPL agreed to conduct specific actions, including the remediation of hypersaline groundwater adjacent to the FPL Turkey Point Power Plant (Turkey Point). The specific objectives of the CA are to demonstrate a statistically valid reduction in the salt mass and volumetric extent of hypersaline water in groundwater west and north of FPL's property without creating adverse environmental impacts and to reduce the rate of, and ultimately arrest, migration of hypersaline groundwater. The specific hypersaline groundwater remediation objectives of the CO are to halt the westward migration of the hypersaline plume from the cooling canal system (CCS) within three years and reduce the westward extent of the hypersaline plume to the L-31E canal within 10 years. Hypersaline groundwater, as defined in the CO and CA, is groundwater with a chloride concentration greater than 19,000 milligrams per liter (mg/L).

FPL initiated the evaluation and design of a recovery well system (RWS) as part of a Remedial Action Plan (RAP) to intercept, capture, and retract hypersaline groundwater west and north of the FPL property boundary in accordance with the requirements of the CA and CO. To design the RWS, FPL developed a groundwater flow and salt transport model, which was extensively reviewed by the South Florida Water Management District (SFWMD), FDEP, MDC, the United States Environmental Protection Agency (USEPA), and the University of Florida. The model and remediation design were ultimately approved by MDC on May 15, 2017. After obtaining all required environmental and well construction permits, FPL initiated the construction of the RWS, which includes 10 groundwater recovery wells, a conveyance pipeline system, and a deep injection well (DIW) more than 3,000 feet (ft) below the base of the aquifer. The system was fully operable on May 15, 2018. FPL submitted an RWS startup report to MDC in October 2018 (FPL 2018a), and quarterly RWS status reports through May 2019 (FPL 2018b, 2019a, 2019b) that provided information on the design and operation of the approved RWS. In addition, an

annual remediation restoration report was submitted in December 2018 (FPL, 2018d) that documented the status of the RWS, CCS canal management actions, Turtle Point and Barge Canal restoration, and monitoring and mitigation actions.

Annual RAASR reports were then subsequently submitted with the first year report (Year 1) covering the period from May 15, 2018, to May 31, 2019 (FPL 2019c). In Year 2, collection of the Aerial Electromagnetic (AEM) survey data was delayed from the originally scheduled end of May 2020 timeframe until September 2020 due to restrictions on international travel and health risks associated with the COVID-19 pandemic. This resulted in the Year 2 RAASR having 16 months of data and being submitted in two parts: groundwater monitoring data from June 2019 to September 2020 (FPL 2020a) and the Year 2 AEM survey (flown September 26–27, 2020) and groundwater model (FPL 2021a). The Year 3 report included groundwater monitoring data collected from October 1, 2020, to September 30, 2021, an updated groundwater model V6, and the Year 3 AEM survey flown June 18 through 22, 2021 (FPL 2021b).

In an effort to return to the pre-COVID 12-month annual remediation assessment schedule, the Year 4 report comprises data collected from July 2021 through June 2022, including the Year 4 AEM survey flown on May 19 and 20, 2022. This timeframe incorporates the June 2022 quarterly sampling event which is used to establish the relationship with bulk airborne transient electromagnetic method (AEM) resistivity measurements from the May 2022 AEM survey.

Data and accompanying analyses in the Year 1 reports indicated a statistically valid reduction in salt mass and a 22% reduction in the volumetric extent of hypersaline groundwater west and north of the FPL property (FPL 2019c). An additional 12% in reductions were observed in the second year of operation which were documented in the Year 2 RAASR (FPL 2021a). In addition to capturing and reducing the plume extent, particle tracking using the Version 5 (V5) updated model demonstrated that the RWS creates a hydraulic barrier that intercepts and contains hypersaline groundwater located beneath the CCS from migrating west and north. In the Year 3 RAASR (FPL 2021b), there was an additional 8% volumetric reduction in the hypersaline plume with a total of 42% reduction since startup of the RWS in May 2018. In addition, data and analyses contained in the Year 3 RAASR show that FPL has successfully intercepted, captured and contained the hypersaline plume and has begun to retract the hypersaline plume within the first three years of operation of the groundwater recovery system.

1.2   SCOPE OF THE REMEDIAL ACTION ANNUAL STATUS REPORT

This Year 4 RAASR report includes the following:

- Information collected from July 1, 2021, through June 30, 2022 although in some instances, data beyond June 30, 2022, have been incorporated into this report for the most updated data trends

- Year 4 RWS operational summary, including analytical results from the RWS wells, salt mass and hypersaline groundwater removal and operation run times

- Data and assessment from monitoring wells in Year 4 and comparisons to baseline conditions and/or previous years

- Year 4 annual AEM survey results with comparisons between the 2022 AEM survey and 2018 baseline AEM survey

- An updated RWS groundwater model description and results, as well as Year 5 and Year 10 remediation forecast results

- Status of activities related to management of the CCS and resulting improvements which includes data up through September 30, 2022

- Appendices containing additional supporting information and data used in the report (Appendices A–H)

Section 2 of this report provides an overview of RWS operations, and it includes a summary of automated and analytical data from the recovery wells and the calculation of total salt removed by the RWS.

Section 3 of the RAASR provides automated data and/or analytical samples from monitoring well sites (up to 26 wells) located within the areal extent of the hypersaline groundwater plume collected from July 1, 2021, to June 30, 2022. These data along with Year 1, Year 2, and Year 3 data were used to evaluate changes and trends in groundwater quality from baseline conditions in March 2018 through June 2022 (52 months). These results were compared to the data collected prior to the startup of RWS to identify changes likely related to RWS operations. Groundwater chloride contour maps for the shallow, middle, and deep monitoring well horizons augmented with AEM data are generated for Year 4 and compared with similarly prepared 2018 baseline contour maps to identify changes in the extent of hypersalinity.

Section 4 of the RAASR includes the results of the Year 4 AEM survey with comparisons to the baseline 2018 AEM survey to document changes to the extent and volume of the hypersaline plume within the CO/CA compliance boundary that have occurred since RWS operations began.

Section 5 of the RAASR encompasses documentation of the updated, recalibrated Turkey Point groundwater flow and salt transport model with predictive model runs for Year 5 and Year 10 of plume remediation.

Section 6 of the RAASR discusses findings observed in the CCS associated with salinity, nutrient, and thermal efficiency management actions.

1.3   STATUS OF CONSENT AGREEMENT/CONSENT ORDER IMPLEMENTATION

> FPL is successfully implementing restoration and remediation activities outlined in the MDC CA and FDEP CO, resulting in significant reductions of hypersaline groundwater volume and improved CCS water quality and conditions.

The RAASR provides information on FPL's progress in meeting the groundwater remediation objectives of the CA and CO along with the status of meeting the additional requirements of these regulatory documents. The CA and CO consist of two categories of required actions: those with deadlines for completion that precede this report (such as design and construct an approved groundwater RWS) and ongoing/future actions (such as implementation of CCS salinity, nutrient, and thermal efficiency management plans and Year 5 and 10 remediation progress reports).

FPL has successfully completed all actions required to be completed prior to this report and is on track implementing all ongoing actions. A summary of all required actions of the CA and CO is included in Appendix A of this report. Additional details pertaining to ongoing actions including salinity, nutrient, and thermal management in the CCS are summarized further in Section 6.

1.4   INDEPENDENT TECHNICAL REVIEW

In support of its review of FPL's Remedial Action Annual Status Reports, MDC DERM retained the services of Arcadis U.S., Inc. (Arcadis) to evaluate FPL's AEM methods, results and statistics, and Groundwater Tek Inc. (GTI) to evaluate site-specific variable density groundwater flow and solute transport modeling. The results of these evaluations were discussed in multiple technical meetings between FPL's and MDC's technical experts and project management staff.

Arcadis' review of FPL's AEM work was detailed, with the overall scope of their evaluations summarized by FPL into the following five categories:

- Review of geophysical data collection

- Review of geophysical data processing and inversion modeling

- Evaluation of alternative mathematical relationships to the correlation between airborne transient electromagnetic (AEM) measured formation resistivity, water resistivity, and chloride concentrations to define the extent and volume of the hypersaline plume

- Evaluation of hypersaline plume volume estimates (conducted for Year 1 report)

- Assessment of approach used to assess statistical significance of changes to plume volume and orientation

The Arcadis conclusions and recommendations were rigorously discussed between FPL and MDC technical and project management staff. As a result of these discussions, FPL addressed the following recommendations in this report as follows:

- Recommendations to standardize geophysical data acquisition, equipment calibration and data verification have been implemented since 2018 and are described in section 4.2.1 of this report and in section 2 of the September 22, 2022, Aqua Geo Frameworks, LLC, report entitled *Report on Advanced Processing and Inversion of 2022 AEM Survey Data and Derived Chloride Concentrations near the Turkey Point Power Plant, Southern Florida* (Appendix G).

- Recommendations for reducing systematic drift between AEM resistivity and monitoring well fluid resistivity by basing regressions on year-specific data pairings rather than multiple year pairings have been implemented by FPL since Year 2. However, this year, this recommendation was also applied to the 2018 baseline survey as discussed in section 4.2.3.2 of this report and section 3.1 of the AGF report (Appendix G).

- Recommendations for alternative methods to those used by FPL and the U.S. Geologic Survey (USGS) to relate AEM formation resistivity to porewater chloride concentrations were examined in section 2.6 of the AGF report (Appendix G). As suggested by Arcadis, rather than incorporating uncertainty associated with the regressions between AEM bulk resistivity and monitoring well laboratory chloride data, the distribution of AEM-measured resistivity values from the 2018 baseline survey through 2022 were qualitatively compared with a focus on changes in orientation of AEM resistivity threshold values of 1.75 ohm-meters or less, which are representative of chloride concentrations of 19,000 mg/L and above. The resulting distributions and retraction of the specified resistivity threshold values compared very well to the chloride conversion approach used by FPL in prior years.

- Six alternative evaluation approaches for assessing hypersaline plume volume estimates from 2018 and 2019 (Year 1 of remediation) were conducted by Arcadis using FPL AEM data. These alternatives produced a range of plume reduction values for the first year of RWS remediation from 16% to 25%, with Arcadis' estimated Year 1 plume volume reduction of 24%; this compared well with FPL's Year 1 volumetric reduction report of 22% (Arcadis 2020). The Arcadis evaluation of alternative methods indicates FPL's methods for calculation of changes in plume volume are consistent with these alternative methods.

- Arcadis's review of the approach FPL uses to assess uncertainty surrounding the regressions that ultimately relate AEM resistivity to chloride concentration focused on how that uncertainty potentially relates to chloride estimation error on a point-by-point scale. While the regression-based relationship between AEM formation resistivity and porewater chloride produce the most probable estimation of 19,000 mg/L chloride hypersaline threshold formation resistivity value, the use of the resulting confidence interval surrounding the regression does not fully represent the range of possible predictive chloride values at any 19,000 mg/L estimated value in the study area. FPL

discussed alternative approaches to assess uncertainty in the estimation of plume volumes with Arcadis and MDC and have included additional approaches (i.e., permutation testing and bootstrap estimation) in this report as described in section 4.2.4.3. and Appendix H. The results of the alternative methods produced very similar volumetric estimates as FPL's original approach.

The GTI review of FPL's variable density groundwater flow and solute transport model versions 3–6 was also detailed and well documented (GTI 2022), with the overall scope of the Year 3 evaluation summarized by FPL into the following five categories:

- Review of FPL's RAASR Year 3 report

- Review of FPL's SEAWAT model V6

- Verification of SEAWAT model runs (i.e., calibration, prediction, and sensitivity analyses)

- Review of salt extraction data and modeling results

- Assessment of model's plume reduction forecast results

The GTI conclusions and recommendations that addressed the model's differences with groundwater monitoring well data and AEM plume orientations and the potential impacts these differences had on remediation forecasts were rigorously discussed between FPL's and MDC's technical and project management staff. The major conclusions and recommendations are summarized by FPL as follows:

- The FPL models overstate the westward extent of hypersalinity as defined by AEM surveys and groundwater monitoring data. Accurate alignment of the western edge of the plume is critical in assessing progress of the remediation.

- The model shows the plume expanding along the base of the Biscayne Aquifer, which is contrary to the conceptual model and is not supported by AEM data. This issue, unless fixed, will prevent the model from accurately predicting the progress of the plume retraction.

- The model as configured shows vertical preferred flow instead of horizontal flow along the bottom of the aquifer (model layers 10 and 11) that, if true, constrains plume retraction along the base of the aquifer. However, this phenomenon is contrary to AEM survey results which show plume retraction along the base of the aquifer is occurring. This inconsistency between the model and the AEM data needs to be resolved.

- Recommendations made by GTI include improved use of parameter estimation targets to achieve better alignment of AEM and modeled initial plume locations, improved calibration that better aligns with groundwater monitoring wells and AEM salinity changes measured since remediation has been implemented, conducting sensitivity

evaluations to determine the relationship between vertical and horizontal flow in the deep layers of the aquifer, and reassessing the capture zone analysis performed by FPL around RWS-5, RWS-6, RWS-7 and RWS-8 in the deep level of the aquifer to verify CCS hypersaline groundwater from beneath the CCS is contained by RWS operations.

These issues were also identified by FPL in the RAASR Year 3 report, and modifications were incorporated into the development of the V7 model. The following modifications, consistent with the recommendations made by GTI, were made to produce the V7 model updates described in greater detail in section 5 and Appendix I in this report:

- Vertical layering of prior versions of the model, informed by the 2016 aquifer performance test (APT) prescribed in paragraph 17.b.i. of the CA, did not include the deep high-flow zone (about 80–90 ft deep) found throughout the Model Lands area. The vertical layering of the V7 model was expanded to include 17 layers, including the deep high-flow zone with the hydraulic conductivities being informed by lithologic core data collected during construction of the RWS production wells.

- CCS seepage to underlying groundwater in prior model versions were much greater than values calculated by the water and salt budget models produced under the 2009 annual monitoring plan. Seepage into and out of the CCS in the V7 model is informed by the calibrated water and salt budget model as documented in FPL Extended Power Uprate Annual Monitoring Reports.

- Initial conditions for the lower portions of the aquifer in prior model versions were informed by low hydraulic conductivity values produced from the 2016 APT test which resulted in conditions that could explain the modeled plume responses that are different from AEM and monitoring data. Initial hydraulic conductivity values of the V7 model were updated with values determined from the RWS and monitoring well core data.

- Model calibration targets and weighting factors were redistributed to better emphasize yearly changes at the Turkey Point groundwater monitoring wells and AEM site salinity changes since remediation began.

2   RECOVERY WELL SYSTEM YEAR 4 OPERATION SUMMARY

2.1   HYPERSALINE EXTRACTION/DISPOSAL OPERATIONS

> The RWS operated 93.8% of the time during the reporting period; there were only 22.8 days out of the year (6.2%) when the entire system was not operational. The majority of outages were related to system enhancements, preventative maintenance activities, lightning strikes, regulatory testing, permit-required testing of the DIW, and during the CSEM survey.

FPL operates 10 recovery wells to extract up to 465 million gallons per month (annual average of 15 mgd) of hypersaline groundwater, preferentially along the base of the Biscayne aquifer. The extraction wells are cased to the lower high flow zone of the Biscayne aquifer (FPL 2018a), allowing hypersaline water to be withdrawn along the base of the plume. As the extraction wells are pumped, hypersaline groundwater from beneath the CCS and from the plume west and north of the CCS flows laterally toward the points of withdrawal. As hypersaline water is removed, the plume shrinks both vertically and laterally with adjacent lower-salinity groundwater replacing the area formerly containing hypersaline groundwater. The extraction of hypersaline groundwater from the lower extent of the Biscayne aquifer along the western margin and north of the CCS accomplishes the objectives listed below:

- Reduces the salt mass and volumetric extent of hypersaline groundwater west and north of the CCS. The retraction of the hypersaline plume is accomplished primarily by direct extraction of hypersaline groundwater, which increases the natural seaward groundwater flow gradient eastward into the RWS capture zone, and secondarily by natural dilution and dispersion of hypersaline water with the lower-salinity waters in the aquifer.

- Creates a hydraulic barrier that intercepts and contains the westward and northward migration of hypersaline groundwater from the CCS. RWS operations extend the hydraulic barrier effect of the interceptor ditch (ID) operation in the upper portion of the Biscayne aquifer to the base of the aquifer.

- Decreases groundwater salinity and mass beneath the CCS, which reduces the driving force that contributed to lateral movement away from the CCS and which is a component of halting the westward migration of hypersaline groundwater from the CCS.

The hypersaline groundwater is pumped from each recovery well into a collection system that consists of an approximately 9-mile-long pipeline that is routed to a deep injection well (DIW) located near the center of the CCS for disposal. The DIW is a 24-inch-diameter permitted underground injection control (UIC) non-hazardous Class I industrial wastewater disposal well (Permit No. 0293962-004-UO/1I) constructed to a depth of 3,230 ft below ground surface into the regionally confined Boulder Zone. Near the end of Year 1, the permitted operating capacity of the DIW was increased from 15.59 mgd to 18.64 mgd (Permit Modification No. 0293962-005-UO/MM) to accommodate additional remediation flows.

The deep injection well.

The Consumptive Use Permit from SFWMD authorizes an RWS annual withdrawal allocation of 5,475 million gallons (15 mgd) and a maximum monthly allocation of 465 million gallons from RWS extraction wells 1 through 10. In early 2020, two UICPWs (UICPW-1 and UICPW-2), co--located with the DIW and constructed to the base of the Biscayne aquifer in a similar manner as the recovery wells, were activated with a rate of approximately 3 mgd each to remove hypersaline groundwater from beneath the CCS. This extracted hypersaline water is disposed in the DIW along with the RWS-extracted hypersaline water, utilizing the DIW UIC permit's injection rate limit.

The groundwater extraction wells are controlled by a Supervisory Control and Data Acquisition (SCADA) system that controls the operation of all wells, has the capability to monitor and regulate individual well withdrawal rates, and maintains real-time-assigned total system extraction capacity in the event of individual well fluctuations. This system assists the operators in maintaining compliance with groundwater withdrawal and disposal permit limits. Flow pumped from each well is measured by totalizers; the combined flow down the DIW is also measured by a totalizer. All RWS and DIW flow meters were checked, calibrated, and certified in June 2022 as part of an annual calibration process.

Overall, the RWS operated 93.8% of the time from July 1, 2021, to June 30, 2022, with only 574 hours (22.8 days) over the year in which the entire system was turned off, primarily related to system enhancements, preventive maintenance activities, lightning strikes, regulatory testing, permit-required testing of the DIW, and during the CSEM survey. There were four outages that lasted more than a day which included the following:

- **November 5, 2021, 15:00 to November 8, 2021, 9:00.** Lightning strike that damaged a transformer which shut down the entire system. The damage was promptly repaired the following business day.

- **February 8, 2022, 10:00 to February 18, 2022, 15:00.** FPL modified the piping configuration at the DIW to allow for more accurate flow measurements at the totalizer and replace corroded production well piping.

- **March 14, 2022, 9:00 to March 17, 2022, 13:00.** A permit required, five-year DIW integrity test.

- **May 15, 2022, 4:00 to May 20, 2022, 14:00.** The whole system was turned off to reduce electrical noise during the CSEM survey.

The system was also turned off on partial days for the following:

- Additional SCADA refinements to optimize flow so that the monthly total extractions are being met and to help ensure that the system does not stop when two or more wells are offline.

- Short-duration maintenance events.

In addition to systemwide RWS outages, individual extraction wells shut down for various reasons including repairs, refurbishment, calibration tests, or preventive maintenance. In these cases, the SCADA system immediately adjusts pumping of the remaining operational wells to continue authorized system total withdrawal rates. Preventive maintenance measures, which are necessary for effective long-term operation of the system, included replacing ductal iron wellhead components and electronic operational components that reach the end of their projected operational life and periodically pulling pumps and motors for rehabilitation based on manufacture's recommendations. Operational run times for each of the RWS wells are shown graphically on Figure 2.1-1.
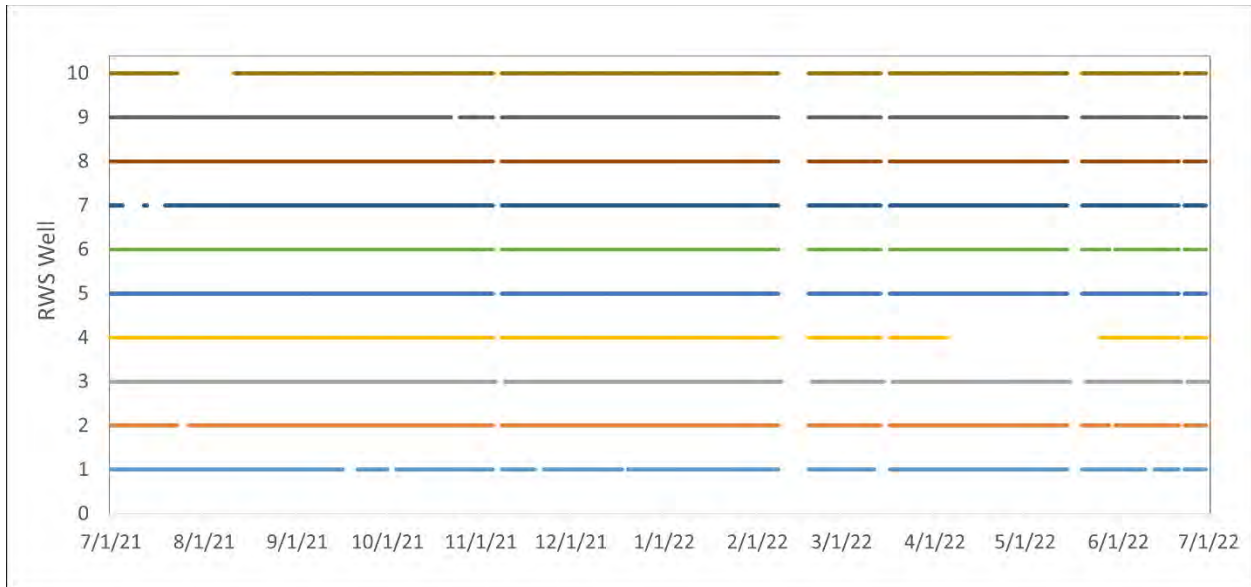
Figure 2.1-1.   Operation of RWS in Year 4 (Pumping with More than 4 Hours of Daily Flow)

2.2   RECOVERY WELL SYSTEM MONITORING RESULTS AND HYPERSALINE GROUNDWATER/SALT MASS REMOVED

During the reporting period, FPL's groundwater remediation actions removed approximately 6.18 billion gallons of groundwater with an average chloride concentration of approximately 27,000 mg/L that contained 2.37 billion pounds of salt. Since inception of the remediation system, approximately 23.43 billion gallons of groundwater with an average chloride concentration of 27,800 mg/L and 9.24 billion pounds of salt have been extracted from the Biscayne aquifer.

Automated flow, salinity, total dissolved solids (TDS), and water elevation data were continuously recorded from each RWS extraction well. Water quality samples were collected from each RWS well monthly and were analyzed for chloride along with field parameters. Pursuant to execution of CA Amendment 2 on August 20, 2019, quarterly sampling of RWS nutrients was implemented in September 2019. All sampling/monitoring was conducted in accordance with the SFWMD-approved FPL Quality Assurance Project Plan (QAPP) (FPL 2013). Water quality data referenced in this RAASR are available in Microsoft Excel tables on the FPL Turkey Point Electronic Data Monitoring System (EDMS) database (https://www.ptn-combined-monitoring.com).

Automated data for all 10 RWS wells and the two UICPW wells are shown in Appendix B. Analytic data are shown in Appendix C, including the field parameters and additional analytes (i.e., nutrients), field sampling logs, data qualifiers, and quality assurance samples. Data usability summary (DUS) reports for the events are provided in Appendix D. Level 4 laboratory reports from the FPL Central Laboratory can be found on FPL's EDMS at https://www.ptn-combined-monitoring.com.

Table 2.2-1 shows a summary of the chloride values for all recovery wells. Chloride values in most of the wells reflect hypersaline conditions, ranging between 21,700 mg/L and 32,400 mg/L in Year 4. The only exception was RWS-1 where all monthly chloride concentrations were less than 19,000 mg/L and ranged between 15,300 mg/L and 18,400 mg/L (Figure 2.2-1). RWS-1 started to frequently have chloride concentrations less than 19,000 mg/L in July 2019.

Table 2.2-1.   RWS Chloride Monitoring Results (mg/L)

Sample ID	2021						2022						Average	
	July	Aug	Sept	Oct	Nov	Dec	Jan	Feb	Mar	Apr	May	June	Current Reporting Period (7/1/21-6/30/22)	Previous Year (7/1/20-6/30/21)
RWS-1	15300	17000	16200	18100	18000	17200	17000	18400	17500	16200	15900	16400	16933	18042
RWS-2	22900	21700	23800	25000	24800	25100	24300	23800	24400	24400	23300	23700	23933	24775
RWS-3	24900	27900	26600	26900	27200	27600	27600	27400	26000	26500	25100	26900	26717	27150
RWS-4	27000	30700	30200	29800	30300	30500	30200	30600	29000	NA	28900	29500	29700	29567
RWS-5	26600	30400	30200	29800	30700	30700	30000	29700	29100	29700	27300	28700	29408	29275
RWS-6	26200	29600	28800	28900	30000	29500	28500	29100	28100	28400	27600	28400	28592	28717
RWS-7	25300	28400	28800	28600	29800	29400	28300	28900	27200	28500	27300	27300	28150	28492
RWS-8	26800	29700	29900	29600	30700	30300	30200	30400	29200	29800	28200	29000	29483	29608
RWS-9	26100	29200	28400	28800	29700	29500	28600	28900	27600	29100	27100	28900	28492	28442
RWS-10	23300	26700	25600	25800	27000	26300	26100	25700	25300	25600	24100	24900	25533	25658
UICPW-1	NA	30400	NA	30700	NA	NA	NA	NA	28100	NA	30400	28000	29520	30817
UICPW-2	28900	NA	32400	NA	30800	30300	29200	29200	NA	29100	28500	NA	29800	30320

Key:

NA = not available/no pumping.
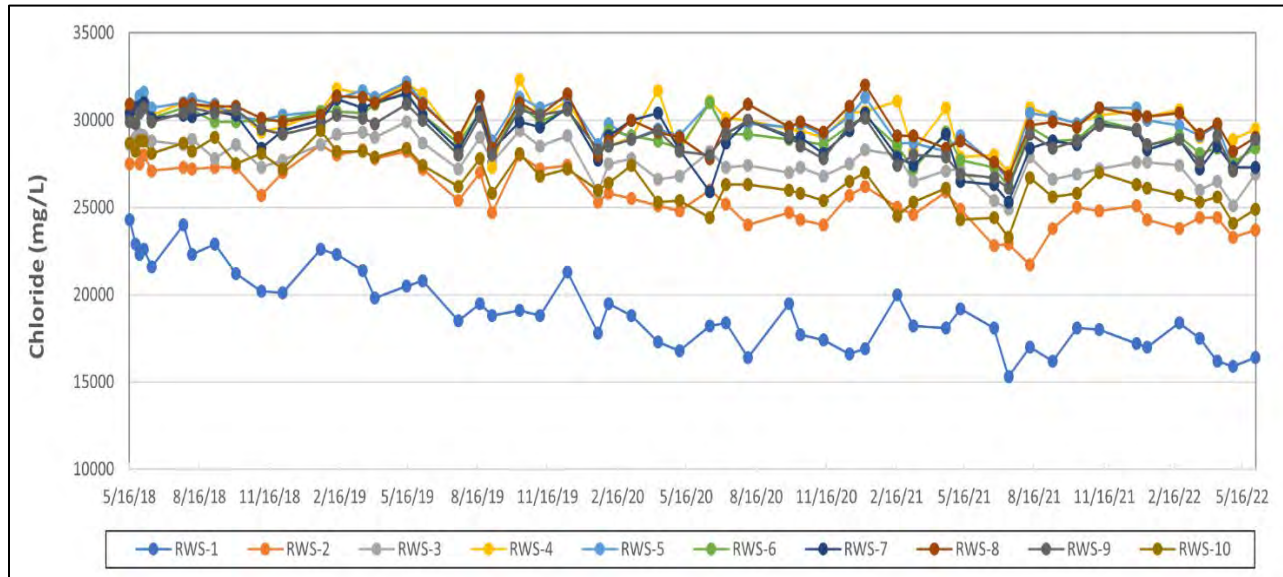
Figure 2.2-1.   RWS Chloride Results (mg/L)

While Mann-Kendall trend analysis conducted on each extraction well for the reporting period shows no trends in chloride, longer-term statistically significant gradual declines in chloride concentrations remain in all the RWS wells using the monthly data from May 2018 through June 2022.

This gradual reduction in salinity of the RWS wells was documented in early modeling of the RWS (Tetra Tech 2016a). The design of the remediation system considers the fluid density of the plume, which is why the extraction wells are open to the base of the aquifer (i.e., dense hypersaline groundwater will naturally "sink" toward extraction points along the base of the aquifer). Accordingly, it is expected that the salinity levels of the extracted water from the RWS wells will remain elevated for an initial period while the thickness of the plume diminishes. As the vertical and lateral extent of the hypersaline plume diminishes over long-term operation of the RWS, larger portions of lower-salinity groundwater from above the extraction horizon mix with hypersaline water moving laterally along the base of the aquifer, resulting in a gradual lowering of the extracted water salinity.

The majority of changes since start-up are modest with both chloride and salinity reductions ranging between 4% and 10%. However, RWS-1, has exhibited greater reduction since the first year of operation as both average chloride and salinity values are now approximately 25% lower than at inception. RWS-1 is located approximately 0.8 mile north of the CCS where the plume is thinner, and CSEM data shows that the plume has diminished significantly in this area since remediation began in 2018. Changes to current pumping operations may be considered when an RWS well produces saline water that is consistently below 19,000 mg/L chloride and when data indicate that CCS hypersaline groundwater within the capture radius of the RWS production well has been sufficiently remediated.

Time Period	Volume (billion gallons)	Salt (billion lbs)
July 1, 2021 - June 30, 2022	6.18	2.37
May 15, 2018 - June 30, 2022	23.43	9.24

Values shown are for total water and salt mass extracted each reporting period and total since startup through June 2022.

Table B.1-1 in Appendix B shows the weekly volume of groundwater pumped from each recovery well. From July 1, 2021, to June 30, 2022, approximately 5.04 billion gallons of water were extracted from the RWS and disposed of via the DIW. This equates to utilizing 92% of the allowed withdrawal of 5,475 million gallons per the Consumptive Use Permit. An additional 1.14 billion gallons of hypersaline groundwater were extracted in Year 4 from the UICPW wells in the middle of the CCS (Table B.2-1), for a total of 6.18 billion gallons of hypersaline groundwater removed from the Biscayne aquifer from July 1, 2021, to June 30, 2022. Since the start-up of the RWS in May 2018, 23.43 billion gallons of hypersaline groundwater have been removed.

Table B.1-1 of Appendix B also shows the automated weekly TDS values and the associated amount of salt mass removed on a weekly basis for each recovery well, which is calculated in accordance with paragraph 29.f of the FDEP CO. Salinity data is provided alongside the TDS values for reference purposes because most people are familiar with salinity. The salt mass values were based on automated flow and TDS data, and the values were then summed for daily and weekly salt mass removal. The TDS value is calculated from specific conductance using a preprogrammed conversion factor of 0.64 (based on empirical data from monitoring wells TPGW-11D and TPGW-13D from 2010–2016). The equation for salt mass removal is as follows:

$$\text{Salt mass removed (lbs/day)} = \frac{\text{Flow}\left(\frac{\text{gallons}}{\text{min}}\right) \text{ x TDS}\left(\frac{\text{g}}{\text{L}}\right) \text{ x 1,000}\left(\frac{\text{mg}}{\text{g}}\right) \text{ x 3.7854}\left(\frac{\text{liters}}{\text{gallon}}\right)}{453,592.37\left(\frac{\text{mg}}{\text{lbs}}\right)} \; x \; 1,440\left(\frac{min}{day}\right)$$

The total amount of salt mass removed varies since the pumping rates, run time, salinity, and TDS differ among wells and/or over time. In Year 4, approximately 1.91 billion pounds of salt was removed from the RWS wells (Table B.1-1) and 0.46 billion pounds for UICPW-1 and UICPW-2 (Table B.2-1), resulting in 2.37 billion pounds removed in the reporting year. Combined with salt mass removed in previous reporting periods, 9.24 billion pounds of salt have been removed from the Biscayne aquifer from May 15, 2018, to June 30, 2022.

2.3　RECOVERY WELL SYSTEM DRAWDOWN ASSESSMENT

> Water table drawdown from RWS operations continue to be negligible (less than 0.10 ft) in Year 4, consistent with previous observations when RWS pumping is occurring.

In the 2019 RAASR (FPL 2019c), FPL determined that the drawdown solely from RWS pumping was approximately 0.11 ft, and the combined drawdown with the RWS and ID was approximately 0.25 ft at TPGW-15S, which is located approximately 710 ft from RWS-3 and just west of the ID. The drawdown in the other depth intervals and at TPGW-1 was of similar magnitude. This amount of drawdown in the shallow portion of the Biscayne aquifer is considered negligible; i.e., it is not considered harmful to wetlands or water resources. The SFWMD regulates drawdown impacts to wetlands and water resources. SFWMD water use rule criteria limit cumulative drawdowns beneath seasonally inundated wetlands to 1 ft during 1-in-10-year drought conditions and maximum authorized withdrawals (SFWMD 2015). Drawdowns that exceed this threshold are considered harmful to wetlands and water resources. Based on the measured drawdowns of the combined impacts of the RWS and ID operations, the combined withdrawals are negligible.

Subsequently, in the Year 2 assessment presented in the 2020 Part 1 RAASR (FPL 2020a), FPL confirmed the above findings of negligible drawdown of 0.10 ft at TPGW-1S and TPGW-15S from solely RWS operations as there was no time during the reporting period when the RWS was turned off and the ID pumps were operating.

For Year 3 of operation, and similar to the previous years, several periods were selected when the RWS wells near TPGW-1 and TPGW-15 were turned off to allow the groundwater to stabilize when there was little to no rainfall (several tenths of an inch) that could mask drawdown. The results supported previous findings of a combined drawdown of approximately 0.25 ft at TPGW-1S and TPGW-15S when RWS and ID pumps are both operational (FPL 2021b).

In Year 4, there was one short period of three days when the RWS pumps near TPGW-1 and TPGW-15 were off and rainfall totals were less than several tenths of an inch (March 14 to March 17, 2022). The results show changes in groundwater levels in TPGW-1 and TPGW-15 of less than 0.10 ft when the RWS wells are turned off and on. Additionally, a review of water levels in TPGW-2 on the same dates of March 14 to March 17 when the entire system was shut down, indicated changes only in the hundredths of a foot in response to RWS operation. There were no times during the reporting period when the RWS was turned off and the ID pumps were operating. ID pumping was triggered only four times (seven days in total) during this reporting year (FPL 2022), which limited the opportunity to assess the combined drawdown effect of ID and RWS operations when both systems were turned off and on. However, since drawdown of water levels in TPGW-1 and TPGW-15 during limited ID operation in April 2022 ranged from 0.10 to 0.20 ft, it is still reasonable to conclude the combined influence of RWS and ID pumping on water levels at TPGW-1 and TPGW-15 is still approximately 0.25 ft.

The impacts of the RWS operations on L-31E stage levels continue to be indiscernible (in the hundredths of a foot) when the pumps are turned on and off. Changes in water levels at nearby L-31E surface water canal sites TPSWC-1, TPSWC-2, and TPSWC-3 are within the range of normal fluctuations due to typical minor meteorological influences (e.g., wind), and do not appear to be a result of RWS operations.

2.4 INTERCEPTOR DITCH OPERATIONS

FPL has reviewed ID operations in conjunction with RWS operations on multiple occasions in accordance with paragraph 17.a.iii of the CA. FPL has presented these findings at various times, including in a meeting with DERM on May 16, 2016, in a letter to DERM dated May 23, 2016, in a presentation to DERM, FDEP, and SFWMD on May 19, 2017, in the RWS Start-Up Report (FPL 2018a), subsequent quarterly status reports (FPL 2018b, FPL 2019a, FPL 2019b), as well as in FPL's Annual Monitoring Reports (FPL 2012, FPL 2016, FPL 2017, FPL 2018c, FPL 2019d, FPL 2020b, FPL 2021c, FPL 2022). Based on these evaluations, modifications to improve the ID function are not warranted at this time due to the following:

- Continued effectiveness of the ID in restricting westward migration of CCS groundwater into the upper portion of the Biscayne aquifer, into wetlands west of the CCS, and into the L-31E canal.

- Continued effectiveness in maintaining the freshwater lens thickness in the Biscayne aquifer west of the CCS.

- Demonstrated lack of harmful impacts to groundwater levels, wetlands, and other water resources in the area as further described in the reports referenced above.

3 GROUNDWATER MONITORING DATA

> Groundwater monitoring to assess RWS performance was conducted on 14 well clusters west and north of the CCS. Most wells have a declining trend since the start of the RWS and many of them show the lowest value on record. The largest reductions thus far have been in the shallow wells while the intermediate and deep well declines have been more gradual. The monitoring well results combined with the area wide CSEM survey and modeling results, provide a robust assessment of changes that are analyzed across the entire landscape west and north of the CCS.

3.1 GROUNDWATER MONITORING

Groundwater monitoring for the assessment of the RWS was performed on well clusters TPGW-1, TPGW-2, TPGW-4, TPGW-5, TPGW-12, TPGW-15, TPGW-17, TPGW-18, TPGW-19, and TPGW-22 and on historical individual wells TPGW-L3, TPGW-L5, TPGW-G21, and TPGW-G28, with samples collected for laboratory analysis in September 2021, December 2021, March 2022, and June 2022 (Figure 3.1-1). With the exception of TPGW-22 included in the 2021 report, these wells are the same ones that were sampled as part of the March 2018 baseline and in Years 1, 2, and 3 RAASRs, with the chloride data used for correlation with CESM data (refer to Section 4) and assessing progress of the remediation. Monitoring sites TPGW-4, TGPW-5, TPGW-G21, and TPGW-G28 are located west of the hypersaline groundwater plume but are useful in the evaluation of the western extent to which RWS operations could influence groundwater salinity. The monitoring horizons for the 3-cluster wells at site TPGW-22 were established by MDC in 2020 independent of the criteria used by FPL to determine the elevations of the three regional high flow zones for the other FPL monitoring wells. Accordingly, the monitoring horizons at this site, particularly the deep monitoring interval, may not be fully comparable with the zones established with the other wells currently in the network. Data from the TPGW-22 monitoring site has been collected since February 16, 2021.

Samples for all events were collected at discrete screen intervals from the well clusters (i.e., shallow, intermediate, and deep intervals), except for the historic L- and G-series, which are continuously screened wells where samples were collected at 18 ft and 58 ft below the top of casing unless noted otherwise. Samples from the groundwater clusters were collected using dedicated tubing and per the methods outlined in the QAPP (FPL 2013) and FDEP Standard Operating Procedures. To aid in the assessment of the RWS, field parameters (i.e., temperature, specific conductance, salinity, density) were measured, and samples from each of the monitoring wells were sent for laboratory analysis of TDS, chloride, and tritium.

In most instances, the data show that the monitoring wells that were or still are hypersaline have lower values this reporting period compared to the baseline values in March 2018. A summary of the Year 4 quarterly chloride and tritium results is included in Tables 3.1-1 and 3.1-2, respectively, along with baseline results for comparison. These results help gauge the progress of remediation, and the chloride data support the calibration of CSEM survey and groundwater modeling updates. Time-series graphs showing quarterly chloride and tritium data from March 2018 (baseline) through June 2022 (end of Year 4 reporting period) are provided in Appendix E and show the extent of change since RWS start-up in well clusters where one or more depths have hypersaline groundwater and historic L–series wells with hypersaline groundwater. Note that in the first year of monitoring, chloride samples were collected weekly for the first month of operation and monthly for the first quarter; data were presented in the 2019 RAASR (FPL 2019c). Chloride trend analyses conducted on monitoring data collected since RWS start-up were based on quarterly data (i.e., early weekly and monthly values were not included) to avoid sample frequency biases.

In addition to analytical data, all the monitoring wells, except TPGW-L3, TPGW-L5, TPGW-G21, and TPGW-G28, are equipped with automated probes that record specific conductance, salinity, and water levels at 1-hour intervals. With the exception of recently installed site TPGW-22, automated data have been recorded since at least April 2018, with several well clusters (TPGW-1, TPGW-2, and TPGW-12) having data that extends back to 2010. For TPGW-22, automated probes were deployed in February 2021. Appendix E shows time-series of average weekly salinity graphs of select wells from the start of RWS monitoring where the entire well cluster at one or more depths have hypersaline groundwater.

Nearly all the analytical and automated data for Year 4 meet the data quality objectives of the QAPP (FPL 2013). Aside from a few sample results, all analytical monitoring well data are usable and exceed the QAPP completeness goal of 90%. Collectively, automated monitoring well water quality data and water level data are over 98% complete in Year 4. Nearly all parameters (i.e., specific conductance, salinity, temperature, and water elevations) in each well are over 90% complete, with the most notable exceptions being water elevations at wells TPGW-22S, TPGW-22M, and TPGW-22D. This well cluster (TPGW-22) had issues, mostly with obtaining valid automated water elevation readings in the first half of the reporting period. There also appears to be stratification that reoccurs in wells TPGW-22S and TPGW-22M where the density of water in the casing may be lower than the density of the water at the screened interval. This can result in water elevation readings that, while accurate, may not fully represent freshwater head equivalents if they were to be calculated.
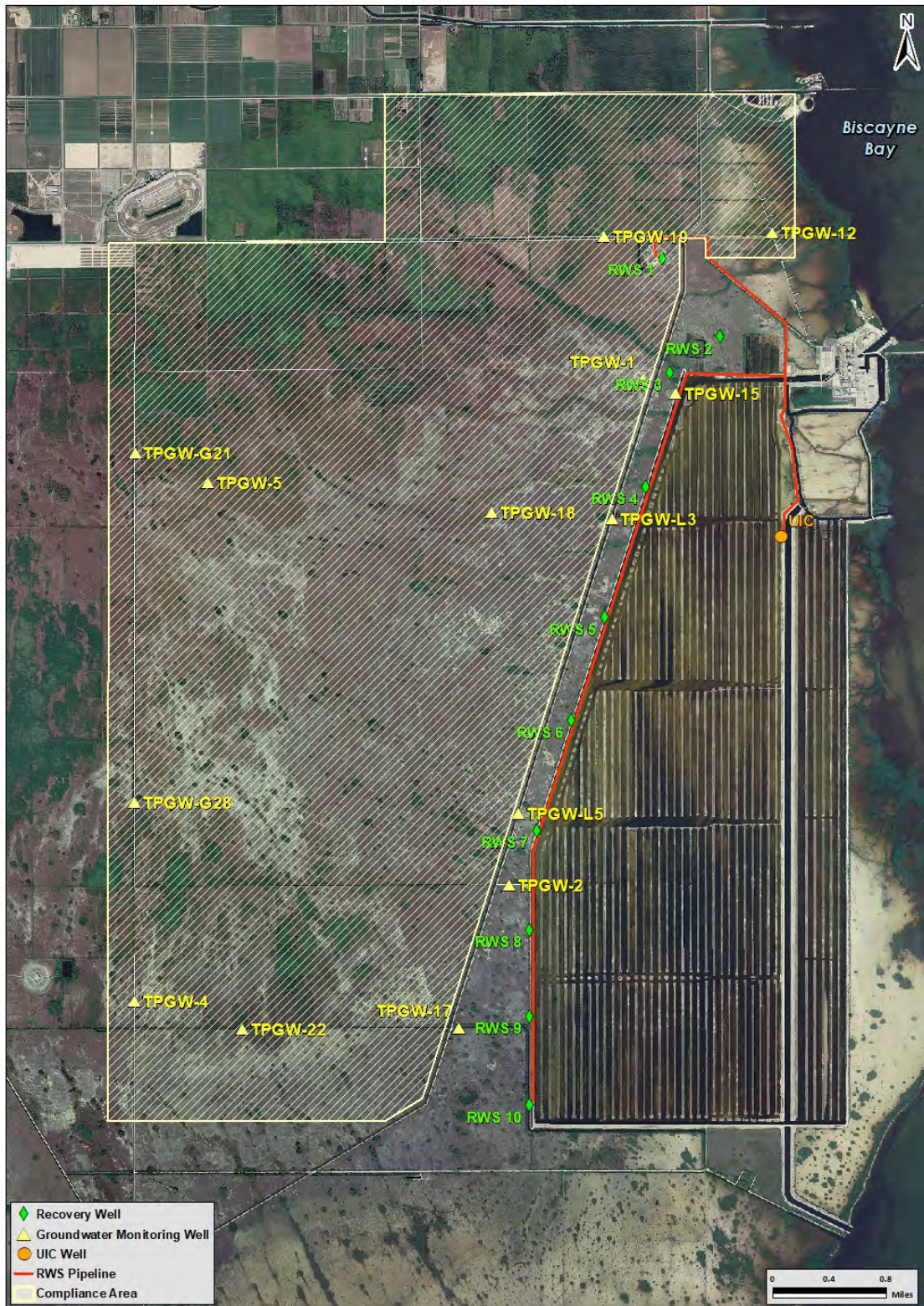
Figure 3.1-1.   RWS and Monitoring Wells West and North of the CCS Used in the Assessment of the RWS

Table 3.1-1.   Monitoring Well Baseline and Year 4 Quarterly (Sept 2021 to June 2022) Chloride Concentration Data

Date	Baseline Chloride (mg/L)	Year 4 Chloride (mg/L)			
	03/2018	9/2021	12/2021	03/2022	06/2022
TPGW-1S	19400	5850	5300	5110	9650
TPGW-1M	27700	25100	25300	24300	23700
TPGW-1D	28500	28000	28700	27800	26700
TPGW-2S	24800	16700	16700	15900	15300
TPGW-2M	29500	29800	30000	28900	28500
TPGW-2D	31300	30800	30300	29500	29000
TPGW-4S	2280	1930	1190	2320	2520
TPGW-4M	15100	15900	15200	14700	14300
TPGW-4D	14800	16400	16100	15700	14700
TPGW-5S	164	153	183	125	138
TPGW-5M	11700	10800	10600	10400	9540
TPGW-5D	13100	14000	13300	13100	12600
TPGW-12S	16500	19300	18900	17700	18400
TPGW-12M	20900	22300	20800	21300	19900
TPGW-12D	24000	26700	26100	26400	24700
TPGW-15S	20100	4970	2710	9850	12800
TPGW-15M	30000	27300	28300	26300	25700
TPGW-15D	28800	29700	31100	28800	27600
TPGW-17S	24900	21400	22100	21400	20300
TPGW-17M	29300	26900	26200	26500	24400
TPGW-17D	28600	28000	28200	27100	26500
TPGW-18S	14200	2810	2610	2590	2230
TPGW-18M	25200	23500	22500	22200	19600
TPGW-18D	26400	23900	23200	22900	22000
TPGW-19S	1830	1350	1030	794	1160
TPGW-19M	26000	20800	20200	19700	19200
TPGW-19D	26800	24600	23600	23400	22800
TPGW-22S	NA	16600	16200	15400	14900
TPGW-22M	NA	22800	21900	21100	20900
TPGW-22D	NA	22400	21900	21000	20400
TPGW-L3-18	2030	142	346	137	124

	Baseline Chloride (mg/L)	Year 4 Chloride (mg/L)			
Date	**03/2018**	**9/2021**	**12/2021**	**03/2022**	**06/2022**
TPGW-L3-58	31400	31700	31600	29700	31500
TPGW-L5-18	1290	87.7	80.4	136	79.5
TPGW-L5-58	29500	30300	29800	27400	28700
TPGW-G21-18	49.2	37.7	29.1	44.0	46.6
TPGW-G21-58	7210	7600	7370	7200	7160
TPGW-G28-18	693	436	573	408	414
TPGW-G28-58	14200	16300	15300	14000	14300

Notes:

1. Laboratory results are reported with 3 digits although only the first 2 are significant figures.

2. Sample at TPGW-L5-18 in December 2021 collected approximately 5 ft deeper.

3. Wells with cells highlighted in tan have or have had chloride concentrations above 19.000 mg/L (hypersaline) and blue highlighted text indicates well has transitioned from hypersaline to saline.

Key:

NA = not available. TPGW-22 was added to the CA sampling requirements in March 2021.

Table 3.1-2.　Monitoring Well Baseline and Year 4 Quarterly (Sept 2021 to June 2022) Tritium Concentration Data

Date	Baseline Tritium (pCi/L)	Year 4 Tritium (pCi/L)			
	03/2018	**9/2021**	**12/2021**	**03/2022**	**06/2022**
TPGW-1S	954	139	107	67.6	293
TPGW-1M	2173	2415	2158	2076	2002
TPGW-1D	2307	1887	1847	1784	1924
TPGW-2S	2166	962	1079	1066	1060
TPGW-2M	3130	2486	2694	2768	3074
TPGW-2D	3123	2472	2545	2558	2594
TPGW-4S	17.4	22.1	2.3	15.5	6.9
TPGW-4M	342	314	274	310	288
TPGW-4D	403	357	341	361	358
TPGW-5S	10.9	17.0	3.7	20.4	13.0
TPGW-5M	271	180	190	187	163
TPGW-5D	362	301	303	342	302
TPGW-12S	46.4	95.2	39.7	43.5	30.5

Date	Baseline Tritium (pCi/L)	Year 4 Tritium (pCi/L)			
	03/2018	9/2021	12/2021	03/2022	06/2022
TPGW-12M	931	424	304	254	221
TPGW-12D	1344	1110	1047	1044	1031
TPGW-15S	1555	116	78.4	306	1562
TPGW-15M	2605	4049	4635	4941	5288
TPGW-15D	2509	3066	3367	2927	3315
TPGW-17S	1482	634	717	676	638
TPGW-17M	2518	1429	1426	1357	1242
TPGW-17D	2272	1729	1751	1754	1800
TPGW-18S	550	25.3	17.1	2.3	17.1
TPGW-18M	1568	1189	1229	1214	1234
TPGW-18D	1600	1252	1233	1175	1205
TPGW-19S	42.9	79.0	46.7	27.6	40.1
TPGW-19M	864	494	521	481	486
TPGW-19D	1082	857	885	848	846
TPGW-22S	NA	382	354	342	307
TPGW-22M	NA	612	597	638	645
TPGW-22D	NA	818	792	860	839
TPGW-L3-18	108	61.2	65.3	98.7	29.2
TPGW-L3-58	3014	4358	4661	4441	5109
TPGW-L5-18	86.7	42.6	96.1	68.5	10.6
TPGW-L5-58	2640	1995	1927	1730	2015
TPGW-G21-18	8.5	-8.8	23.0	16.2	7.4
TPGW-G21-58	40.0	50.6	58.1	54.9	38.2
TPGW-G28-18	7.3	20.4	8.5	5.8	0.9
TPGW-G28-58	333	322	280	313	316

Notes:
1. Sample at TPGW-L5-18 in December 2021 collected approximately 5 ft deeper.
2. Wells with cells highlighted in tan have or have had chloride concentrations above 19.000 mg/L (hypersaline) and blue highlighted text indicates well has transitioned from hypersaline to saline.
Key:
NA = not available. TPGW-22 was added to the CA sampling requirements in March 2021.

3.2 YEAR 4 WATER QUALITY CONDITIONS AND TRENDS

> A multi-factored objective data assessment was used to identify meaningful changes in groundwater quality associated with the ongoing groundwater remediation. The assessment identified that 21 of the 26 RWS monitoring wells exhibited statistically significant declining trends in either chlorides, salinity, and/or tritium since remediation began in May 2018. Changes in shallow, middle, and deep wells indicate positive progress in meeting the objectives of the CA and CO.

To assess trends and influence of RWS operations, a multifactor data screening process was applied to analytical and automated groundwater monitoring data. This included comparing Year 4 data against periods of record low values and conducting objective statistical trend analyses (i.e., linear regression and Mann-Kendall trend) for chloride, tritium, and salinity. Assessments for tritium help confirm chloride and salinity trends and can be a potential precursor to declining chloride and salinity trends as lower tritium may indicate a reduction in CCS-sourced water. Regression analyses were conducted using Statistix v. 10 (Analytical Software Inc., Tallahassee, Florida), while Mann-Kendall analyses were conducted with XLStat (Addinsoft Inc., Paris, France). Additional information and graphical plots for both sets of analyses are included in Appendix E.

Wells used in these analyses were located west and north of the CCS where one or more of the depths had hypersaline groundwater. This includes all the wells in well cluster TPGW-1, TPGW-2, TPGW-12, TPGW-15, TPGW-17, TPGW-18, TPGW-19, and TPGW-22 in addition to non-automated stations TPGW-L3-58 and TPGW-L5-58 for a total of 24 wells with automated data and 26 wells with analytical data. TPGW-22 has hypersaline groundwater in two of the wells, but since it has a relatively short period (6 quarters) of analytical data available, comparisons of data values to the period of record at this time is premature. However, TPGW-22S, TPGW-22M and TPGW-22D are included in the automated weekly Mann-Kendall salinity and regression analyses. There are 4 wells in this group (TPGW-12S, TPGW-18S, TPGW-19S and TPGW-22S) that were never hypersaline during the historical period of monitoring, leaving a total of 22 hypersaline monitoring wells. Three of the 22 wells have since transitioned during RWS operations from hypersaline to saline. Table 3.2-1 and Figure 3.2-1 provide a summary of this assessment which include the following findings:

- The weekly average salinity during this reporting period was less than the historical period of record (comprising the start of data collection through June 2021) and the RWS operational period (March 2018 through June 2021) for 9 (3 shallow, 4 intermediate, and 2 deep depth) out of 21 wells with automated probes. Of the current hypersaline monitoring wells with automated salinity data, 7 recorded the lowest weekly value for the period of record during this reporting period.

- One or more chloride concentrations for the reporting period were less than the historical period of record and the prior RWS operational period in 9 (4 shallow and 5 intermediate depth) out of 23 wells. Of the current hypersaline monitoring wells with 2 or more years

of quarterly chloride data, 5 have the lowest quarterly chloride concentration this reporting period.

- One or more tritium concentrations for the reporting period were less than the historical period of record and the prior RWS operational period in 11 (3 shallow, 5 intermediate, and 3 deep depth) out of 23 wells. Of the current hypersaline monitoring wells with 2 or more years of quarterly tritium data, 8 have the lowest quarterly tritium concentration this reporting period.

The Mann-Kendall trend analysis and linear regression analysis for automated salinity using weekly average values from March 2018 through June 2022, and a similar analysis for chloride and tritium using quarterly sampling results showed the following:

- 17 wells had a declining trend for weekly salinity out of 24 wells with automated data, including TPGW-22 wells (automated data are not collected from TPGW-L3 and L5) based on Mann-Kendall analysis and 18 wells based on regression analysis. Of the current hypersaline monitoring wells with automated salinity data (17 wells total), 12 have a declining trend based on Mann-Kendall analysis and 13 wells based on linear regression analysis.

- 13 wells had a declining trend for chloride out of 23 wells (excluding the three TPGW-22 wells due to the short period of quarterly monitoring data) based on Mann-Kendall analysis and 14 wells based on regression analysis. Of the current hypersaline monitoring wells with 2 or more years of quarterly chloride data (17 wells total), 9 have a declining trend based on Mann-Kendall analysis and 10 based on linear regression analysis.

- 17 wells had a declining trend for tritium (one less well this reporting period) out of 23 wells based on Mann-Kendall analysis and 16 wells based on regression analysis. Of the current hypersaline monitoring wells with 2 or more years of quarterly tritium data (17 wells total), 13 have a declining trend based on Mann-Kendall analysis and 12 based on linear regression analysis.

In total, 21 of the 26 RWS monitoring wells exhibited statistically significant declining trends in either chlorides, salinity, and/or tritium since remediation began in May 2018.
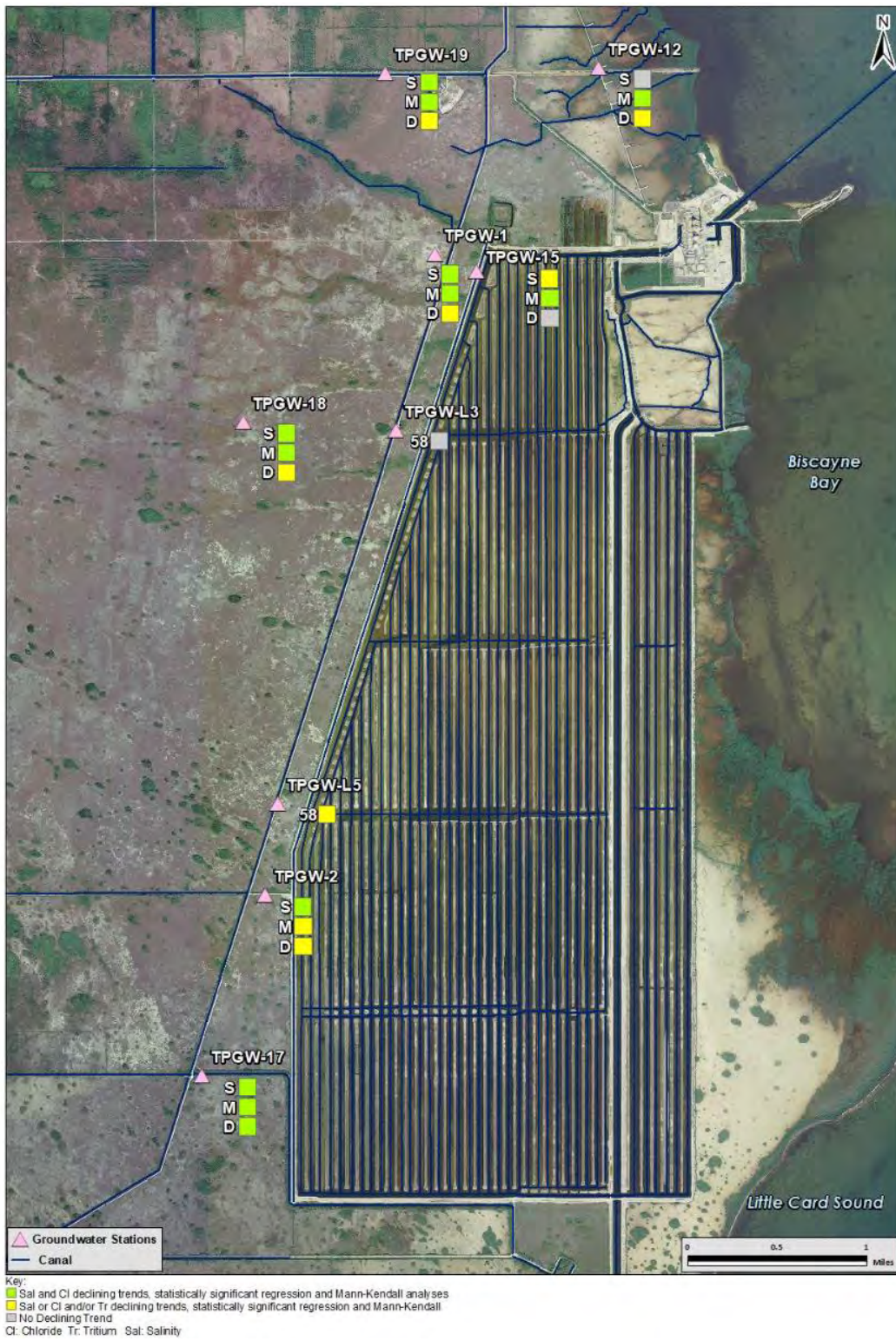
Figure 3.2-1. Summary of Monitoring Well Influences in Year 4 RWS Operations

Table 3.2-1. Summary of Monitoring Well Influences from RWS Operations in Year 4

Assessment:	Analytical Quarterly Chloride Data				Analytical Quarterly Tritium Data				Automated Salinity Data[2]			
	Period of Record low in Year 4?	Year 4 minimum < Year 1, 2, 3 & baseline minimum chloride?	Statistically significant declining linear regression?	Mann-Kendall chloride trend	Period of Record low in Year 4?	Year 3 minimum < Year 1, 2 & baseline minimum tritium?	Statistically significant declining linear regression?	Mann-Kendall tritium trend	Period of Record low in Year 4?	Year 4 minimum < Year 1, 2, 3 & baseline minimum weekly salinity?	Statistically significant declining linear regression?	Mann-Kendall average weekly automated salinity trend
Period of Review:	Start[1] – June 30, 2022	July 2021 – June 2022 vs. March 2018 – June 2021	March 1, 2018 – June 30, 2022	March 1, 2018 – June 30, 2022	Start[1] – June 30, 2022	July 2021 – June 2022 vs. March 2018 – June 2021	March 1, 2018 – June 30, 2022	March 1, 2018 – June 30, 2022	Weekly Average Start[1] to June 30, 2022	July 2021 – June 2022 vs. March 2018 – June 2021	March 1, 2018 – June 30, 2022	March 1, 2018 – June 30, 2022
TPGW-1S	Yes	Yes	Yes	Decrease	Yes	Yes	Yes	Decrease	Yes	Yes	Yes	Decrease
TPGW-1M	Yes	Yes	Yes	Decrease	No	No	No	No Trend	Yes	Yes	Yes	Decrease
TPGW-1D	No	No	No	No trend	No	No	Yes	Decrease	No	No	Yes	Decrease
TPGW-2S	Yes	Yes	Yes	Decrease	Yes	Yes	Yes	Decrease	Yes	Yes	Yes	Decrease
TPGW-2M	No	No	No	No trend	No	No	No	Decrease	No	No	No	No Trend
TPGW-2D	No	No	Yes	No trend	No	No	Yes	Decrease	No	No	No	Decrease
TPGW-12S	No	No	No	Increase	No	No	No	No Trend	No	No	No	No Trend
TPGW-12M	Yes	Yes	Yes	Decrease	Yes	Yes	Yes	Decrease	No	No	Yes	Decrease
TPGW-12D	No	No	No	No trend	Yes	Yes	Yes	Decrease	No	No	Yes	Decrease
TPGW-15S	Yes	Yes	No	No trend	Yes	Yes	No	No Trend	No	No	Yes	Decrease
TPGW-15M	No	No	Yes	Decrease	No	No	No	Increase	No	No	Yes	Decrease
TPGW-15D	No	No	No	No trend	No	No	No	Increase	No	No	No	Increase
TPGW-17S	No	No	Yes	Decrease	No	No	Yes	Decrease	No	No	Yes	Decrease
TPGW-17M	Yes	Yes	Yes	Decrease	Yes	Yes	Yes	Decrease	Yes	Yes	Yes	Decrease
TPGW-17D	No	No	Yes	Decrease	Yes	Yes	Yes	Decrease	No	No	Yes	Decrease
TPGW-18S	Yes	Yes	Yes	Decrease	No	No	Yes	Decrease	Yes	Yes	Yes	Decrease
TPGW-18M	Yes	Yes	Yes	Decrease	Yes	Yes	Yes	Decrease	Yes	Yes	Yes	Decrease
TPGW-18D	No	No	Yes	Decrease	Yes	Yes	Yes	Decrease	Yes	Yes	No	No Trend
TPGW-19S	No	No	Yes	Decrease	No	No	Yes	Decrease	No	No	Yes	Decrease
TPGW-19M	Yes	Yes	Yes	Decrease	Yes	Yes	Yes	Decrease	Yes	Yes	Yes	Decrease
TPGW-19D	No	No	No	No trend	No	No	Yes	Decrease	Yes	Yes	Yes	Decrease
TPGW-22S	-	-	-	-	-	-	-	-	-	-	No	Increase
TPGW-22M	-	-	-	-	-	-	-	-	-	-	No	Increase
TPGW-22D	-	-	-	-	-	-	-	-	-	-	Yes	No Trend
TPGW-L3-58	No	No	No	No trend	No	No	No	Increase	-	-	-	-
TPGW-L5-58	No	No	No	No trend	Yes	Yes	Yes	Decrease	-	-	-	-

NOTES:
TPGW-22 came online in February 16, 2021 so limited data for comparative and trend analysis.
Wells with cells shaded in tan indicate station has had chloride values >19,000 mg/L.

Wells highlighted in blue have transitioned from hypersaline to saline in Year 1 or year 3 of RWS operation, and chloride concentrations have stayed below 19,000 mg/L.

Text highlighted in green are indications of postive RWS influence.

KEY:

[1] Startup period varies: TPGW-1 to -12 started reporting around mid-2010; TPGW-15 started to report in September 2015; TPGW-17 and -19 started on January 10, 2018. TPGW-18 came online April 15, 2018.

[2] Actual date ranges may vary by a few days based on the beginning and ending date of full week of data.

- No analysis for salinity since stations TPGW-L3 and TPGW-L5 do not have automated instrumentation. No analytical data comparisons or trend analysis at TPGW-22 to previous reporting periods due to short period of record or limited quarterly data.

The assessment in Table 3.2-1 includes multiple factors and time periods as some of the changes may be relatively small and within the range of laboratory or field reading accuracy. However, with sufficient and different types of data, trends can be ascertained. A single affirmative answer in Table 3.2-1 may not indicate significance, but a number of affirmative factors likely indicate that something positive is happening. Of those factors, linear regression analysis and the Mann-Kendall analysis represent powerful tools to objectively assess if the data, since the start-up of the RWS, is indicating a statistically significant trend.

> The fact that a majority of wells have a declining trend since the start of the RWS and a number of the wells, including intermediate and deep wells, continue to show lower chloride, salinity, and/or tritium concentrations each year, indicates positive progress in meeting the objectives of the CA and CO.

Further details related to changes in specific conductance, chloride, and tritium at select wells used to monitor the progress of remediation are discussed below. These findings are similar to observations in the 2022 annual monitoring report (FPL 2022) with minor differences due to slightly differing time periods (i.e., the 2022 Annual Report time period was June 2021 through May 2022 while the Year 4 RAASR time period was July 2021 through June 2022).

3.2.1   Shallow Wells

> While variable, there is a net decline of chloride in the shallow wells west of the RWS from March 2018 through May 2022. This coincides with automated probe-specific conductance reductions at those stations and are statistically significant per Mann-Kendall trend analyses and regression analyses.

The shallow zone in wells west of the CCS show the greatest amounts of saltwater constituent decline since the start of remediation (Figure 3.2-2). However, the rate of decline is decreasing in some wells as the salinity is much lower now, and conditions may be approaching a new salinity equilibrium range. Four shallow wells were hypersaline at the start of remediation (TPGW-1S, TPGW-2S, TPGW-15S and TPGW-17S), with only one well still hypersaline (TPGW-17S) this reporting year. The other shallow wells, including TPGW-12S, TPGW-18S, TPGW-19S and TPGW-22S, were never hypersaline; however, they are of interest as remediation progresses because they are in the compliance area and provide insights as to how remediation is affecting the shallow zone. The percent reduction of saltwater was most evident in TPGW-1S, TPGW-2S, and TPGW-15S as the average annual salinity values during the reporting period for these three wells (11.7 PSU, 27.3 PSU, and 13.0 PSU) were 65%, 42%, and 49% lower respectively, compared to the historic period of record (33.4 PSU, 47.3 PSU, and 25.4 PSU). These reductions were associated with RWS operations.
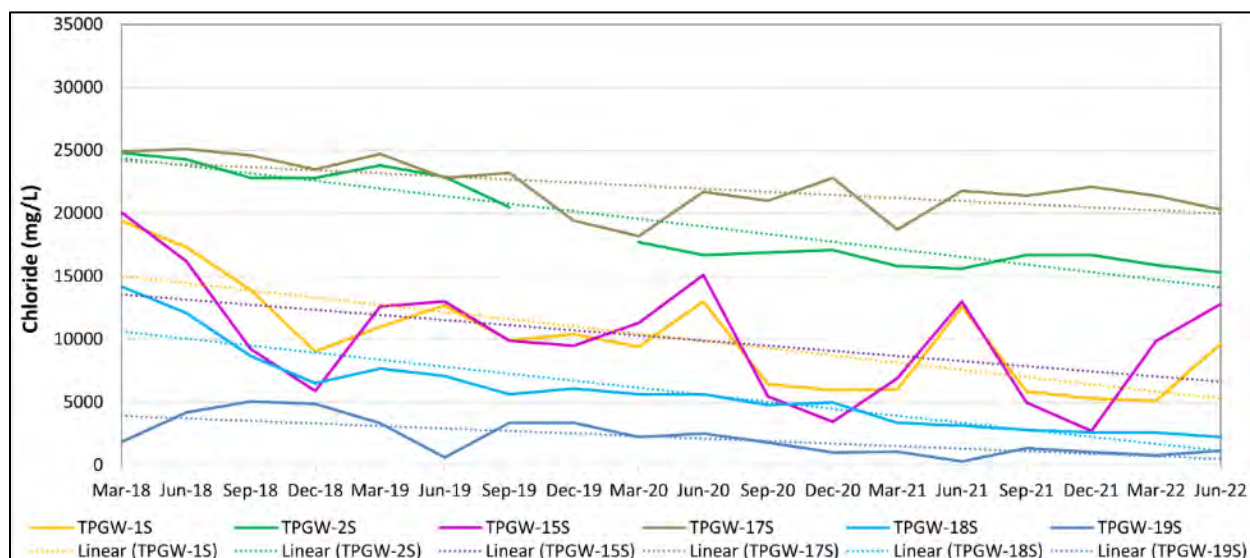
Note: TPGW-1S, TPGW-2S and TPGW-15S **have transitioned below 19,000 mg/L after RWS start-up and have remained below 19,000 mg/L through Year 4. (TPGW-22S is not shown due to limited data.)**

Figure 3.2-2. Reductions in Chloride Concentrations in Shallow Wells West of the CCS

Similarly, the average annual chloride concentrations for the reporting period at TPGW-1S, TPGW-2S, and TPGW-15S (6,478 mg/L, 16,150 mg/L, and 7,583 mg/L) were 60%, 37%, and 47% lower than the historic period of record (16,284 mg/L, 25,739 mg/L, and 14,401 mg/L), respectively. The average tritium concentrations this reporting period at TPGW-1S, TPGW-2S, and TPGW-15S (152 picocuries per liter [pCi/L], 1,042 pCi/L, and 516 pCi/L) are 82%, 60% and 52% lower than the historical period of record annual average (845 pCi/L, 2,596 pCi/L, and 1,068 pCi/L), respectively. Since significant reductions in saltwater constituents and tritium have already occurred, the rate of reduction is lower this year compared to previous years. In future years, it is anticipated that reductions in these three wells will generally be similar to or smaller than this reporting period and, in some years, will have slightly higher values reflective of variability in groundwater concentrations.

TPGW-17S, located near the southwest end of the CCS, is of interest since it is the only shallow well west of the CCS that is still hypersaline with the lowest value this period reported at 20,200 mg/L (note that chloride levels were below 19,000 mg/L in March 2020 and March 2021). The Mann-Kendall and regression analysis for chloride and salinity showed a declining trend in saltwater concentrations since startup of the RWS; however, there has been very little change observed this year compared to the prior 12 months. The USGS induction log in the annual monitoring report (FPL 2022) for TPGW-17S also showed an overall notable net reduction in bulk conductivity since 2018 just above the screened interval. It is anticipated that these reductions will be reflected in time at the shallow screen interval as the freshening continues vertically downward and with retraction of the hypersaline groundwater back towards the CCS. Since the retraction of the plume is being observed first in shallow monitoring wells closer to the CCS and recovery wells, distance from the CCS is also a factor of when shallow wells will transition from hypersaline to saline. TPGW-17S is approximately 0.5 miles west of the CCS

and over 0.25 miles further west than TPGW-1S and TPGW-2S; thus, it is taking longer to observe meaningful salinity reductions at TPGW-17S.

The other shallow wells, including TPGW-12S, TPGW-18S, TPGW-19S and TPGW-22S, were never hypersaline; but they are of interest as remediation progresses. Declines in specific conductance, chloride, and tritium were observed at TPGW-18S and TPGW-19S during the reporting period. These two wells are located within 1 mile west or northwest of the CCS (Figure 3.1-1). The biggest percent reduction in salinity and chloride this reporting period in any of the 23 wells occurred in TPGW-18S. The average automated salinity this reporting period at TPGW-18S (4.7 PSU) was 35% lower this reporting period compared to the previous 12 months. Chloride concentrations at TPGW-18S this reporting period (2,560 mg/L) was 37% lower compared to the previous year (4,065 mg/L). Tritium concentrations in TPGW-18S are slightly less than the previous reporting year, but the values are low (i.e., 15 pCi/L compared to 24 pCi/L), indicating little to no CCS groundwater contribution. The USGS induction logs in the annual monitoring report (FPL 2022) showed appreciable declines in bulk conductivity in shallow groundwater at the shallow well screens in TPGW-18S, TPGW-19S, TPGW-1S, TPGW-2S, and TPGW-15S, confirming freshening of the shallow zone.

No decreasing trends were noted at TPGW-12S and TPGW-22S. The salinity and chloride at TPGW-12S are affected by Biscayne Bay with limited influence from the CCS. The average annual tritium concentration this reporting period was 52 pCi/L with a low value of 30 pCi/L in June 2022. Since TPGW-22 is a relatively new monitoring well (i.e., FPL started collecting automated data from mid-February 2021, with the first quarterly analytical sample taken in March 2021), and because conditions prior to RWS operations at this location are unknown, it is not possible to assess the effects of the RWS operations since startup at this site. Chloride values at TPGW-22S have ranged from 13,900 mg/L to 16,200 mg/L with no discernible pattern. Mann-Kendall analysis based on limited weekly salinity data shows a slight increasing trend at TPGW-22S with values at the end of February 2021 around 27.4 PSU and values at the end of June 2022 around 28 PSU (note that these small differences are within the error band of automated data).

3.2.2   Intermediate and Deep Wells

Nearly all the intermediate and deep wells west and north of the CCS used in the remediation assessment showed a statistically significant decline in one or more parameters (i.e., specific conductance, chloride, tritium) since the inception of the RWS. The only exceptions are TPGW-15D (located between RWS-3 and the CCS), TPGW-L3-58 (located near well cluster TPGW-15), and TPGW-22M (which has too short of a period of record to observe a declining trend). Reductions of saltwater and tritium in the intermediate and deep wells continue to be observed, although these declines are smaller than in the shallow wells (Figure 3.2-3). For wells that only show a declining trend in tritium, these trends may be a precursor to a reduction in saltwater concentrations.

At the time of this report, there are 10 hypersaline intermediate monitoring wells (TPGW-1, TPGW-2, TPGW-12, TPGW-15, TPGW-17, TPGW-18, TPGW-19, TPGW-22, TPGW-L3-58 and TPGW-L5-58), with 5 of those wells (TPGW-1, TPGW-12, TPGW-18, TPGW-19, and

TPGW-22) in the compliance area west of the L-31E canal and north of the FPL property. There
are 8 deep horizon monitoring wells (same as above excluding TPGW-L3-58 and TPGW-L5-
58), 5 of which are in the compliance area (same locations as the intermediate wells). The
TPGW-23 well cluster site, located along the L-31E canal road 0.5 miles north of Palm Drive,
was completed; and data collection began in mid-August 2022. Preliminary data indicate that
both intermediate and deep wells are hypersaline.

During the reporting period, no intermediate or deep hypersaline monitoring wells transitioned to
saline groundwater (i.e., chloride concentration <19,000 mg/L), but three intermediate depth
wells (TPGW-12M, TPGW-18M and TPGW-19M) reported at least one chloride concentration
below 20,000 mg/L during this reporting year. All of these wells have a statistically significant
declining trend in chloride and salinity.
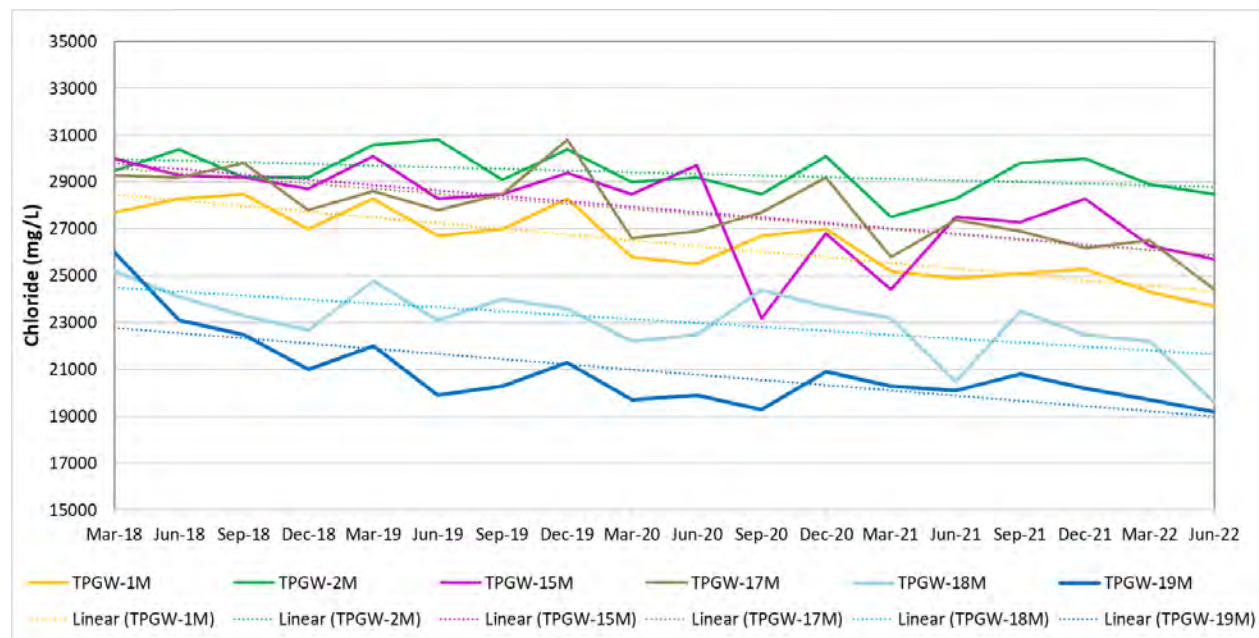
Note: TPGW-22 is not shown due to limited data.

Figure 3.2-3. Reduction in Chloride Concentration in Intermediate Wells West of the CCS

Monitoring well TPGW-19M (shown as the dark blue line in Figure 3.2-3) has been fluctuating
from 19,000 mg/L to 21,000 mg/L for approximately the past 3 years, and it is the closest
intermediate or deep well to transition from hypersaline to saline. As discussed in the annual
monitoring report (FPL 2022), the induction log at TPGW-19 shows reduction in bulk
conductivity has occurred in the upper 70 ft of the well since 2018.

As previously discussed, there are 22 groundwater monitoring wells used in this assessment of
RWS operations that have been or still are hypersaline (9 of which are in the compliance area)
with the majority of them being intermediate and deep wells. Figure 3.2-4 shows the chloride
concentration in March 2018 for most of the wells prior to the start of RWS operations (top of
the orange color of the bar) and the chloride concentration at the end of this reporting period in
June 2022 (top of the blue color of the bar). There are two wells in March 2018 that appeared to

have biased high chloride levels (TPGW-19M and TPGW-19D) and one well with biased low (TPGW-12M) chloride concentrations based on prior and subsequent near-term data; for these 3 wells, June 2018 chloride values were used in the graph. The June 2018 data for these 3 wells did not appear to be affected by RWS operations, so use of the June 2018 data is a reasonable surrogate for the March 2018 baseline data. The orange portion of the bar shows how much the chloride concentration has dropped from 2018 to 2022 while the blue portion of the bar shows how much more the concentration would need to drop from the June 2022 concentration to reach the 19,000 mg/L target. Other than TPGW-12D and TPGW-L3-58, all the wells show reductions in chloride concentrations with the three shallow wells (TPGW-1S, TPGW-2S, TPGW-15S) no longer hypersaline and several other wells close to the 19,000 mg/L threshold.
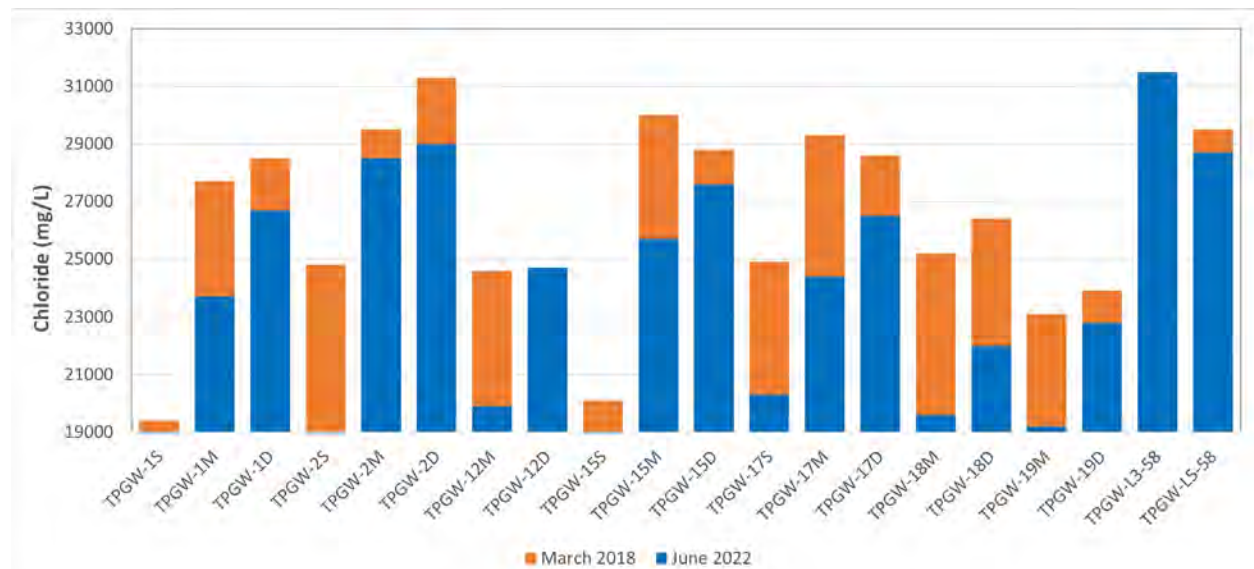
Figure 3.2-4. Chloride Concentrations in March 2018 and June 2022

Average tritium concentrations in the intermediate and deep wells for the reporting period range from 496 pCi/L (TPGW-19M) to 4,728 pCi/L (TPGW-15M), indicating varying degrees of CCS groundwater influence with concentrations in excess of 1,000 pCi/L within approximately 1 mile of the CCS. Approximately half of the intermediate and deep monitoring wells west and north of the CCS used in monitoring the progress of RWS remediation, have lower annual average tritium concentrations this reporting period compared to the previous 12 months and to the historical period of record (Table 3.2-1). Monitoring wells TPGW-17M, TPGW-19M, and TPGW-L5-58 show the greatest tritium reduction this reporting period compared to the previous reporting period (18.6%, 9.3%, and 8.1% respectively) while TPGW-17M and TPGW-L5-58 show the greatest reduction compared to the historical period of record (20.2% and 32.1%, respectively). The tritium concentrations this reporting period were 1,364 pCi/L at TPGW-17M, and 1,917 pCi/L at TPGW-L5-58 (historic period of record averages were 1,981 pCi/L and 2,823 pCi/L, respectively), so the percent reductions are appreciable drops in tritium concentrations. These two wells, TPGW-17M and TPGW-L5-58, along with TPGW-17S (previously mentioned) are located near the southwestern boundary of the CCS and indicate reductions in CCS-sourced groundwater in that area.

TPGW-2M, which is in the same general vicinity as TPGW-17M and TPGW-L5-58, had a 12% increase in tritium (2,755 pCi/L average for reporting period) compared to the previous 12-month average. Note that the tritium values at TPGW-2M are 11% lower compared to the historical period of record, and there is an overall declining trend since RWS startup through May 2022. The data indicate that changes are not spatially uniform, and variations between years may occur even though an overall trend is observed.

There were a few wells (TPGW-15M, TPGW-15D and TPGW-L3-58) that showed increasing trends in tritium since the start of RWS operations through the end of this reporting period. The increases at TPGW-15M and TPGW-15D are likely related to RWS pumping as this well cluster is situated between the CCS and RWS-3 (RWS-3 is less than 0.5 mile northwest of the CCS). The screen interval at TPGW-15M is -48 to -51 ft (NAVD 88) while TPGW-15D is -80 to -84 ft (NAVD 88). These depths are within the targeted ranges for extraction at RWS-3 (-72 to -90 ft [NAVD 88]). It is suspected that groundwater from under the CCS may be pulled past TPGW-15 at depth, thereby increasing the percentage of CCS-sourced groundwater as reflected in higher tritium concentrations. Due to the proximity of TPGW-L3-58 to the TPGW-15 well cluster, it is also suspected TPGW-L3-58 could be similarly affected.

Well data provides a localized assessment of changes. Given the volume of the hypersaline plume, distance between the wells, hypersaline boundary, and the gradual vertical reductions in the thickness of the hypersaline plume in response to remediation to date, it is not surprising that reductions of chloride in the intermediate and deep wells are more modest compared to the shallow wells which were/are closer to the hypersaline interface. The CSEM survey results that are presented in Section 4 provide a more robust assessment of changes since data are analyzed across the entire landscape west and north of the CCS.

3.2.3   Other Observations

> Chloride reductions in the compliance area in the middle well at TPGW-5, which is over 3 miles west of the RWS, is an indication of the lateral reach of the withdrawal system.

Well clusters TPGW-4 and TPGW-5 and wells TPGW-G21 and TPGW-G28 are the next series of wells west of the hypersaline plume. Monitoring sites TPGW-4, TPGW-5 and TPGW-G28 are approximately 3 miles west of the CCS while TPGW-G21 is approximately 3.7 miles west. These wells are of general interest in assessing the lateral extent of RWS operations on reducing groundwater salinity levels. Based on a review of the data, there appears to be relatively few meaningful salinity trends other than a statistically significant declining trends in chloride, tritium, and salinity at TPGW-5M over the reporting period. Chloride (10,335 mg/L) and salinity (18.2 PSU) were approximately 15% and 6.2% lower, respectively, this reporting period compared to the previous year; and the time series automated salinity data show a clear declining trend. Tritium concentrations at TPGW-5M were slightly lower this reporting period (180 pCi/L) compared to the previous reporting period (209 pCi/L) and over 25% lower than the historical period-of-record average (242 pCi/L). Collectively, the data from this site potentially

indicate some influences of RWS operations at this mid-depth well located over 3.1 miles west of the CCS.

> While gradual reductions in chloride are occurring in the intermediate and deep wells, large declines, and transitions from hypersaline to saline groundwater will not occur until the edge of the hypersaline plume reaches the narrow monitoring interval at that well location.

3.2.4   Monitoring Well Data Considerations

Several factors should be considered when evaluating monitoring well water quality data and trends for the purpose of gauging progress in plume remediation rates and spatial extent. These factors include the nature of geology of the Biscayne aquifer in the Model Lands area, the design and location of the monitoring well network, the effects of fluid density on the characteristics and remediation of the plume, and the design of the RWS. The combined influences of these factors, discussed below, are expected to result in transitions from hypersaline to saline in shallow monitoring wells prior to middle and deep monitoring wells; and such transitions will occur comparatively quickly following a period of relatively small reductions in chloride concentrations.

Lithologic core and geophysical logging data from the Biscayne aquifer in the Model Lands indicate the presence of three thin high flow zones, localized lower permeable tight limestone beds and variable occurrences of sandy silts reflective of the Tamiami Formation interspaced with higher permeable limestones along the lower portions of the Biscayne aquifer (JLA Geoscience, Inc. 2010). These variations in vertical and horizontal permeability affect the orientation and spatial extent of hypersaline groundwater originating from beneath the CCS with groundwater being able to move laterally more freely in high flow zones while being restricted by lithologies characterized by lower permeabilities. As a result, the vertical and lateral extent and concentrations of the hypersaline plume are complex and variable as shown in AEM mapping and borehole induction logs.

The monitoring wells used to assess the progress of plume remediation are constructed to monitor these three high flow zones (with the exception of the L and G monitoring wells which are open hole to over 60 ft and, possibly TPGW-22). These high flow zones are on the order of 2 to 5 ft thick, and the monitoring well intervals were constructed to the same thickness. Prior to the initiation of remedial actions, hypersaline groundwater preferentially moved through the high flow zones, which represents the greater lateral extent of the plume. Many of the wells are located on upland and roadways either near the CCS or along Tallahassee Road to avoid impacts to wetland areas. Monitoring wells in the vicinity of Tallahassee Road are west of the hypersaline plume and have not contained hypersaline groundwater, while monitoring wells near the CCS (particularly those constructed into the middle and deep high flow zones, contain hypersaline groundwater with the highest concentrations. The lateral extent of the plume in the middle and high flow zone was mapped in 2018 to be as far west as 1 to 2 miles west of the CCS, with the edge of the plume closer to the CCS in the shallow high flow zone due to fluid-

specific density factors and in the lower high flow zone due to occurrences of lower permeability sediments at depth in the aquifer (FPL 2019c).

The orientation and extent of hypersalinity is also influenced by the specific gravity and density of the fluid compared with lower salinity native coastal waters. Higher specific gravity hypersaline water, formed in the CCS when evaporation exceeded rainfall, sank through the Biscayne aquifer beneath the CCS until low permeable lithologies along the base of the aquifer restricted vertical flow, after which the hypersaline groundwater flowed laterally along more permeable pathways. These factors combined to form narrow or sharp interfaces between hypersaline and saline groundwater.

The Agency-approved RWS is designed to extract hypersaline water near the base of the aquifer, which induces lateral and vertical flow of hypersaline groundwater into the extraction wells. As hypersaline groundwater is removed along the base of the aquifer, the plume narrows in thickness and retracts along the outward edge as hypersaline groundwater moves eastward and downward to replace the hypersaline water being extracted at depth. This process results in salinity reduction along the western and northern edge of the plume in wetland areas without many monitoring wells and along the top of the plume in shallow monitoring wells closer to the CCS.

This is illustrated by the borehole induction log for TPGW-2 on Figure 3.2-5. Lithologies having high permeabilities and containing high salinity groundwater have comparatively higher bulk conductivity values compared to lower permeable materials. As permeability of earth materials don't change much with time, the shifts in measured bulk conductivity over the years (represented by different color traces on the figure) are due to change in borehole salinity. Depth intervals where bulk conductivity decreases with time are areas where pore water salinity is decreasing. This can be seen to varying degrees at each of the three monitoring intervals at monitoring site TPGW-2. At the shallow monitoring interval (-28 to -30 ft), there has been a significant reduction in bulk conductivity from 2018 (green trace) to 2022 (black trace) in the upper high flow zone since remediation began. This is reflected by chloride level trends in TPGW-2S which have dropped from approximately 25,000 mg/L immediately prior to the start of remediation withdrawals to less than 15,000 mg/L in 2022.

The interval immediately below the TPGW-2S monitoring interval, from approximately -32 to -48 ft, has low bulk conductivity which has not changed in value from 2011 to 2022. This area and deeper areas with similar low conductivity values that remain consistent over years are interpreted to be low permeable lithofacies that impede the flow of groundwater. The middle (-54 to -56 ft) and deep (-89 to -91 ft) high flow zones show progressively less reductions in bulk conductivity since remediation began, which is reflected in the chloride monitoring data that shows no significant trend during the first four years of remediation. Note that despite chloride concentrations of 30,000 mg/l in TPGW-2D, the maximum bulk conductivity is significantly less than the two shallower monitor horizons containing lower chloride concentrations. This is most likely due to interbedded, comparatively lower permeable layers of rock and sandstone in the lower portion of the aquifer at this site that could slow the extraction of hypersaline groundwater at depth.
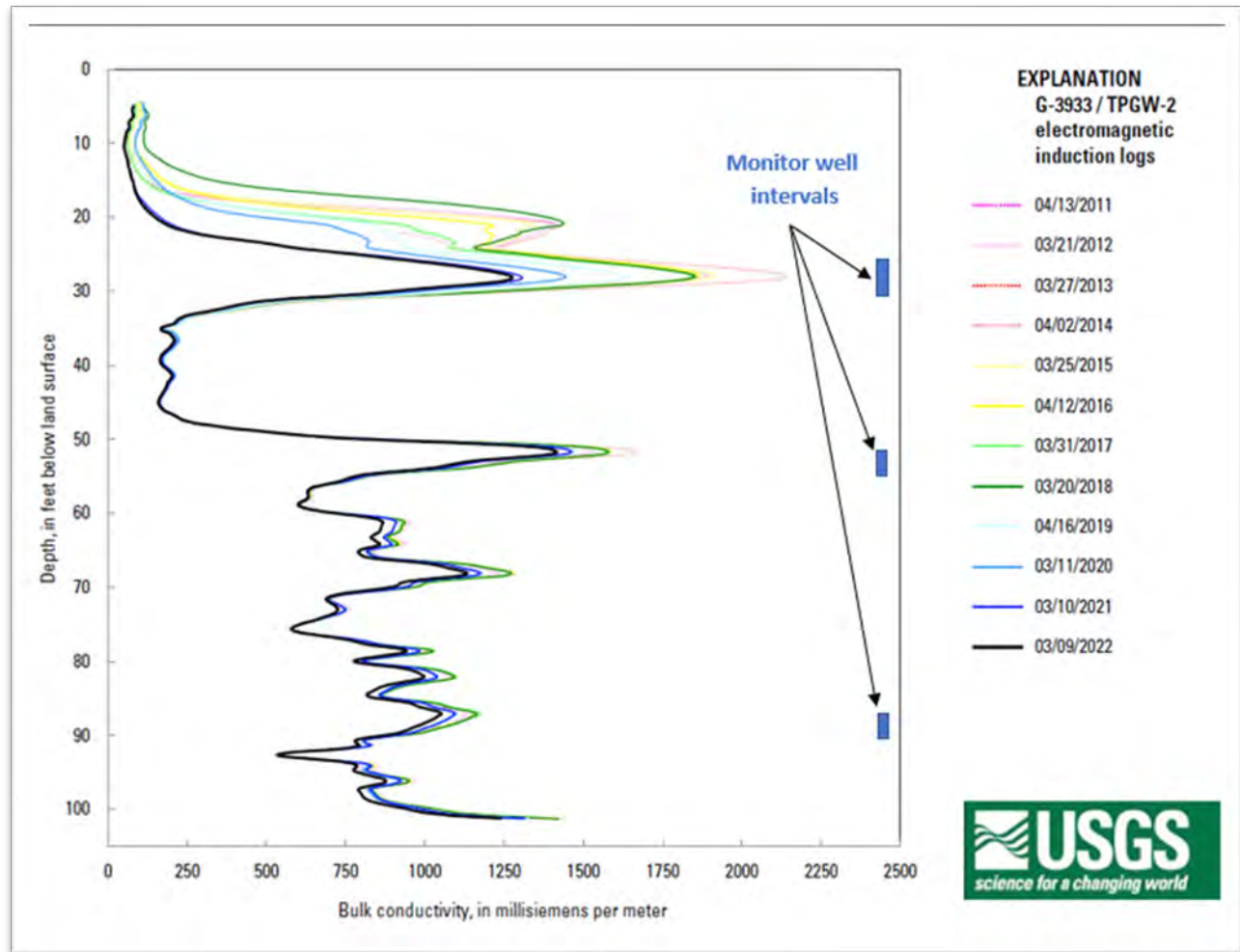
Figure 3.2-5. Monitoring Well TPGW-2 Borehole Induction Log: 2011 through 2022

Documentation of both the sharpness of the hypersaline-saline water interface and the vertical retraction of the plume while deep salinity levels remain unchanged is also documented by open hole monitoring wells TPGW-L3 and TPGW-L5 located along the L-31E canal, west of sections 1 and 3 of the CCS. Figure 3.2-6 shows the measured depth to the 19,000 mg/l chloride interface from 2011 through June 2022, including the last 4 years of remediation. These elevations are collected at 1-ft intervals over the depth of the well (FPL 2022). These data show a progressive expansion of the thickness of the overlaying fresher water lens by approximately 6 ft at TPGW-L5 and about 10 ft at TPGW-L3 and the thinning of the deeper hypersaline plume at these two monitoring sites during the four years of remediation. The data also show the saline-hypersaline interface is sharp, with chloride values transitioning from 5,000 to 19,000 mg/L in approximately 5 ft (FPL 2022). However, while the thickness of the hypersaline plume at this location is narrowing at these locations, the chloride concentrations at a depth of -58 ft have shown no statistically significant trend since remediation began (Table 3.2-1).
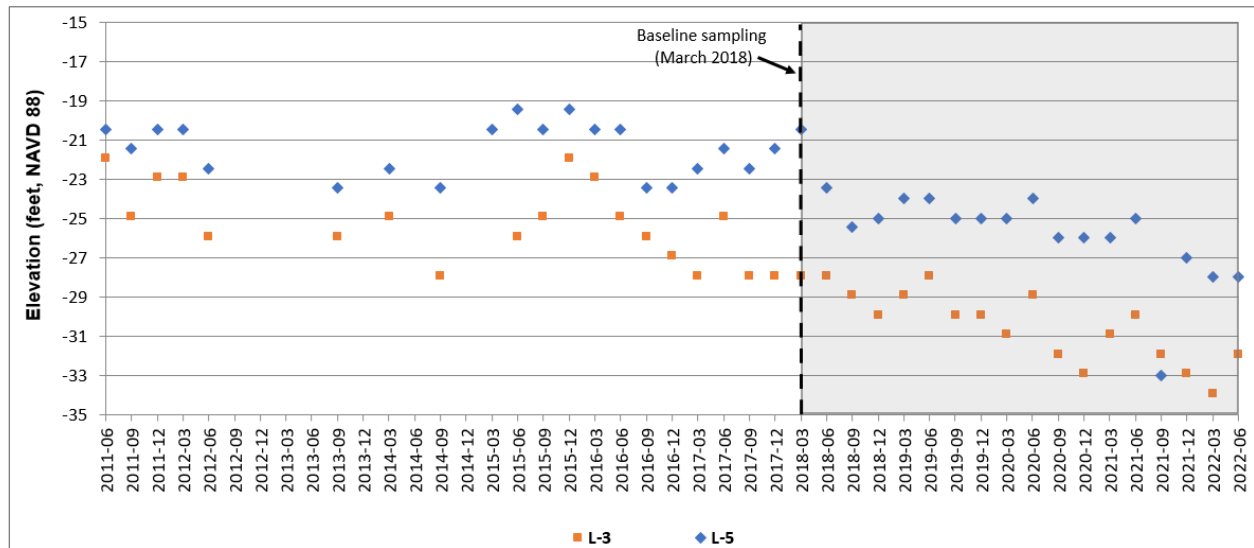
Note: Area in gray indicates RWS operational period.

Figure 3.2-6. Trends in the Depth to the Hypersaline Interface in wells TPGW-L3 and TPGW-L5

Monitoring well data provide information on water quality from a 2- to 5-ft length of the Biscayne aquifer over a radial distance of a foot or two. Due to lithologic variability in the Biscayne aquifer, it is not possible to produce technically based conclusions regarding the progress of the remediation of the plume west and north of the CCS on these data alone. However, these data play a critical role in assessing remediation progress when used in conjunction with other monitoring and analytic methods, including AEM and groundwater modeling. As a result, the lack of large declines in hypersaline chloride concentrations in middle or deep monitoring wells located near the CCS should not be construed to mean the plume is not being reduced in volume or extent, rather that the edge of the hypersaline plume has yet to reach the particular monitoring interval at that well location.

3.3 CHLORIDE CONCENTRATION CONTOUR MAPS

> Comparison of the 2018 and 2022 maps show the 19,000 mg/L contour line is being retracted closer to the CCS for all three depth horizons, which is supported by other data findings reported in this Year 4 RAASR.

As requested by MDC, plan view chloride concentration contour maps were created for the shallow, middle, and deep monitoring horizons using chloride measurements from up to 22 monitoring well sites and nine CSEM chloride measurement sites for comparison of the estimated location of the 2022 versus 2018 baseline orientations of the 19,000 mg/L chloride isochlor contour lines. The contours were objectively generated by Earth Volumetric Studio, a program developed by C Tech Development Corporation, using kriging algorithms. Isochlors were generated using the kriging software and contoured for chloride levels of 1,000, 4,000,

9,000, 14,000, 19,000, and 24,000 mg/L. These figures were modified to clip or blank isochlors that trend into areas not supported by monitoring data or outside of the remediation compliance area east and south of the CCS.

To reduce some of the uncertainty in spatial data gaps between monitoring wells in the area between the CCS and Tallahassee Road which covers the western extent of the hypersaline plume and CSEM survey data, chloride estimates from the CSEM survey were added for mapping purposes at nine different areas at shallow, middle, and deep layers. The CSEM chloride values were added at midpoints between monitoring wells to place the CSEM points in locations that were least represented by monitoring well data. The added CSEM locations and their spatial relationships to the monitoring wells are shown graphically in Figures 3.3-1 through 3.3-6. Chloride concentrations for the 2022 TPGW and CSEM monitoring points used in these figures are provided in Table 3.3-1.

The 2022 chloride contour maps for the shallow, middle, and deep layers are shown on Figures 3.3-1 through 3.3-3 while Figures 3.3-4 through 3.3-6 show comparative positions of the 19,000 mg/L chloride contour for the 2018 baseline conditions and the 2022 Year 4 conditions. Comparison of the 2018 and 2022 maps show the 19,000 mg/L contour line is being retracted closer to the CCS for all three depth horizons, which is supported by other data findings reported in this Year 4 RAASR. Any definitive conclusions in specific areas, however, are constrained in accuracy by the spatial distances between the existing monitoring wells, the degree that chloride concentrations change spatially, differing vertical depths or relative depths of monitoring well screens, differences between the CSEM and laboratory determination of chloride concentration, the size of the study area, and the assumptions of hydraulic continuity among all monitoring wells in each layer.

Table 3.3-1. Chloride concentrations for the 2022 TPGW and CSEM monitoring points

Data point	Shallow			Middle			Deep		
	Chloride (mg/L)	Elevation (ft)	Relative position[1] (%)	Chloride (mg/L)	Elevation (ft)	Relative position[1] (%)	Chloride (mg/L)	Elevation (ft)	Relative position[1] (%)
TPGW-1	9650	-25.3	28.6	23700	-49.3	55.5	26700	-82.7	92.9
TPGW-2	15300	-25.4	25.8	28500	-52.9	53.2	29000	-83.1	83.4
TPGW-3	22500	-25.5	24.3	24300	-51.4	49.2	26300	-88.3	84.6
TPGW-4	2520	-22.3	32.7	14300	-40.2	58.6	14700	-61.8	89.5
TPGW-5	138	-23.5	31.8	9540	-45.8	61.2	12600	-64.2	85.4
TPGW-6	263	-22.5	27.7	7870	-51.8	61.9	8290	-82.5	97.7
TPGW-7	32.4	-25.1	30.9	44.2	-51.4	61.2	4290	-79	93
TPGW-8	28.3	-20.7	36.8	27.5	-35.2	60.6	33.9	-50.3	85.4
TPGW-9	21.9	-11.8	24.7	22.4	-29.1	56.3	24.9	-45.1	85.4
TPGW-10	20500	-33.3	25	21100	-50	38	27900	-121.6	93.9
TPGW-11	21200	-37.4	28.4	22600	-86.8	70.6	27600	-118.1	97.3
TPGW-12	18400	-28.3	27.9	19900	-53.8	52.4	24700	-89.9	87.1
TPGW-13	31100	-30.1	31.6	31200	-56.4	58.6	32100	-81.8	84.7
TPGW-14	22000	-23.7	19.6	23600	-50.6	45.4	27600	-95.3	88.3
TPGW-15	12800	-26.9	29.2	25700	-49.5	53	27600	-83.4	88.8
TPGW-16	24000	-30.2	28.3	29400	-51.6	47.8	29600	-68.7	63.4
TPGW-17	20300	-25	26.7	24400	-48.2	51.2	26500	-82.3	87.3
TPGW-18	2230	-28.3	31.6	19600	-55.1	61.2	22000	-73.7	81.8
TPGW-19	1160	-23.2	26.9	19200	-43.3	49	22800	-80	89.2
TPGW-20	N/A	N/A	N/A	N/A	N/A	N/A	2420	-80.2	98.2
TPGW-21	25.8	-17.2	23.8	26.9	-39.7	53.6	30.7	-69.6	93.3
TPGW-22	14900	-29.2	37.8	20900	-54.1	69.4	20400	-65.7	84.1
CSEM1	1225	-23.1	27.7	11835	-50	58.5	5574	-80.4	93.3
CSEM2	171	-23.5	30.7	1274	-48.2	60.3	9506	-68.7	85
CSEM3	555	-24.4	29.5	2560	-41.1	49.3	4779	-67.4	80.3
CSEM4	1023	-25.6	30.3	10511	-51	59.9	7558	-68.9	80.8
CSEM5	8034	-28.1	31.6	9814	-51.4	57.9	17132	-71.4	80.5
CSEM6	2317	-20.9	24.9	12616	-48.5	57.5	13676	-67.9	80.3
CSEM7	930	-20.2	27.5	9905	-43.2	58.4	12839	-59.6	80.6
CSEM8	4084	-23.8	28.8	19246	-52	62.1	15646	-70.6	83.9
CSEM9	6138	-24.8	26.8	21120	-52.2	57.1	19904	-79.3	87

1 computed as: -(elevation) / thickness
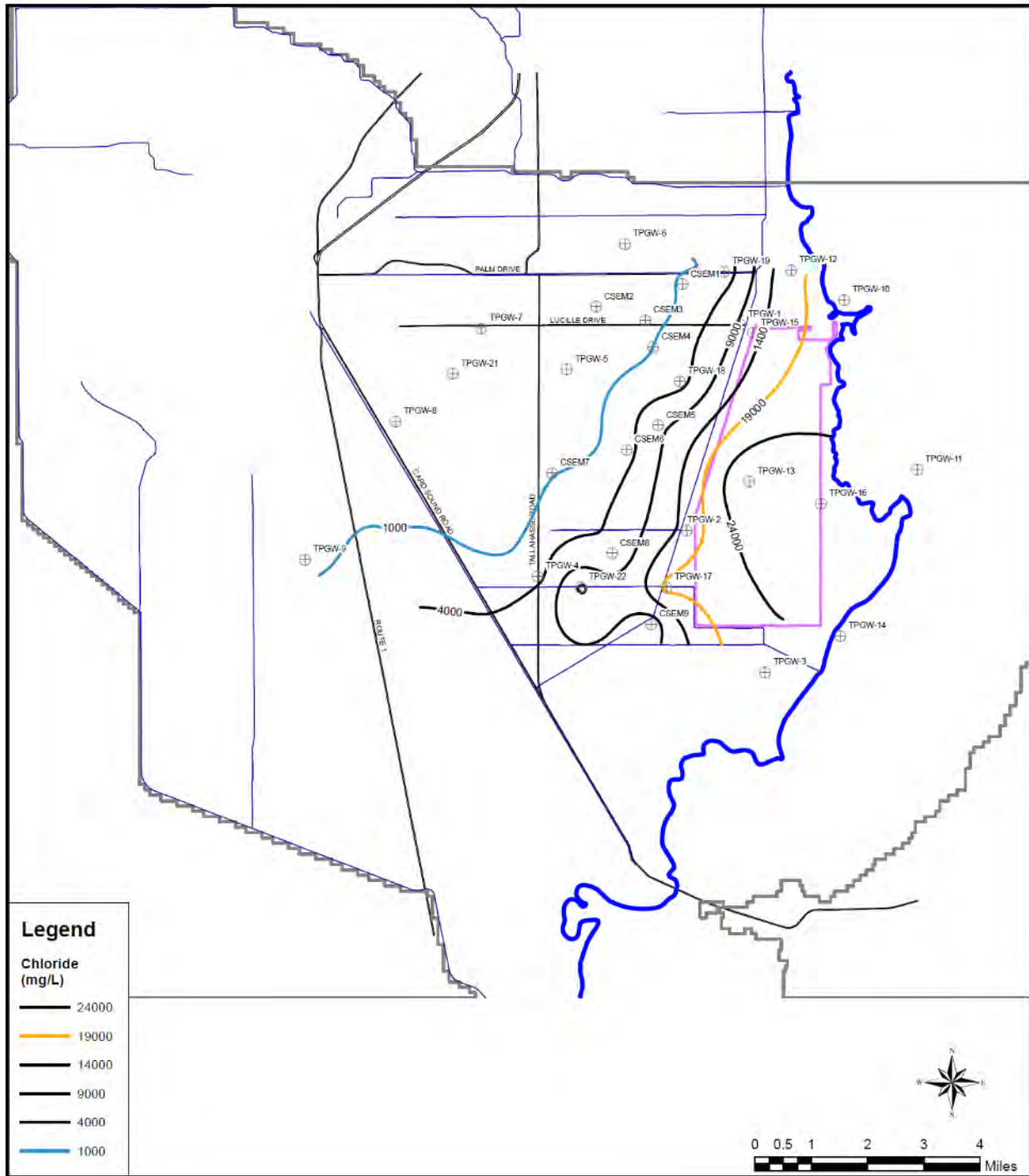
Figure 3.3-1. Groundwater Chloride Contour Map based on 2022 Shallow Monitoring Well Data and CSEM Horizon Chloride Values
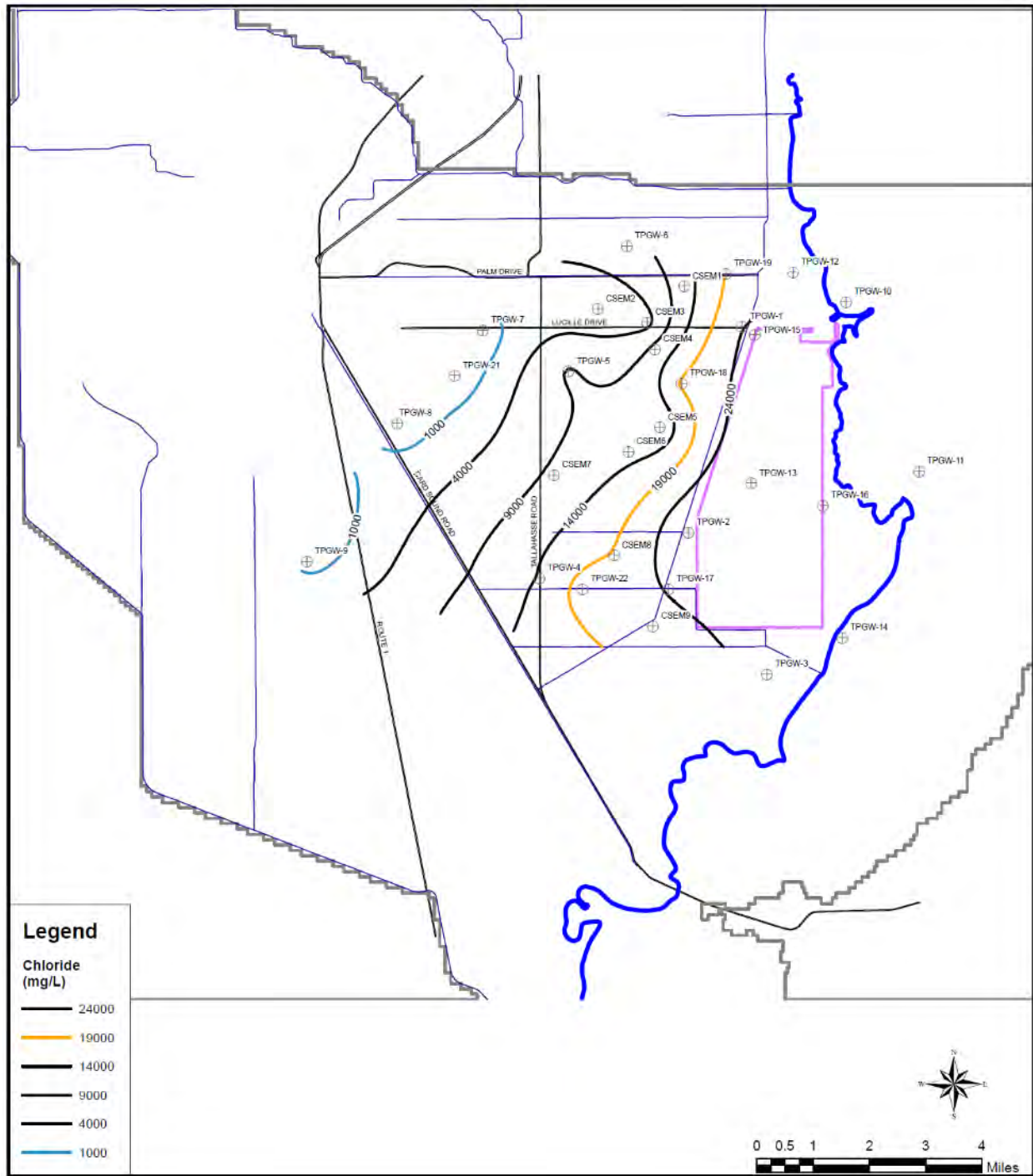
Figure 3.3-2. Groundwater Chloride Contour Map based on 2022 Middle Monitoring Well Data and CSEM Horizon Chloride Values
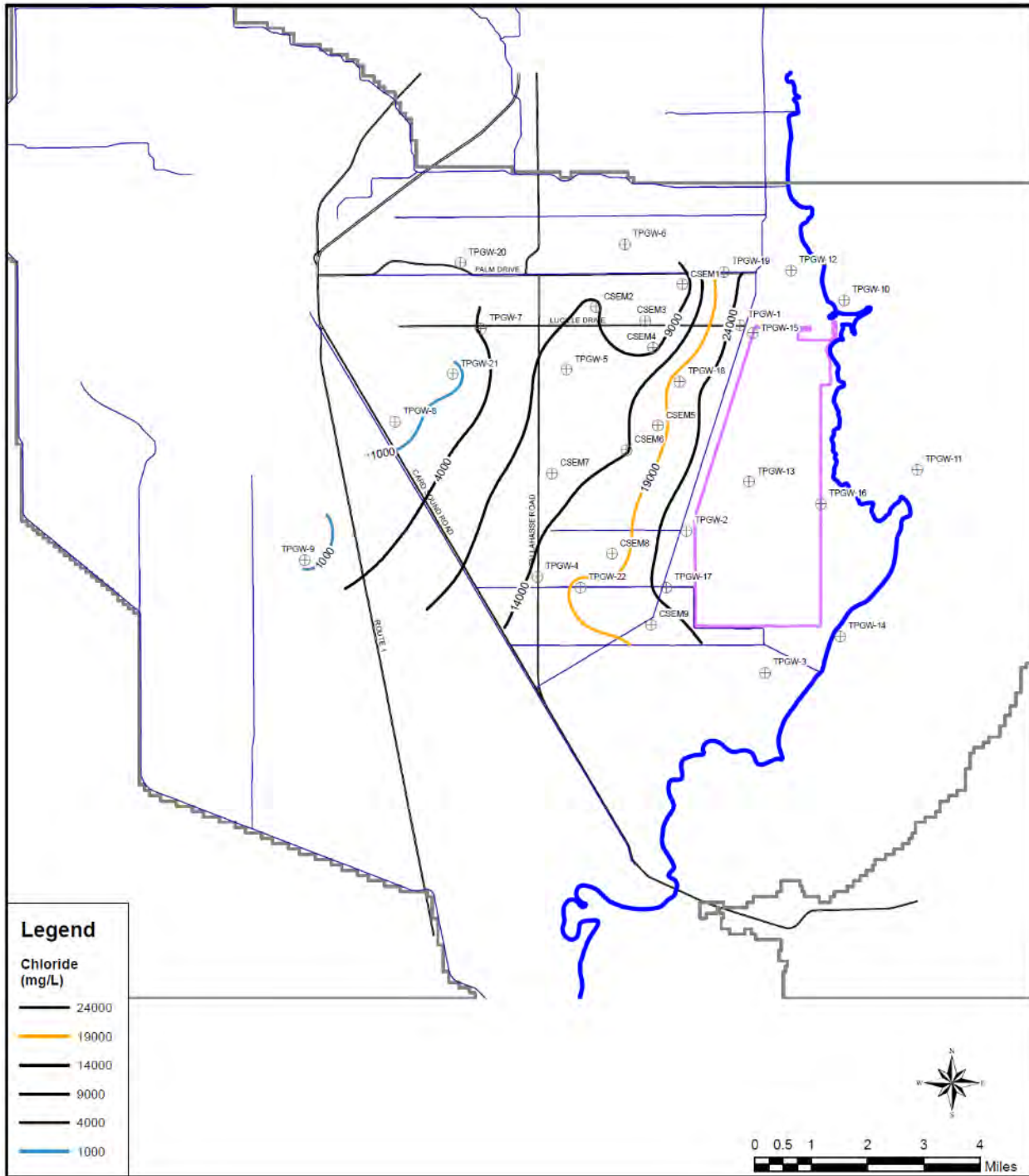
Figure 3.3-3. Groundwater Chloride Contour Map based on 2022 Deep Monitoring Well Data and CSEM Horizon Chloride Values
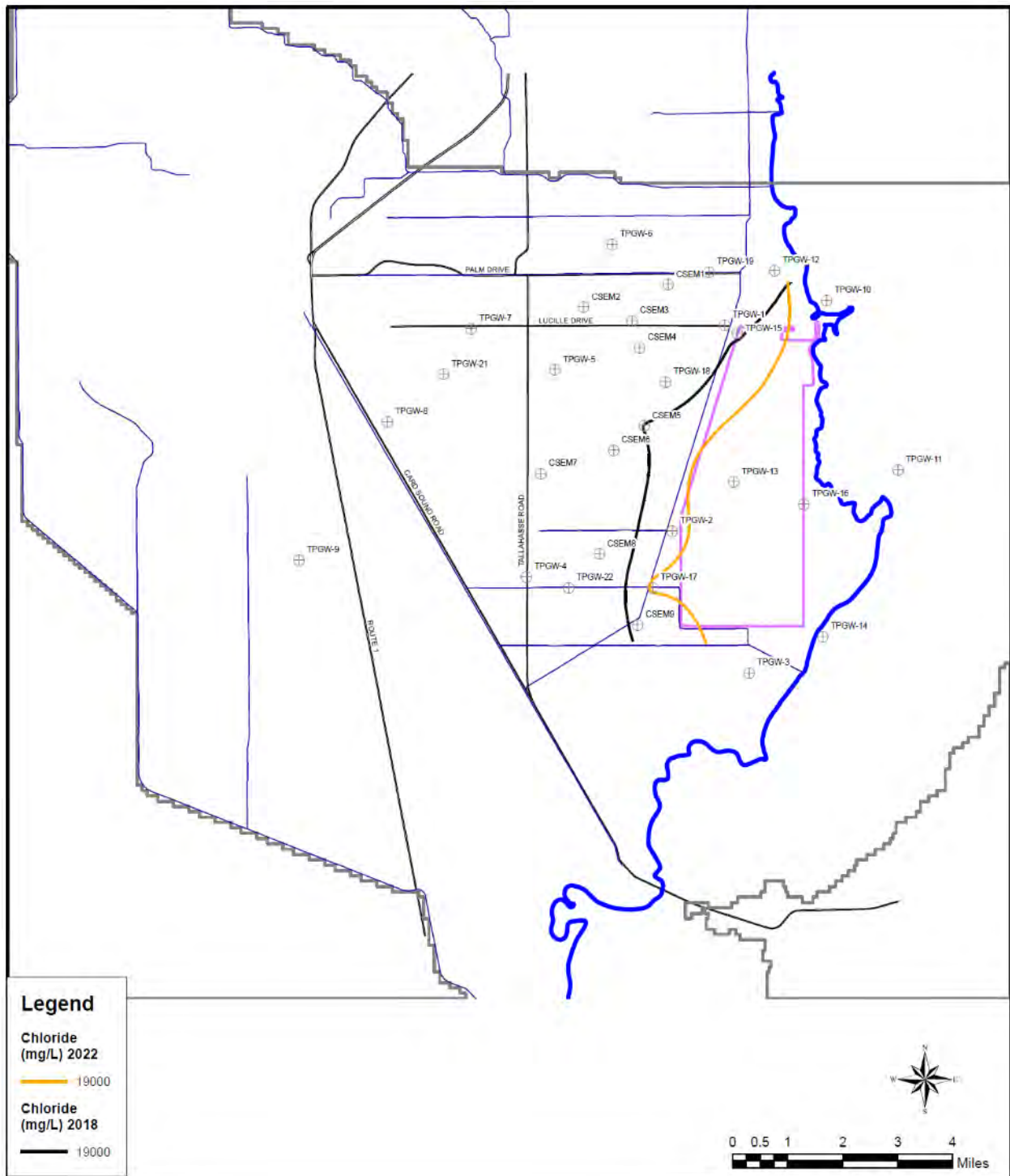
Figure 3.3-4.   Comparison of the 2018 Baseline and 2022 Year 3 Inland Extent of Hypersaline Groundwater (19,000 mg/L Chloride Isochlor) based on Shallow Horizon Monitoring Well Data
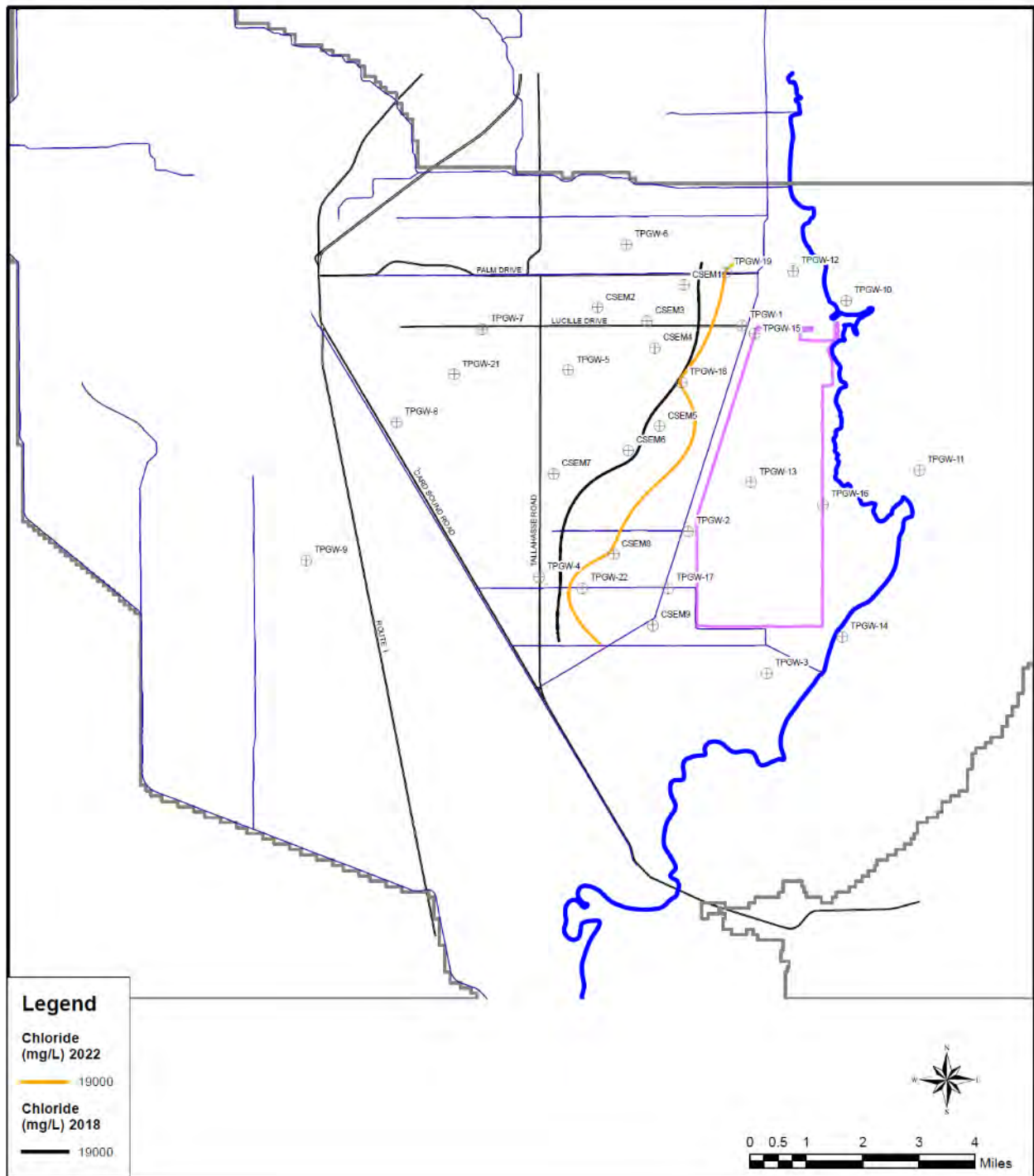
Figure 3.3-5. Comparison of the 2018 Baseline and 2022 Year 3 Inland Extent of Hypersaline Groundwater (19,000 mg/L Chloride Isochlor) based on Middle Horizon Monitoring Well Data
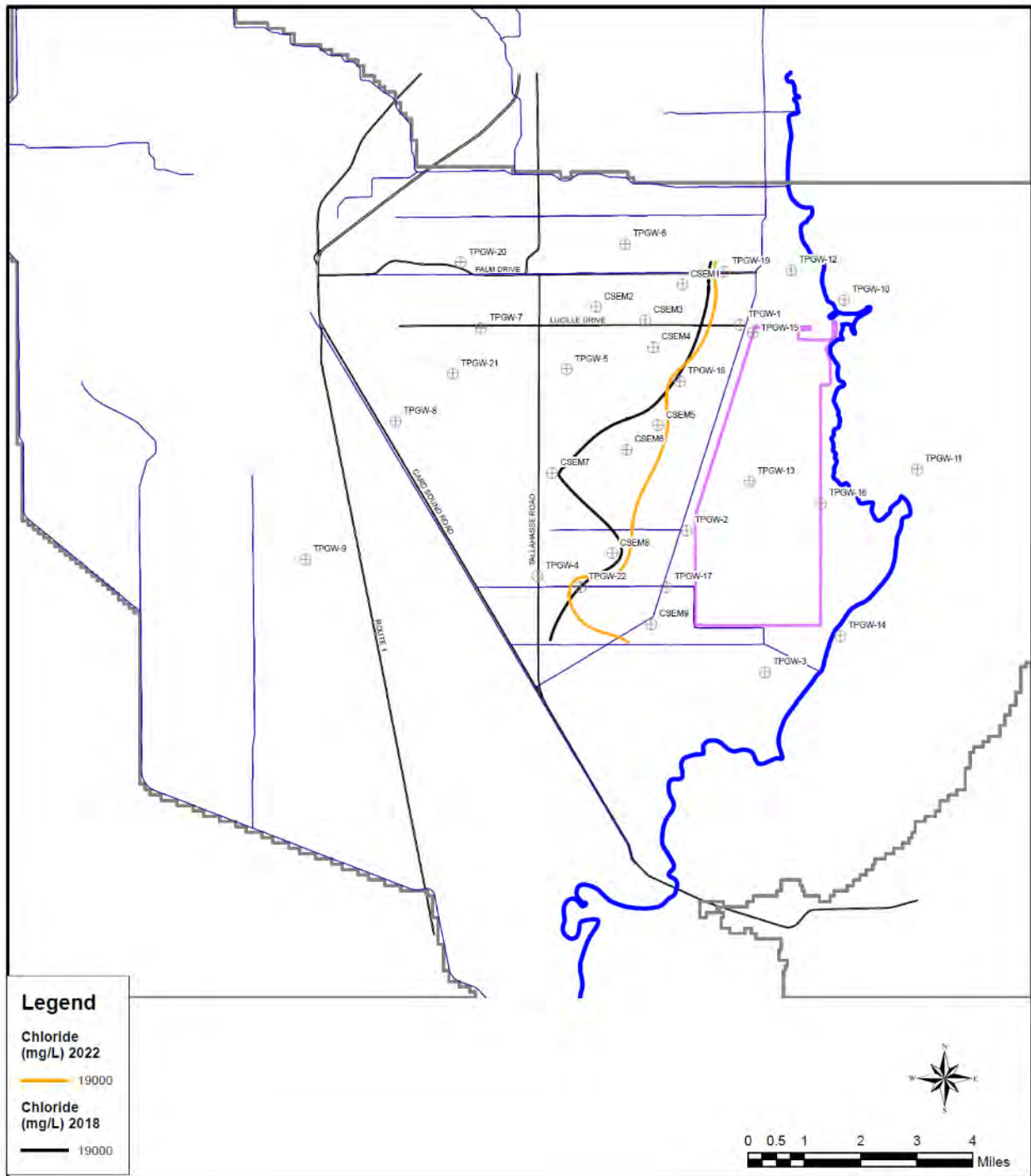
Figure 3.3-6. Comparison of the 2018 Baseline and 2022 Year 3 Inland Extent of Hypersaline Groundwater (19,000 mg/L Chloride Isochlor) based on Deep Horizon Monitoring Well Data

3.4 GROUNDWATER LEVEL TRENDS

Groundwater levels in the area vary seasonally, with levels generally higher during the wet season and lower during the dry season. However, the groundwater levels can also vary daily and rise within hours of a rainfall event and, in some wells, change hourly with tides. Despite these complicating factors, groundwater contouring can provide broad insights into regional gradients, flow directions, and flow rates. Figures 3.4-1 and 3.4-2 show groundwater elevation contour maps generated from daily average automated water level data for two separate days (April 1, 2022, representing dry season conditions and September 24, 2021, representing wet season conditions) collected from shallow monitoring wells TPGW-1S, TPGW-2S, TPGW-4S, TPGW-5S, TPGW-6S, TPGW-7S, TPGW-12S, TPGW-15S, TPGW-17S, TPGW-18S, TPGW-19S and TPGW-22S. The contours were developed using manual linear interpolation contouring methods and best professional judgment and informed by the above-referenced monitoring wells and additional wells (TPGW-10, TPGW-13, and TPGW-21) which are part of other monitoring efforts.

The representative groundwater contour maps for the dry (Figure 3.4-1) and wet (Figure 3.4-2) seasons indicate a generally eastward flow direction, with a slightly steeper gradient during the wet season relative to the dry season. These maps are based on measured water levels and are not adjusted for freshwater head equivalents, so care must be taken to interpret the results. Because of the variable fluid densities in the Biscayne aquifer, modeling tools are needed to more accurately represent groundwater flow rates, direction, and gradients.

Regionally, the groundwater levels on September 24, 2021, (the wet season) were approximately 0.5 to 1.0 ft higher than April 1, 2022 (the dry season). Continuous eastward groundwater gradients with stages equal or above sea level are generally considered helpful in reducing saltwater intrusion and aid in plume remediation.
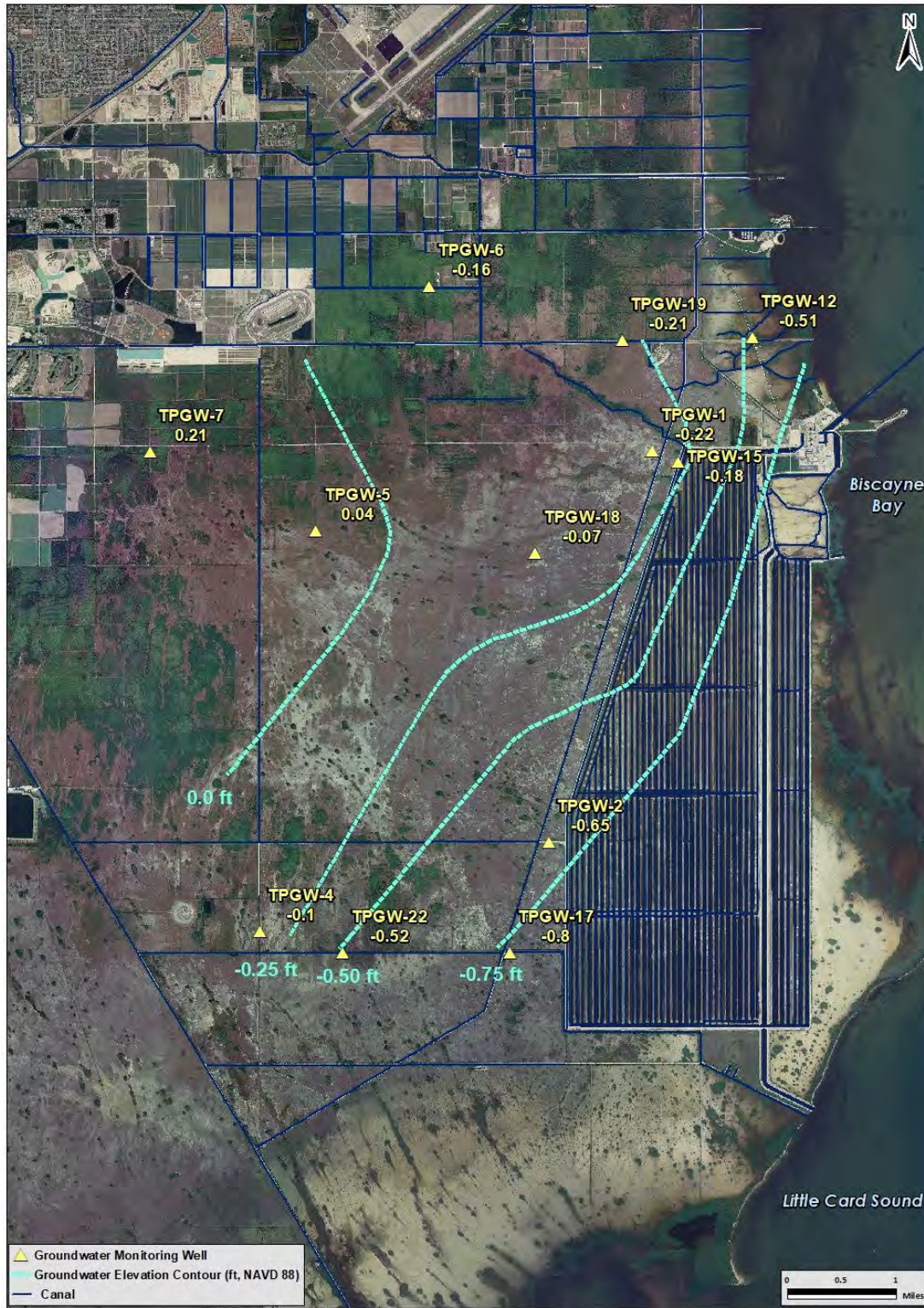
Figure 3.4-1. Dry Season Water Level Contour Map (April 1, 2022)

Figure 3.4-2. Wet Season Water Level Contour Map (September 24, 2021)

4 CONTINUOUS SURFACE ELECTROMAGNETIC MAPPING SURVEY SUMMARY

Year 4 CSEM survey results were compared against the 2018 baseline survey and indicate net westward migration of the hypersaline plume has been halted and the volumetric extent has been reduced by 67% after four years of RWS extraction.

4.1 INTRODUCTION

Pursuant to the FDEP CO requirements of paragraph 29.a., MDC CA paragraph 17.d.iii, and as requested in item 3.b. in a letter provided to FPL by MDC dated May 15, 2017, FPL conducted the 2018 baseline CSEM survey from March 31 to April 6, 2018, using aerial electromagnetic (AEM) methods (described in ENERCON 2016). As AEM is the methodology employed for the CSEM surveys, the acronym will be used when referring to the survey processes, procedures, and data. The purpose of the 2018 baseline survey was to map the hypersaline plume west and north of the FPL property adjacent to Turkey Point prior to the initiation of RWS operations.

Paragraph 17(d)(iii) of the MDC CA and paragraph 29(b) of the FDEP CO required that an AEM survey be conducted 30 days after the first year of RWS operation, which was initiated on May 15, 2018. The first year AEM survey was conducted from May 24 through 26, 2019, and the results were presented in the November 15, 2019, Remedial Action Annual Status Report (RAASR). Due to restrictions on international travel and health risks associated with the COVID-19 pandemic, collection of the Year 2 survey data was delayed from the originally scheduled May 2020 timeframe until September 26–27, 2020. The Year 3 survey was conducted June 18–22, 2021, and data acquisition for the Year 4 survey (the subject of this report) occurred May 19–20, 2022.

Information on data collection, data analysis, error assessment, three-dimensional (3D) mapping of the distribution of hypersaline chloride concentrations within the Biscayne aquifer and comparisons of the 2022 results with those of the 2018 baseline AEM survey are provided in the following sections and detailed in the *Report on Advanced Processing and Inversion of 2022 AEM Survey Data and Derived Chloride Concentrations near the Turkey Point Power Plant, Southern Florida* provided by AGF (Appendix G). Plan and profile color-flood maps of bulk resistivity and AEM-derived chloride concentrations for the 2018 and 2022 surveys and 3D chloride views are provided in Appendices F (2018 baseline) and G (Year 4, 2022). Year 4 AEM data confirms prior documentation that there is no net westward movement in the leading edge of the hypersaline plume. The data also demonstrate a statistically significant reduction of

67% in the volume of the hypersaline Biscayne aquifer materials in 2022 as compared to 2018. In addition, there is no CCS-sourced hypersaline water in layers 1 through 4 (upper 15 feet of the aquifer) west of the L-31E canal and north of the FPL property; and there has been net retractions in the western and northern extent of the CCS-sourced hypersaline plume in layers 5 through 14.

4.2 APPROACH AND METHODS

To collect transient AEM data, an electrical current is sent through a large loop of wire consisting of multiple turns which generates an electromagnetic (EM) field. The EM field switches off and on at rapid rates. When the EM field is generated, it passes into the ground where it dissipates and decays with time, traveling deeper and spreading wider into the subsurface. The rate of dissipation is dependent on the electrical properties of the subsurface and is controlled by the material composition of the geology, including the amount of mineralogical clay, the water content, the presence of dissolved solids, and the percentage of void space. At the moment the EM field is turned off, a secondary EM field, which also begins to decay, is generated within the subsurface. The decaying secondary EM field generates a current in a receiver coil. This current is measured at several different moments in time, each moment being within a time band called a "time gate." From the induced current, the time rate of decay of the magnetic field, B, is determined (dB/dt). When compiled in time, these measurements constitute a "sounding" at that location. Short time measurements present data on near-surface conditions while longer timed measurements collect data from greater depths below land surface. Thus, data on the decay of the magnetic field over multiple progressively longer time bands break up each sounding into sequential depth layers. By maintaining a consistent elevation of the transmitter/receiver (minor flight elevation variations are adjusted during post-processing), and using consistent time gates, the thickness of each individual earth layer derived from the field data is constant across the surveyed area relative to the land surface, with layer thickness being thinnest near the surface while deeper layers average data over progressively greater thicknesses. Additional details of data acquisition and processing are contained in the 2022 Aqua Geo Frameworks, Inc. (AGF) report (Appendix G).

The AEM survey area encompasses approximately 30 square miles of mostly wetlands located to the west and north of the CCS. Figure 4.2-1 presents Turkey Point, the CCS, the survey area and compliance boundary, monitoring well sites used to correlate chloride concentrations, and 2022 AEM survey flight lines.

Figure 4.2-1. 2022 AEM Survey Area, Flight Lines, Monitoring Well Locations and Designation of Compliance Area Boundary (Black Line)

The 2022 AEM survey was performed using the same airborne platform and EM technique used for the 2018 through 2021 surveys: a helicopter-borne transient EM (TEM) system developed and implemented by SkyTEM Canada, Inc. (SkyTEM) that provided nearly continuous (i.e., one sounding every 6 feet along each flight line) EM survey data within the coverage area. The geophysical data are collected using TEM sounding equipment suspended from an airborne platform flown along prescribed flight lines (transects) over the target area. In this application, the individual transects primarily run from west to east with north to south tie lines (as shown in Figure 4.2-1) and cover the entire region of interest.

The AEM survey measures bulk resistivity of the ground. For water-saturated materials, bulk resistivity, or its inverse, bulk conductivity, is principally determined by pore fluid conductivity and porosity. When pore water chloride ion content is high, bulk conductivity and fluid conductivity have a nearly 1:1 relationship. This allows the measurement of fluid conductivity from bulk resistivity or conductivity values obtained from geophysical surveys. Consequently, the high electrical conductivity of saline groundwater makes it an excellent target for electrical geophysical methods. Due to lithologic effects, the relationship between bulk electrical properties and fluid conductivity must be calibrated with local water quality data. ENERCON established a relationship for the Biscayne aquifer near the CCS during performance of the proof of concept 2016 AEM survey as reported in *PTN Cooling Canal System, Electromagnetic Conductance Geophysical Survey, Draft Final Report, Florida Power and Light Turkey Point Power Plant* (ENERCON 2016). ENERCON supplemented those data with the 2018 baseline AEM survey and 2018 water quality data as presented in Appendix G of the Recovery Well System Startup Report (FPL 2018a) and amended the reported hypersaline volumes as described in Section 4.2 of this report. The relationship between bulk AEM resistivity and laboratory chloride content was developed for the 2022 data sets as described in Section 4.2.3 below. The process conducted by ENERCON to assess the vertical and horizontal extents of a hypersaline plume in the Biscayne aquifer in the vicinity of the CCS is similar to the USGS method previously conducted for the Biscayne aquifer (Prinos et al. 2014).

4.2.1   Data Acquisition and Field Processing

Airborne EM data acquisition was conducted by SkyTEM during May 19–20, 2022. As changes in hypersaline extent over time are based on comparisons between baseline and current EM survey responses, multiple steps are taken prior to, during, and immediately after AEM field acquisition flights to help ensure consistent data acquisition and processing from year to year. Steps to provide consistency in the data include the following:

- **Use of consistent hardware.** The EM304 hardware and software has been consistently used since 2016. Since AEM systems go through constant updates and replacements that may complicate direct comparisons, SkyTEM has dedicated the EM304 unit used in our studies for use over the entire 10-year project. All software updates are provided to AGF who evaluate impacts to consistency of annual surveys. Adjustments to data processing are made and documented if software changes would otherwise result in inconsistency between survey years.

- **Implement consistent flight plans.** Prior to flights, the detailed flight plan is reviewed with the pilot. The flight plan details flight line locations, ground speed, elevations, flight direction, ground hazards such as powerline locations, and any areas of potential EM interference. Attention and care are given to attempt to fly as close as practical the same flight path as 2018. In addition, as described in Appendix G, constant details of flight conditions, global positioning system (GPS) locations, altimeter, tilt, fight speed, etc. are recorded and reviewed after each flight. If any flight lines are found to fall out of consistency specifications, the out-of-spec flight lines are re-flown.

- **Equipment calibration.** Prior to deployment of the EM304 system hardware to the site, it is calibrated to a ground test site in Lyngby, Denmark. After delivery to the Turkey Point site, the calibration is verified through a series of test flights that include measurement of the transmitter waveforms, verification that the receiver is properly located in a null position, and verification that all positioning instruments were functioning properly. A high-altitude test, used to verify system performance, is also conducted prior to the beginning of the survey's production flights.

- **In-field preliminary data verification and review.** Raw flight data are transmitted upon landing to AGF for verification and quality control. If flight data were found to fall outside quality specifications, the flight segment would be re-flown and verified before proceeding to the next flight segment. This field-based quality control protocol helps ensure that the field data are complete and verified prior to completing the airborne data acquisition phase of the survey. In addition, a review of acquired raw data by SkyTEM in Denmark for primary field compensation (PFC) is conducted prior to continued data processing by AGF (Schamper et al. 2014). The primary field of the transmitter affects the recorded early time gates, which in the case of the Low Moment measurements (LM), are helpful in resolving the near-surface resistivity structure of the ground. The LM uses a sawtooth waveform which is calculated and used in the PFC correction to correct the early time gates.

Multi-zoned groundwater monitoring wells (Figure 4.2-1) were sampled during June 2022, and samples were analyzed for dissolved chloride using procedures and methods described in the approved Turkey Point QAPP (FPL 2013). The water quality data were used in the calibration and conversion of the AEM data to chloride concentrations. In addition, continuous borehole induction logging was conducted by USGS from the deepest monitoring well at each monitoring well site during March 2022 and were used as an independent comparison and verification of the airborne resistivity data.

Following data acquisition by SkyTEM, the field data were delivered directly to AGF for post-processing. The AGF-ENERCON team conducted the data processing, interpretations, method calibration, data correlations with monitoring well induction logs and water quality, and prepared the survey reports. At each sounding along a flight line, the theoretical field response of a layered earth model was calculated and compared to the actual field data and adjacent data points. The resistivities of the model layers were adjusted until the differences between the calculated (model) response and the observed field response were minimized. This spatial

averaging produced laterally-constrained inversions (LCIs) and spatially-constrained inversions (SCIs) of the data collected. AGF produced LCIs and SCIs of collected data with the SkyTEM system during daily flight operations to verify and confirm the functionality of the SkyTEM system and eliminate drift or calibration concerns. These inversions were conducted using the Aarhus University Geophysics Workbench software that allowed for editing of the AEM data to remove EM couplings (i.e., noise) from power lines and pipelines. AGF also provided integration of continuous borehole induction log data as a qualitative check against field resistivity data. The inversions were then combined into an electrical resistivity model of the area which generates calibrated resistivity estimates for the survey area along each flight line.

Table 4.2-1 lists the thicknesses of the layers within the AEM model, including the upper 14 layers that account for the estimated thickness of the Biscayne aquifer in the area based on USGS maps (Fish and Stewart 1991). Layer thicknesses increase with depth as AEM resolution decreases. Layer 1 has a thickness of about 3 ft, while layer 14, with a bottom depth of approximately 100 ft, has a thickness of about 13 ft. The data in this AEM survey were inverted at each sounding, converted into two-dimensional (2D) resistivity plan view sections versus depth and displayed as resistivity profiles by layer. The plan and profile views of the AEM resistivity model for the 2022 survey are presented in Appendix G-2 and G-3.

4.2.2   Quality Control of the AEM Data Inversion

4.2.2.1   Magnetic Field Noise

The raw field data acquired along flight lines are filtered and processed to improve data quality and reliability. The data are converted to a uniform transmitter coil height above the ground using the helicopter altimeter data, and a GPS location is determined for each data point. An analysis is made of background EM interference (noise) that originates from sources such as thunderstorms, large electrical motors, and power lines. Data points that are "too noisy" (i.e., where the signal is obscured by excessive background interference to a degree the data are unreliable) are "blanked" and not included in the data inversion. The data are examined for spikes that occur over pipelines and other conductive objects. The spikes are also blanked. Figure 4.2-2 shows the locations of the decoupled and removed data (red lines) along the AEM flight lines and the data used in the inversion (blue lines) in the 2022 project area. A noisy area near the RWS appeared during the 2019 survey. The noise was presumed to be associated with power delivery and operation of the RWS electric pump motors. As recommended in the 2019 report, the RWS was temporarily shut down during acquisition of the 2020 through 2022 AEM data. The result was a quieter EM setting for these surveys, resulting in less filtering and interpolation than in 2019.

Table 4.2-1.   Thickness and Depth to Bottom for each Layer in the AEM Model

Layer	Depth to Bottom (m)	Thickness (m)	From (ft)	To (ft)	Thickness (ft)
1	1.0	1	0	3.3	3.3
2	2.1	1.1	3.3	6.9	3.6
3	3.3	1.2	6.9	10.8	3.9
4	4.7	1.4	10.8	15.4	4.6
5	6.2	1.5	15.4	20.3	4.9
6	7.9	1.7	20.3	25.9	5.6
7	9.8	1.9	25.9	32.1	6.2
8	11.9	2.1	32.1	39.0	6.9
9	14.2	2.3	39.0	46.6	7.5
10	16.8	2.6	46.6	55.1	8.5
11	19.7	2.9	55.1	64.6	9.5
12	22.9	3.2	64.6	75.1	10.5
13	26.4	3.5	75.1	86.6	11.5
14	30.3	3.9	86.6	99.4	12.8
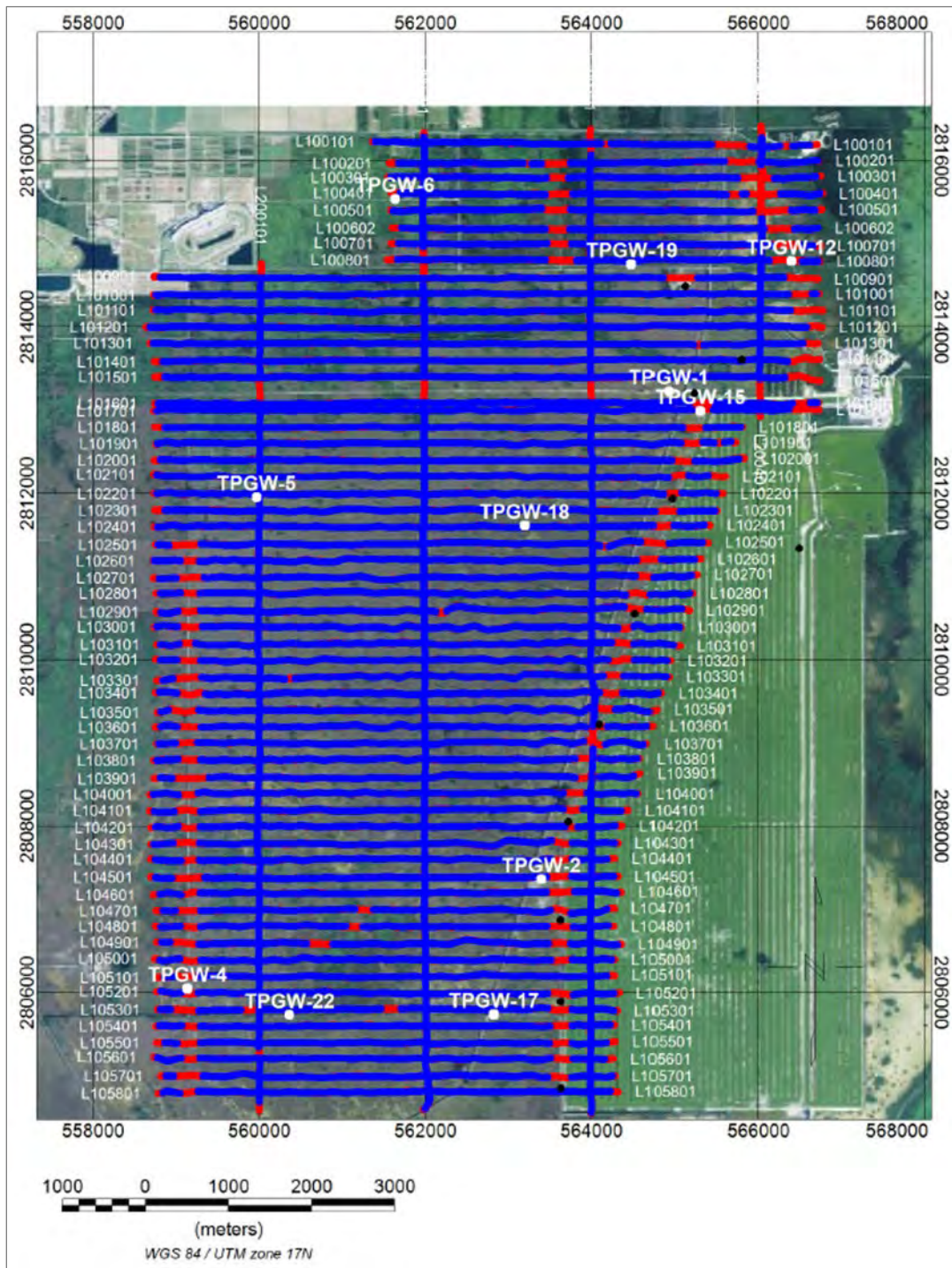
Figure 4.2-2. Locations of the Decoupled and Removed Data (Red Lines) Along the AEM Flight Lines and the Data Used in the Inversion (Blue Lines)

4.2.2.2   Resistivity Model Verification

Continuous surface electromagnetic mapping resistivity measurements are generally in close agreement with U.S. Geologic Survey induction (resistivity) logs collected from monitoring wells within the survey boundaries. This, combined with the good calibration with chloride samples from multi-layered monitoring wells, provides an independent check on the efficacy of the EM data processing method in estimating groundwater salinity concentrations within the study area.

Borehole induction logging was conducted by the USGS at each deep well within the TPGW series monitoring sites located within the survey area. The induction logs were acquired with a single frequency EM logging tool that measures the bulk resistivity of the earth materials and pore fluids up to approximately 1 meter (m) outside the well bore. Details regarding the borehole induction logging and the result for each site are published in Appendix J of the 2022 Turkey Point Annual Monitoring Report (FPL 2022). The induction logs provide a continuous record of localized (i.e., tens of centimeters surrounding the borehole) EM electrical resistivity with depth at each well where the induction log data were obtained.

The layer inversions (resistivity model) from the AEM data were compared to the induction log data to verify that the parameters chosen in the AEM inversion software were producing layer resistivities that are in general agreement with the borehole induction logs. However, there are several differences between the two methods that make direct alignment of the data technically infeasible. Therefore, care needs to be taken when comparing results from the borehole induction logs and the AEM layer resistivities, as comparing trends is appropriate rather than attempting to match absolute resistivity values. Factors that prevent direct comparisons of resistivity values between the two methods include the following:

- **Differences in measuring geometry.** The AEM footprint is large compared to the data acquisition distances within centimeters of a borehole for induction logs. Accordingly, there are typically vertical differences between the location of the borehole screen and the associated AEM layer which provides data for the layer with thickness greater than the screened zone.

- **Lateral differences in data acquisition locations.** Not all wells are located on flight lines; but several wells that were close to or within a few hundred feet of a flight line were used in the verification.

- **Uncalibrated borehole logging tool.** The borehole logging tool is generally uncalibrated for the full range of resistivities measured in the survey area. Additionally, various logging tools have been used within the survey area leading to potential data biases.

AEM bulk resistivity inversion profiles were compared to induction logs obtained at wells TPGW-1, TPGW-2, TPGW-4, TPGW-5, TPGW-6, TPGW-12, TPGW-15, TPGW-17, TPGW-18, TPGW-19 and TPGW-22 shown in Appendix G-2. Where a TPGW monitoring well induction log was performed near an AEM flight line profile, the induction log resistivity is shown on the profile using the same color scale as the AEM resistivity. The bulk resistivity inversion profiles along each flight line generally compare well with the borehole induction logs, indicating that the inversion has produced estimates of the variation of bulk resistivity versus depth comparable to values obtained in observation wells. A detailed discussion of the USGS induction log/AEM resistivity comparison is presented in the 2022 AGF Report (Appendix G).

4.2.3   Conversion of AEM Resistivity to Estimated Chloride Concentrations of Ground Water

Quarterly water quality data from the TPGW monitoring wells were used to develop an equation for conversion of AEM resistivity to equivalent groundwater chloride concentration (i.e., chlorinity). The calculations used the relationship established between the June 2022 laboratory samples for the TPGW wells (Table 4.2-2) and AEM resistivity. Normal seawater has a salinity of about 34 PSU and will have a chlorinity of about 19,000 milligrams per liter (mg/L). The CO, paragraph 8, and CA, paragraph 9, delineate 19,000 mg/L of chloride to be the boundary between normal salinity seawater and hypersaline groundwater. Chloride concentrations greater than 19,000 mg/L equate to standard seawater salinity greater than 34.32 PSU.

The calibration of the AEM data was conducted using a two-step approach, similar to that presented in Fitterman and Prinos (2011) and Fitterman et al. (2012). First, a mathematical relationship was established between AEM resistivity and the resistivity of groundwater samples from discrete depth intervals in the TPGW monitoring wells (water resistivity is the inverse of specific conductance). The mean values of the AEM resistivity sounding located within a 175-m radius (574 ft) of each corresponding TPGW monitoring well were selected to develop a statistical range in bulk resistivities for the AEM model layer that was at an equivalent depth to the screened intervals in the TPGW wells.

Table 4.2-2.   June 2022 Water Quality Data from TPGW Wells

Well ID	Well Screen (from Top of Casing)				CI (mg/L)	Salinity (PSU)	Specific Conductance (µS/cm)
	From (ft)	To (ft)	From (m)	To (m)			
TPGW-1S	32.00	34.00	9.76	10.37	9,650	18.28	29,601
TPGW-1M	52.10	54.10	15.88	16.49	23,700	43.58	64,475
TPGW-1D	85.30	89.30	26.01	27.23	26,700	47.83	69,913
TPGW-2S	27.97	31.97	8.53	9.75	15,300	28.24	43,898
TPGW-2M	53.88	55.88	16.43	17.04	28,500	50.99	73,997
TPGW-2D	88.79	90.79	27.07	27.68	29,000	52.12	75,380
TPGW-4S	23.20	25.20	7.07	7.68	2,520	5.08	9,116
TPGW-4M	38.10	43.10	11.62	13.14	14,300	26.45	41,343
TPGW-4D	61.60	65.60	18.78	20.00	14,700	27.31	42,535
TPGW-5S	28.60	32.60	8.72	9.94	138	0.46	933
TPGW-5M	49.30	54.30	15.03	16.55	9,540	17.87	28,975
TPGW-5D	67.00	72.00	20.43	21.95	12,600	23.33	36,900
TPGW-6S	25.09	27.09	7.65	8.26	263	0.73	1,453
TPGW-6M	51.61	55.61	15.73	16.95	7,870	14.79	24,410
TPGW-6D	84.70	88.70	25.82	27.04	8,290	15.25	25,063
TPGW-12S	25.19	27.19	7.68	8.29	18,400	33.52	51,161
TPGW-12M	59.21	63.21	18.05	19.27	19,900	35.83	54,259
TPGW-12D	93.24	97.24	28.43	29.65	24,700	45.27	66,655
TPGW-15S	24.32	29.32	7.41	8.94	12,800	23.30	37,003
TPGW-15M	44.39	49.39	13.53	15.06	25,700	46.23	68,050
TPGW-15D	79.31	84.31	24.18	25.70	27,600	49.84	72,666
TPGW-17S	32.11	37.11	9.79	11.31	20,300	36.95	55,776
TPGW-17M	49.95	54.95	15.23	16.75	24,400	43.90	64,903
TPGW-17D	86.81	91.81	26.47	27.99	26,500	47.58	69,644
TPGW-18S	35.25	40.25	10.75	12.27	2,230	4.62	8,330
TPGW-18M	63.25	68.25	19.28	20.81	19,600	39.91	59,647
TPGW-18D	84.27	91.27	25.69	27.83	22,000	39.48	59,076
TPGW-19S	27.37	31.37	8.34	9.56	1,160	2.45	4,601
TPGW-19M	48.39	52.39	14.75	15.97	19,200	35.65	53,961
TPGW-19D	84.35	89.35	25.72	27.24	22,800	40.93	60,952
TPGW-22S	29.00	32.00	8.84	9.75	14,900	27.76	43,156
TPGW-22M	54.00	57.00	16.46	17.37	20,900	37.25	56,083
TPGW-22D	69.00	72.00	21.03	21.94	20,400	37.59	56,532

4.2.3.1   Year 2022 Chloride Conversion

The 2022 AEM chloride conversion process is described in detail in Appendix G, including details of the conversion process and calibration data sets used during previous surveys. The process is summarized below.

The 2022 water quality data, using the baseline or "core" 24 monitoring well set, were plotted on a log-log plot with the mean AEM resistivity value from the analogous resistivity model layer on the x-axis and the corresponding groundwater sample resistivity on the y-axis. A regression equation was fitted to the plot producing a power function of the form:

$$Water\ Resistivity = 0.12038 \cdot (AEM\ Resistivity)^{1.194945} \qquad (1)$$

with $R^2 = 0.826$ (Figure 4.2-3). R^2 is the percent of the variance in the dependent variable (i.e., water resistivity) explained by the variance of the independent variable (i.e., AEM resistivity). The value of the Pearson correlation coefficient, r, is the square root of R^2. For an R^2 of 0.83, r is 0.91. For the number of samples, n, equal to 24, the significance of r is $p < 0.0001$ indicating that the regression between water resistivity and AEM resistivity is highly significant statistically.

The second step in the calibration process is to mathematically relate laboratory chloride to field measured borehole water resistivity. As chloride concentration increases, water resistivity decreases. In groundwater influenced by seawater, the dominant and most conductive ions are chloride and sodium. The chloride ion comprises 55% of the TDS of seawater, so it is expected that there will be a statistically strong relationship between water resistivity and chloride ions. Again, a log-log plot is constructed with water resistivity of well samples on the x-axis and chloride concentration of well samples on the y-axis.

A regression equation is fitted to the data and has the form:

$$Chloride\ Concentration = 2{,}639.6 \cdot (Water\ Resistivity)^{-1.19036} \qquad (2)$$

with $R^2 = 0.99$ (Figure 4.2-4). For a sample number of 24, the statistical significance of the correlation coefficient for the regression equation is $p < 0.0001$. Equations (1) and (2) are combined to form an equation that defines chloride concentration as a function of AEM resistivity. This equation is then used to convert AEM resistivity to chloride concentration.
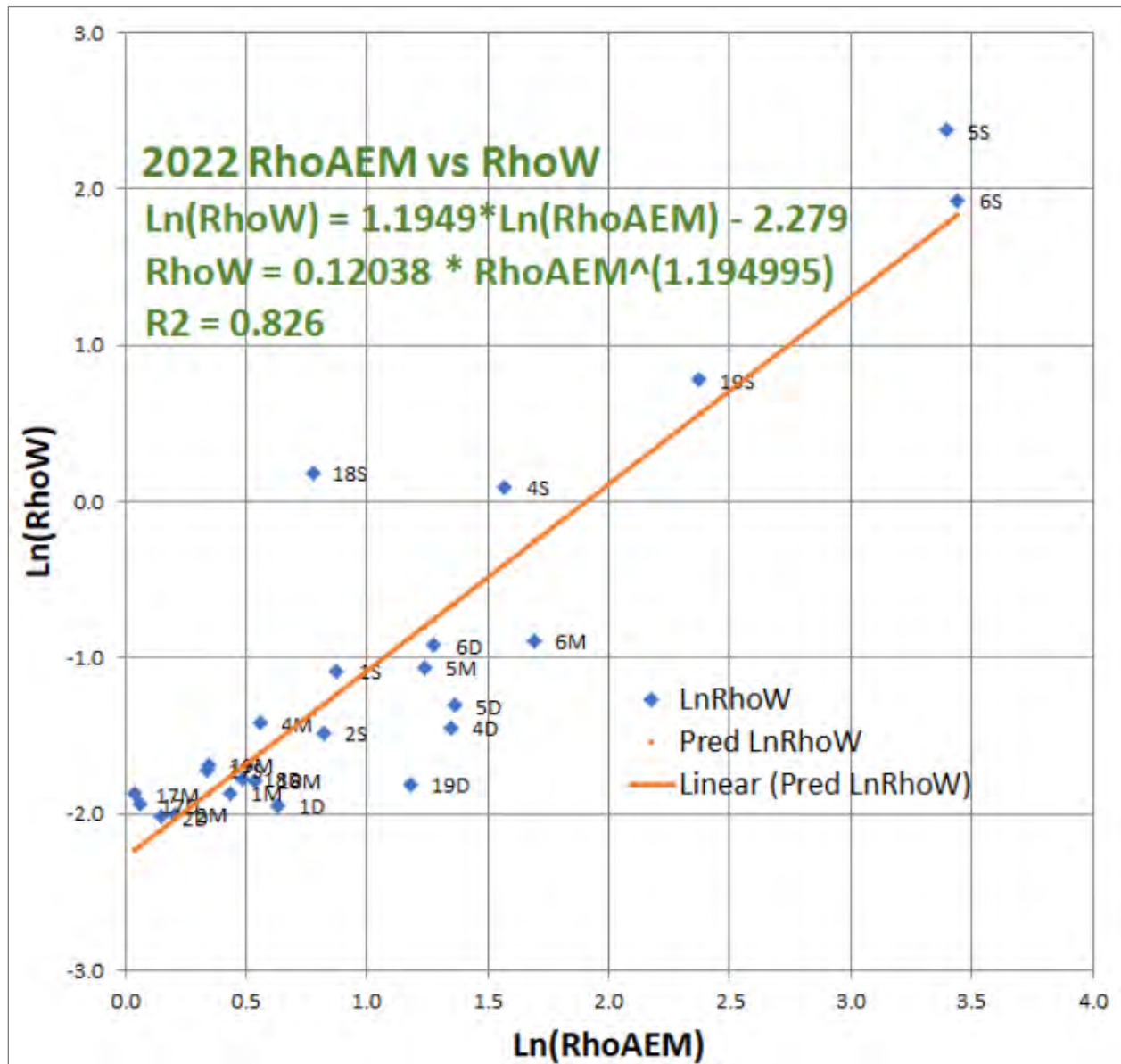
Figure 4.2-3. Comparison of 2022 Field Water Resistivity (RhoW) versus AEM Resistivity (RhoAEM)
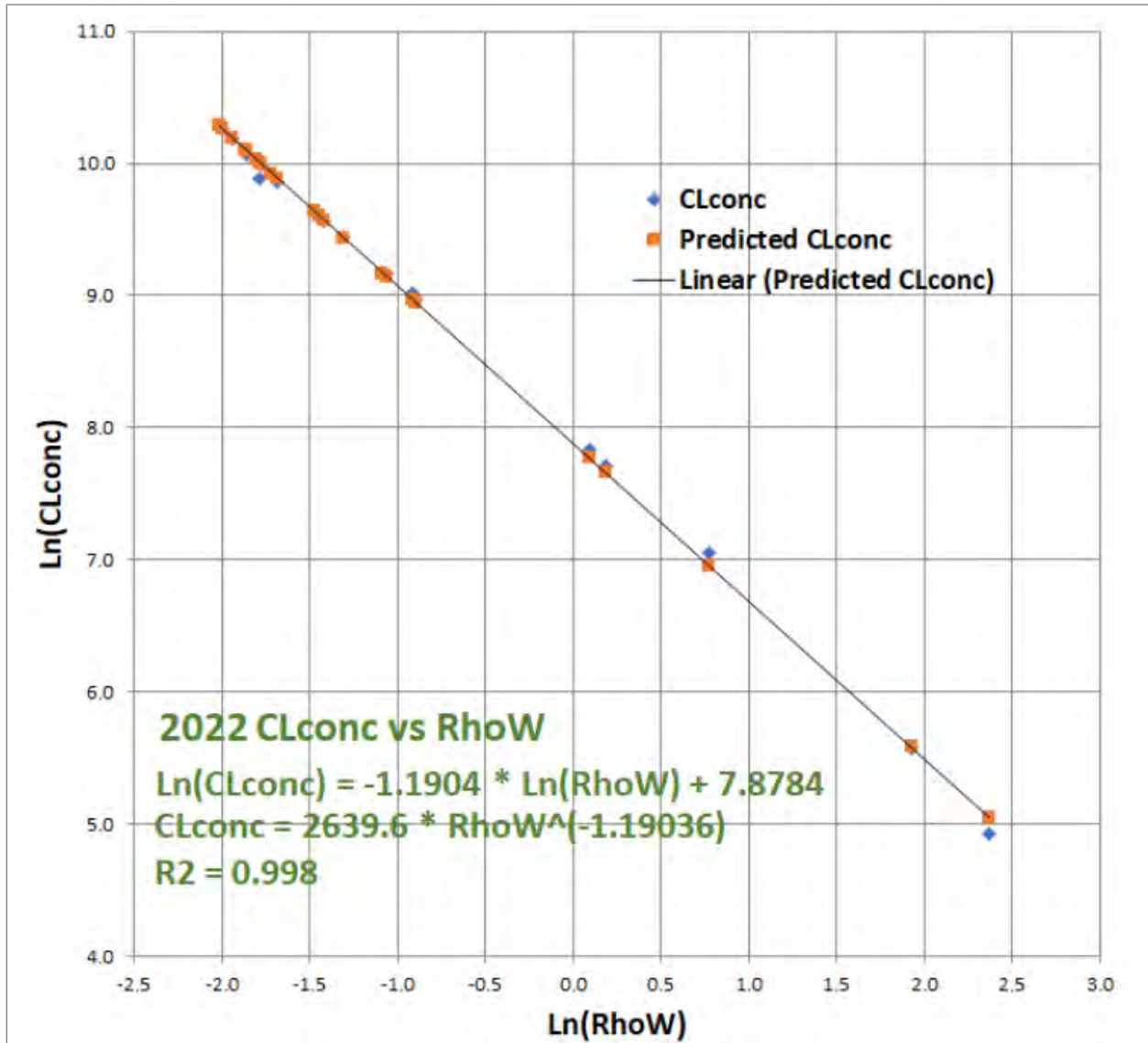
Figure 4.2-4. Comparison of 2022 Field Water Resistivity (RhoW) versus Laboratory Chloride Concentration (CLconc)

The correspondence of chloride concentration calculated from AEM resistivity and laboratory-determined values of chloride concentration from TPGW wells is graphically illustrated by superimposing the TPGW well-derived chloride values on AEM-derived chloride concentration versus depth profiles, using the same color-coded contour intervals (Appendix G, Attachment 3). On the vertical profiles, the agreement between the AEM predicted chloride value and the chloride value obtained from samples taken from the monitor wells can be visually compared. A quantitative comparison between AEM-estimated chloride and laboratory-determined chloride at monitor wells is found in Table 4.2-3. Note that the sample area of each AEM-estimated chloride value is different in every case from the corresponding sample area of the monitoring well. Accordingly, at any given point, the correspondence is affected by many factors, including porosity variations, the location of the screened interval with respect to the assigned AEM layer, distance between monitoring well locations and flight lines, EM noise, and the documented wide range of vertical variability in bulk conductivity documented in the borehole induction logs.

Monitoring well chloride data collected in 2022 are also posted on the 2022 AEM color-flood depth layers for comparison (Appendix G, Attachment 4). The monitoring well data are posted only on applicable AEM layers where the well screened interval is contained within the layer. Monitoring well chloride data for well screens that are at or across a layer interface are posted on both layers. As discussed in Appendix G, although TPGW-12, TPGW-15, and TPGW-22 chloride values were not included in the AEM calibration data set (Section 4.2.3.3), they are posted on the appropriate AEM layer maps as a means to compare AEM-derived chloride with laboratory chloride from these wells.

Monitoring well data are from the Biscayne aquifer only. Consequently, the calibrated equation relating AEM resistivity to groundwater chloride concentrations is constrained to the data collected from the CA/CO network of monitoring wells. For this reason, use of this empirically derived relationship between AEM resistivity and chloride concentrations should not be applied to AEM resistivities from geologic units below the Biscayne aquifer not monitored under the CA/CO monitoring network.

4.2.3.2   AEM Layers and High Flow Zones

Monitoring wells within and surrounding Turkey Point are constructed into high permeability zones in the upper, middle, and lower Biscayne aquifer that are based on review of pilot well lithologic and borehole geophysical data. As the elevations of the screens in the monitoring wells vary in depth and the elevations of the AEM layers are constant across the survey area, the AEM layers that represent the upper, middle, and lower flow zones of the Biscayne aquifer can vary. Table 4.2-3 lists the TPGW monitoring wells screen interval depths, corresponding AEM layer, June 2022 monitoring well chloride values and the estimated chloride value for the analogous AEM layer. For example, the upper flow zone is present in AEM layers 6 through 8, the middle flow zone is present in AEM layers 10 and 11, and the lower flow zone is present in AEM layers 12 through 14. The three AEM layers that include the most upper, middle, and lower monitoring well intervals are AEM layers 7, 10, and 14, respectively.

Table 4.2-3.   Correspondence Between TPGW Screened Zones and the AEM Model Layer – 2022 Data

Well ID	Depth Below Land Surface				2022 Chloride (mg/L)	CSEM Model Layer	CSEM Estimated Layer Cl (mg/L)
	From (m)	To (m)	From (ft)	To (ft)			
TPGW-4S	7.1	7.7	23.2	25.2	2,500	6	3,524
TPGW-15S	7.4	8.9	24.3	29.3	12,800	6	2,216*
TPGW-6S	7.6	8.3	25.1	27.1	263	6	245
TPGW-12S	7.7	8.3	25.2	27.2	18,400	6	21,410*
TPGW-2S	8.5	9.7	28.0	32.0	15,300	7	10,223
TPGW-5S	8.7	9.9	28.6	32.6	138	7	262
TPGW-6S	7.6	8.3	25.1	27.1	263	7	245
TPGW-15S	7.4	8.9	24.3	29.3	12,800	7	2,216*
TPGW-19S	8.3	9.6	27.4	31.4	1,160	7	1,119
TPGW-22S	8.8	9.8	29.0	32.0	14,900	7	6,503
TPGW-1S	9.8	10.4	32.0	34.0	9,650	8	9,445
TPGW-17S	9.8	11.3	32.1	37.1	20,300	8	20,331
TPGW-18S	10.7	12.3	35.3	40.2	2,230	8	10,900
TPGW-4M	11.6	13.1	38.1	43.1	14,300	9	14,801
TPGW-18S	10.7	12.3	35.3	40.2	2,230	9	10,900
TPGW-15M	13.5	15.1	44.4	49.4	25,700	9	16,304*
TPGW-15M	13.5	15.1	44.4	49.4	25,700	10	16,304*
TPGW-1M	15.9	16.5	52.1	54.1	23,700	10	17,753
TPGW-2M	16.4	17.0	53.9	55.9	28,500	10	24,441
TPGW-5M	15.0	16.6	49.3	54.3	9,540	10	5,660
TPGW-6M	15.7	17.0	51.6	55.6	7,870	10	2,949
TPGW-17M	15.2	16.8	50.0	55.0	24,400	10	31,030
TPGW-19M	14.8	16.0	48.4	52.4	19,200	10	20,126
TPGW-22M	16.5	17.4	54.0	57.0	20,900	10	14,623
TPGW-12M	18.1	19.3	59.2	63.2	19,900	11	20,331*
TPGW-4D	18.8	20.0	61.6	65.6	14,700	11	4,831
TPGW-22M	16.5	17.4	54.0	57.0	20,900	11	14,623
TPGW-4D	18.8	20.0	61.6	65.6	14,700	12	4,831
TPGW-5D	20.4	22.0	67.0	72.0	12,600	12	4,734
TPGW-18M	19.3	20.8	63.3	68.3	19,600	12	15,296
TPGW-22D	21.0	21.9	69.0	72.0	20,400	12	8,428
TPGW-15D	24.2	25.7	79.3	84.3	27,600	13	25,618*
TPGW-1D	26.0	27.2	85.3	89.3	26,700	13	13,367
TPGW-6D	25.8	27.0	84.7	88.7	8,290	13	5,348
TPGW-18D	25.7	27.8	84.3	91.3	22,000	13	16,375
TPGW-19D	25.7	27.2	84.3	89.4	22,800	13	6,123
TPGW-1D	26.0	27.2	85.3	89.3	26,700	14	13,367
TPGW-2D	27.1	27.7	88.8	90.8	29,000	14	26,566
TPGW-6D	25.8	27.0	84.7	88.7	8,290	14	5,348
TPGW-17D	26.5	28.0	86.8	91.8	26,500	14	30,200
TPGW-18D	25.7	27.8	84.3	91.3	22,000	14	16,375
TPGW-19D	25.7	27.2	84.3	89.4	22,800	14	6,123
TPGW-12D	28.4	29.6	93.2	97.2	24,700	14	20,331*

Note: AEM-derived Cl produced from average resistivity within 175 m radius of borehole and converted to Cl using regression equation.
* TPGW-12 and TPGW-15 AEM estimated chloride data are calculated from nearest Cl voxel due to locations within EM noise.

4.2.3.3   AEM System Response Shift

In the 2019 RAASR, the AGF-ENERCON team considered using the regression equations derived from the 2016 and 2018 data in the two-step process to convert 2018 AEM bulk resistivity values to estimated pore water chloride content for defining the baseline hypersaline spatial extent and volume prior to initiation of the RWS remediation to be used as the basis of comparison for all subsequent annual AEM surveys. An inherent assumption of this approach is that the AEM instrument response to a given bulk earth resistivity does not change over time or from survey to survey; and by compounding AEM resistivity versus chloride data over progressively more years, the expanded data set would reduce uncertainty in the regressions. The SkyTEM system firmware and software are frequently updated to reduce noise, improve signal to noise ratios, and provide better resolution of the resistivity of very shallow layers. While the AEM instruments are calibrated at a test site, there may be small changes from year to year in the instrument response to a given earth resistivity. These changes may fall below the SkyTEM calibration criterion for the instrument which is more commonly used for mineral exploration with greater resistivity contrast.

In 2020, after accumulating two years of survey data, FPL independently began conducting evaluations of the potential for system drift in resistivity response. Additionally, a review by MDC (Arcadis 2020) of the 2019 AEM survey, recommended that a procedure be implemented to evaluate and reduce the effects of any year-to-year variations in the instrument response to a given earth resistivity. To determine whether there had been any change in instrument response, an analysis was conducted of the change in the AEM bulk resistivity value that correlates to an estimated pore water chloride value of 19,000 mg/L from 2018–2022 on the basis of the regression equations specifically developed for each survey year which are based on that year's specific water quality and AEM data. The results indicate that there have been small and consistent changes in instrument responses over time (Table 4.2-4). To eliminate the effects of this instrument bias or shift, consistent with the MDC recommendation, the AEM survey results in each survey year are calibrated against water samples collected during that year. This procedure produces a unique AEM resistivity to chloride relationship for each survey, eliminating the consequences of any shift in SkyTEM system resistivity response that may occur from year to year.

Table 4.2-4.   AEM Resistivity Associated with 19,000 mg/L Chloride Listed by Survey Year

Survey Year	AEM Resistivity (ohm-m) at 19,000 mg/L
2022	1.4682
2021	1.6556
2020	1.7185
2019	1.8795
2018	2.0569

It is important to recognize that the systematic drift in resistivity does not affect the chloride model results, as each survey's unique resistivity field is correlated with chloride data collected near the time of the AEM survey. For each survey, the resistivity field is paired with the associated chloride data; and the chloride model is developed based on this unique relationship, which eliminates the effects of the resistivity drift in chloride space.

Accordingly, the AGF-ENERCON team used the 2022 calibration between 2022 AEM resistivity and 2022 water quality data to derive estimated pore water chloride values from AEM resistivity data. This procedure normalizes the instrument response from year to year, produces an independent AEM resistivity to chloride relationship, and allows a comparison of the 2022 survey year to 2018 baseline distribution of pore waters with chloride content >19,000 mg/L. This procedure was also used for the 2020 and 2021 surveys to address the recommendation provided by MDC (Arcadis 2020) to initiate a procedure to address any potential year-to-year variation in the response of the SkyTEM system. As the AEM-derived chloride distribution for each year is independently calculated, the system response drift does not impact the volume calculations or AEM-derived chloride distribution.

The 2018 baseline results used data obtained from both the 2016 proof of concept and the 2018 baseline surveys. To address year-to-year variation, AGF reprocessed the 2018 baseline data conversion using only 2018 water quality and bulk resistivity data (i.e, the 2016 data were excluded from the regressions to eliminate any impact of instrument drift). The resulting regression equation was very similar to the original. However, for consistency, a new 2018 baseline survey result was established to compare with the current annual AEM survey results. A comparison of the layer by layer and total volumetric differences between the 2018 baseline produced using 2016–2018 data regressions versus the 2018 year-specific regressions is shown in Table 4.2-5. As an example of how this change translates to the spatial extent of hypersaline groundwater on a layer-by-layer basis, Figure 4.2-5 shows the location of the 19,000 mg/L contour in model layer 7, resulting from both the original and new baseline data conversions. Maps of the comparisons between the original 2016–2018 baseline and the survey-specific (i.e., 2018 only) baseline for all layers are contained in Appendix G-7C.

In order to consistently address systematic drift in the baseline condition and subsequent years, the 2018 year-specific regression volumes for the 2018 baseline condition will be used in this report and for all subsequent reports.

Table 4.2-5   Comparison of 2018 Baseline Volumes Developed Based on 2016+2018 Water Quality Data and Volumes Produced Using 2018 Survey-Specific Water Quality Data

Layer	2018 Volume > 19,000 mg/L (m^3) Based on 2016+2018 Data	2018 Volume > 19,000 mg/L (m^3) Based on 2018 Survey Specific Data
1	1,920,000	1,930,000
2	2,026,000	2,047,500
3	1,587,000	1,644,500
4	858,000	923,000
5	2,595,500	2,508,500
6	12,672,000	12,304,000
7	22,896,000	22,572,000
8	20,480,000	20,480,000
9	33,770,000	33,440,000
10	68,281,500	67,399,500
11	92,840,000	92,207,500
12	89,822,500	89,029,500
13	63,181,000	63,817,500
14	43,050,000	43,540,000
Totals:	**455,979,500**	**453,843,500**
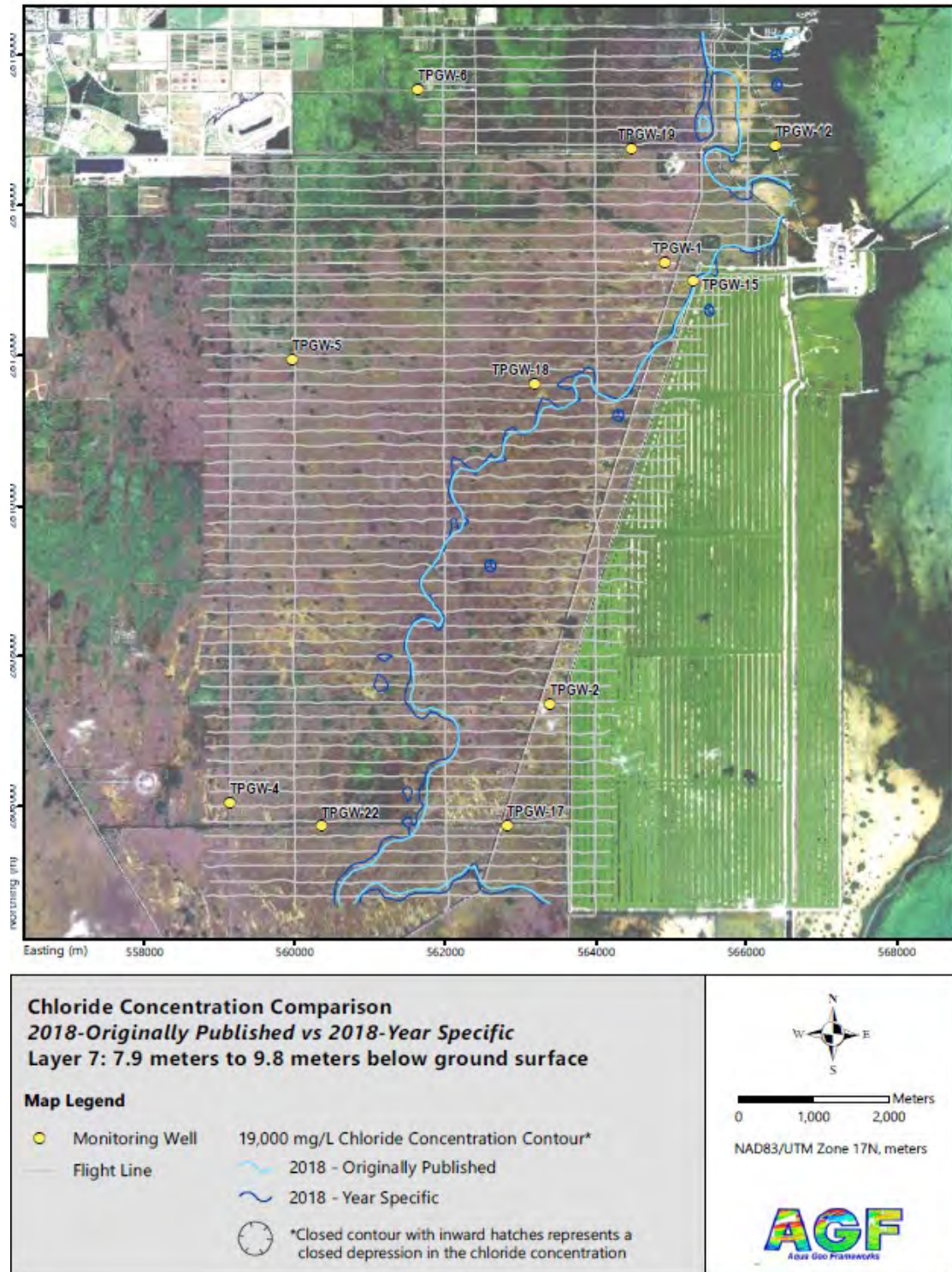
Figure 4.2-5. Layer 7 Comparison of Original 2016/2018 Baseline AEM-Derived 19,000 mg/L Chloride Contour and Contour Resulting From 2018 Year-Specific Data Set

4.2.3.4   The Calibration Data Set

> Introduction of monitoring data not included in the original 2018 baseline calibration data set results in shifts in the AEM resistivity versus pore water resistivity regression equation. Such shifts in the regression affect the hypersaline voxel volume, creating discontinuities between hypersalinity volumes calculated before and after any new monitoring station is added. To resolve this, annual volumetric hypersalinity calculations are based on regressions calculated using year-specific (i.e., survey-specific) pore water chloride data collected from a consistent set of 24 'core' monitoring wells.

An important objective of the AEM survey is to assess change in the volumetric extent of the hypersaline plume within the defined boundaries. To consistently assess the effect of the RWS on AEM-estimated hypersaline pore water volume, the year-to-year AEM survey calibration must use the same wells that were used in the baseline survey. These wells are considered the core monitoring well data set (sites TPGW-1, TPGW-2, TPGW-4, TPGW-5, TPGW-6, TPGW-17, TPGW-18, and TPGW-19 shallow, middle, and deep monitoring zones) and are used to form the regression equation converting AEM resistivity to AEM-derived chloride. Data obtained from any newly installed wells will be used in comparisons with borehole induction logs, on vertical profiles of AEM-estimated pore water chloride, and (x, y) contour and color-flood maps of AEM-estimated pore water chloride values.

An important underlying assumption related to the AEM bulk resistivity measurements is they are made without consideration for naturally occurring variations in porosity of earth materials. Said another way, the AEM surveys consider the Biscayne aquifer to be isotropic and homogeneous with respect to porosity. Porosity is an important factor in the saturated portion of the aquifer as pore spaces are filled with mineralized water that is a much better conductor of electricity than rock. Lithologies with high porosities and high percentages of water will produce lower AEM bulk resistivity measured values than the same lithology having low porosity, even if the chloride concentration is the same in both lithologies. As a result, it is possible that an AEM layer transect flown over an area with a constant chloride concentration and comprising a lithology that laterally transitions from low porosity to high porosity would produce a chloride map that shows chloride concentrations increase commensurate with increasing porosity even though the actual pore water chloride does not change. Areas like this are characterized as discontinuous lenses of elevated salinity that is not connected to a source of higher salinity. In addition, since rock porosity does not change significantly over time, such areas of apparent elevated salinity will not change, even though salinity levels in layers above or below will change in response to remediation actions. There appear to be such areas within the compliance area, most notably an area west of the southern portion of the CCS between the L-31E canal and Tallahassee Road in AEM layer 9.

An AEM resistivity versus monitor well fluid resistivity plot shows some wells plotting above and some below a regression trend line. Because porosity and well locations are fixed, those wells would consistently plot in the same geometric offset position relative to the regression line for each survey. This consistent offset or non-random error is what we observe in the year-

specific regression plots. Wells consistently plot in the same general geometric positions (Figure 4.2-6). If the error was random, we would expect the position of a given well to exhibit random scatter on the plot for multiple surveys. Since the pattern is consistent, we expect this to be representative of porosity differences among wells.

Newly installed wells may plot above or below the trend line affecting the regression equation and compromising the ability to compare against the baseline survey for which the new wells did not exist. Due to the relatively few data points available to develop the regression equation, any new data points that plot offset from the regression line carry a proportional weight in producing a change in the regression equation that cannot be reproduced in the 2018 baseline regression data.
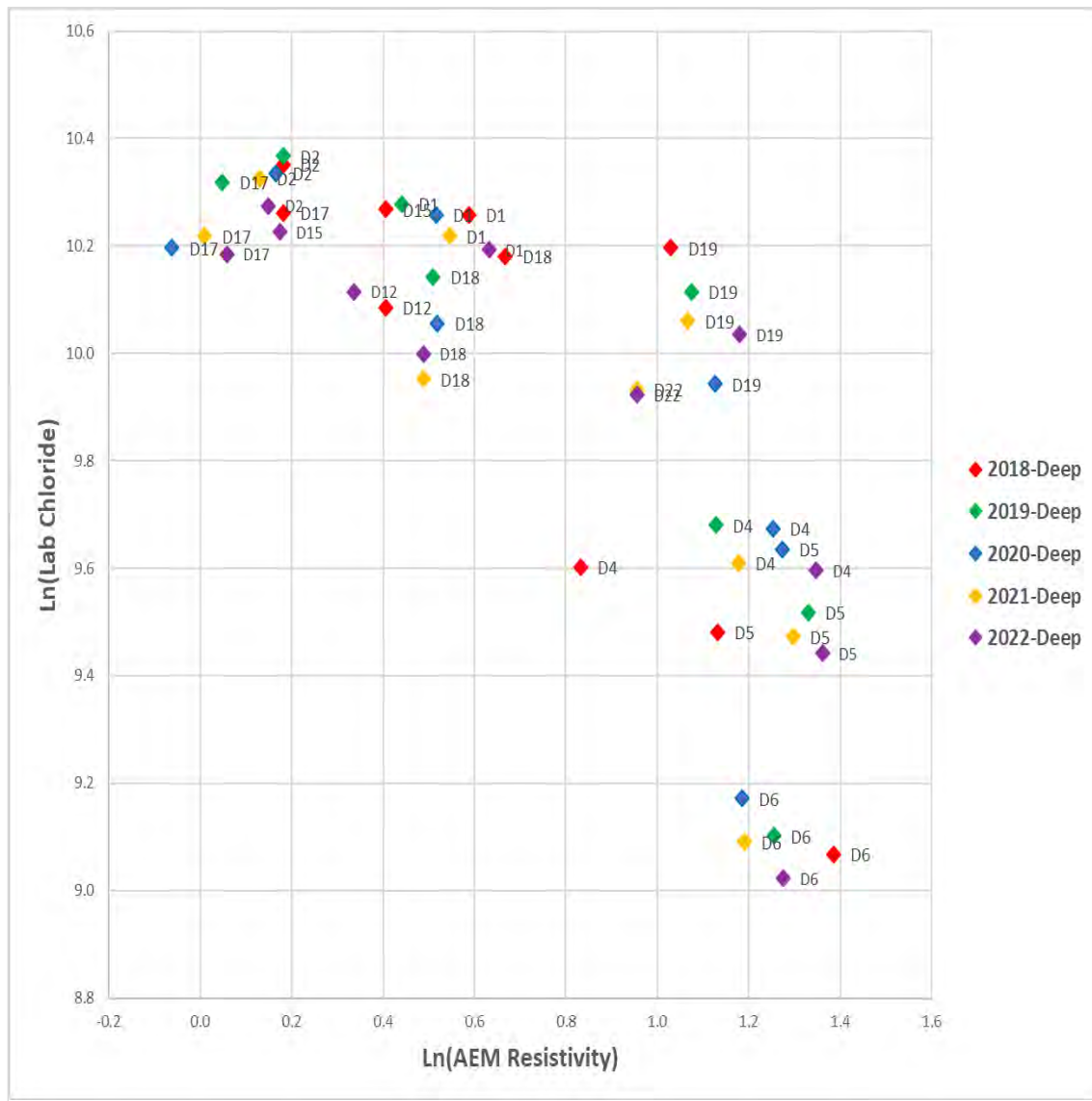
Figure 4.2-6. 2018-2022 Plot of Laboratory Chloride versus AEM Resistivity for Deep Well Screened Zones

4.2.4   Sources of AEM Method Uncertainty

The AEM results are used to map relative changes in the spatial extent and volume of the hypersaline plume both horizontally and vertically. Appendix G-7A shows the AEM 19,000 mg/L chloride contour lines produced from year-specific regressions for years 2018 and 2022. Statistically, the mapped position of the 19,000 mg/L contour is the most probable location of the 19,000 mg/L contour based on the year-specific data used to produce the laboratory derived versus AEM-estimated chloride regressions. However, the estimates of pore water chloride levels derived from AEM resistivity vary from measured chloride levels at discrete monitoring intervals. In addition to the differences in lateral and vertical locations of the comparative AEM and monitor well measurements and the wide range of vertical variability in bulk conductivity documented in the borehole induction logs, an important source of differences between AEM-estimated chloride and laboratory-determined chloride is the assumption of constant porosity. As discussed earlier, the equation that relates AEM bulk resistivity to chloride uses the regression equation derived from a plot of AEM bulk resistivity versus pore water resistivity measured at wells. This equation uses the best fit relationship between AEM bulk resistivity and measured pore water chloride levels.

Variation of porosity horizontally and vertically introduces some geologic noise to the AEM chloride estimates. This geologic noise causes the locations of the specific AEM bulk resistivity versus monitor well resistivity pairing to deviate to varying degrees from the best fit regression line as shown on Figure 4.2-3 above. These deviations from the regression line are included in the overall assessment of the error in AEM chloride estimates. The additional time series monitoring well data and density-dependent solute transport groundwater modeling that FPL performs complements the AEM survey and, together, provides a comprehensive representation of the remedial action progress.

Another source of error is the spatial displacement of the water quality samples taken from discrete intervals in the monitoring wells and the location of the nearest AEM data on a flight line. None of the monitoring wells available for calibration of the AEM data are on a flight line: all well screens are shorter than the thickness of AEM layers, and some well screens are divided by two AEM layers (see Figure 4.2-7). In addition, the AEM data average the instrument's response to variations in chloride content over distances of a few tens of meters to over 100 m, while well samples come from small-diameter well screens about 1 m in length. It can be reasonably assumed that changes in pore water chloride content are smooth and not abrupt over distances of tens of meters, and the effects of spatial errors are included in the overall assessment of AEM-estimated chloride values.
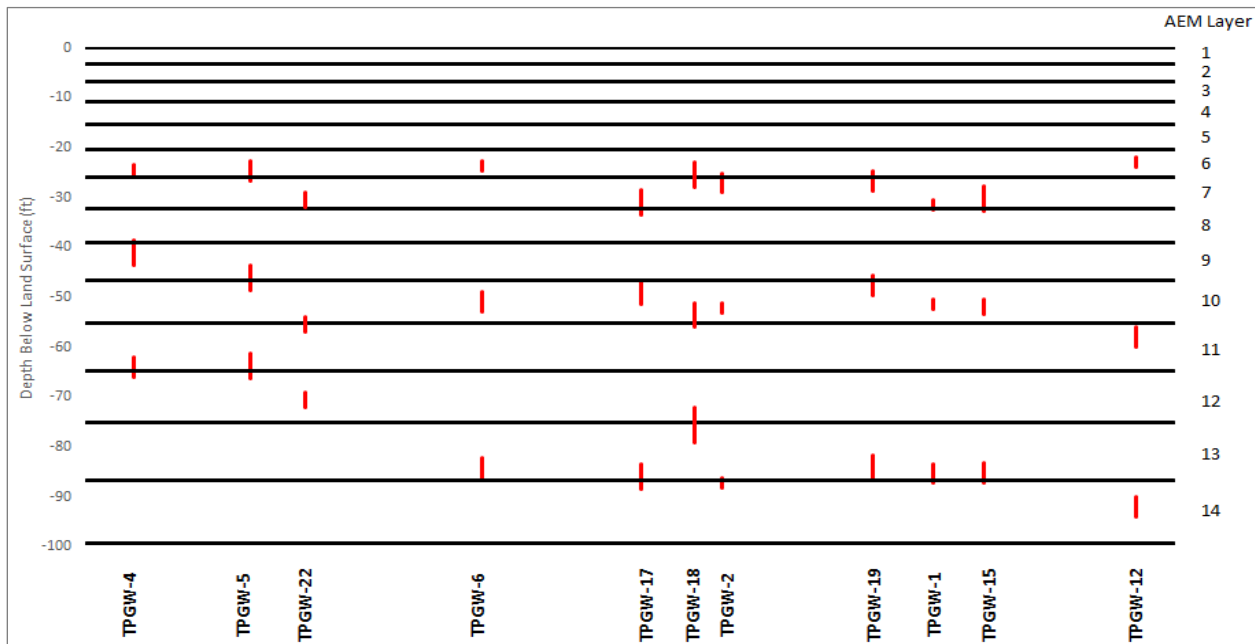
Figure 4.2-7. Monitor Well Screened Zone versus AEM Layer

4.2.4.1   Definition of AEM Survey Error

> Statistically, the mapped location of the AEM-estimated 19,000 mg/L contour is the most probable location of the 19,000 mg/L physical boundary.

The basis for evaluating the accuracy of the AEM surveys is in the comparison between measured aquifer pore water chloride data obtained from the TPGW multi-level monitoring wells and adjacent AEM-estimated chloride value. Each well cluster has three screened intervals corresponding to the upper, middle, and lower flow zones within the Biscayne aquifer. Water quality data are available from the TPGW monitoring well system. For comparison to AEM data, water quality data closest in time to the AEM survey were selected for wells that are close to an AEM flight line (i.e., there are no wells on a flight line) and at screen intervals that correspond to AEM layers. Where the well screen elevations span two AEM layers, the average of the two AEM layers is used for comparison. Figure 4.2-7 shows relative position and length of monitoring well screens (shown in red) versus AEM layers. The water quality samples used in the error analysis are the same samples used to establish the baseline relationship between AEM bulk resistivity and pore water chloride content, as these samples were used to establish the transfer function converting AEM resistivity to chloride concentrations, as described in Section 4.2.3.

The AEM estimates of pore water chloride levels are obtained as described in Section 4.2.3 and listed along with monitoring well chloride in Table 4.2-3. The error between AEM-estimated

chloride values and chloride levels obtained from monitoring wells is defined as the ratio of the AEM-estimated chloride value to the closest monitoring well value:

$$AEM\ Error = [AEM\ estimated\ chloride]/[monitor\ well\ chloride]$$

A perfect correlation between AEM estimates of chloride and monitoring well data would have a value of 1.0. Values >1.0 indicate an overestimation of chloride by the AEM data, and values <1.0 indicate an underestimation of chloride by the AEM data.

An alternative error measure is the algebraic difference between the AEM estimates and the water quality data:

$$AEM\ Error = [AEM\ estimated\ chloride] - [monitor\ well\ chloride]$$

However, the magnitude of this difference error varies with the chloride level: larger for high chloride values and smaller for low chloride values. The error defined as a ratio maintains the relative error between AEM and water quality data across a wide range of chloride values. It is similar to a percent error, where:

$$\%\ Error = 1 - \frac{[AEM\ estimated\ chloride]}{[monitor\ well\ chloride]} * 100$$

4.2.4.2   Distribution of Error

For 2022, the relative error of AEM chloride estimates was assessed using only 2022 data in order to reduce any effects of changes in instrument response that may have occurred between 2018 and 2022. The standard error is the standard deviation of the relative error between AEM-estimated chloride and laboratory-measured chloride, divided by the square root of the sample size. The standard error for the 2022 data is 0.07. The equation for the 95% confidence interval is

$$CI_{95} = (average\ error) * (1.96) * (s/n^{0.5})$$

where s is the standard error and n is the number of samples.

For the 2022 data points greater than the minimum reliable chloride concentration of 10,000 mg/L (Section 4.2.5), n is 15, and the 95% confidence interval is 0.13, or about ±13%. As applied to the 19,000 mg/L estimated chloride value, the 95% confidence interval is ± 2,470 mg/L, or approximately 16,500 mg/L to 21,500 mg/L. Plan view maps showing the 19,000 mg/L contour for the 2018 and 2022 surveys are contained in Appendix G-7A.

4.2.4.3   Statistical Significance of Plume Volume Changes 2018–2022

Additional analyses of statistically significant changes in the volume of hypersaline water from 2018–2022 in the compliance area, as defined by the AEM data, has been performed using permutation testing and bootstrapping and is summarized below by Kirk Cameron, PhD. Dr. Cameron is the principal author of the 2009 *Unified Guidance for the Statistical Analysis of*

Groundwater Monitoring Data (EPA 2009) and Principal for MacStat Consulting, Ltd. A detailed report of the data and analyses are contained in Appendix H.

If the RWS is ineffective or the AEM method has large errors in estimated chloride, then the year-by-year changes in the AEM-derived hypersaline volume within the compliance area will be random and statistically unrelated to the time of pumping by the RWS. This null hypothesis, that there is no statistically significant change in the volume of the hypersaline volume with time, can be tested statistically. Two methods have been applied to the voxel volume data to test the null hypothesis: permutation testing and bootstrap estimation. The data used in these analyses are the gridded chloride voxels derived from the regression-based, AEM-estimated pore water chloride values, as summarized in Section 4.2.6 and described in detail in the AGF report (Appendix G).

Permutation Testing

Permutation tests were first introduced by two early pioneers in the statistics field, Fisher (1935) and Pitman (1937). Permutation tests are also known as randomization tests, involving a hypothetical calculation of the possible ways in which a data set can be randomly rearranged, and then comparing the observed arrangement to the set of possible rearrangements, to assess the level of statistical significance.

Permutation testing and bootstrap estimation are highly empirical, computationally intensive techniques. Neither one requires fitting or identification of exact statistical models. The most critical assumption relates instead to the overall data generation process. In order to compare the extent of the hypersaline plume across years, it is assumed that the data generating mechanism remains essentially the same with each year consisting of the steps described above. Then, regardless of the overall level of statistical uncertainty, under a null hypothesis of no actual change in plume extent or volume, one would expect year-to-year differences to be random, e.g., some years showing the number of hypersaline voxels lower and some years higher, but not trending over time or space in a particular direction. If, instead, the hypersaline plume is shrinking (or growing), the pattern of change across voxels from year to year will tend to exhibit a trend; and that trend can be positively identified as statistically significant using a combination of permutation testing and bootstrap estimates.

When comparing two or more groups of data, the general algorithm for conducting a permutation test is based on a straightforward idea: under the null hypothesis of no difference between the groups (often representing a hypothesis of no physical difference between the underlying populations), the observations from each group should be exchangeable. That is, random shuffling of the measurements between the groups should not affect the observed difference. Or, from another perspective, random relabeling of the observations (i.e., renaming elements of group 1 as group 2, group 3, etc.) should not change the magnitude of difference between the groups.

In practice, a permutation test involves the following steps:

1. Select an appropriate test statistic (t) to numerically gauge any difference between the groups.

2. Calculate the test statistic for the observed data as collected (t_0).

3. Enumerate all (if feasible) or a large, randomly-selected subset of the possible group label rearrangements (permutations).

4. Compute (t) on each permuted version of the data to construct the permutation distribution.

5. Compare t_0 to the permutation distribution to determine what fraction (p) of the permuted statistics t exhibits a group difference as or more extreme than t_0. This fraction is the *p* value of the test.

6. If the *p* value (p) is large (e.g., $p \geq 0.05$ or $p \geq 0.01$), accept the null hypothesis of no group difference; but if p is small (e.g., $p < 0.05$ or $p < 0.01$), declare a statistically significant difference.

To implement permutation testing for the Turkey Point RWS, the only exchangeable voxels are those with the same spatial coordinates but estimated in different years. That is, the same voxel estimated in, say, 2018, can be randomly swapped with its paired counterpart in 2019, 2021, and so on; but it cannot be swapped with a different voxel from one of those successive years. Consequently, the strategy tailored to the Turkey Point remediation is denoted as a spatial permutation test and looks akin to a kind of paired, two-sample test, where the natural pairing occurs between identically-located voxels estimated in different years.

The steps for the spatial permutation testing are similar to those of a general permutation test, but with specific adjustments:

1. Define hypersaline chloride volume as the proportion of voxels within the study or comparison area of interest with chloride above 19,000 mg/L. Select year-to-year percentage change in hypersaline volume as the test statistic (t).

2. Compute the observed percentage change (t_0) in hypersaline volume for each comparison of interest, e.g., baseline (2018) versus 2019, 2020, 2021, and/or 2022 for the overall hypersaline plume, any specific depth layer of the plume, or any subarea of the site.

3. For each comparison, generate a large number (e.g., 10,000) of random spatial permutations of the data (i.e., by randomly swapping identical voxels between the years being compared), and then compute t on each permutation to construct the permutation distribution for that case.

4. Compare t_0 to the distribution of t to compute the *p* value and assess the statistical significance of each desired comparison.

The results of the spatial permutation testing algorithm were computed for the chloride voxel models from 2018 compared to years 2019–2022. The comparisons of interest were changes in the overall hypersaline plume proportion, as well as similar changes calculated separately for each depth layer. For the overall plume, the observed relative drop in hypersaline volume from the baseline year of 2018 was 22.4% in 2019, 34.6% in 2020, 42% in 2021, and 66.9% in 2022. These observed changes were very strongly different from the respective permutation distributions, so much so that the *p* values in all cases were essentially zero. These annual reductions in plume volume compare well with those reported in prior RAASR reports (22% after Year 1 of remediation, 34% in Year 2, and 42% in Year 3). Separate spatial permutation tests were conducted on a layer-by-layer basis. The results of these evaluations also are very similar to those reported in prior RAASR reports. The *p* values associated with the vast majority of the depth layers in each year were also essentially zero and document a highly statistically significant percentage decrease in hypersaline plume volume. The exceptions at fairly shallow depth layers indicate a net increase in hypersaline plume volume, including statistically significant increases in depth layers 4 and 5 that were documented in prior reports. The source of hypersalinity in these shallow layers was from evaporation of bay water transported inland northeast of the Turkey Point Plant by Hurricane Irma.

Bootstrap Estimation

Bootstrapping was first introduced in the late 1970s (Efron 1979, Efron and Tibshirani 1986). The flexibility and usefulness of bootstrapping has made it commonly employed by statisticians. While permutation tests are mostly limited to group comparisons, bootstrapping can be applied to a wide variety of problems, including estimates of statistical variation from a single group or population. The bootstrap is especially powerful in constructing confidence intervals on test statistics for which the underlying statistical model is complex or unknown. As such, bootstrapping is often employed as a nonparametric technique when it may be difficult or impossible to fit the underlying data to a standard statistical distribution/model. The core idea behind the bootstrap is that the observed data can be assumed to adequately represent and substitute for the underlying, unknown population. Any statistical model must assume that the collected data are in some sense representative of the underlying population from which the observations came. But bootstrapping takes this assumption a step further by recognizing that the empirical (observed) distribution (or density) can be repeatedly resampled in order to mimic what would occur if access were available to the "true" distribution, and not simply to its empirical representative. In the simplest case, a nonparametric percentile bootstrap confidence interval around a desired statistic (t) can be computed as follows:

1. Select an appropriate (test) statistic (t) to summarize the desired population characteristic.

2. Note the sample size (n) of the observed data.

3. Compute t for the observed sample data, yielding the observed statistic (t_0).

4. Construct a large number of bootstrap samples (B∗) by repeatedly resampling n observations with replacement from the observed data.

5. Compute t on each bootstrap sample B∗, leading to the bootstrap distribution of t.

6. Select a confidence level, $1 - \alpha$.

7. Calculate lower and upper percentiles of the bootstrap distribution so that the range between the percentiles covers a proportion of $1 - \alpha$ of the total bootstrap density (e.g., for 95% confidence, compute the 2.5th and 97.5th percentiles).

Results of bootstrap estimation for the Turkey Point RWS are shown on Figure 4.2-8 which presents the calculated 99% bootstrap confidence intervals around the proportion of hypersaline chloride in each of the years 2018–2022, both overall and for each depth layer separately, using 10,000 bootstrap samples in each calculation. The trend in decreased overall hypersalinity is evident as well as the general 'tightness' of the confidence intervals, so that no overlap in the combined confidence intervals is recorded between the respective years. These results are consistent with the permutation testing outcomes; but instead of providing a *p* value, they show a range of statistical uncertainty around each estimate.

Results of Statistical Tests

The results of the permutation testing are contained in Appendix H. The probability that the observed changes in plume volume with time are random (the *p* value) is much less than 0.001 for the full plume volume and AEM layers 1–3 and 6–14. The null hypothesis is rejected. Layers 4 and 5 show an increase in chloride as a result of tidal inundation in 2017 during Hurricane Irma in the coastal area north of the CCS bounded by the Turkey Point Power Plant access road and the L-31E berm. These waters were concentrated by evaporation and moved downward from 2018–2022 through layers 1–3 to layers 4 and 5.

The results of the bootstrap testing are contained in Tables 2 and 3 and Figure 4 of Appendix H and are reprinted below as Figure 4.2-8. The *p* values for layers 1–3 and 6–14 are <<0.001 and the null hypothesis is rejected for the overall plume volume in layers 1–3 and 6–14. Again, layers 4 and 5 show an increase in plume volume from 2018–2022 in the coastal area north of the CCS.
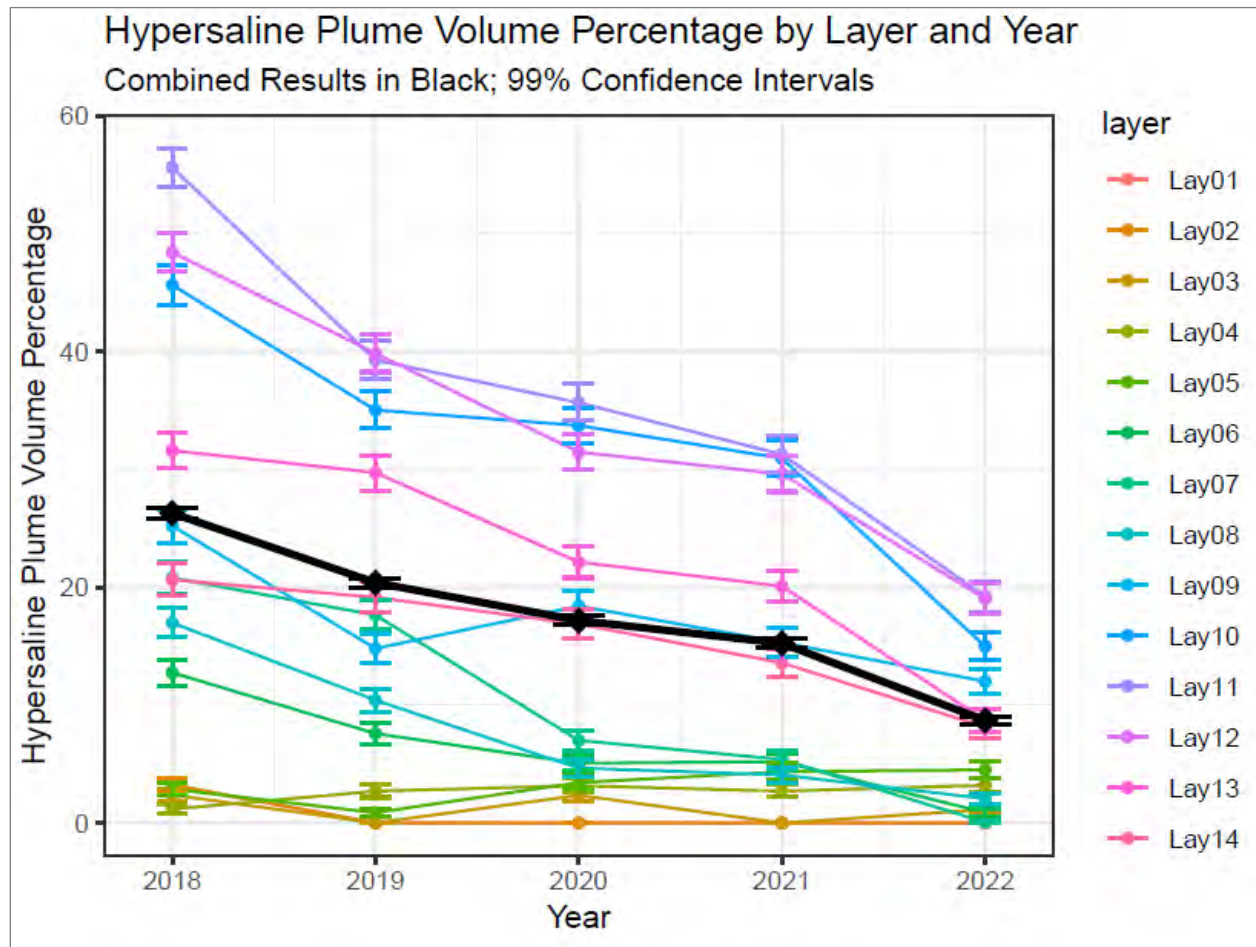
Figure 4.2-8. Bootstrapped Trend in Percent Hypersaline Plume Volume (from Cameron 2022 included as Appendix H)

In summary, the statistical testing of the changes in the volume of the hypersaline plume, both overall and by layer, demonstrates that the changes are highly significant statistically. This demonstrates that the RWS is effectively reducing the volume of the hypersaline plume, and that the AEM results are producing statistically significant estimates of the change in plume volume from year to year.

4.2.4.4   Verification of AEM Resistivity Changes

> An alternative approach to calculate changes over time of measured formation resistivity within the compliance area west and north of the CCS confirms the reductions in high conductivity estimated using the chloride regression methods.

As explained in the previous sections, and as with any empirical data analyses, there is uncertainty associated with correlation of AEM-estimated chloride and measured chloride

values. To verify the magnitude of AEM-derived chloride changes that have occurred from the 2018 baseline and that the measured changes in AEM-derived chloride are independent of the AEM resistivity to chloride conversion process, AEM resistivity distributions from each survey were compared independent of conversion to chloride. AGF conducted the analyses and gridded resistivity models for each survey (2018–2022). Details of the analyses are reported in detail in Appendix G. Part of the analysis included comparisons of the multilayered AEM resistivity models for each survey to evaluate how AEM resistivities associated with hypersaline water were changing with time. For this evaluation, the average of values shown on Table 4.2-4 above, 1.75 ohm-m, was selected to represent 19,000 mg/L chloride (if resistivity alone was to be used to assess yearly changes rather than chloride, the year-specific resistivity to chloride values from the table would be used for each year). Resistivity values of 1.75 ohm-m or less were tracked and resistivities above that value (non-hypersaline) were discarded. The AEM resistivity soundings were then gridded to provide a 3D resistivity model. This approach is similar to an alternative approach suggested by MDC (Arcadis 2020). Figure 4.2-9 provided by AGF, illustrates how AEM resistivity has been reduced over time in layer 7 (as an example).

The analysis is independent of the chloride conversion step, and the reduction of AEM resistivity verifies that the annual changes in the volume of the hypersaline portion of the aquifer in the compliance area are consistent with the observed changes in measured resistivity.
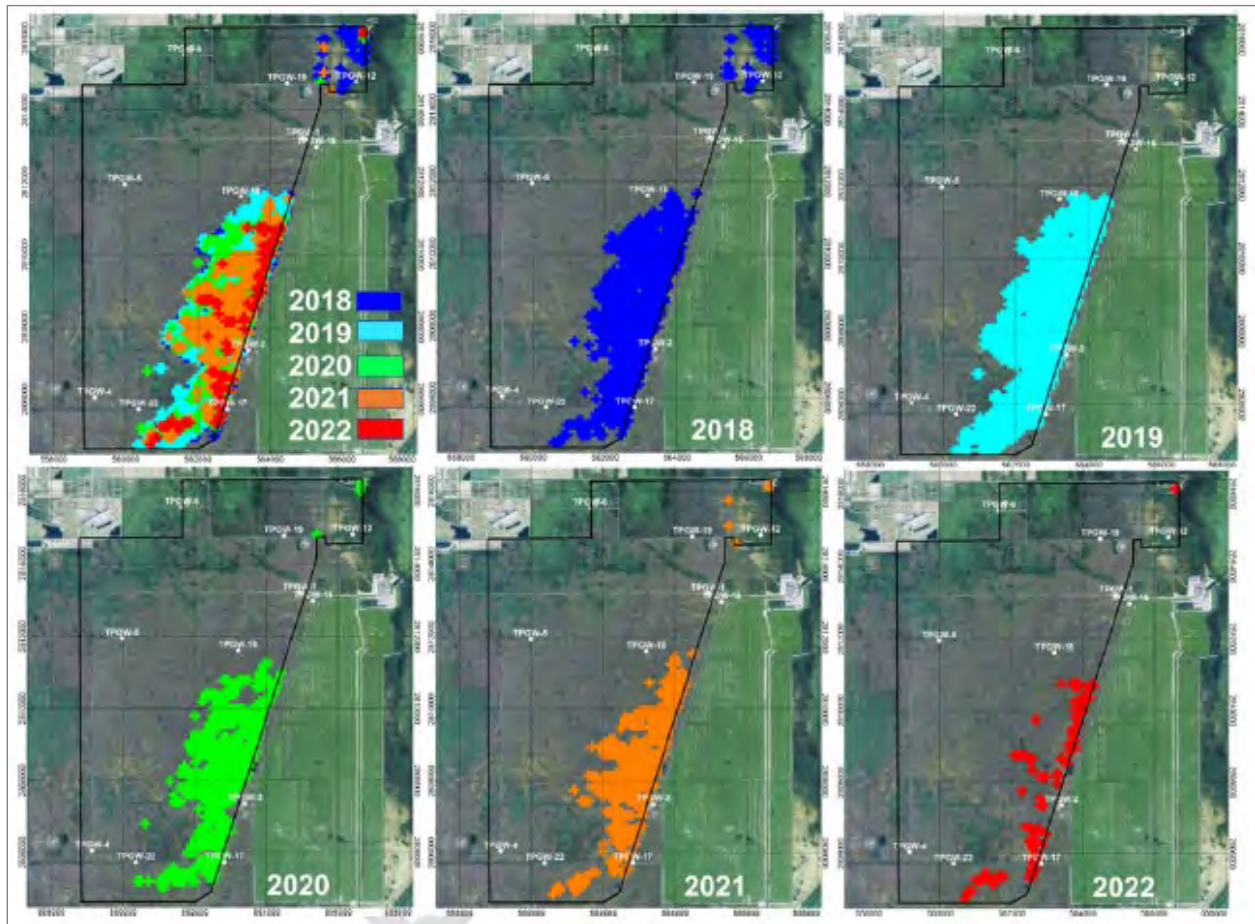
Figure 4.2-9. Example of Changes in Resistivities Less than 1.75 ohm-m over Time (2018–2022) in Layer 7

4.2.5   Method Minimum Reliable Chloride Concentration

While the AEM time-domain resistivity survey at Turkey Point was designed to map the extent of aquifer pore waters with greater than 19,000 mg/L chloride concentration, as the predominant bulk resistivity response at those concentrations is directly attributable to chloride within the formation of the Biscayne aquifer, FPL was asked by MDC to assess the method reliability for portions of the aquifer containing lower salinity concentrations. Appendix G of the *Turkey Point Recovery Well System Startup Report* (FPL 2018a) provides a discussion on the derivation of the minimum reliable chloride reporting limit. As discussed, prediction accuracy decreases significantly for pore water chloride ion contents <10,000 mg/L. Based on this analysis, the reliable lower limit of the AEM survey for mapping chloride concentration within the Biscayne aquifer is 10,000 mg/L.

4.2.6   Creation of a 3D Chloride Ion Voxel Grid

A voxel is a 3D grid cell, or "volume element." The AEM-derived chloride values were interpolated to a uniform voxel grid to allow for more effective graphical visualization of the chloride ion distribution. Each voxel has lateral (x, y) dimensions of 328 ft x 328 ft (100 m x 100 m) and a thickness equivalent to the individual 3D AEM resistivity layers (Table 4.2-1). The bottom of layer 14 is at a depth of about 100 ft below land surface (30.3 m). As a result of the interpolation process to develop the voxel model, AEM-derived chloride concentrations near monitoring wells located in blanked areas due to excessive background EM noise can be compared to water quality data obtained from those wells and used to assess remediation progress. For example, TPGW-12 and TPGW-15 were excluded from the AEM bulk resistivity model because there were no usable AEM data within the radial criterion of 175 m due to EM noise and proximity of flight line data. However, these data points are useful for comparison with AEM-derived chloride in the plan view and cross-sectional maps.

All depth slices, profile views, and 3D views of the AEM-derived chloride concentrations are provided in Appendix G for the 2022 survey. Chloride concentrations between 10,000 mg/L and 19,000 mg/L are shown in shades of gray; chloride concentrations above 19,000 mg/L are shown with a colored scale, with red representing the highest concentrations (up to ~40,000 mg/L) and blue representing the lowest concentrations (~19,000 mg/L). An example of a chloride depth slice is shown in Figure 4.2-10, representing AEM layer 12.
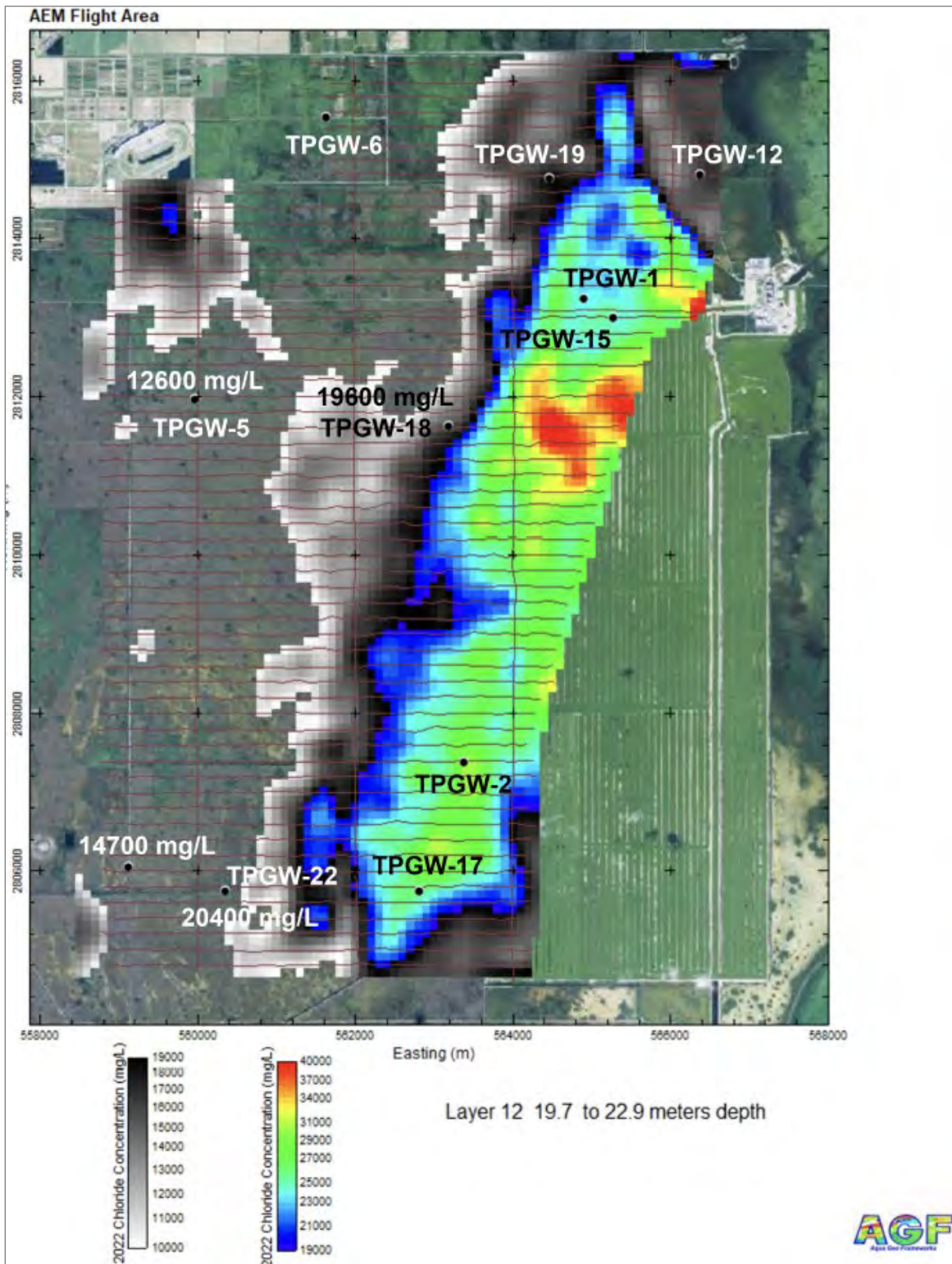
Figure 4.2-10. Chloride Depth Slice (Layer 12) for 2022 AEM Survey

4.3 DISCUSSION OF FINDINGS

AEM data demonstrate there has been significant retraction of the leading edge of the hypersaline plume by as much as 1.25 miles after four years of remediation. The data also demonstrate a statistically significant reduction of 67% in the volume of the hypersaline Biscayne aquifer materials in 2022 as compared to 2018. In addition, there is no CCS-sourced hypersaline water in layers 1–4, and remediation of the plume in layers 5 and 6 is nearly complete.

4.3.1   Natural Occurrence of Hypersaline Water

Two sources of hypersaline groundwater occur within the AEM survey area adjacent to the CCS. Per the groundwater model, the predominant source is CCS groundwater while the other source is naturally occurring non-CCS-sourced evaporated seawater that originates in the coastal wetland margins (referred to as "the white zone") and documented by USGS (Prinos et al. 2014). Salinities exceeding 40 PSU (>22,000 mg/L) have been documented to occur in coastal waters in western Florida Bay and Taylor River, well outside of any influences from the CCS (SFNRC 2012), and north and south of the CCS as discussed in Section 4.3.3.1. Hypersaline surface water with fluid densities greater than underlying groundwater will sink into groundwater, resulting in both shallow and deep expressions of hypersaline groundwater. This is significant to the RWS remediation assessment, as the CA and CO do not require FPL to extract naturally occurring hypersaline groundwater.

Fitterman et al. (2012) used helicopter electromagnetic (HEM) surveys to map the distribution of saline groundwater in the C-111 and Model Lands basin areas of southeast MDC. The HEM data were presented as resistivity depth profiles. Comparison of geophysically determined formation resistivity and salinity concentrations from well samples (Fitterman and Prinos 2011) shows that formation resistivities of 1–2 ohm-m represent geologic units saturated with groundwater close to or at normal seawater chloride concentrations of 19,000 mg/L. Formation resistivities with values of 1 ohm-m or less represent hypersaline groundwater with chlorinity greater than 19,000 mg/L. Fitterman et al.'s (2012) HEM data show that at a depth of approximately 17 ft (5 m), hypersaline groundwater is present between Card Sound Road and U.S. Highway 1 (US 1) in a coast-parallel band 4,000 to 6,000 ft wide. Hydrologically, the hypersaline groundwater in this coastal band is not from the CCS as there is no mechanism for coast-parallel flow of hypersaline groundwater from the CCS southwest past US 1. This hypersaline water corresponds to a coast-parallel zone of lower vegetative density in the coastal wetlands as viewed from satellite images. It is common in coastal wetlands for evaporation of seawater to form hypersaline groundwater that moves downward into the sediments under a density gradient (Prinos et al. 2014). Salinities in shallow groundwater in coastal wetlands can reach 60–100 PSU (34,000–56,000 mg/L) (Stringer et al. 2010) and will migrate downward due to the increased density as compared to normal seawater. Close to the coast, evaporation of seawater can create a wide band of hypersaline groundwater. The HEM data of Fitterman et al. (2012) suggest that this band of naturally created hypersaline groundwater extends to the base of the Biscayne aquifer between Card Sound Road and southwest past US 1. It is likely that this

band of naturally occurring hypersaline water extended northward along the coast prior to construction of the CCS in the early 1970s at Turkey Point.

Shallow Hypersaline Occurrence North of the Cooling Canal System

A shallow zone of >19,000 mg/L chloride porewater occurs north of Palm Drive and east of the L-31E levee. The shallow zone of hypersalinity was observed in the 2018 baseline survey, which was conducted approximately six months after the Hurricane Irma storm surge of 3–5 ft inundated the costal reaches of the Model Lands basin. Seawater that flooded the coastal wetlands up to the L-31E levee and the Turkey Point entrance road north of the Plant was trapped and became concentrated via evaporation during the dry season. This evaporative-sourced hypersaline groundwater was limited to the upper 7–10 ft of the aquifer as shown in 2018 AEM survey layers 1–3 (Appendix F, Figures 1a, 2a, 3a). At the same time, at depths of 20–25 feet (AEM layers 4 and 5), groundwater salinities were lower with chloride levels similar to or less than seawater. From 2018– 2022, this more-dense, naturally sourced hypersaline groundwater has migrated downward under a density gradient, from layers 1–3 to layers 4 and 5 (see Appendix G-5 and Section 4.3.3). In layers 4 and 5, this shallow hypersaline water is not connected to the main hypersaline plume just north of the CCS. The AEM data do not show continuity of hypersalinity in the inundated area with the CCS-sourced hypersaline plume. As this area is tidally influenced and periodically producing hypersaline waters in the upper layers that migrate downward, it is expected that the measured hypersaline volumes by layer will continue to change cyclically.

4.3.2   Spatial Extent AEM-Derived Chloride Concentrations

Color-flood maps that illustrate the 2D plan view variation in AEM-estimated chloride content of groundwater (i.e., representation of "groundwater contours" utilizing AEM) for the 2022 survey (Year 4) are provided in Appendix G-5. Consistent with the CA, too further assess changes in the spatial extent of the hypersaline plume edges before and after four years of RWS operations, contour maps were created to compare the location of the 19,000 mg/L contour in the 2018 baseline results with the location of the 19,000 mg/L contour for Year 4 (2022). These comparisons are shown for each AEM layer in Appendix G-7A, and an example is shown below in Section 4.3.3. While there is uncertainty in the estimated 19,000 mg/L chloride values produced from the AEM survey, the contour lines represent the most probable location of the 19,000 mg/L boundary in 2018 and 2022.

4.3.2.1   Spatial Comparison and Volumetric Determination Methodologies

As described above, the AEM pore water chloride estimates were interpolated to a voxel grid with horizontal dimensions of 100 m x 100 m for each grid cell. The thickness of each cell is the thickness of a given AEM layer (Table 4.2-1). The voxels with estimated chloride values >19,000 mg/L can be counted, and their volumes calculated. This allows an estimate of the volume of the hypersaline plume (>19,000 mg/L) to be made. This comparison of hypersaline volume can be made layer by layer or for the entire thickness of the Biscayne aquifer. Likewise, the spatial extent of hypersaline earth materials is determined by locating the westernmost and northernmost positions of adjacent voxels along each flight line. The locations of each "edge"

position are manually identified by AGF; and the contour of the 19,000 mg/L chloride extent on a layer-by-layer basis is produced. To assess changes in the orientation of the extent hypersalinity in the Biscayne aquifer after four years of RWS operations, the positions of both the 2018 and 2022 19,000 mg/L contours are produced for each AEM layer.

4.3.3   Comparison of the 2018 and 2022 AEM Survey Results

4.3.3.1   Comparison of 2018 and 2022 Spatial Extent of AEM-Estimated Hypersalinity

Comparison of the 19,000 mg/L chloride contours generated from the 2018 and 2022 AEM surveys show reductions in the westward and northern extent of CCS-sourced hypersaline groundwater in all layers of the compliance area except layers 4 and 5 which show increases in non-CCS-sourced hypersaline groundwater as discuss above (Appendix G). The lateral extent of CCS-sourced hypersalinity in all AEM layers exhibit movement of the western and northern plume extent back toward the CCS and RWS extraction wells. However, there are localized areas in each layer where the leading edge of the plume does not show significant retraction toward the CCS; and in limited areas, there are some small areas exhibiting movement to the west. It is expected these westward deviations in localized areas will be resolved over time as the remediation continues.

On a layer-by-layer perspective, the spatial extent of hypersaline water in layers 1–5 north of Palm Drive and east of the L-31E levee are reflective of non-CCS-sourced hypersaline water that formed from seawater encroachment into the coastal marsh areas during Hurricane Irma. In this area, the spatial extent of this evaporative hypersaline groundwater found in the shallow portion of the Biscayne aquifer waxes and wanes over time as the denser water sinks. While the coastal evaporative formation of hypersalinity occurs regionally along the Model Lands and south Florida peninsular margin, only a small area northeast of the FPL property falls within the compliance zone and is measured by the AEM surveys. While the extent of hypersalinity in the upper five layers of the aquifer is comparatively small, there is no other hypersalinity in these layers throughout the entire compliance area. As such, variations in extent are small while percentage of changes in volume as the hypersaline water sinks from layer to layer are disproportionately large.

Layers 6–14, for which the hypersalinity within the compliance area are predominantly CCS-sourced, show reductions in the western and northern extent of hypersalinity from 2018–2022 with retraction of the plume ranging from 0.5 to over 1.25 miles.   The amount of retraction varies from layer to layer based on several factors, including the degree to which hypersaline groundwater existed in the layer, the hydraulic characteristics of the layer, the distance between the RWS wells and the edge of the plume, and the concentration of the plume.

The survey indicates there is no CCS-sourced hypersaline groundwater west of the L-31E canal or north of the FPL property in the upper 15 ft (4.7 m) of the aquifer, with small areas remaining in layers 5, 6 and 7 which have otherwise seen the plume retracted back to or east of the L-31E canal. The 2022 survey also indicates reductions in chloride concentration within the plume that

further reflects progress of the RWS operations in reducing CCS-sourced hypersalinity within the compliance area.   A more detailed description of changes within each layer follows.

Layer 6

The AEM data indicates that there are no CCS-derived waters >19,000 mg/L west of the L-31E canal except for a small area between TPGW-2 and TPGW-17, and a very small, isolated area north of TPGW-2. AEM data from 2018 and 2022 show the hypersaline volume in the compliance area for this layer has been reduced by over 93%. The AEM data shows a significant eastward retraction of the 19,000 mg/L boundary in the southern third of the compliance area with the 2018 western edge of the plume retreating east by as much as 1 mile near monitoring sites TPGW-2 and TPGW-17.

Layer 7

Layer 7 most closely represents the upper high flow zone in the Biscayne aquifer near the CCS (see Figure 4.3-1). This layer shows a 99% reduction in the volume of hypersaline water within the compliance area between the 2018 and 2022 AEM surveys (Table 4.3-1). For AEM layer 7, there is very little hypersaline water west of L-31E in 2022, with the 2018 western edge of the plume retreating east by as much as 1.25 miles from just south of monitoring site TPGW-18 to the southern extent of the CCS.

Layer 8

The main, unbroken 19,000 mg/L contour is largely east of the L-31E canal in the 2022 AEM survey. There are isolated areas of >19,000 mg/L estimated chloride south and southeast of TPGW-18, west of TPGW-12, and at TPGW-17. AEM data from 2018 and 2022 show the hypersaline volume in the compliance area for this layer has been reduced by 88%. In general, there is significant eastward movement of the 19,000 mg/L boundary (ranging between 0.5 to over 1 mile) in layer 8 from monitoring well site TPGW-18 to the southern extent of the CCS.
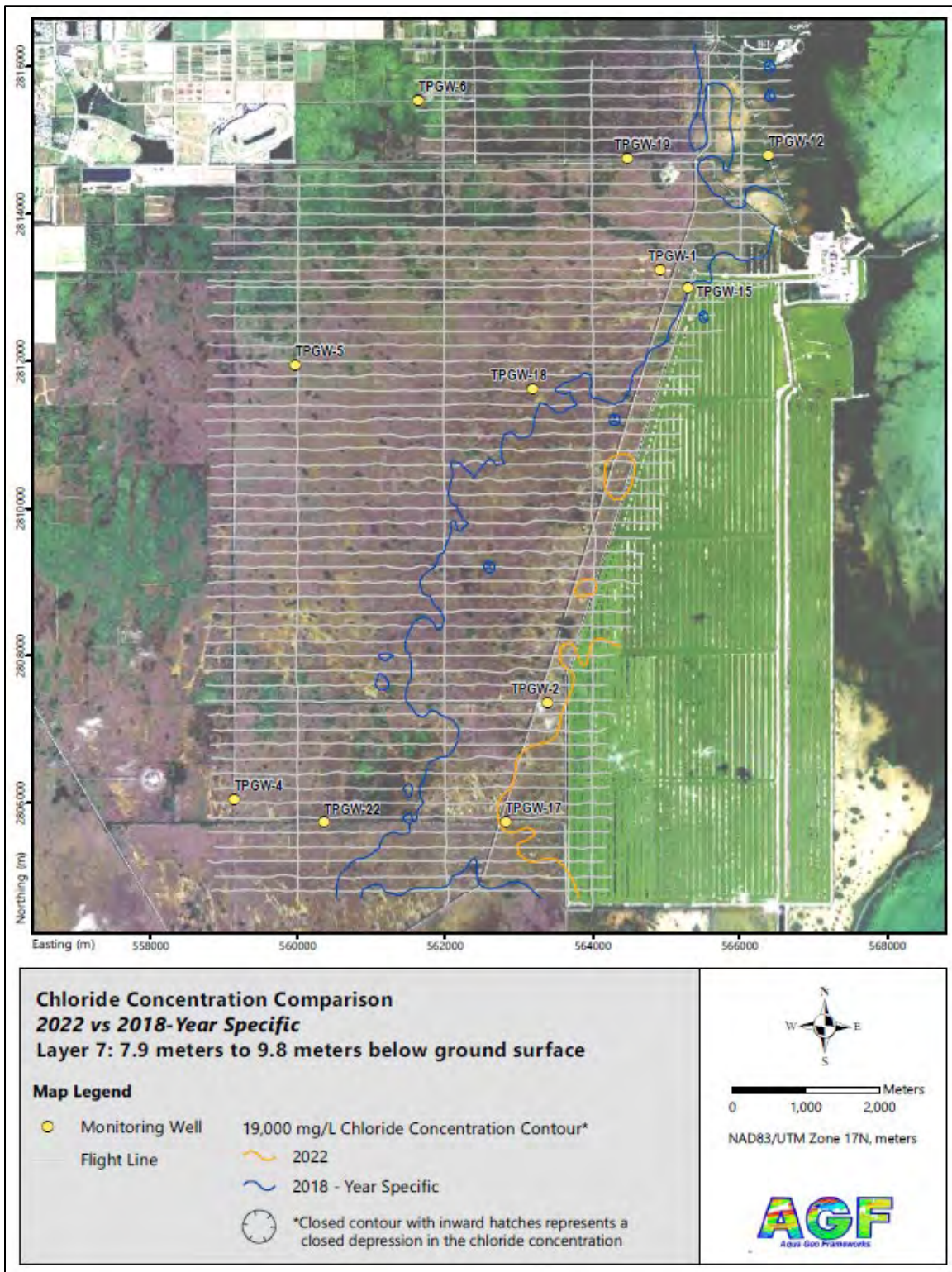
Figure 4.3-1. Layer 7, 19,000 mg/L Chloride Concentration Contours for 2018 and 2022

Table 4.3-1.   Year-Specific AEM-Derived Chloride Volume Estimates of Hypersaline Aquifer Material for the 2018 Baseline and the 2022 Year 4 survey by Layer (m³)

Layer	2018 Volume > 19,000 mg/L (m³)	2022 Volume > 19,000 mg/L (m³)	Percent Volumetric Change by Layer (2018 to 2022)	Percent Volumetric Change by Layer (2018 to 2022) Relative to Total Volume
1*	1,930,000	0		-0.4
2*	2,047,500	0	-100	-0.5
3*	1,644,500	793,500	-52	-0.2
4*	923,000	2,509,000	172	0.3
5*	2,508,500	3,944,000	57	0.3
6	12,304,000	848,000	-93	-3
7	22,572,000	72,000	-99	-5
8	20,480,000	2,500,000	-88	-4
9	33,440,000	15,928,000	-52	-4
10	67,399,500	22,123,500	-67	-10
11	92,207,500	31,845,000	-65	-13
12	89,029,500	34,983,500	-61	-12
13	63,817,500	17,520,500	-73	-10
14	43,540,000	17,185,000	-61	-6
Totals:	**453,843,500**	**150,252,000**	**-67**	**-67**

 * Note: Hypersaline volumes located in the northeast corner of the compliance area (east of the L-31E levee and north of Palm Drive) in these layers are from evaporated seawater and not sourced from the CCS.

Layer 9

Overall, layer 9 shows a 52% reduction in the volume of the aquifer with AEM-estimated chloride values >19,000 mg/L from 2018–2022, with much of the discontinuous hypersaline area in the southwest survey area remaining unchanged while significant retraction has occurred in the area of hypersalinity contiguous to the CCS. Significant retraction of the contiguous hypersaline plume has occurred west and north of the CCS during the first four years of remediation.

A broad area 1 to 2 miles west of TPGW-2 and TPGW-17 shows isolated discontinuous lenses of hypersalinity in both the 2018 and 2022 surveys (Figure 4.3-2). The contour lines show a broad area of isolated lenses with pore water chlorinity at or near 19,000 mg/L (as shown in Appendix G-5). There is little discernible significant change in the position of the 19,000 mg/L contour between 2018 and 2022 in this area. Lithologic, acoustic imaging, and seismic borehole logs for TPGW-2 and TPGW-4 (JLA 2010) and data described in Fish and Stewart (1991) (E-E' geologic cross section) suggest that at least the upper part of layer 9 is a lower permeability sandstone or sandy limestone near the bottom of the Ft. Thompson Formation. The driller's log for TPGW-22

shows extensive high-porosity silty materials. As discussed above, variations in formation porosity affect AEM estimations of chloride concentrations with higher porosities resulting in elevated estimates of chlorinity. The area of slightly hypersaline to slightly less than hypersaline aquifer pore waters located in the southwest corner of the AEM survey may be caused by higher porosity localized lithology. Laboratory chlorides for TPGW-4M from September 2010 to present have consistently averaged around 15,000 mg/L while chloride levels from TPGW-22M are around 21,000 mg/L. Additional evaluation of this are will be conducted to verify or refute the chloride concentrations in this area.

Layer 10

Layer 10 (Figure 4.3-3) most closely represents the middle flow zone of the Biscayne aquifer near the CCS. Overall, the 2022 Year 4 AEM survey shows a 67% reduction of the hypersaline plume volume from 2018–2022. Areas showing significant retraction of the northern and western extent of >19,000 mg/L aquifer materials occur north of the CCS where the extent of the plume has retracted into an isolated area between TPGW-19 and TPGW-1 from 2018–2022, and into areas north and west of TPGW-2 and TPGW-17 where the western extent of the plume has retracted east by as much as 1.5 miles since 2018. There is an isolated area of >19,000 mg/L between TPGW-5 and TPGW-18 that is unconnected to the main plume similar to the lenses in layer 9. (see Appendix G-5). Future AEM evaluations will show whether this area persists, indicative of a high-porosity lithologic sequence or dissipates as a result of RWS operations.

Layers 11 and 12

Layers 11 and 12 showed a 66% and 61% volumetric reduction of the hypersaline plume, respectively, since 2018, with the western extent of the 19,000 mg/L chloride retracting over 1 mile toward the CCS after four years of remediation (Figures 4.3-4 and 4.3-5). This is significant as it indicates the remediation is working in the lower portion of the aquifer and at significant distances west of the CCS. Factors that could be contributing to reductions in chlorinity at distances further west than the capture radii of the RWS extraction wells include the prevailing east-southeasterly groundwater gradient, the halting of net westward flow of hypersaline groundwater from beneath the CCS, and reduction in fluid density west of the CCS due to decreasing salinity concentrations resulting from RWS operations, thus facilitating increased inflow of fresher groundwater from the west.

Layer 13

Layer 13 shows a 73% reduction in hypersaline plume volume in 2022 as compared to 2018. The movement of the plume boundary eastward is similar to that of layer 12 with the largest amounts of retraction (0.75 to 1 mile) occurring in the area between TPGW-18 and TPGW-2.

Layer 14

Layer 14 shows 61% in reduction of the volume of the hypersaline plume from 2018 to 2022. The plume boundary is east of L-31E from TPGW-15 to southeast of TPGW-18.
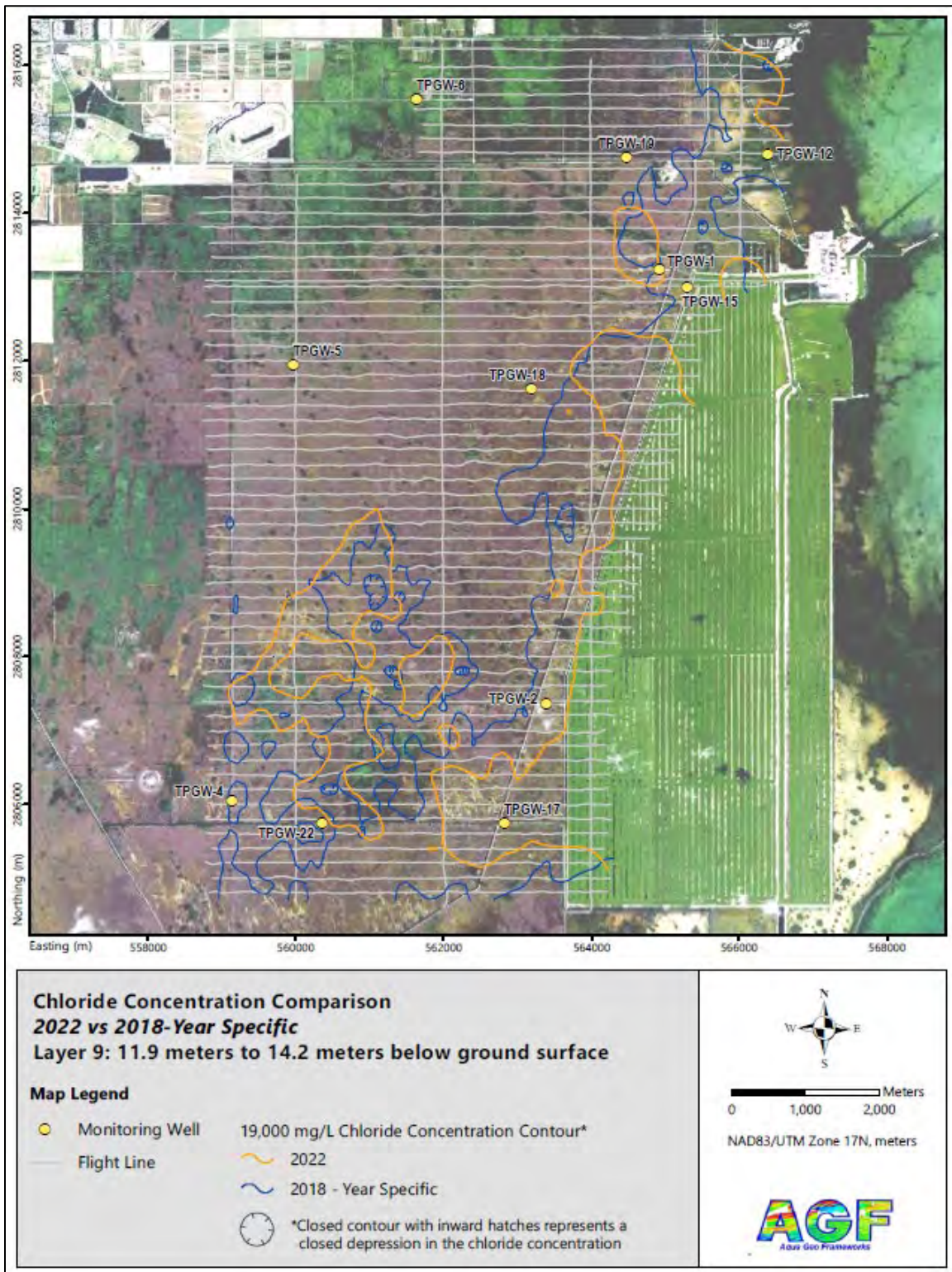
Figure 4.3-2. Layer 9, 19,000 mg/L Chloride Concentration Contours for 2018 and 2022
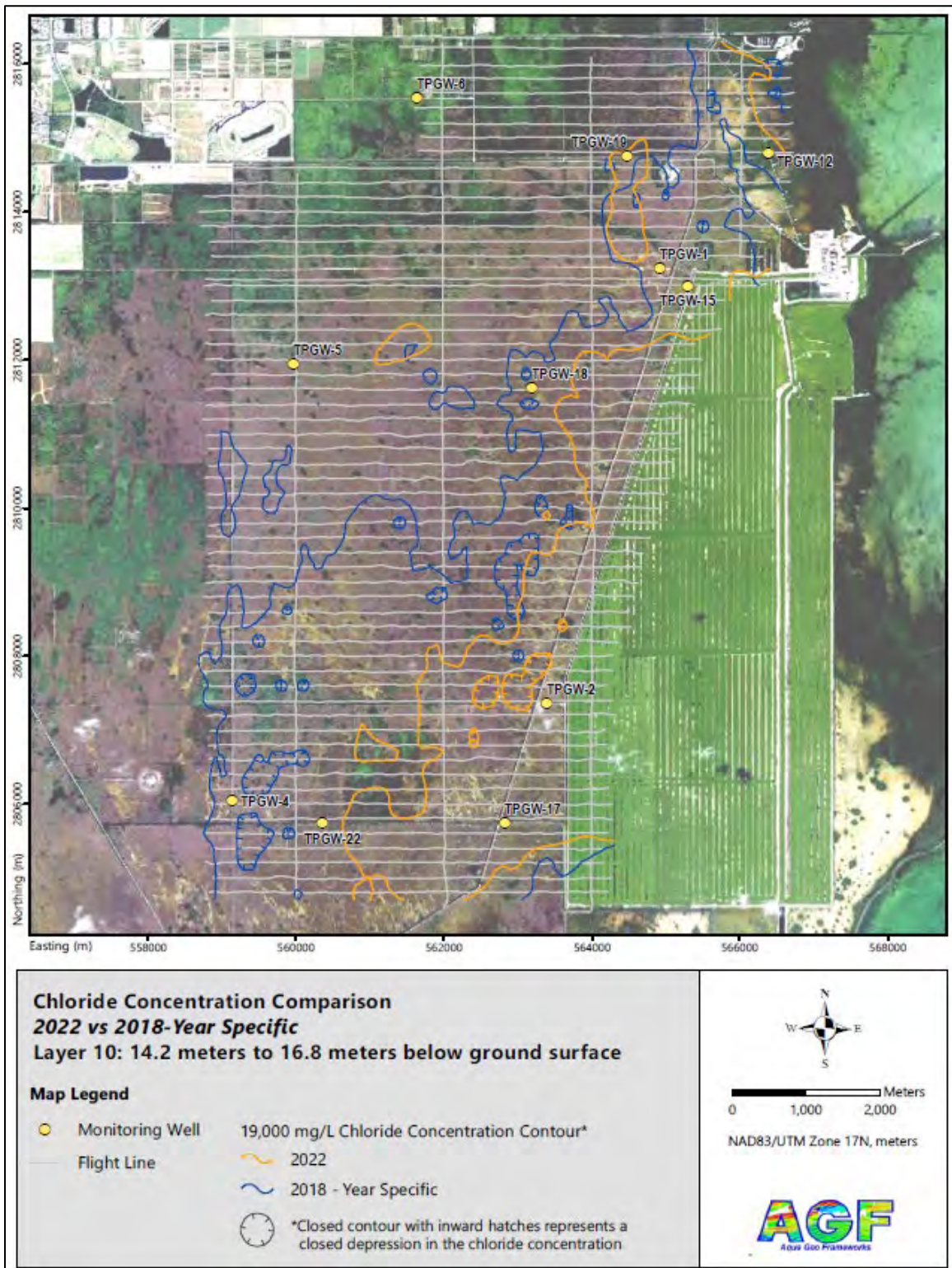
Figure 4.3-3. Layer 10, 19,000 mg/L Chloride Concentration Contours for 2018 and 2022
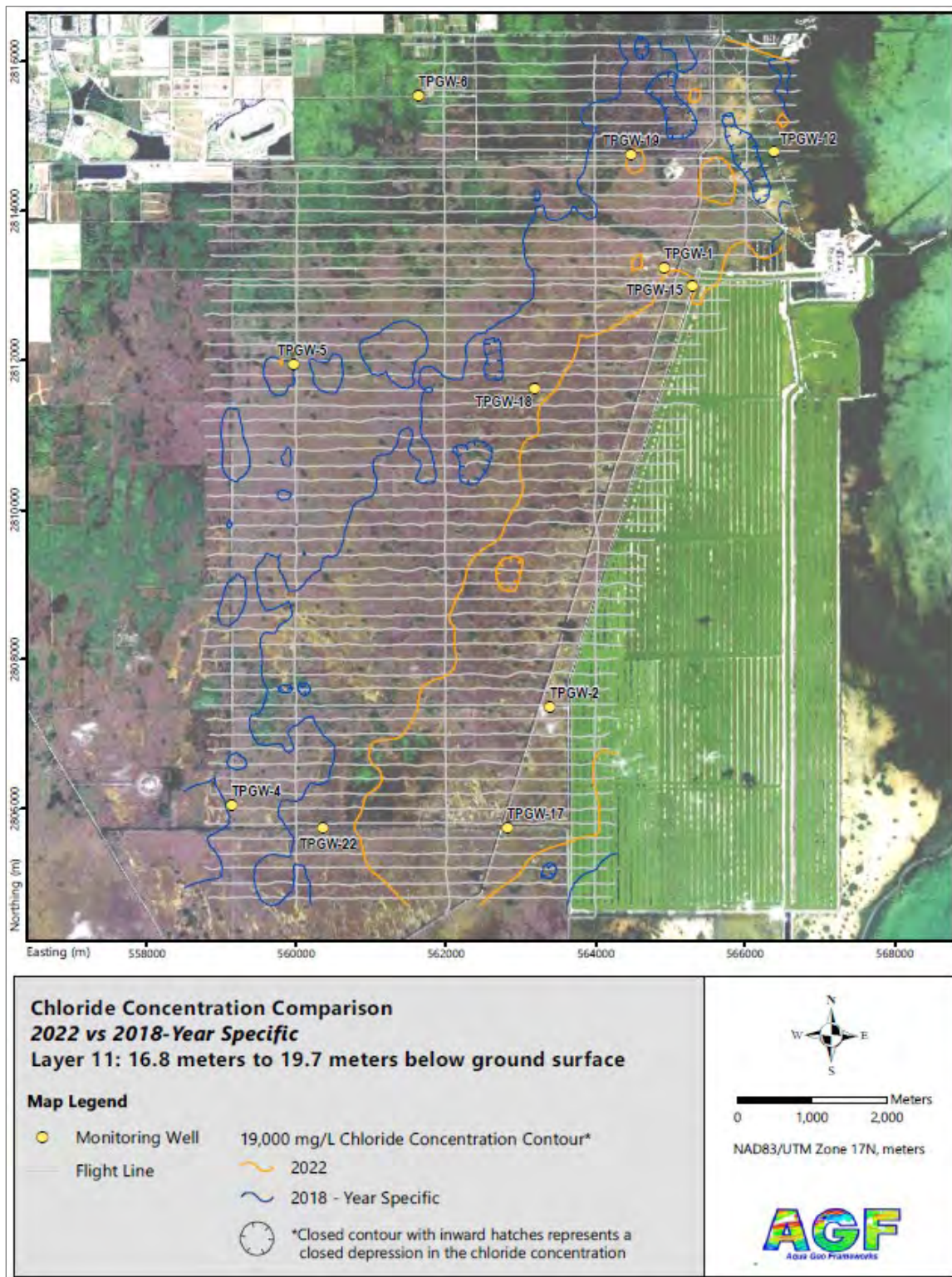
Figure 4.3-4. Layer 11, 19,000 mg/L Chloride Concentration Contours for 2018 and 2022
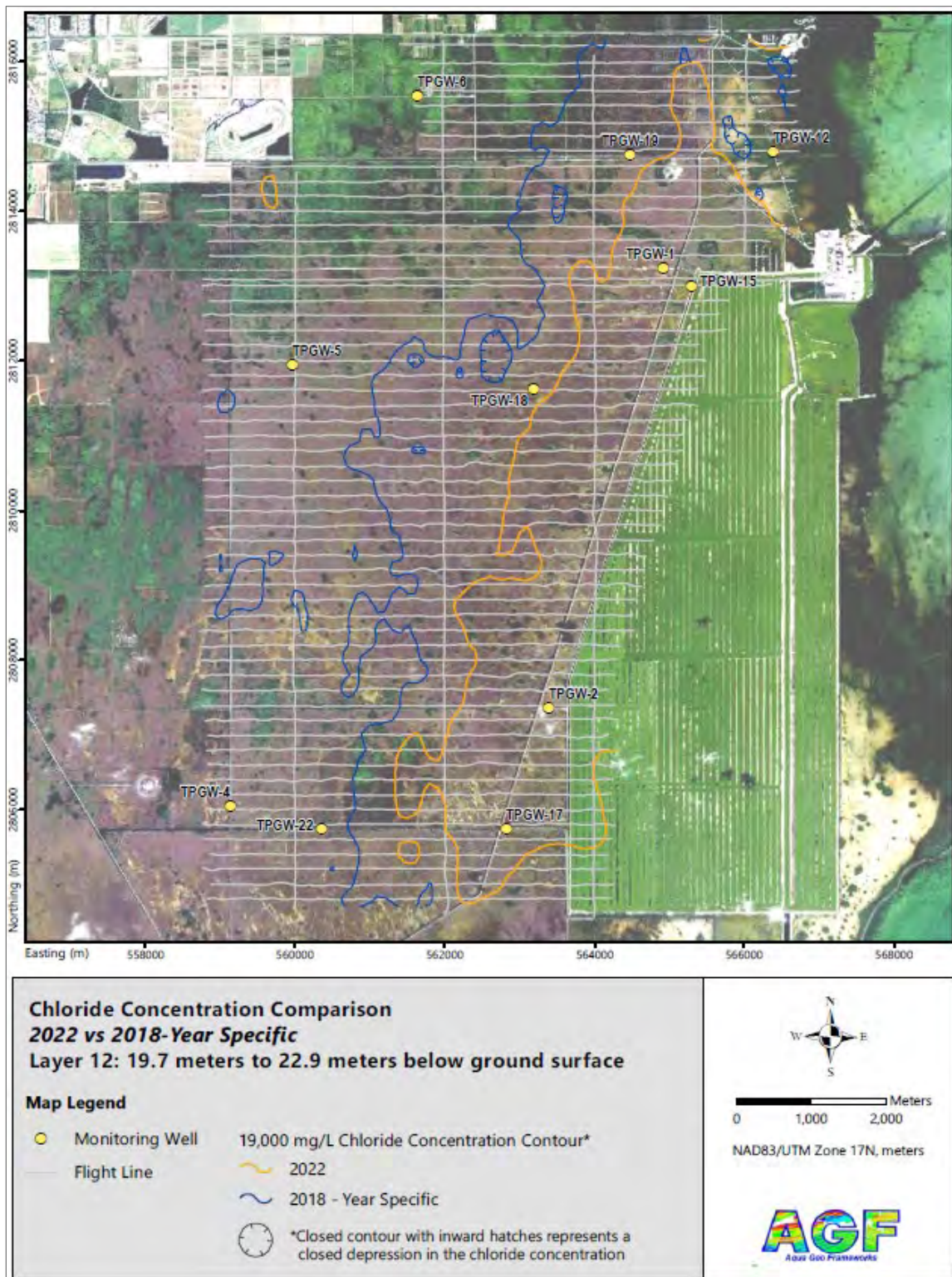
Figure 4.3-5. Layer 12, 19,000 mg/L Chloride Concentration Contours for 2018 and 2022

4.3.4   Volume of the Hypersaline Plume

> There has been a 67% total reduction in the volume of hypersaline Biscayne aquifer materials through Year 4, with layer volume reductions of CCS-sourced hypersaline materials from 53% to 99%.

The volume of the hypersaline plume is estimated by summing the volume of the AEM grid cells (voxels) that have an estimated chloride level >19,000 mg/L. This has been done for all 14 layers of the baseline 2018 and Year 4 2022 surveys. It is very important to note that the volume of each voxel represents the aquifer matrix measured by the resistivity survey to be hypersaline and consists of rock matrix plus aquifer pore water. The majority of the voxel volume is rock, while a smaller percentage (approximately 20% to 30%) is groundwater. As a result, the reduction in volume of the Biscayne aquifer saturated with aquifer pore water with chloride content >19,000 mg/L should not be construed as the volume of hypersaline water "removed" from within the aquifer. Table 4.3-1 lists the measured volume of hypersaline aquifer matrix by layer for the 2018 and 2022 AEM surveys and summarizes the volumetric changes by layer from 2018–2022, expressed both as a percent change in a layer and as a fraction of the total volume. The reduction of hypersaline volume between the 2018 baseline survey and the Year 4 survey is 67%. The volumes are illustrated in Figures 4.3-6 and 4.3-7.

As previously described, the AEM layer geometry and the volumes of the voxels increase with depth. As a result, care should be exercised when comparing the percent reduction of the volume of the aquifer saturated with hypersaline water for different layers. The lower AEM layers have substantially greater volume per voxel than the shallowest layers. To illustrate a relative change in hypersaline aquifer volume between the 2018–2022 AEM surveys, the 2018 and 2022 hypersaline voxel volumes are tabulated and plotted (Table 4.3-1 and Figure 4.3-6). Figure 4.3-7 clearly illustrates that most of the reduction in hypersaline plume volume between 2018–2022 occurred in layers 6–14, corresponding to the three zones of preferential flow in the Biscayne aquifer. Columns 4 and 5 of Table 4.3-1 list the relative percent change in hypersaline voxels by layer between 2018–2022 (positive percentages indicate an increase from 2018). The changes in layer volumes are reported as percentages of the 2018 total volume. The sum of the individual layer changes is the 67% change in the total plume volume from 2018–2022. The layer percentages represent the relative contribution of each layer to the total volume change.
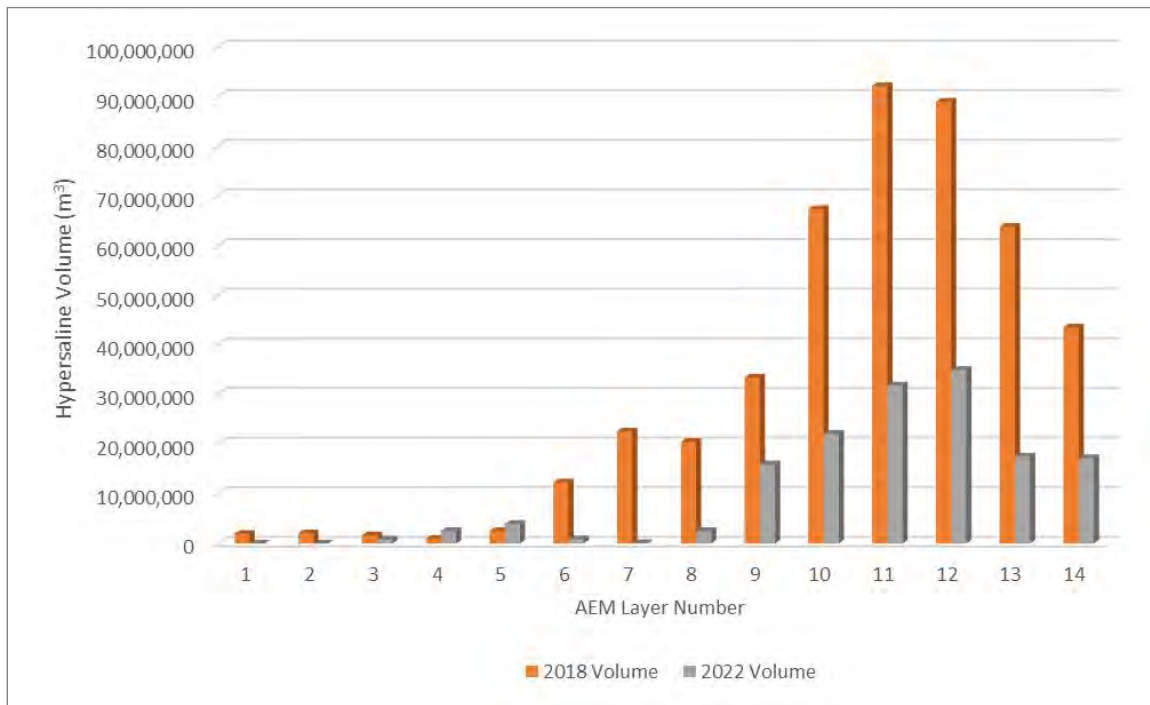
Note: Increases in hypersaline volumes in layers 4 and 5 are from non-CCS sources.

Figure 4.3-6. 2018 and 2022 Hypersaline Volumes (>19,000 mg/L) by Layer
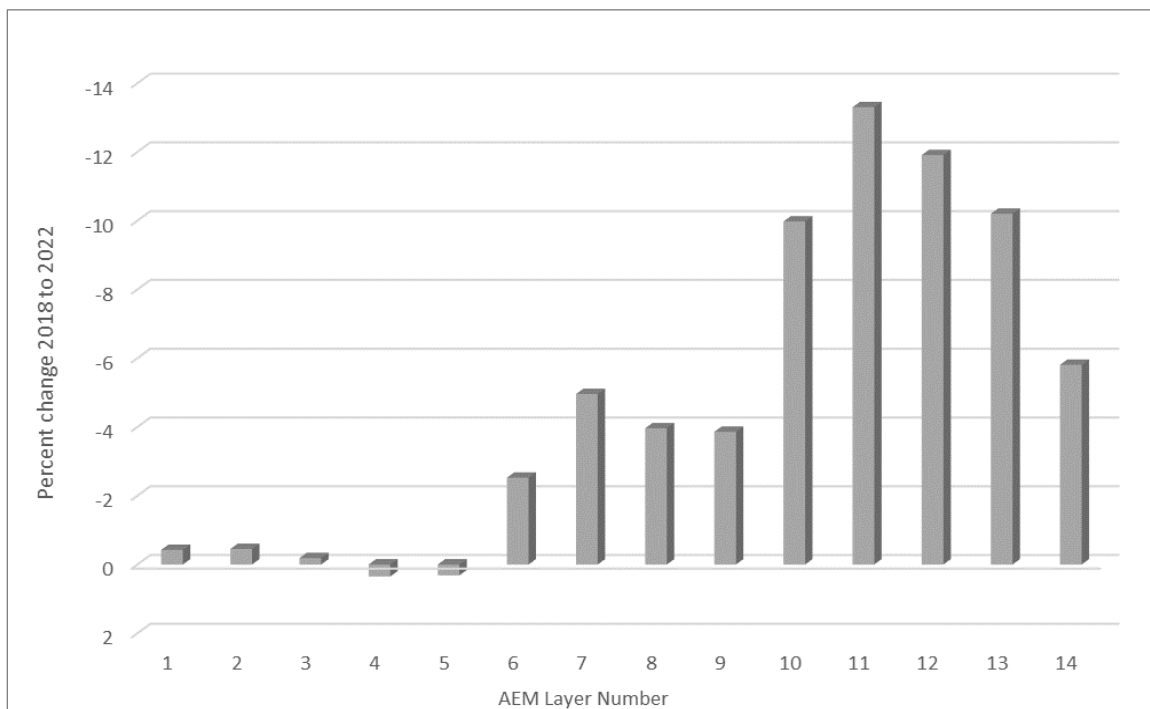
Figure 4.3-7. Normalized Percent Change: 2018 to 2022 (>19,000 mg/L) from the Total 2018 Volume

4.3.5   Summary of Comparison of 2018 and 2022 AEM Survey Results

There has been a statistically significant reduction in the volume of the hypersaline Biscayne aquifer materials of 67% in 2022 as compared to 2018. There is no CCS-sourced hypersaline water in layers 1–4 (upper 15 feet of the aquifer) west of the L-31E levee and most of the hypersaline groundwater in layer 5 is from a non-CCS source. Plume remediation is continuing in all layers and at distances of more than 1 mile from the RWS wells. The volume of the hypersaline plume decreases between 2018 and 2022 in AEM layers 1–3 and 6–14, with the largest volume decreases in layers 7–14. The area of hypersalinity located in layers 1 and 2 in 2018 in the northeastern corner of the compliance area is not sourced from the CCS and has migrated into layers 4 and 5, resulting in net increased hypersalinity in these layers. Layers 1–3 did not contain pore waters >19,000 mg/L in 2022.

4.3.6   Factors for Additional Evaluation

As described above, changes in hypersaline extent over time are based on comparisons between baseline and subsequent AEM survey responses. Accordingly, great care is taken prior to, during, and immediately after AEM field acquisition flights to help ensure consistent data acquisition and processing from year to year. By assuring data acquisition is acquired identically and processed consistently with electromagnetic noise filtered, measured variations in bulk resistivity reflect changes in fluid ionic strength from year to year. Accordingly, AEM's continuous measurement of changes in bulk resistivity produces the most complete data-sourced expression of salinity dynamics available. Nonetheless, FPL plans to conduct additional evaluations to determine whether better alignment between monitoring well data, groundwater model-based plume dynamics, and AEM results can be achieved.

FPL plans to evaluate the following in preparation for the Year 5 RAASR:

- **Extent of retraction of the leading edge (i.e., westward, northern) of the plume.**
  Layer-by-layer comparisons of the of the 2018 baseline and subsequent years 19,000 mg/L isochlor contours, as shown in Appendix G, indicate the reductions in plume volume are largely occurring at distances farthest away from the RWS system and in the thickness of the plume closer to the RWS wells. This west to east retraction is expected and has been represented by the groundwater model (with the exception of the lower model layers where plume retraction may be under-simulated due to hydraulic conductivity assumptions that are also being evaluated). However, in some cases, AEM results have shown hypersaline retraction has occurred at locations farther west than the modeled extent of the RWS well capture radii. In addition, lateral retractions are occurring west of existing monitoring wells. Additional evaluation to refine the AEM documented changes along the western edge of the plume is prudent to further verify the progress made in plume retraction and better inform the model calibration and resulting remediation forecast reliability.

- **Nature of isolated lenses of hypersalinity located in the southwest portion of the compliance area in layer 9.** AEM hypersaline plume maps identified several isolated

island-like occurrences of low hypersalinity (19,000 to 21,000 mg/L chloride) in the vicinity of Tallahassee Road approximately 2.5 to 3 miles west of the southern portion of the CCS in AEM layers 8 and 9. These lenses lacked vertical or lateral continuity with the CCS prior to remediation and have persisted through year 4, primarily in layer 9. As discussed prior in this section, such an expression of apparent elevated chloride could be associated with a change in lithology to a high-porosity clay and silt sequence. Further evaluation will help determine whether CCS-sourced hypersaline groundwater exists at that location or whether the AEM expression is caused by lower salinity water in high-porosity lithology.

- **AEM identified areas of lower salinity groundwater located along the base of the aquifer beneath AEM identified hypersaline layers.** In the area west of the southern portion of the CCS, AEM surveys have shown the western edge of the continuous CCS plume in layers 10 and 11 are farther west than the deeper layers 13 and 14, resulting in areas in the aquifer where fresher groundwater is located beneath higher density hypersaline groundwater. While such a phenomenon could occur where there is an aquitard preventing vertical flow, such occurrences are rare in the Biscayne aquifer. FPL plans to evaluate the potential that high-conductive fluids could be biasing the flow of the AEM signals to deeper layers.

- **Areas where AEM-estimated chloride values are consistently significantly lower than adjacent monitoring well values.** As shown on Table 4.2-3, there are several monitoring wells, mostly monitoring the lower high flow zone, where AEM chloride values are much lower than monitoring measured values (TPGW-1D, TPGW-4D, TPGW-5D, TPGW-19D and TPGW-22D).The large differences between AEM-calculated and monitor well measured chlorides have occurred in the same wells over all four years of comparative data suggesting there is a time invariant feature, such as a variation in geology or a sharp change in salinity, between the well interval and the surveyed AEM layer. FPL plans to evaluate the cause and the lateral extent of the differences to determine whether it is a localized condition or a large-scale factor.

5 GROUNDWATER MODEL

> Data from the 2018 baseline and Years 1 through 4 remediation operations have been incorporated into and assessed in the Turkey Point variable density dependent solute transport model to provide a better understanding of the hydrogeology of the study area, improve the model's ability as a predictive tool, and contribute to the assessment of the progress of remediation.

5.1 MODEL OVERVIEW AND EVOLUTION

5.1.1 Objectives

The variable density flow and salt transport model developed for the design of the RWS has been updated and recalibrated using data from the fourth year of operation of the RWS. This update represents the seventh version of the model. The objectives of the update and recalibration are to inform and reduce the uncertainty of the model and to improve the model's simulation of saltwater conditions throughout the full aquifer vertical profile and the model's capability to predict the plume response to the groundwater recovery system. Revised five- and 10-year model predictions and milestones to evaluate the system's performance with respect to achieving the objectives of paragraph 17.b., of the CA are provided.

These objectives were addressed by the following actions:

- Performance of a sensitivity analysis with the model used in the prior RAASR (V6) to investigate the potential causes of that model's inability to align the saline-hypersaline interface (HSI) position along the base of the aquifer and retract the HSI in a manner consistent with monitor well and CSEM data.

- Incorporation of the results of the sensitivity analysis into the Version 7 model calibration process.

- Restructuring the vertical resolution of the model from 11 layers to 17 to represent the presence of the third high flow zone and the dynamics of density-dependent flow and transport more accurately in the lower parts of the Biscayne Aquifer.

- Assignment of revised depth-discrete hydraulic conductivities based on reinterpretation of drill cores and geophysical logs as starting values in the model calibration.

- Incorporation of leakance (hydraulic conductivity/sediment thickness) zones from the water and salt balance of the CCS to align the modeled water and salt flux with that derived from the CCS-focused balance model.

- Incorporation of the salinity, water level, and mass extraction data (RWS and UIC test production wells) collected during the fourth year of the recovery system operation.

- Increasing calibration target weights on annual salinity changes during remediation to further emphasize the accurate simulation of the movement of the saline and hypersaline interfaces during the fourth year of RWS operation.

The revised model was then used to predict RWS impacts on the degree of CCS sourced hypersaline groundwater plume retraction at Years 5 and 10 of remediation and update Years 5 and 10 plume retraction milestones based on the V7 forecasts.

5.1.2 Model Versions

The current groundwater flow and salt transport model documented in Appendix I is the seventh version (V7) of a 3D regional model developed by FPL to evaluate various projects associated with the Turkey Point CCS. The model has undergone an evolutionary process as the objectives of the modeling changed, as progressively more data are added, and as the knowledge base expands. The evolution of the model to date is summarized in Table 5.1-1 and presented in detail in Appendix I.

FPL originally developed a 3D SEAWAT (Langevin et al. 2008) model wherein density varied as a function of both salinity and temperature (Tetra Tech 2016). This model is referred to as the V1 model. The purpose of the V1 model was to evaluate alternatives for compliance with the MDC CA and FDEP CO that required stopping the westward migration of hypersaline water and retracting hypersaline water north and west of the CCS to the L-31E canal and the FPL property. This model simulated the period from pre-development (early 1940s) through 2015 and was calibrated by manual methods to measured water levels and salinity. The model was used to evaluate a number of potential groundwater remediation projects that resulted in the selection of Alternative 3D, which involved implementing a groundwater RWS consisting of 10 wells screened to the base of the Biscayne Aquifer capable of pumping 15 mgd of hypersaline groundwater that would be disposed in an existing UIC DIW. Based on the V1 model (with minor modifications requested by the reviewing agencies) and the associated results related to the retraction of the hypersaline plume, the model's application in the assessment of Alternative 3D was conditionally approved by MDC on September 29, 2016.

In addition to using the model to aid in the evaluation and selection of a groundwater remediation system, FPL was directed by FDEP to use the variable density 3D groundwater model developed under the MDC CA to allocate relative contributions of the CCS and other entities or factors on the movement of the saltwater interface. In order to conduct this evaluation, several modifications, including many of those required by MDC, were necessary and incorporated into what is referred to as the Version 2 or V2 model. The results of the V2 modeling were presented to FDEP on June 19, 2019.

Table 5.1-1.   Summary of Groundwater Model Versions

	Version 1	**Version 2**	**Version 3**	**Version 4**	**Version 5**	**Version 6**	**Version 7**
Date	June 2016	June 2018	October 2019	September 2020	April 2021	September 2021	October 2022
Purpose	Design RWS	FDEP attribution analysis	Year 1 verification of RWS	Year 1 Calibration to RWS	Year 2 Calibration to RWS	Year 3 Calibration to RWS	Year 4 Calibration to RWS
Calibration Method	Manual	Automated (PEST)	Automated (PEST)	Automated (PEST)	Automated (PEST)	Automated (PEST)	Automated (PEST)
Hydraulic Conductivity Representation	Uniform within layers	Heterogeneous in layers 4,8,9,10,11	Heterogeneous in layers 4,8,9,10,11	Heterogeneous in layers 4,8,9,10,11	Heterogeneous in layers 4,8,9,10,11	Heterogeneous in layers 4,8,9,10,11. Contrast between 5,6, and 7; 9,10, and 11 based on JLA Associates	Heterogeneous in layers 4 and 7-17. Contrast between 7 and 8; 10 and 11; 12, 13, and 14; 15,16, and 17 based on JLA Associates
Recharge Formulation	Net	Precipitation and Evapotranspiration	Precipitation and Evapotranspiration	Precipitation and Evapotranspiration	Precipitation and Evapotranspiration	Precipitation and Evapotranspiration	Precipitation and Evapotranspiration
CSEM Data Used?	No	Yes	Yes	Yes	Yes	Yes	Yes
Predictions	10-year forward	40-year backward	10-year forward	9-year forward	8-year forward	7-year forward	6-year forward
Primary Change / Focus	Assess alternatives for compliance; selected alternative 3D	Differentiate between Recharge and ET, detailed surface water representation, CSEM targets evaluate causal factors of regional saltwater intrusion	Second round of CSEM and recent TPGW & RWS wells as targets; verify with stress (RWS)	Recent TPGW & RWS wells as targets; incorporation of geologic information at TPGW and RWS locations	Third round of CSEM and recent TPGW & RWS wells as targets; revision to CSEM targets to eliminate localized significant changes in salinity	Fourth round of CSEM and recent TPGW & RWS wells as targets; porosity as a spatially variable parameter, sensitivity analysis to guide calibration	Fifth round of CSEM and recent TPGW & RWS wells as targets; subdivision of lowermost layers and inclusion of a lower high flow zone; initial hydraulic conductivity from JLA Associates, use of water/salt balance to determine CCS leakance

In compliance with paragraph 17.b.ii., and 17.d.v., of the MDC CA, as amended on August 20, 2019, FPL has annually updated the variable density flow and salt transport model informed with data collected during operation of the RWS. In addition to inclusion of additional RWS pumping rates and mass extracted, TPGW well water levels and salinities, CCS stage and salinity, and CSEM salinity data, each version of the model was modified with new findings or modeling techniques and recalibrated. Examples of these modifications include: (1) use of the automated parameter estimation technique called PEST, (2) incorporation of compatible elements of the surface water routing package developed by USGS and implemented by Hughes and White (2014), (3) incorporation of geologic information obtained during and after the installation of the RWS and TPGW monitoring wells, (4) use of an averaging procedure to create a smoother CSEM salinity distribution that contained less apparent outliers than the prior versions, and (5) inclusion of layer-wide heterogeneity of porosity instead of the layer-wide homogeneity used in the prior models.   Following calibration, the models were used to make projections regarding the performance of the RWS over the remaining years of operation. In addition to the V2 model, four model updates have occurred annually such that the current model is referred to as the Version 7 or V7 model.

5.1.3   Sensitivity Analysis with the Version 6 Model

Several of the recommendations in the Year 3 RAASR (FPL 2021b) and in the independent model review conducted by Groundwater Tek Inc on behalf of MDC DERM (GTI 2022), sought to obtain a more accurate present-day location of the hypersaline interface as the Version 6 (V6) modeled plume appeared to be more extensive than suggested by the CSEM data. To investigate the causes of the model's inconsistent alignment of both the saline-hypersaline interface position along the base of the aquifer and the retraction of the saline-hypersaline interface (HSI) with respect to monitor well and CSEM data, sensitivity analyses were performed using the V6 model to identify potential changes to model parameters, boundary conditions, initial conditions, or calibration techniques that have the greatest influence on hypersaline plume location and retraction. A model sensitivity analysis involves a series of simulations where model inputs are varied from their calibrated values in a systematic manner to enable quantitative evaluation of effects of those variations on model outputs. The insights gained through the sensitivity analyses are used to improve model responses and calibration of the year 4 RAASR Version 7 (V7) model.

Table 5.1-2 shows details of the sensitivity evaluations that were performed with the V6 model. Five categories of evaluations were performed: effects of initial conditions on PEST calibration, effects of explicitly adding the lower high flow zone, correlation between horizontal and vertical hydraulic conductivity, use of water and salt balance to inform CCS connection to the aquifer, and calibration targets and weights. For many of the categories, the evaluation involved multiple simulations to either represent both the historical and future aspects of the modeling or to obtain a true sense of sensitivity by various degrees of parameter perturbation.

Table 5.1-2.   Description of Sensitivity Evaluations and Simulations Performed with the V6 Model

Evaluation No.	Sensitivity Description	Question to be Answered	Why Important?
1	Use geologist estimated hydraulic conductivities as initial condition subjected to PEST gradient search calibration	Does the geologist estimated hydraulic conductivities provide a better calibration than produced by PEST?	Hydraulic conductivity values influence containment, interface location, and retraction.
2	Effect of adding Lower High Flow Zone	Does explicit inclusion of lower high flow zone improve match to saltwater interface and remediation progress?	Lower high flow zone provides a direct avenue for plume movement in the lower (and pumped) part of the aquifer.
3	Correlation between horizontal and vertical hydraulic conductivity	Can a better calibration be attained with different ratios of Kh to Kv?	Relationship between horizontal and vertical ease of flow affects lateral capture distances.
4	Use of CCS water and salt balance data to inform CCS connection to aquifer	What is the effect of a more informed timeseries of CCS/aquifer inflows and outflows?	How the model simulates CCS hypersaline discharges to the aquifer prior to RWS operations affects the spatial extent of the plume.
5	Calibration targets and weights	Can different calibration targets be identified and weighted to better reflect plume extent and remediation?	Accurate representation of plume extent and remediation supports the usefulness of the model for evaluating remediation enhancements.

Based on the results of the sensitivity simulations, updates associated with the formulation of the V7 model included the following items: 1) restructuring the vertical resolution of the model from 11 layers to 17 to represent the presence of three high flow zones and the dynamics of density-dependent flow and transport more accurately in the lower parts of the Biscayne Aquifer, 2) specification as starting values in the model calibration of depth-discrete hydraulic conductivity surfaces based on reinterpretation of drill cores and geophysical logs to the 17-layer vertical resolution, 3) incorporation of leakance zones from the water and salt balance of the CCS to align the modeled water and salt flux with that derived from the CCS-focused balance model and 4) increasing calibration target weights on overall salinity changes during remediation to further emphasize the accurate simulation of the movement of the saline and hypersaline interfaces during the fourth year of RWS operation. Additional details regarding the V6 model sensitivity analyses are presented in Chapter 4 of Appendix I.

5.1.4   Description of Version 7 Model

Detailed descriptions of the V7 model assembly, calibration, and predictive simulations are included in Appendix I. The V7 model uses the same basic plan-view framework as the prior V1 though V6 models. It simulates a 276-square-mile area that is subdivided from west to east into 274 columns and from north to south into 295 rows. The width of the rows and columns vary between 200 ft and 500 ft, with smaller grid cell dimensions located near the CCS. The model domain overlain by the model grid is shown on Figure 5.1-1.

A significant change to the model included in this update was a revision to the vertical layering that had been used in prior models. Layering in model versions 1 through 6 were informed by data produced from an aquifer performance test as prescribed in paragraph 17. B. I., of the CA and consisted of 11 layers that included two thin high flow zones located in the upper portion of the Biscayne Aquifer and comparatively lower hydraulic conductivity layers assigned to the lower portion of the aquifer. However, subsequent lithologic data produced from the construction of the RWS and additional monitoring well identified a persistent third high flow zone that appears as a discontinuity within the lower sequence of the Fort Thompson Formation. This deeper high flow zone is also identified in the original FPL Extended Power Uprate (EPU) monitoring well network throughout the region. The lack of the deep high flow zone and the associated low hydraulic conductivities assigned to the lower layers of the prior model versions is thought to be a potential reason why prior models produce different representations of hypersaline groundwater than those reflected in groundwater monitoring data and AEM surveys. Based on a sensitivity analysis with the V6 model it was determined that inclusion of a deep high flow zone was important for accurately representing the results of RWS operation.

Accordingly, the layering and vertical framework of the V7 model has been modified from the V6 model, with the Biscayne Aquifer divided into 17 layers in the V7 model.   The uppermost model layers (layers 1 through 4) represent the Miami Oolite. The thicker Fort Thompson Formation was divided into thirteen layers (layers 5 through 17). Well borings and geophysical logs were analyzed to define geologic contact elevations containing zones with large, connected voids to determine the regional hydrostratigraphy. Consequently, three such high flow zones were represented in the regional model based on their relatively higher hydraulic conductivity. The upper high flow zone (layer 4) occurs at the base of the Miami Oolite, the middle high flow zone (traversing layers 7 through 11 across the model domain) is located in the approximate middle of the Fort Thompson formation, and the deep high flow zone (traversing model layers 11 through 17 across the model domain) is located near the base of the Fort Thompson formation.

800390, 337650 (SPE83 feet)

Legend

▢ Study Area	– – – Cross Section Location Row 116	North
▢ Model Grid	0 1 2 Miles	
▢ Inactive		

GIS\modelgrid_sec.mxd
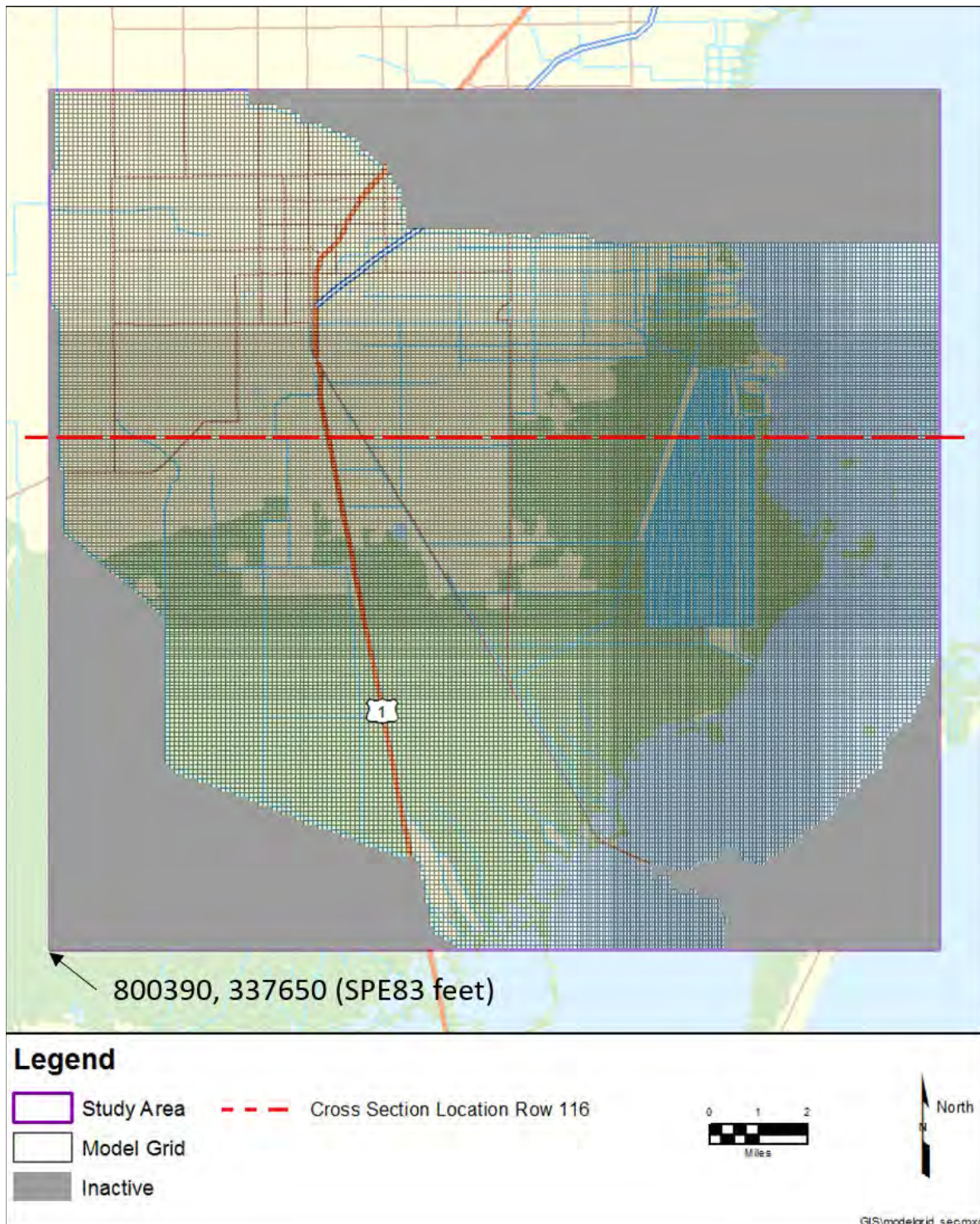
Figure 5.1-1.   Model Study Area Overlain by the Active Model Grid; Red Dashed Line Represents the Location of the Model Cross Section Shown in Figure 5.1-2

Refinement of the layers in the model's lower half was also important to better represent the dynamics of density-dependent flow in the area of highest salinity. The V1-V6 layer structure was maintained for ease of comparison of results of the V7 to prior models by subdividing the prior layers into even multiples. As such former layer 7 was subdivided into two layers (new layers 7 and 8); former layer 9 was subdivided into two layers (new layers 10 and 11); former layer 10 was subdivided into three layers (new layers 12, 13, and 14); and former layer 11 was subdivided into three layers (new layers 15, 16, and 17). Horizontal hydraulic conductivity estimates, based on geologic cores and geophysical logs collected from TPGW monitoring wells and RWS production wells, were interpreted for each model layer by JLA Associates (2022). These values were kriged to form hydraulic conductivity arrays for each model layer. This methodology allowed the high-conductivity zones to be discontinuous or to be present in multiple layers. Figure 5.1-2 provides a cross-sectional view of the 17 layers of the V7 model and how they correspond to the hydrogeologic formations. The location of this cross section, along row 116 of the model, is shown on Figure 5.1-1. Unlike the prior models, the interpreted values were used as the starting values in the calibration with the opportunity for adjustment based on the ability of the model to replicate measured heads and concentrations.

The representation of the connection between surface water in the CCS and the underlying groundwater system, or leakance, has been modified in the V7 model. The V6 and prior models used a single leakance value to represent the entire CCS. The value of the leakance varied with time depending upon conceptualization of the effect of siltation and dredging. The V7 model uses four zones of leakance, as derived from the water and salt balance model of the CCS (FPL 2012) and shown in Figure 5.1-3. Use of zones of leakance is consistent with the conceptual model that sediment thicknesses and characteristics may vary due to velocity dependent siltation, dredging, and/or vertical flow direction (inflow or outflow). Use of values from the water and salt balance ensures consistency between the models, but moreover provides parameter values that are derived specifically from calibration to CCS stage and salinity dynamics.

The USGS groundwater flow and solute transport modeling tool SEAWAT V4 (Langevin et al. 2008) was used in this analysis and the prior (V1 through V6) modeling analyses. This SEAWAT version includes: (1) solute transport simulations through the integrated MT3DMS process (Zheng and Wang 1998); and (2) variable density flow (VDF) simulation through the VDF process. SEAWAT's VDF package was used to simulate the density effects of both temperature and salinity. SEAWAT inputs and outputs are specified in terms of "point-water heads" (Langevin et al. 2008), which represent the hydraulic head at a given location based on salinity and temperature. SEAWAT solves the groundwater flow and transport equations after converting point-water heads to "reference heads" or "equivalent freshwater head at the reference temperature."

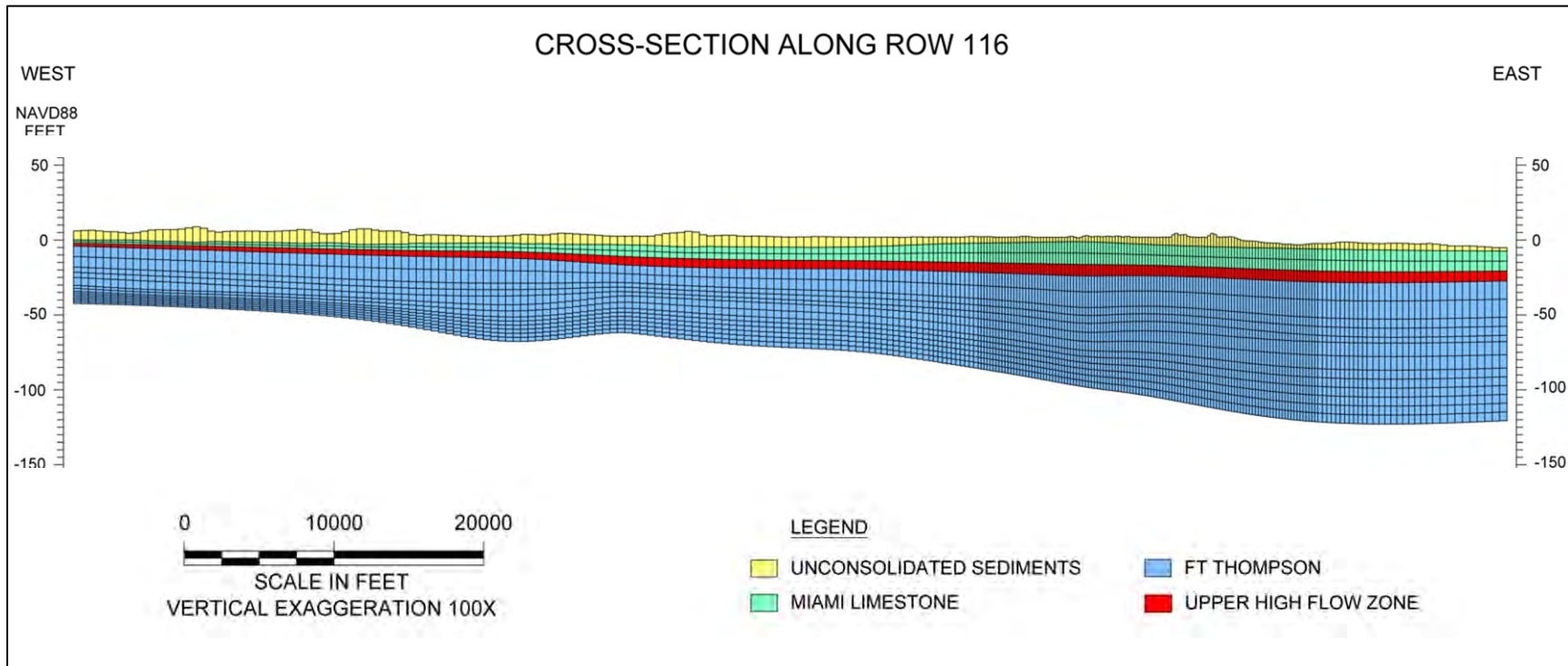**Figure 5.1-2.   Cross Section Showing Model Layering and Hydrogeologic Formations (Location of Cross Section Shown in Figure 5.1-1)**
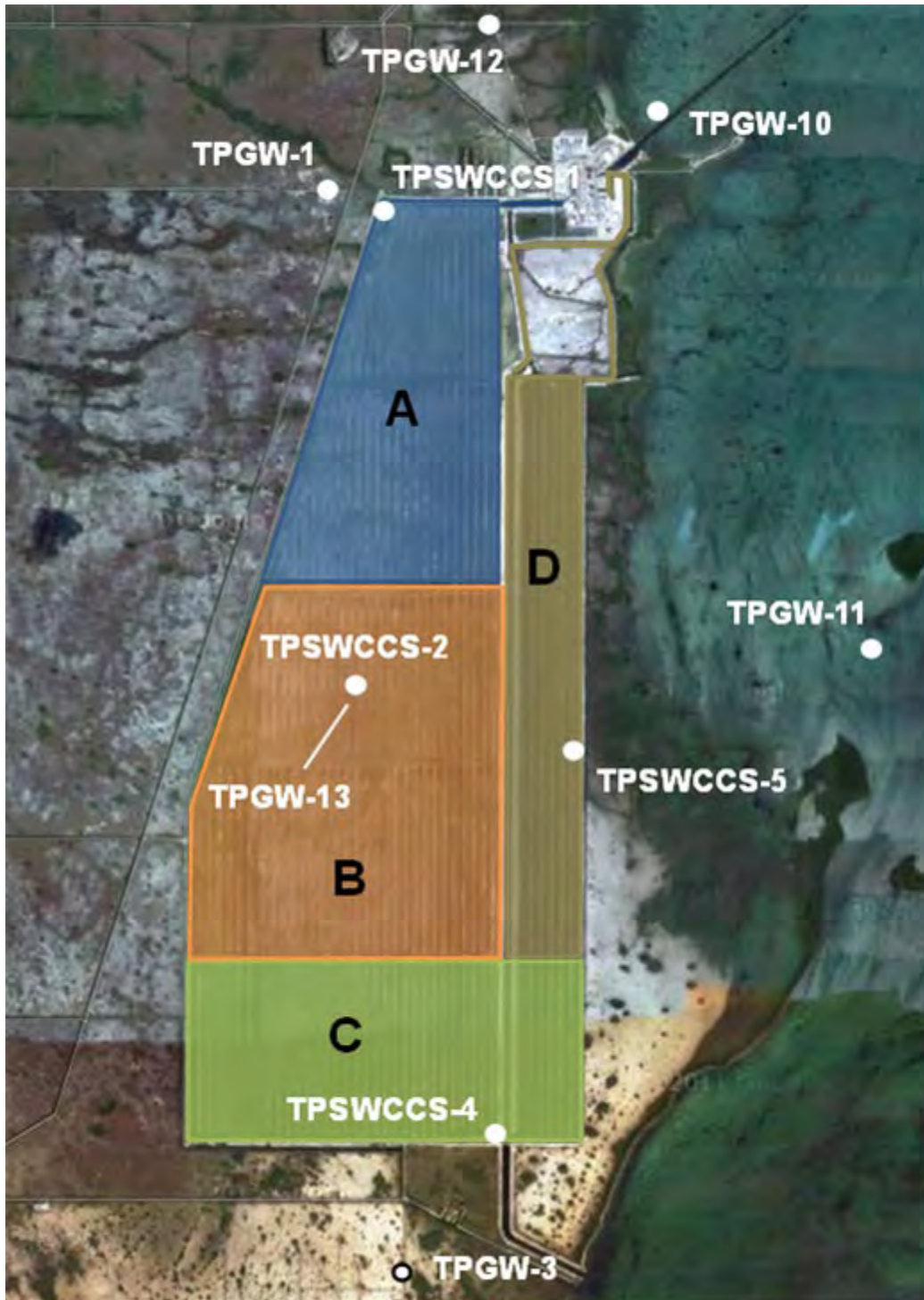
Figure 5.1-3.   Representation of the CCS with Four Zones of Leakance from the Water and Salt Balance Model

The boundary conditions applied to the V7 model are also very similar to those applied in the prior models. Namely, specified head-boundary conditions are used to simulate the effects of temporal changes in Biscayne Bay and the various canals (including the CCS) on groundwater flow and transport. General-head boundaries are used to simulate the exchange of groundwater across the model's lateral boundaries on all sides. Next Generation Radar (NEXRAD)-based rainfall rates and historical patterns (spatial and temporal) in land use are used to estimate the amount of groundwater recharge throughout the model domain. Reference evapotranspiration (ET_o) data and land use/land cover data are used similarly to estimate groundwater evapotranspiration (ET) rates as a function of groundwater head. Consumptive use of groundwater for agricultural purposes and some industrial uses (e.g., the Blue Water Industries and Card Sound quarries) are simulated as specified withdrawals; and they were estimated based on land cover, estimated local rainfall/recharge, and ET rates. Municipal and other industrial groundwater uses are also simulated as specified withdrawals and are based on data as much as possible. The temperatures and salinities assigned to water entering from the various boundaries simulated are also based on actual data, as much as possible.

The V7 model incorporates canal hydraulics and groundwater interactions based on Hughes and White's (2014) modeling for MDC that were added in the V2 model. Details of these additions are included in Appendix I.

5.2   MODEL MODIFICATIONS/CALIBRATION

> The model was calibrated to 82 years of data, including Years 1 through 4 of operation of the RWS. The resulting calibration indicates the model is a reasonable tool to be used in conjunction with monitoring data and CSEM results to assess progress in meeting the groundwater remediation objectives of the MDC CA and FDEP CO. However, improvements in the model's alignment with CSEM and monitoring well data at the edge of the hypersaline plume in 2018, prior to remediation and during subsequent remediation years, is needed to improve reliability of long-range remediation forecasts.

5.2.1 Model Calibration Process

In order to perform reliable predictions and satisfactorily meet the objectives of this modeling effort, the SEAWAT model required calibration. Model calibration is the process of adjusting parameters and boundary conditions within reasonable ranges to match historical observations reasonably well. The ability to replicate past conditions in the calibration period provides confidence that the model can simulate future conditions in the model applications. The process for developing a model capable of providing accurate projections of RWS operation involves calibration of the model to prior measured data that are similar to those of the projections it is to make. This model calibration involved matching: (1) water level and salinity observations; and (2) salinity estimates based on spring 2018, spring 2019, fall 2020, summer 2021, and summer (June) 2022 CSEM data set. The calibration period includes the V6 model calibration period (i.e., pre-development through June 2021) plus an additional 12 months. This 12-month period includes the June 2022 CSEM data set. The calibration model is subdivided into four timeframes,

each of which simulates the development and movement of the saltwater wedge under different hydrologic and anthropogenic stresses. These periods are defined as follows:

- Pre-development steady-state flow model (prior to 1940)
- Steady-state flow and transient transport calibration model (1940–1968)
- Seasonal transient flow and transport calibration model (1968–2010)
- Monthly transient flow and transport calibration model (2010–2022)

The final period includes the first, second, third, and fourth year of RWS operation. Operational pumping rates for each RWS well are input monthly. All available precipitation and boundary condition (i.e., canal stage) data are also used. Model results for water levels, salinities at monitoring wells, CSEM salinity distribution, and mass extracted by the RWS are compared to measured values.

Calibration was performed primarily using automated PEST, which seeks to minimize the summation of weighted residuals, or differences between the sought observed / measured values and the interim calibrated values of targets, using a systematic mathematical optimization procedure.

5.2.2 Model Calibration Results

The calibration results for water levels and relative salinities are shown in Table 5.2-1. Seasonal and monthly transient model water levels and relative salinities are shown separately in Appendix I. In general, the monthly data set is considered more reliable than the seasonal data set because it uses the multi-depth and short-screened TPGW wells at which groundwater levels and salinity are measured on an hourly basis. As a result, the monthly data set also has considerably more data despite its shorter duration (2010-2022). A robust assessment of model calibration quality and statistics is provided in Appendix I.

Table 5.2-1. Calibration Statistic Summary for the V7 Model

Model	Target Type	Units	ME	MAE	RMSE	MAE ÷ Range
Seasonal (1968-2010)	Hydraulic Head	ft	-0.130	0.464	0.614	6.8%
	Relative Salinity	R.S.	0.013	0.090	0.163	5.4%
Monthly (2010-2022)	Hydraulic Head	ft	-0.162	0.325	0.447	5.2%
	Relative Salinity	R.S.	0.034	0.161	0.216	8.4%
CSEM (2018 through 2022)	2018 CSEM Survey	R.S.	0.017	0.230	0.313	11.2%
	2019 CSEM Survey	R.S.	0.066	0.252	0.343	12.2%
	2020 CSEM Survey	R.S.	0.086	0.241	0.332	11.7%
	2021 CSEM Survey	R.S.	0.091	0.229	0.319	11.2%
	2022 CSEM Survey	R.S.	0.142	0.245	0.346	11.9%

<u>Note</u>: One Relative Salinity (R.S.) Unit = 35 PSU = 19,400 mg/L Cl

Figures 5.2-1 and 5.2-2 show comparisons of the modeled hypersaline interfaces to the 2022 CSEM layer equivalent interface orientations and the TPGW monitor well supplemented with CSEM points (presented in Figures 3.3-1 through 3.3-3) locations. These figures illustrate that the model generally under-simulates the extent of the interface relative to the other interface locations in shallow layers as represented by layer 9 but over-simulates the edge of hypersalinity in deep layers such as layer 16. The over-simulation of the extent of the hypersaline compared with AEM and monitoring well generated interface locations is consistent with prior versions of the model. The perceived over-simulation is an area that continues to be investigated with sensitivity analysis and alternative conceptual models.

The model responds similarly to the actual hydrologic system during the first four years of RWS operation in that salinity changes are only observed in wells relatively close to the RWS (e.g., TPGW-1). Except TPGW-17, salinity changes in wells near the RWS are observed only in shallow and intermediate wells. Model versus measured change in salinity since 2018 for wells TPGW-1, TPGW-2, TPGW-4, TPGW-15, TPGW-17, TPGW-18, TPGW-19, and TPGW-22 are shown on Figure 5.2-3. Comparison of model to measured salinity change is very good for these wells, though inexact. Where simulated changes in salinity notably deviate from observed changes (TPGW-1M, TPGW-15M), the model over-simulates salinity decline.

Figure 5.2-1.   Location of the Modeled, CSEM, and TPGW-Supplemented Hypersaline Interfaces in Layer 9
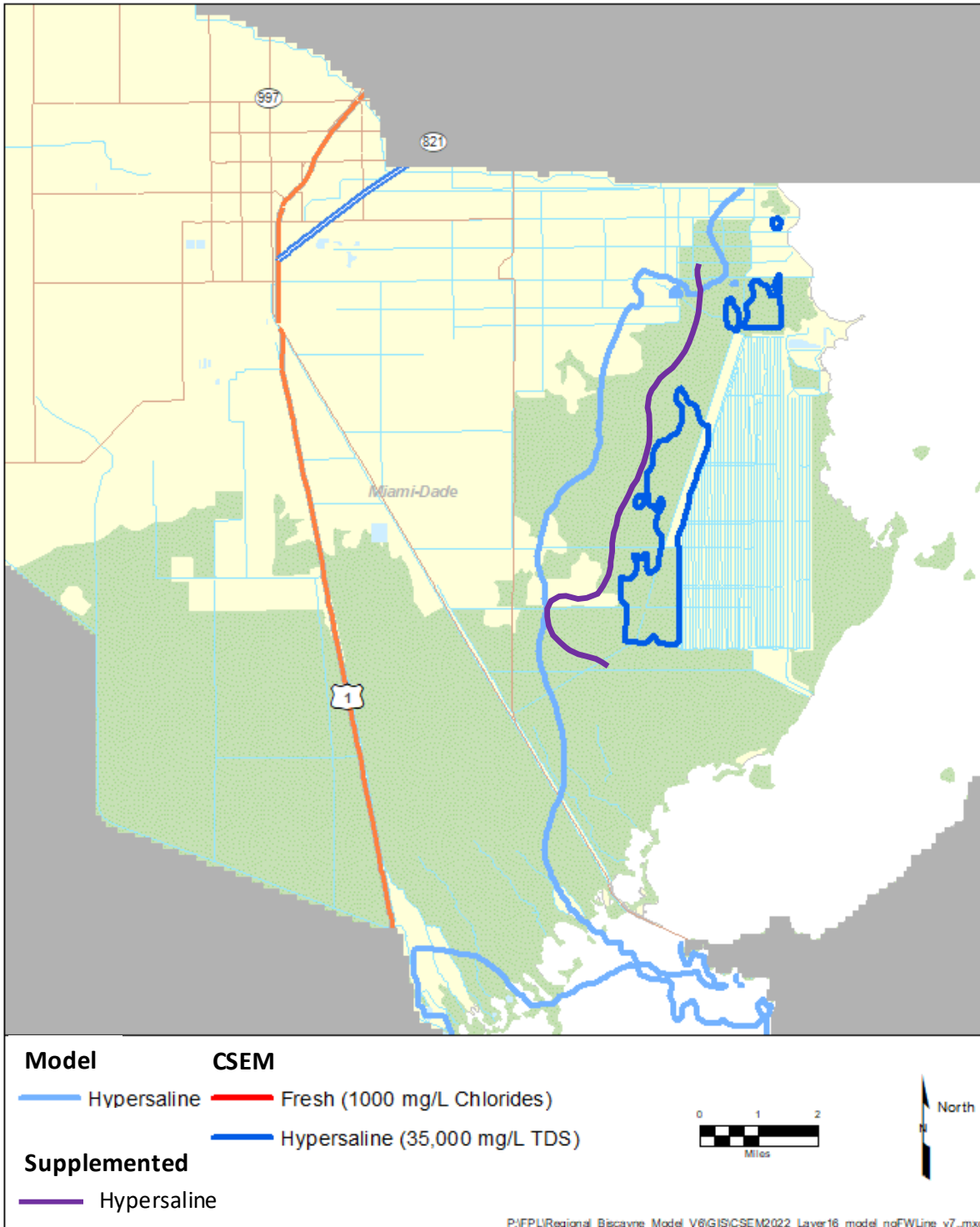
Figure 5.2-2.   Location of the Modeled, CSEM, and TPGW-Supplemented Hypersaline Interfaces in Layer 16
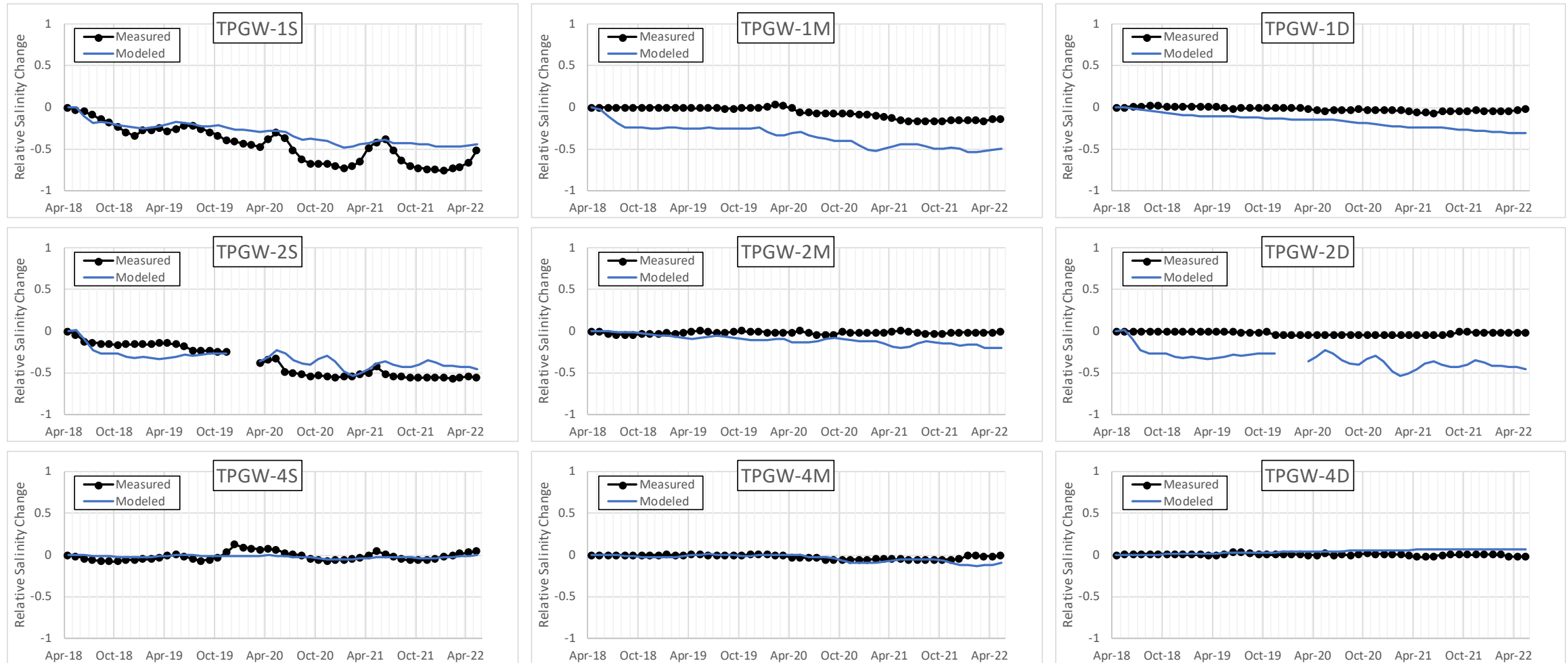
Figure 5.2-3.   Comparison of Model and Observed Changes in Relative Salinity with Time by Well Between April 2018 and May 2022
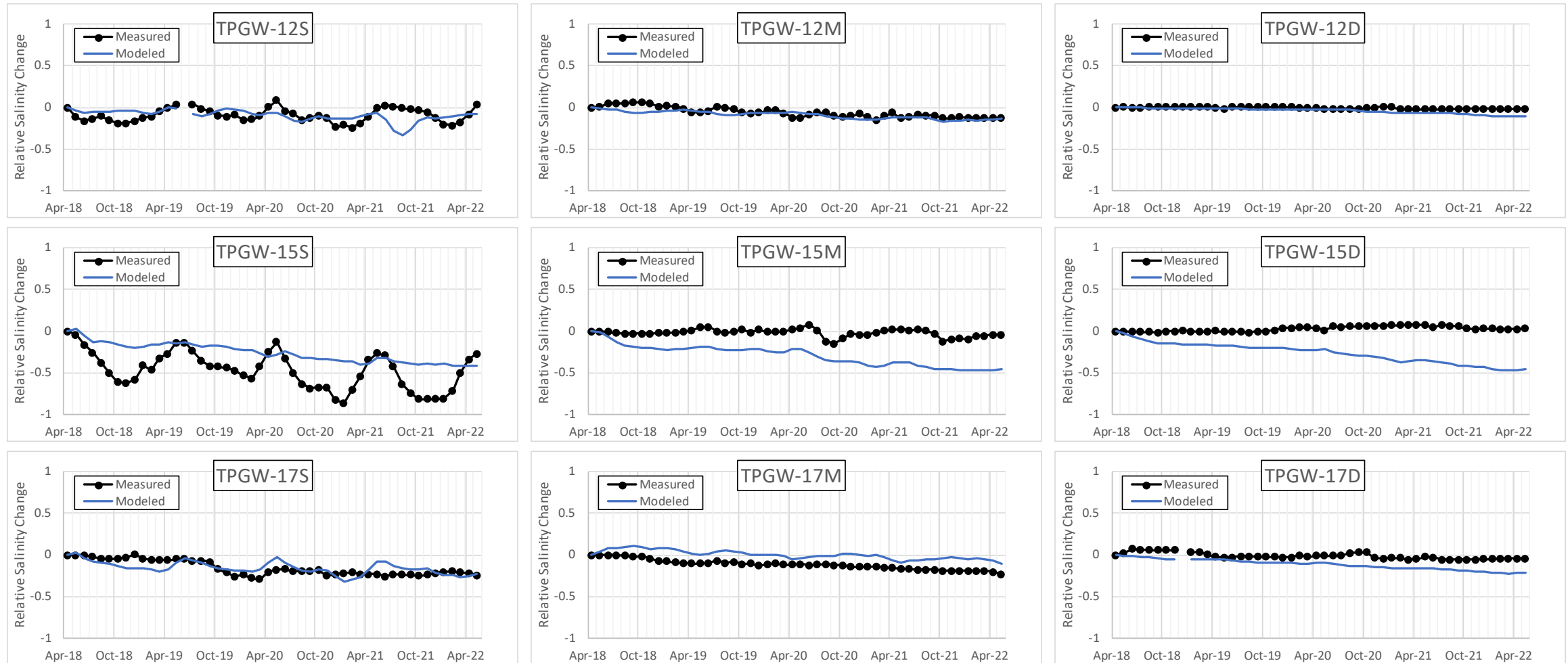
Figure 5.2-3 (continued). Comparison of Model and Observed Changes in Relative Salinity with Time by Well Between April 2018 and May 2022
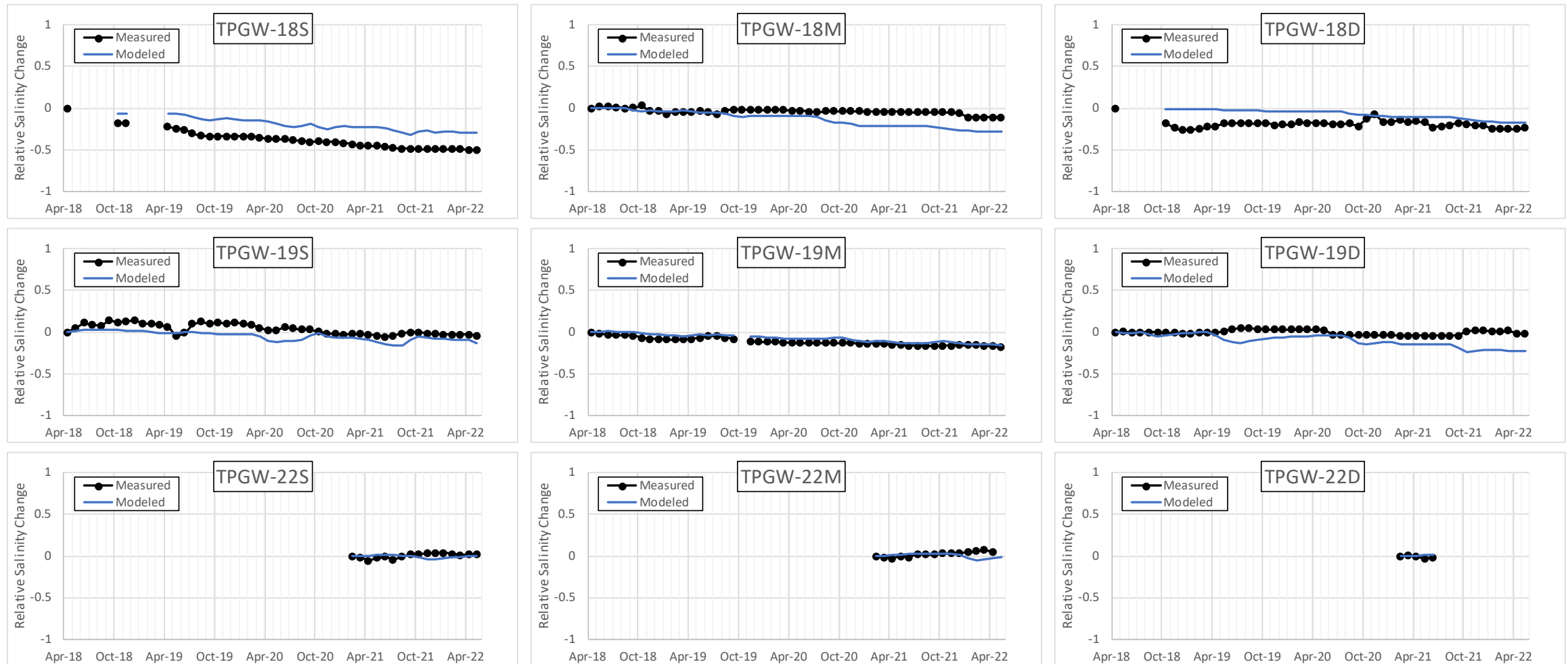
Figure 5.2-3 (continued). Comparison of Model and Observed Changes in Relative Salinity with Time by Well Between April 2018 and May 2022
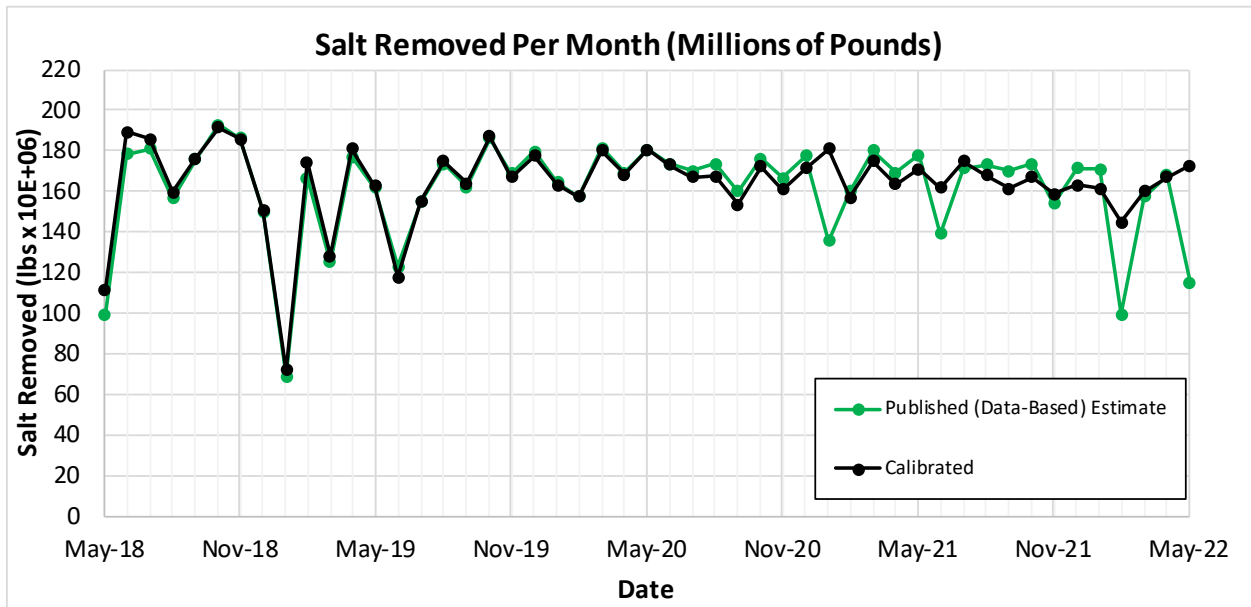
Figure 5.2-4.   Comparison of Model and Observed Total Mass Extracted by the RWS Between May 2018 and May 2022
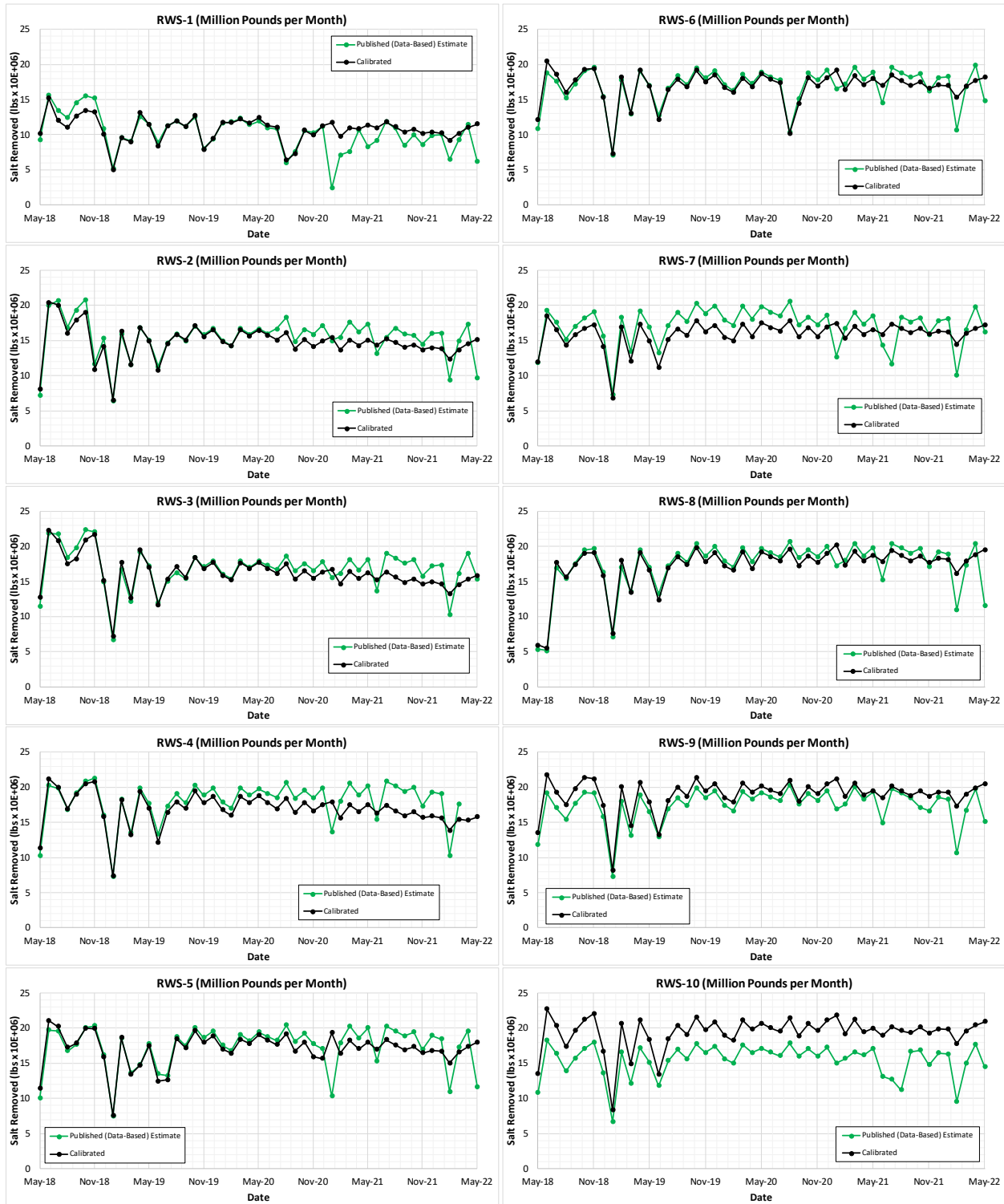
Figure 5.2-5.   Comparison of Model and Observed Mass Extracted by Well Between May 2018 and May 2022

5.3   REMEDIATION YEARS 5 AND 10 FORECAST

> Predictive model runs indicate the RWS will fully retract the hypersaline interface in the upper two thirds of the Biscayne Aquifer (layers 1-10) to the FPL property within 10 years of RWS operation. The simulations indicate the hypersaline interface retracts towards FPL property in layers 11 through 15 and the westward expansion slows or halts in layers 16 to 17. However, the results in the lower model layers differ from CSEM-measured changes suggesting additional evaluation of the model forecast and CSEM trends are needed.

5.3.1   Description of Remediation Simulations

The construction of the predictive model uses the calibrated V7 data and conditions represent a recent time frame of varied hydrologic conditions. The model is well calibrated and its use to simulate Years 5 and 10 potential plume responses to continued RWS operations is presented here. It is recognized that there are areas for improvement in the alignment of the remedial responses documented by the monitoring well network, the AEM surveys and the groundwater model.   Continued analysis of all three methods used to assess progress in plume remediation is ongoing and will continue in 2022-2023 with the intent of improving the collective understanding of the plume and its response to remediation actions. Accordingly, modeled forecasts generated by the V7 model may differ from forecasts produced by subsequent model versions.

The projected results of the operation of the RWS during Year 5 through Year 10 were simulated in a similar fashion as the operations of the RWS during Years 1 through 4. The initial conditions for the simulation were the ending conditions (i.e., salinity, temperature, and water level) of the final period of the calibration simulation (June 2022). Climate conditions (e.g., precipitation, evaporation, canal stages) for the 2018-2022 period used in the calibration were repeated during the predictive period; the first four years of the prediction mimicked the 2018 to 2022 timeframe, and the 2018 to 2020 timeframe informed the final two years of the prediction. In the Model-Land ArcHydro Enhance Database watershed west of the CCS, the average annual (June to May) precipitation during the period 2010 to 2022 is 47.2 inches (DBHYDRO 2022). Over the 2018 to 2022 4-year timeframe, the average annual rainfall is 48.7 inches. This 4-year sequence is marked by precipitation that is below average for the first year (41.7 inches), above average for the second and fourth years (50.3 and 54.6 inches, respectively), and close to average for the third year (48.2 inches) (DBHYDRO, 2022). The RWS was simulated to operate according to the design: 1.5 mgd extraction from each RWS well, for a total of 15 mgd withdrawal. The CCS was set at a salinity of 34 PSU for the duration of the predictive period. In addition, the UIC test production wells were set to withdraw a total of 3 mgd from beneath the CCS for the duration of the remediation period.

5.3.2   Remediation Forecast

Model forecasts of the position of the hypersaline/saline water interface in Years 5 and 10 of remediation were determined using the V7 model, and they are similar to prior forecasts. Retraction of the hypersaline plume to the L-31E canal is achieved in the upper 10 model layers (approximately two thirds of the Biscayne Aquifer thickness) by year 10 of remediation. Figures 5.3-1a, b, c and d illustrate the Years 5 and 10 plume retraction in model layers 4, 9, 13, and 16. Plume positions for Year 5 and 10 for additional model layers are shown in Appendix I. In layers 11 through 15, the plume is retracting toward the FPL property through Year 10 but remains west of the L-31E canal. Due west of the southern portion of the CCS in layers 16 and 17, however, the plume is shown to expand further west through year 5 and halts or slows by Year 10 of remediation. This forecast is contrary to Year 4 CSEM survey results that show net retractions of the plume exceeding 60% along the base of the aquifer has already occurred from 2018 through 2022 as shown on Table 4.3-1 and visually in Appendix G 6A.

At this point, it is not clear whether the differences between the model forecast retraction in the lower portion of the aquifer compared with AEM measured retraction achieved during the first four years of remediation is a result of a physical phenomenon or inaccuracies in either the model or AEM. The physical phenomenon of the complexities of CCS leakance (temporal variability caused by siltation and dredging, spatial variability of sediment thickness and hydraulic conductivity) may play a role in the extent of the historical location of the hypersaline interface. The leakance terms associated with the CCS canals are a controlling influence on the quantity of hypersaline water and salt mass that is released to the aquifer. Additionally, based on the geologic/geophysical logs (JLA Associates 2022) horizontal hydraulic conductivities in the screened zones of the RWS vary significantly from well to well. For example, the average hydraulic conductivity in layers 15 through 17 is 1,587 ft/d in RWS-7 and 16,260 ft/d in RWS-9, a difference of over an order of magnitude. The RWS wells that withdraw from layers assigned with lower hydraulic conductivities have steeper cones of depression and hence narrower capture zones than RWS wells with higher hydraulic conductivities. As a consequence of the steeper cones of depression, these wells may obtain more water vertically than horizontally. This conceptual model is supported by the layer 16 capture zones near RWS-5, RWS-6, and RWS-7 being smaller than the capture zones in overlying but unpumped layers.

In addition, there appears to be contribution from non-CCS, coastal, evaporative-formed hypersaline groundwater that is recharging the hypersaline plume north and south of the CCS. The V7 and earlier versions of the model have shown this process to be simulated with the surface-formed hypersalinity migrating vertically in the aquifer and recharging the lower model layers. Retraction in southern areas surrounding the CCS could be hampered by continued addition of non-CCS sourced hypersaline water from the south. Additional evaluation of the model's representation and extent of this process should be evaluated to determine the degree to which this source of hypersalinity could impact the CCS remediation objectives.
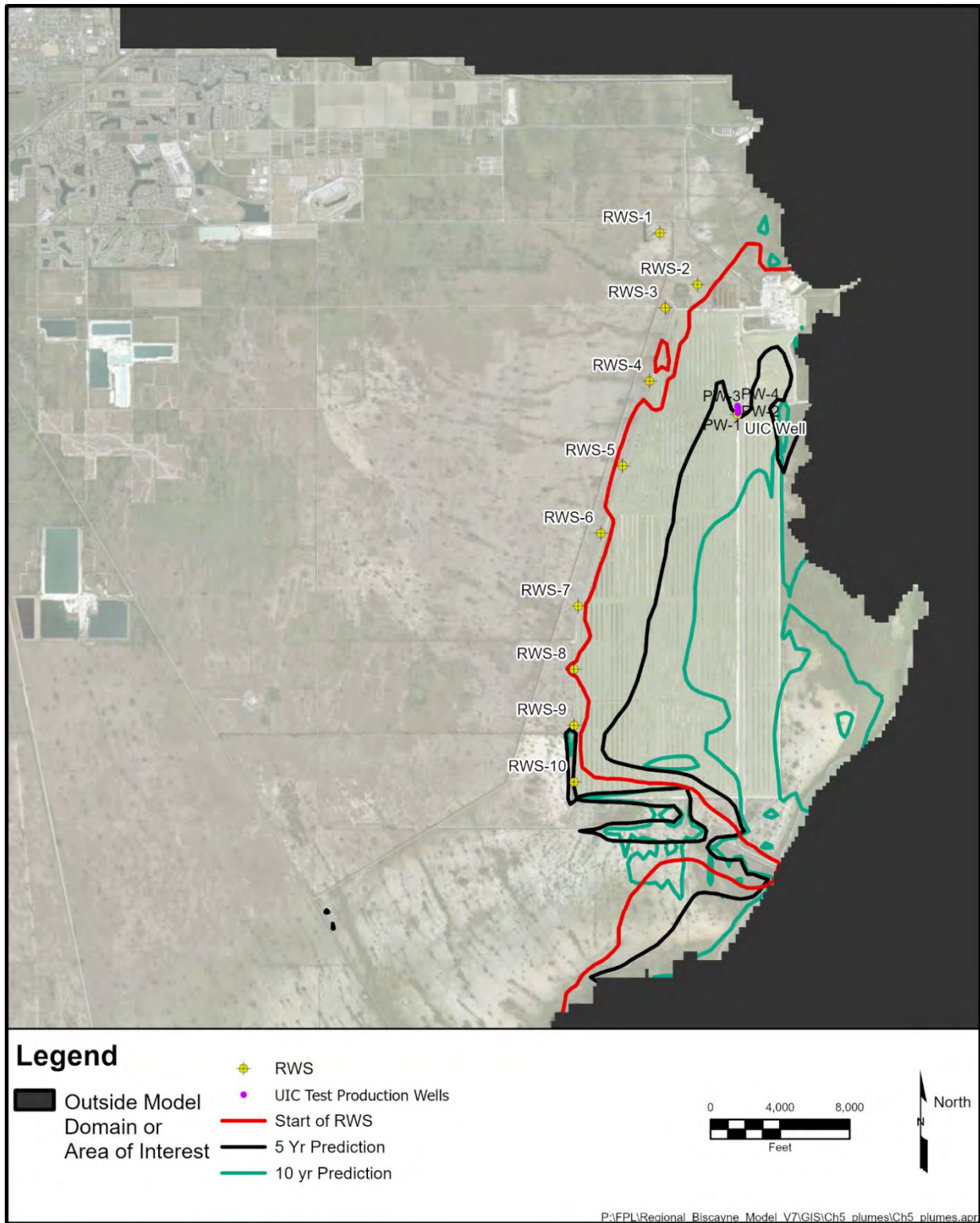
Figure 5.3-1a. Location of Initial, Year 5, and Year 10 Hypersaline Interface in Model Layer 4
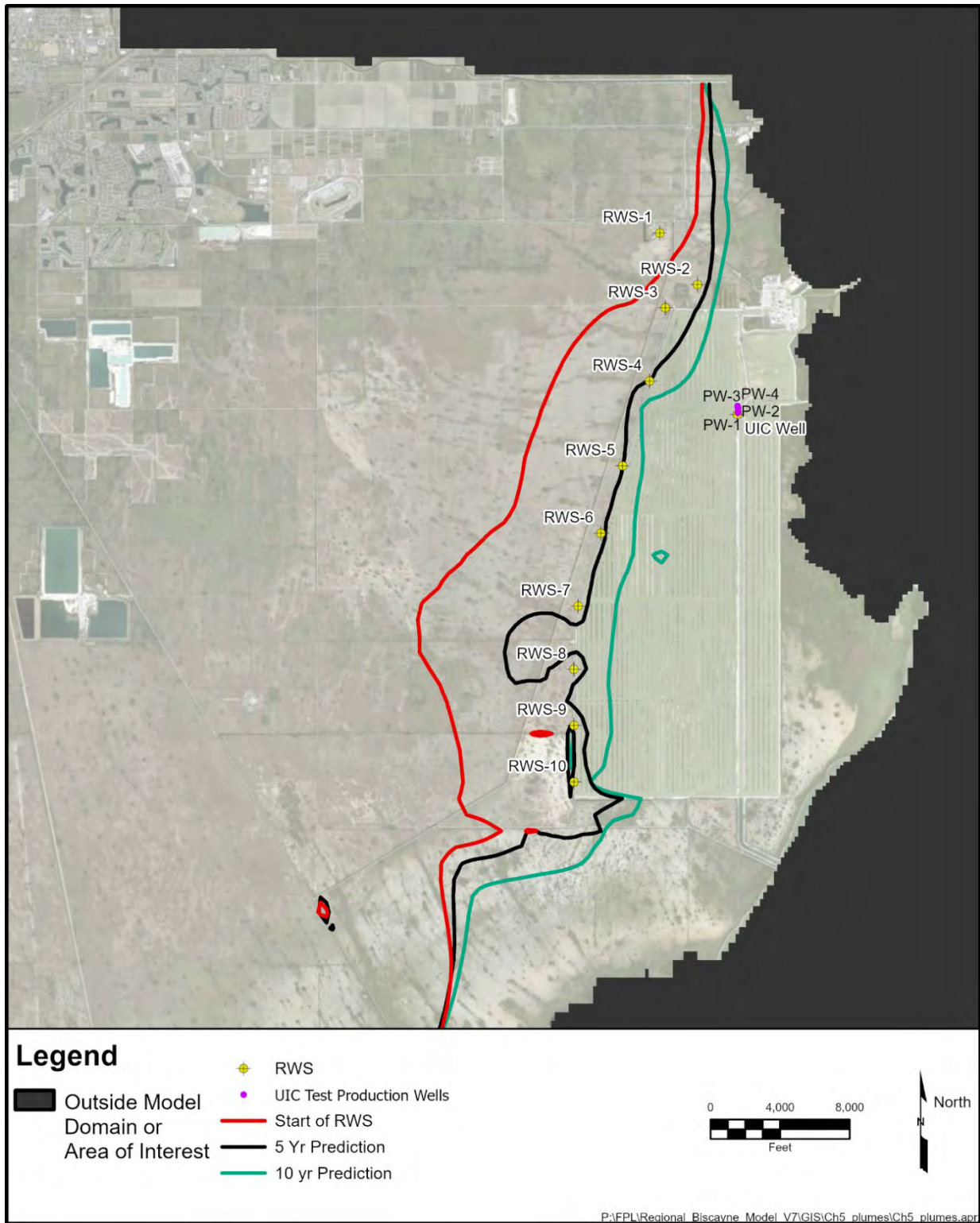
Figure 5.3-1b. Location of Initial, Year 5, and Year 10 Hypersaline Interface in Model Layer 9
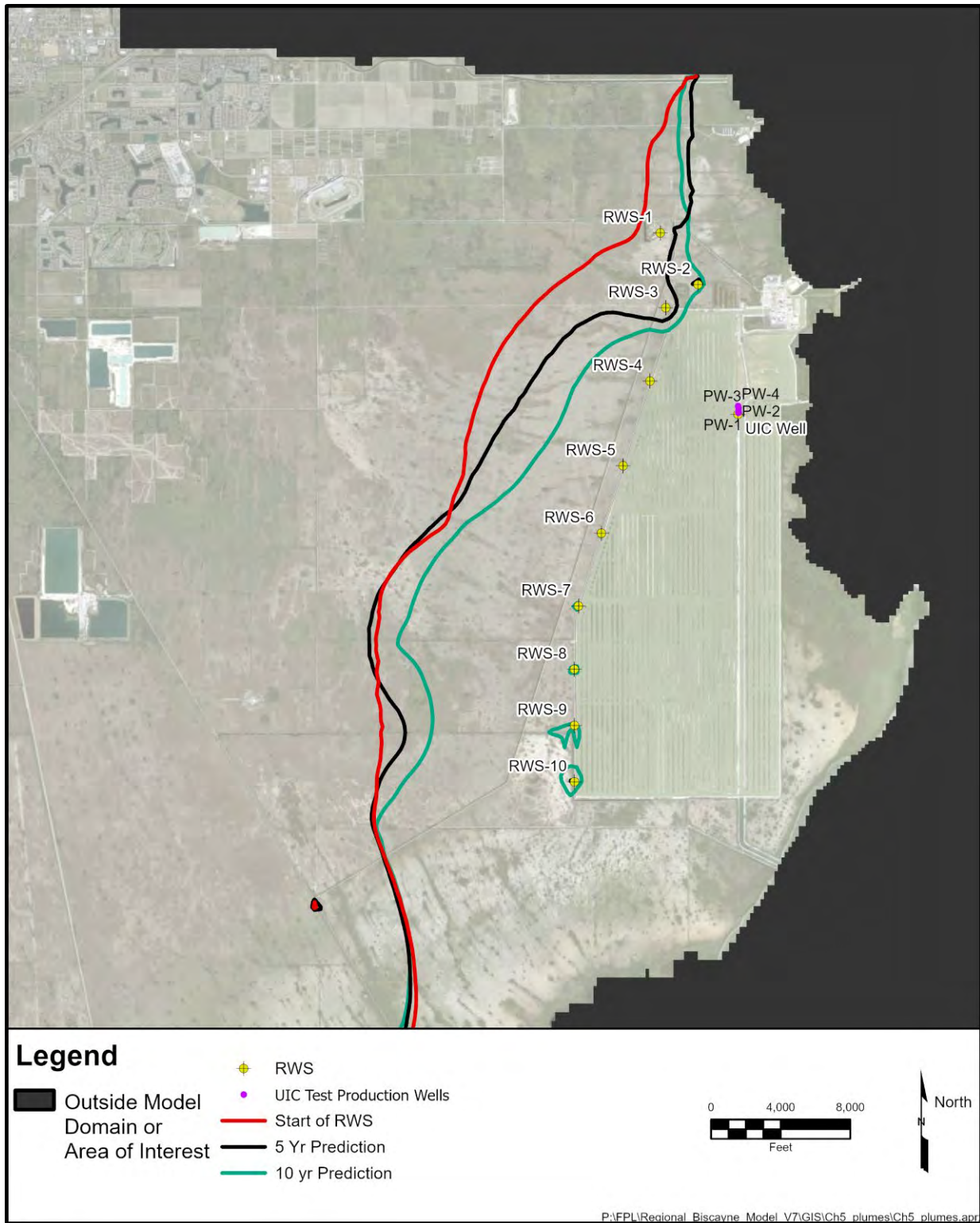
Figure 5.3-1c. Location of Initial, Year 5, and Year 10 Hypersaline Interface in Model Layer 13
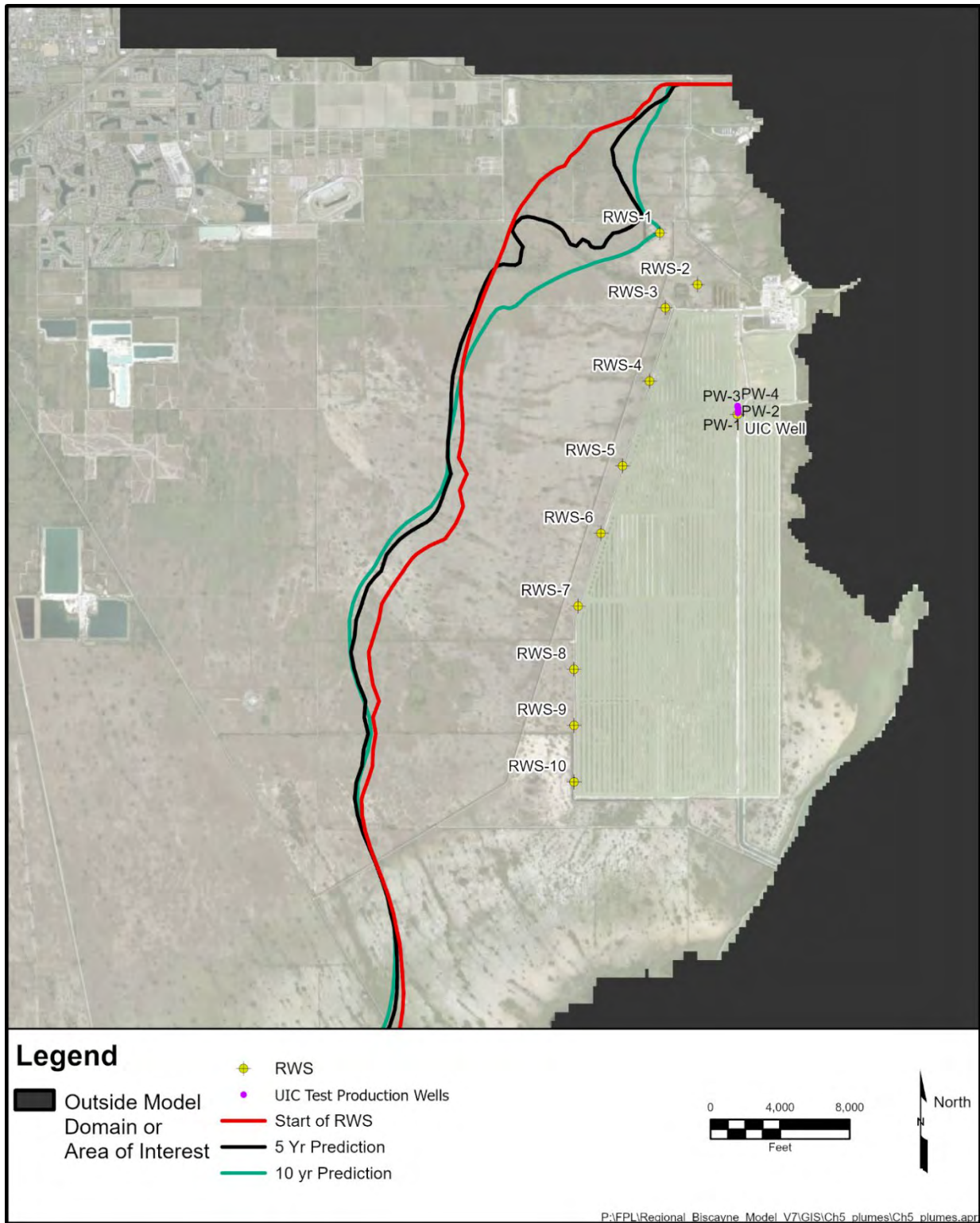
Figure 5.3-1d. Location of Initial, Year 5, and Year 10 Hypersaline Interface in Model Layer 16

Particle tracking, conducted using the V7 model (Figure 5.3-2), confirmed the hypersaline water from the CCS is intercepted, captured, contained and no longer recharges the plume within the compliance zone. Figure 5.3-2 shows the predicted capture zones of layers 4, 6, 9, 10, 13, and 16. This analysis was conducted for all model layers from initiation of the RWS operations through 10 years of remediation. These figures are generated by initializing particles in cells in the areas shaded gray in Figure 5.3-2 and highlighting the starting locations of each particle that ends at the RWS in orange. This evaluation indicates the operation of the RWS provides a hydraulic constraint to the migration of hypersaline groundwater from beneath the CCS. A gap in the layer 16 capture zone appears to exist between RWS well 6 and 7 and to a lesser degree between RWS wells 5 and 6. This gap was investigated further and indicated that particles in this area are either stagnant, appear to oscillate in direction with no clear destination, or traverse along circuitous pathways that require travel times of greater than 10 years to reach their final RWS well destination. As discussed above, it appears that the narrower capture zones in this area are related to the relatively low hydraulic conductivities that occur at these wells. The pumping stress at these wells is transferred upward such that more water is obtained from above than laterally, as desired. This conceptual model is supported by the comparatively more extensive capture zones that exist in layers that are above the pumped zone (Figure 5.3-2).
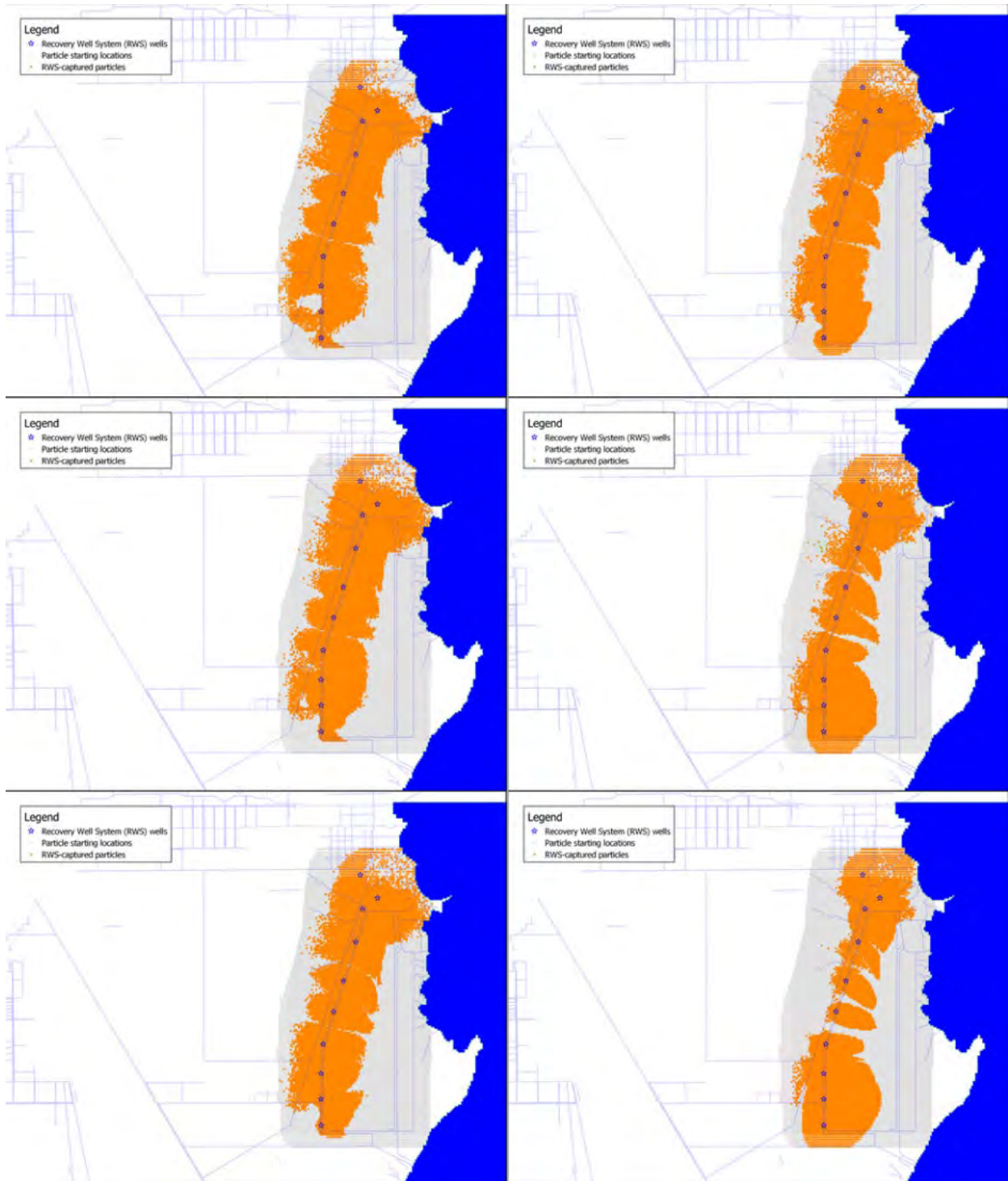
Figure 5.3-2.   Predicted nine-year capture zones for model layers 4 (top left), 6 (center left), 9 (bottom left), 10 (top right), 13 (center right), and 16 (bottom right)

5.3.3 Sensitivity Simulations

Two sensitivity simulations were performed with the V7 calibration and prediction models. The simulations suggest the importance of accurate quantification of the initial plume and a plausible conceptual model to reproduce the monitoring well and CSEM-derived plume configurations.

Two sensitivity simulations were performed to 1) assess the influence on remediation of the hypersaline plume being aligned with the CSEM data and 2) evaluate the efficacy of a conceptual model in better aligning the hypersaline plume with CSEM and monitor well data.

The first sensitivity simulation was made to test the effect of the accuracy of the location of the hypersaline plume at the start of the RWS operations. It has been recognized for some time that model calibration tends to result in an initial plume that extends further west than supported by the CSEM data (see Figure 5.2-2). Oversimulating the extent of the edge of the plume away from the RWS wells would result in the model forecasting either longer timeframes for plume remediation or not retracting the interface in areas outside the capture zones of the wells. It was not clear how much of a change in the plume retraction forecast would result from a less extended initial plume location. This condition was evaluated by replacing modeled salinities within the compliance zone with data from the 2022 CSEM study as initial conditions for the simulation of RWS operation.

The results of this simulation are similar to the original simulation in the upper 7 layers. The plume for this simulation is less extended to the west in the lower layers than in the original model, with a salinity below 45 PSU in layer 12 that is within the compliance zone. However, the movement of the interface in layers 13 and 17 (Figures 5.3-3 and 5.3-4) shows mixed results with westward movement in some areas during the 10-year remediation period. These results are generally consistent with the capture zone figures for these layers (Figure 5.3-2) which show limited lateral reach west of the RWS in some areas. The interface continues its westward movement under the influence of hydraulic and density gradients when located outside the capture zone. This simulation suggests that the model's inability to align interface movement with the CSEM data is related to the representation of the near-RWS flow system. The sensitivity simulation highlights the importance of having the model construction and hydraulic properties reproduce the CSEM initial plume more accurately. More refinement of the near-RWS conceptual model is needed to improve alignment between the model and CSEM results which would produce different forecast results. These factors of the conceptual model include vertical hydraulic conductivities of the aquifer, leakance of the CCS, and source/sink representation of L-31E.
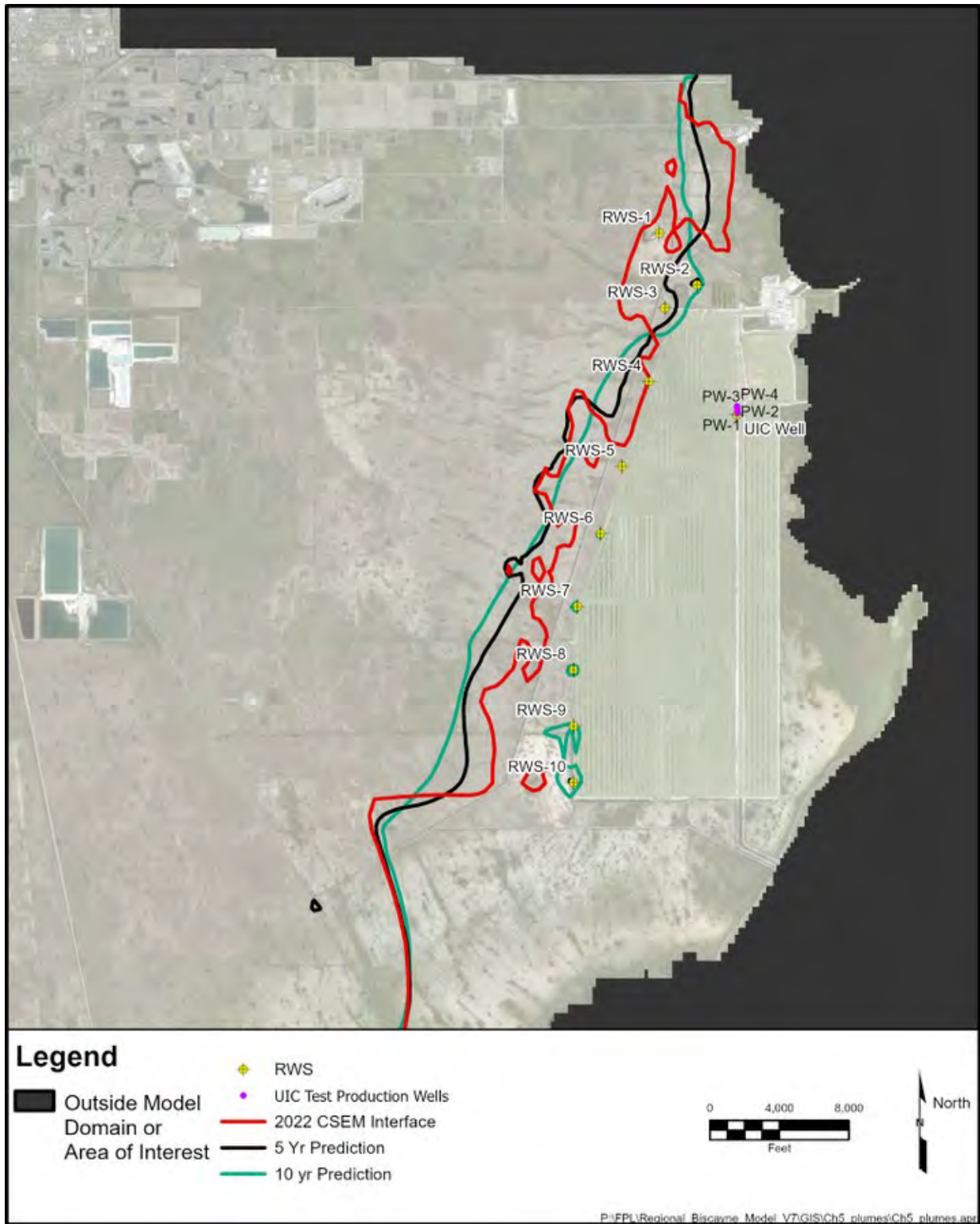
Figure 5.3-3.   Location of Initial, Year 5, and Year 10 Hypersaline Interface in Model Layer 13 for the First Sensitivity Simulation
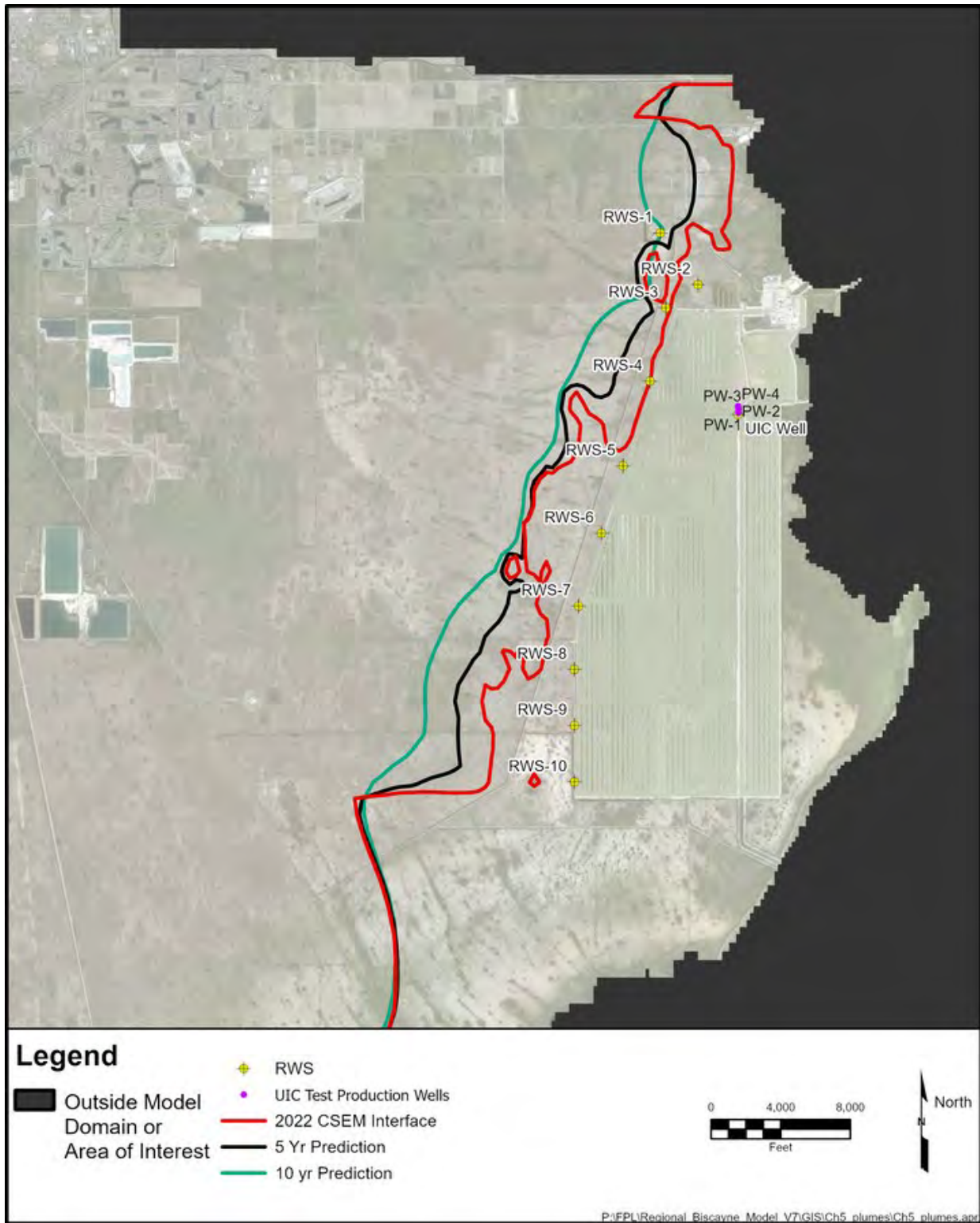
Figure 5.3-4. Location of Initial, Year 5, and Year 10 Hypersaline Interface in Model Layer 16 for the First Sensitivity Simulation

As a follow up to the findings of the first sensitivity simulation, a second sensitivity simulation was made to evaluate the effect of the modeled boundary representation of the L-31E drainage canal has on the hypersaline interface location. The V1-V7 models have represented this boundary with the "river package" which allows flow out of the aquifer when the aquifer head is greater than the canal stage and into the aquifer when the aquifer head is less than the canal stage. It is plausible that L-31E is primarily an outflow or drain boundary condition and that allowing flow into the aquifer provides an artificial source of water to the RWS water demand that more appropriately would come from aquifer storage or a more distal source. The L-31E water source would tend to reduce the lateral and upgradient capture zones of the RWS wells and thereby cause the model to under-represent plume retraction. Evidence for "short-circuiting" of water from the L-31E to the RWS wells in the model are the subtle rings of low salinity water that surround some of the RWS wells in the color-flood plots of plume salinity.

To test this hypothesis, the modeled representation of L-31E was changed from a "river package" to a "drain package" boundary condition. The entire historical model was run to 2022 with this representation. As shown in Figure 5.3-5 the modeled mass extraction is not degraded from the original calibration model. Moreover, the hypersaline interface is closer to the CCS than in the original V7 calibration model (Figure 5.3-5). The prediction model also shows greater retraction (Figures 5.3-6 and 5.3-7) than the original V7 predictive model. The sensitivity simulation presents a possible conceptual model for consideration in the V8 model for the Year 5 RAASR.
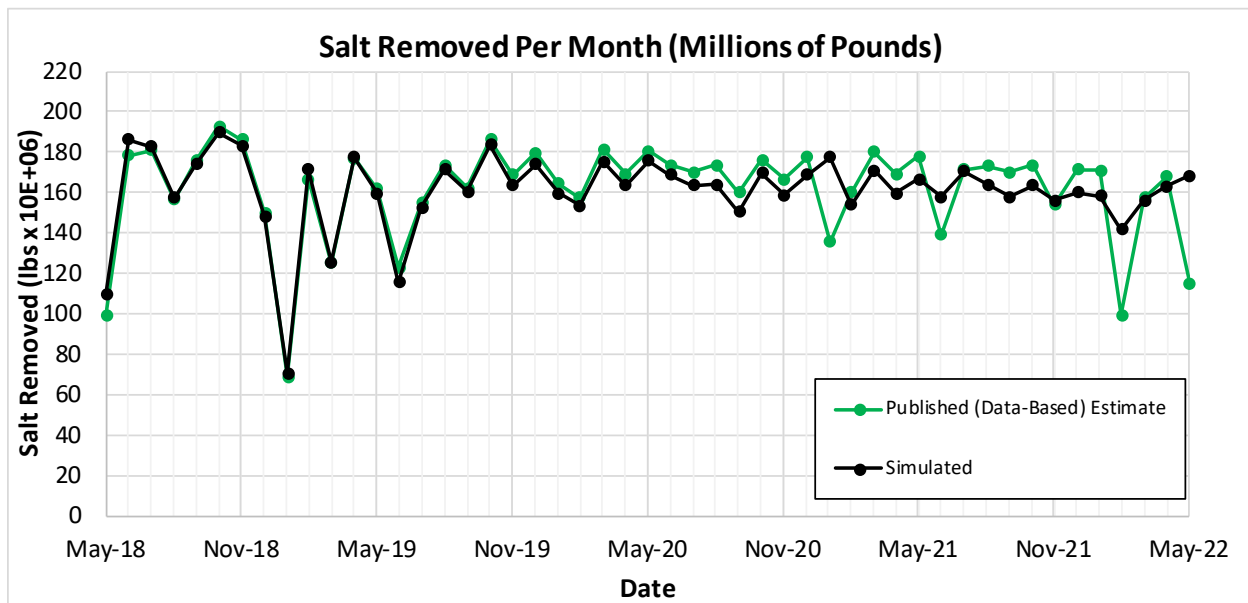
Figure 5.3-5.   Comparison of Model and Observed Mass Extracted by Well Between May 2018 and May 2022 for the Second Sensitivity Simulation
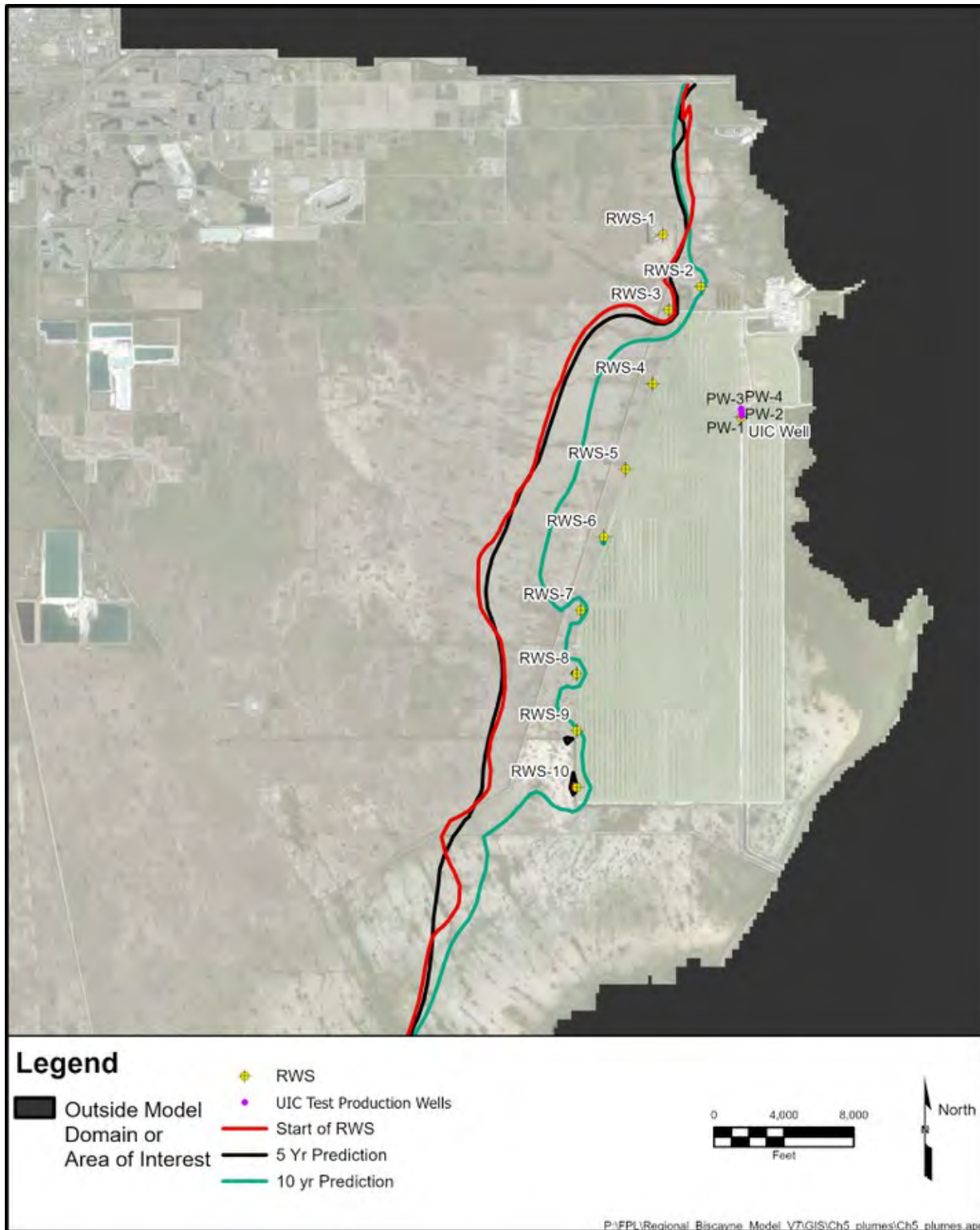
Figure 5.3-6. Location of Initial, Year 5, and Year 10 Hypersaline Interface in Model Layer 13 for the Second Sensitivity Simulation
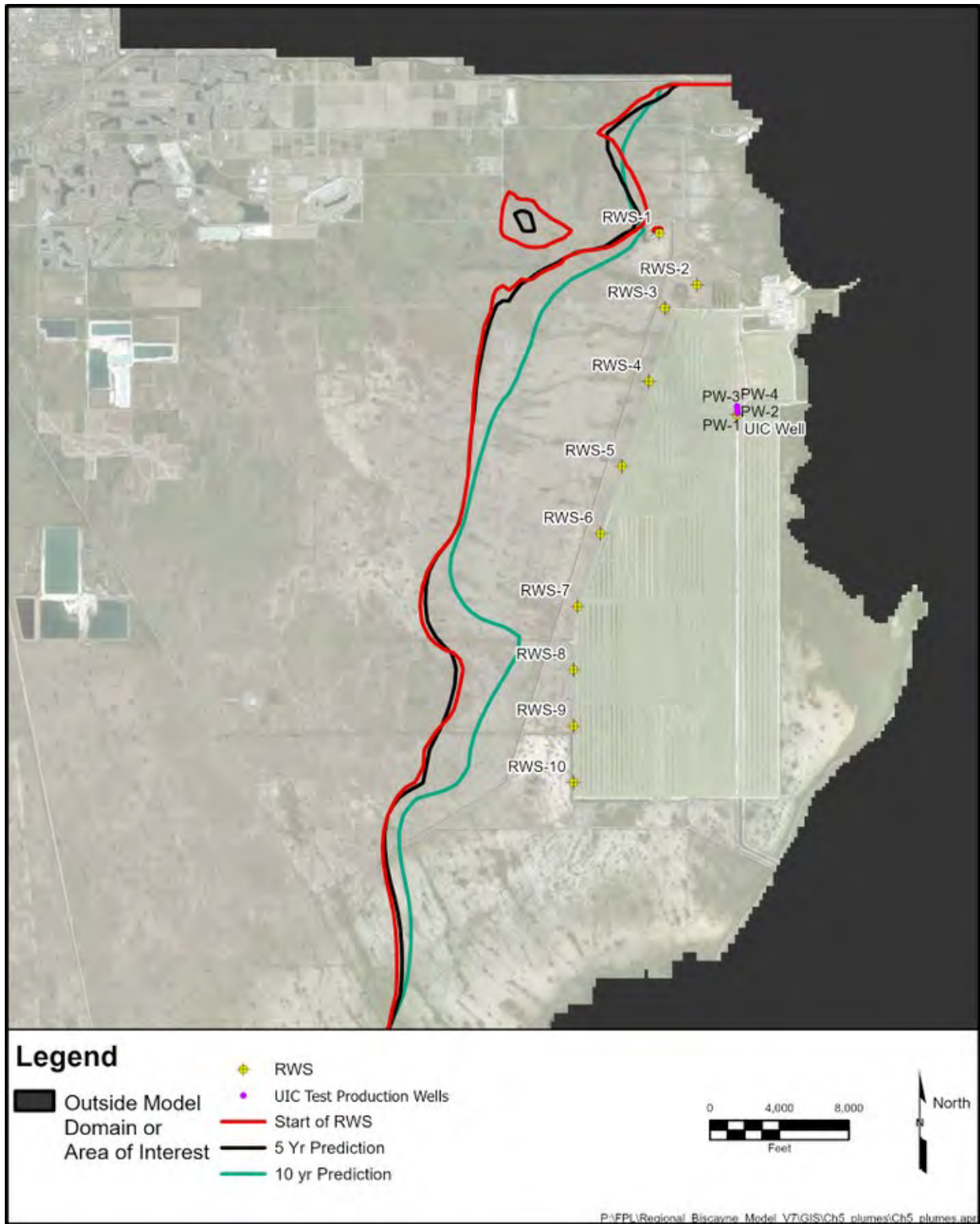
Figure 5.3-7.   Location of Initial, Year 5, and Year 10 Hypersaline Interface in Model Layer 16 for the Second Sensitivity Simulation

5.3.4 Model Recommendations

Six recommendations for future evaluations of system performance are offered:

- Refine the technique for using inputs from the water and salt balance in the groundwater flow and saltwater transport model.

- Continue to explore alternative conceptual models of the near-RWS flow system to align the modeled hypersaline interface more closely with those characterized by CSEM and monitor well data.

- CCS salinities and climate conditions should continue to be monitored and the model updated and recalibrated with more data reflective of longer RWS operations. The longer period of RWS operation and consequent changes to salinities over a progressively larger area will help inform the model and increase its accuracy in simulating the effect of the RWS and forecasting longer-term performance.

- Additional analysis to understand the hypersaline plume development and retraction in the lower model layers.

- Evaluations should be conducted to verify the degree to which model-generated, non-CCS hypersaline groundwater impacts remediation objectives.

- Use the groundwater model to assist in the evaluation of potential CCS management and RWS operations.

6   COOLING CANAL SYSTEM MANAGEMENT

As a result of FPL management activities in the CCS, the average annual salinity value of 36.1 PSU is the lowest since 1977; and the thermal efficiency of 86.2% is well above the minimum target of 70%. Total nitrogen and algae concentrations are declining along with more recent reductions in chlorophyll-*a* concentrations and increases in light penetration and dissolved oxygen. Commensurate with these improvements, seagrass beds are expanding and crocodile nests and hatchlings are at record highs.

FPL has implemented multiple measures to improve conditions in the CCS, several of which are directly or indirectly linked to the remediation of the hypersaline groundwater plume. These management activities have been focused on reducing salinity and nutrients in the CCS and enhancing thermal efficiency for ensuring a long-term sustainable operation. Objectives, approaches and targets for managing nutrients are described in the Turkey Point Cooling Canal System Nutrient Management Plan (NMP; FPL, 2016b) and for thermal efficiency, in the Turkey Point Cooling Canal System Thermal Efficiency Plan (TEP; FPL, 2016c).

6.1 COOLING CANAL SYSTEM SALINITY MANAGEMENT

Paragraph 20.a., of the CO requires FPL to achieve a CCS average annual salinity of at or below 34 PSU two out of every three years, beginning in reporting year June 2022 through May 2023. Reducing CCS salinity is a component of remediating the hypersaline plume west and north of the CCS. One tool FPL uses to manage salinity within the CCS is to freshen the canals with brackish Upper Floridan aquifer (UFA) water. Freshening is authorized by the Turkey Point site certification PA 03-45F. In October 2021, FPL received a modification to the site certification to increase its freshening allocation to 10,950 million gallons per year (30 mgd) with monthly total withdrawals not to exceed 1,033.6 million gallons (34 mgd). Based on automated daily average data from seven stations in the CCS, the average annual CCS salinity level for the most recent reporting period, June 1, 2021, to May 31, 2022, was 36.1 PSU, which is the lowest annual average value since June 1976 through May 1977 (35.6 ppt) and the second lowest annual average salinity value since data first started being recorded in 1974 (FPL 2022). Salinity reductions were achieved by above-average rainfall and by adding UFA freshening water during the reporting period. Almost 5.29 billion gallons of UFA water (less than half of the authorized allocation of the freshening wells) were added to the CCS, which was instrumental in reducing CCS salinities by offsetting much of the evaporative losses of water from the CCS during the drier periods of the year.

Figure 6.1-1 shows a time series of average salinity in the CCS (all stations) from July 2015, just prior to the start of FPL's CO-directed CCS freshening efforts, through September 2022.

Freshening actions during this period included short-term use of marine groundwater (intermittently from July 2015 to August 2017) and fresh L-31E surface water (intermittently from August through November 2015) but evolved to the use of brackish UFA groundwater to offset evaporative losses that result in increased CCS salinity. Based on the regression line, the figure shows a declining trend in salinity of approximately 30 PSU over the past 7 years.

Figure 6.1-1.   Time Series Declining Trend in CCS Salinity

Reductions in CCS salinity are important as they correspond with reductions in the specific gravity of the CCS waters, thereby reducing the driving head of the canal water which, in turn, reduces and ultimately halts seepage of hypersaline canal water into the underlying aquifer and improves groundwater plume remediation to the west of the CCS. Another benefit of reducing canal salinity is the reduction of the dominant hypersaline-tolerant CCS blue-green algae (*Synechocystis* sp.). Concurrent with sustained salinities below 40 PSU are declines in nutrients and algal populations in the canals as discussed below. Sustained CCS salinities below 40 psu is a target identified in the NMP for reducing the severity and persistence of algae blooms.

FPL continues to successfully implement CCS salinity management measures using the UFA freshening water authorized under the site license. The average CCS salinity since the last average annual salinity (covering June 1, 2021 through May 31, 2022) value of 36.2 PSU was calculated was 33.2 PSU (June 1, 2022 through September 30,2022), which was 6.7 PSU lower than the average over the same period last year when salinities reached the lowest annual average level since 1977.

6.2 COOLING CANAL SYSTEM NUTRIENT MANAGEMENT PLAN

Paragraph 20.a., of the CO required FPL to submit a detailed report outlining the potential sources of the nutrients found in the CCS and included a plan for minimizing nutrient levels in the CCS. FPL has been implementing the FDEP required Turkey Point CCS NMP since July 2017 although several actions to improve CCS nutrient levels preceded the plan. The NMP includes both short-term actions and long-term objectives. Short-term actions include nutrient

and algae reduction, CCS sediment and vegetative management, and reduction of CCS salinity. Long-term objectives of the plan focus on re-establishing seagrass meadows to stabilize nutrient levels over the operational life of the CCS. The plan includes both "acceptable" and "good" targets for achieving the plan objectives. These targets are specific to total phosphorus (TP; <0.035 and <0.02 mg/L, respectively), total nitrogen (TN; <5.0 and <2.5 mg/L, respectively), water clarity (between 2 and 10 ft to >10 ft respectively), and salinity (between 40 to 50 PSU and less than 40 PSU respectively). The plan identifies that "achieving the target levels will reduce the severity and persistence of algae blooms and provide the environmental conditions necessary to support re-establishment of submerged aquatic vegetation in the system."

Nutrient management activities conducted during the reporting period included continued removal of non-native Australian pine (*Casuarina equisetifolia*) from the internal canal berms and along the perimeter berms which impede airflow and are a significant source of biomass entering the canals. The trees are either girdled, spiked with herbicide and left in place to die, or completely felled with the stumps treated with herbicide and the felled trees burned in place. Since 2018, removal of Australian pines on over 1,423 acres across the CCS has occurred and is an ongoing annual management activity.

Along with active removal of the Australian pines, FPL has planted native grasses on berms to aid erosion control and improve berm stability. To date, approximately 448,000 units of native salt-tolerant grasses have been planted on 10 berms and shorelines across the CCS; these plantings have been successful and are naturally expanding. Periodic control burns, when conditions warrant, help to control regrowth of Australian pines while sustaining grasses and native vegetation on the berms.

In addition to grasses on the berms, the NMP includes reestablishment of native seagrasses within the canals. Seagrasses planted within the CCS at 24 sites from 2018–2021 have also been successful, with 16 of the sites established and expanding. Due to the concentrations of nutrients in the foamy CCS water that is produced at the plant discharge, FPL designed, constructed, and maintains operation of a foam collection, condensation, and disposal system. Beginning July 25, 2019, through September 2022, the system has removed 8,156 pounds of nitrogen and 167 pounds of phosphorous from the CCS.

While not a component of the NMP, the RWS operations have also minimized the inflow of groundwater-sourced nutrients to the CCS from the western face and bottom seepage and have captured groundwater nutrients from below, west, and north of the CCS. During this reporting period, an estimated 235,000 pounds of nitrogen and 3,000 pounds of phosphorus were removed from the groundwater under, and in proximity to, the CCS. Since startup of the RWS and UICPW operations, approximately 760,000 pounds of TN and 10,000 pounds of TP have been removed from the groundwater.

TN and TP data collected at CCS monitoring stations TPSWCCS-1 and TPWCCS-6 from April 2019 through September 2022 are shown on Figure 6.2-1. These data show a significant decline in TN, while TP fluctuated during this 3.5-year period, with the majority of the values within the acceptable or good target ranges identified in the NMP (below 0.35 mg/L). Notably, the CCS is a phosphorus-limited system; therefore, any bio-available phosphorus is scavenged, incorporated

by the living organisms within the system, and rapidly recycled within the system when it is available.
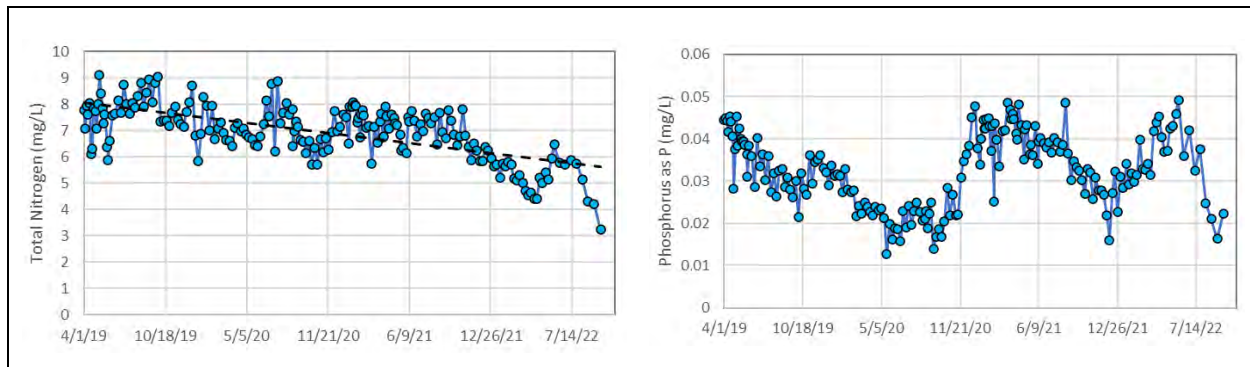
Figure 6.2-1.   CCS Average TN and TP Concentrations

Nutrients within the CCS are primarily within the algal community. The retention of TN and TP within the CCS water column for many years was likely a function of the rapid turnover and uptake of the algae within the system, which was often in excess of 1,000,000 cells per milliliter (mL). Increases in the rate of reductions in total nitrogen since June 2021 appear coincident with declines in algae as nitrogen levels approach the acceptable NMP target level of 5 mg/L or less. Further discussion of algal trends is found in section 6.4.

6.3 COOLING CANAL SYSTEM THERMAL EFFICIENCY PLAN

Paragraph 20.b., of the CO required FPL to submit a thermal efficiency plan (TEP) that includes a detailed description of actions for the CCS to achieve a minimum of 70% thermal efficiency. The FDEP required plan has been implemented since July 2017 although several actions to improve CCS thermal efficiency preceded the plan.

During the reporting period, TEP activities have included collecting thermal imagery to measure thermal performance of the CCS canals, removing 400 acres of large Australian pine trees on the CCS berms which impeded air flow across the canals, and removing sediment in strategic cooling canals. The ongoing removal of Australian pine benefits both CCS nutrient management and thermal efficiency objectives.

Thermal imagery indicated that flows through discharge cooling canals 1–5 in sections 1–3 could be improved by sediment removal. During the reporting period, approximately 100,000 cubic yards of canal sediment were removed.

Implementation of the TEP has not only improved the amount of heat released from the canals as water travels from the plant discharge point to the intake location (an average of 9 degrees Celsius [ºC] or 16.2 degrees Fahrenheit [ºF] during the reporting period), but it has also contributed to a long-term downward trend in CCS temperature. Figure 6.3-1 shows the daily average CCS temperature from all stations for June 2013 through May 2022 which documents an

overall declining trend of nearly 2.5°C (4.5º F) below post-Uprate temperatures (FPL 2022). CCS thermal efficiencies have significantly exceeded the CO minimum value (70%) since 2016, with the annual average CCS thermal efficiency for the period from June 2021 through May 2022 being 86.2% (FPL 2022).
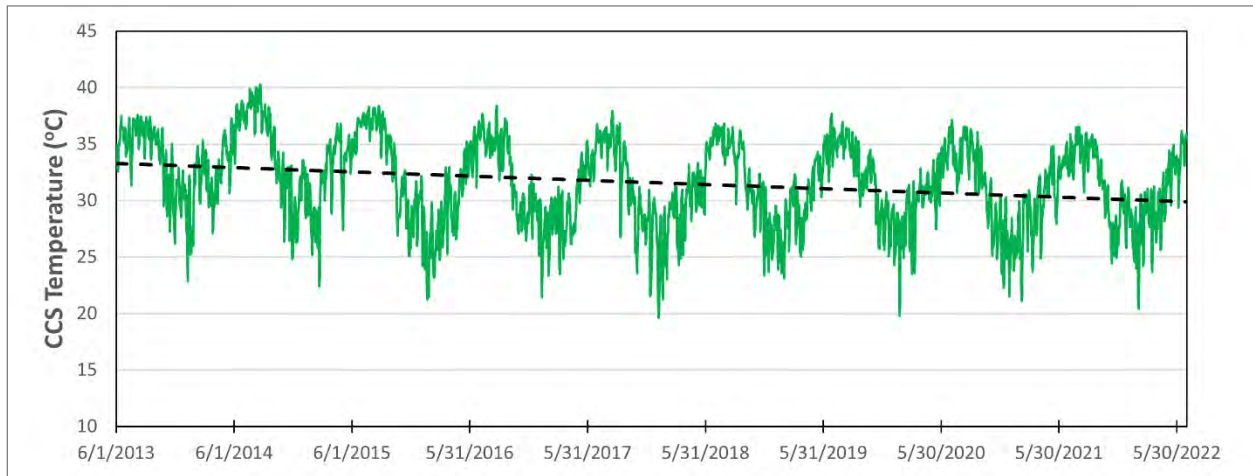
Figure 6.3-1.   Time Series Declining Trend in CCS Temperature Since Unit 3 and 4 Uprate (FPL 2022)

6.4 COOLING CANAL BIOTIC RESPONSES

> Salinity, nutrient, and thermal management actions appear to be driving the CCS ecosystem towards a new equilibrium which is currently characterized by lower algal densities, lower particulate nutrient loads, improved water clarity, and coincident increases in biodiversity.

Implementation of FPL's nutrient, thermal efficiency, and salinity management plans have resulted in gradual sustained improvements in water quality. As a result, positive ecological developments are occurring. The NMP identifies salinity, water clarity, TN and TP levels that, if achieved and sustained, would likely reduce the blue-green algae, support the re-establishment of native seagrasses to moderate nutrients, and return the CCS to its original status as a thermally efficient, ecologically sustainable industrial cooling system.

To monitor progress in working toward these goals, FPL has collected algal data at TPSWCCS-1 to improve the understanding of algal dynamics in the CCS and assess potential impacts to operations of the plant. Algal counts from April 2019 through September 2022 are shown on Figure 6.4-1, along with related water quality parameters including turbidity, chlorophyll-*a* and secchi disk depth, with linear trend lines for the 3-year, 5-month data period. More recently, beginning approximately June 2021, there has been an increasing rate of decline in algal concentrations, biomass, turbidity, chlorophyll-*a*, and nitrogen and an increase in light penetration.
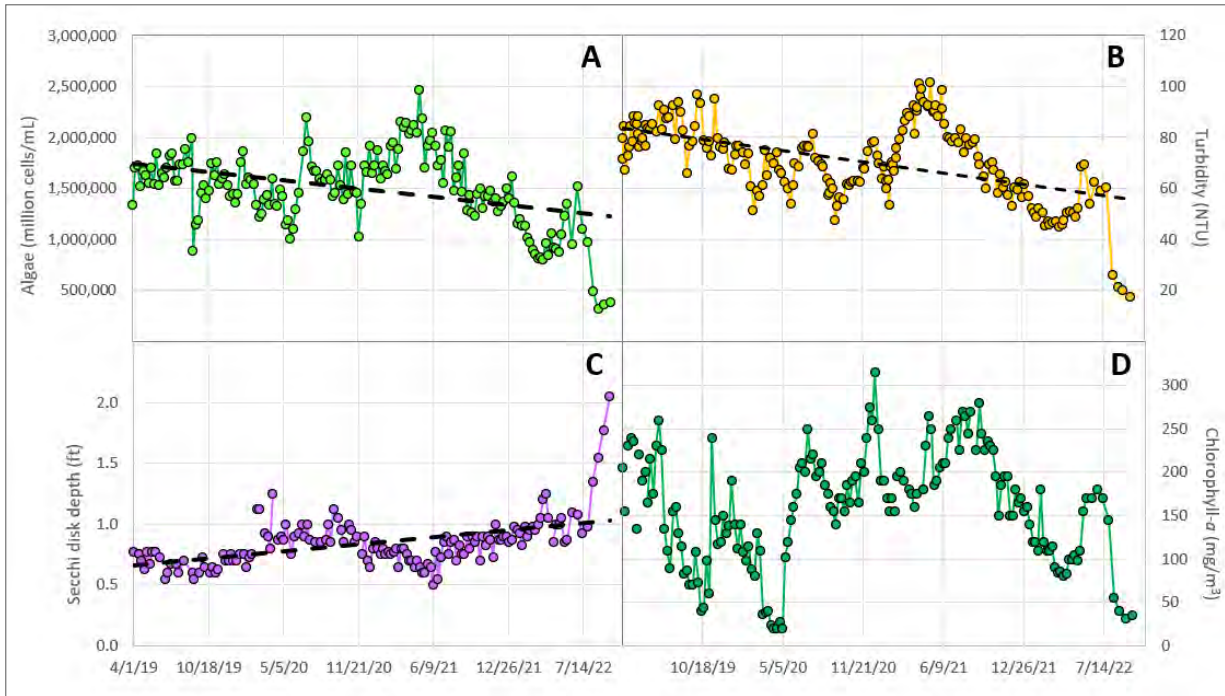
Figure 6.4-1.   Time Series of (A) CCS Algae Concentrations, (b) Turbidity, (c) Secchi Disk and (d) Chlorophyll-*a* Concentrations

In addition, dissolved oxygen (DO) is measured quarterly at seven monitoring stations in the CCS. In the first year of monitoring in 2010/2011, the average annual DO was 5.39 mg/L. However, in the 2014/2015 time frame, the average annual DO dropped to 2.53 mg/L. In subsequent years with the implementation of various CCS management activities, DO began to trend upward (see Figure 6.4-2) with average DO values around 5 mg/L from October 2020 through June 2022.
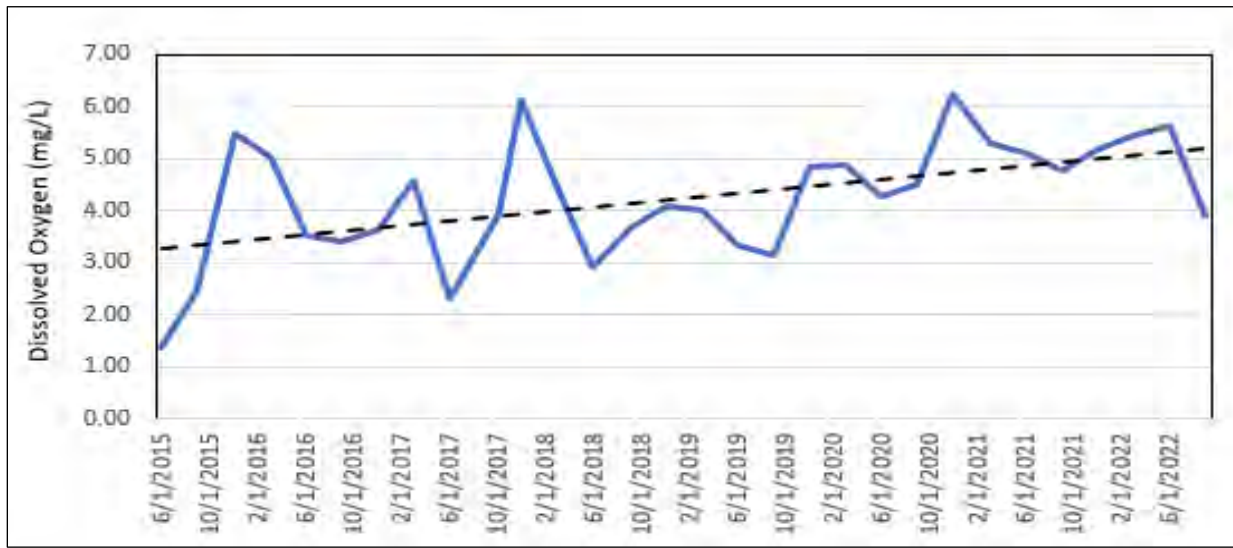
Figure 6.4-2   Average Quarterly CCS Dissolved Oxygen: 6/2015 through 9/2022

FPL has taken actions to improve DO levels in the CCS. Lower DO levels occur at the intake and discharge sides of the plant due to inflow of anoxic groundwater associated with canal drawdowns from the circulation pumps. As a result, aerators were added in intake and discharge canals beginning in 2016. In addition, reducing orifice plates and upturned spray assemblies are placed on the UFA freshening wells 2 through 7 to highly aerate freshening discharges into the CCS. These actions along with changes in algae levels and lower nutrient levels likely play a role in the increased DO levels of the CCS.

Continued efforts by FPL have resulted in CCS waters approaching the ambient salinity levels characteristic of Biscayne Bay (Figure 6.1-1). Reductions in salinity and TN appear to be driving the CCS ecosystem toward a new equilibrium which may be characterized by lower algal densities, lower particulate nutrient loads, improved water clarity, and coincident increases in biodiversity. The stability in lower salinity over the last 2 years, coupled with the range of nutrient management efforts have, over time, likely contributed to this decline in algal biomass. This reduction of algae biomass has resulted in concomitant improvements of water clarity within the CCS as observed by turbidity and Secchi disk readings (Figure 6.4-1).

Despite the decrease in algal concentrations within the CCS water column, chlorophyll-*a* concentrations from April 2019 through August 2021, while fluctuating, remained rather stable. However, since September 2021, there has been a clear decreasing trend in chlorophyll-*a* concentrations which parallels the decline in algae concentrations.

As discussed in prior RAASRs, FPL began test planting the native seagrass, *Ruppia maritima*, in 2018 when CCS salinity levels were declining to assesses viability under the CCS water conditions at that time. As documented in the NMP, the reintroduction of this seagrass species, previously found within the CCS, is recommended for nutrient management. This species once occupied large areas of the CCS bottom, so reintroducing this species is preferred for initiating the shift within the CCS from an algal-based system to a more ecologically stable seagrass system. Seagrasses sequester nutrients within their biomass and also help maintain the stability

of CCS sediments by capturing loose flocculent material within the bottom of the canal. Additionally, the nutrient turnover within a seagrass system is much slower when compared to an algal-dominated system, resulting in more consistent and manageable nutrient and water quality. Many of the seagrass sites planted between 2018–2021 have successfully established; and although these patches are currently small (estimated to be 100 to 3,500 square ft), they are self-propagating and expanding. As water clarity improves, these grasses will likely be able to expand geographically and into deeper CCS waters, thereby reducing turbidity and further accelerating improvements to water clarity.

Commensurate with the thermal efficiency, salinity and water quality improvements, there are also preliminary indications of improved habitat quality for various organisms within the CCS resulting in increased non-algal biomass and biodiversity. During periods when CCS salinities were very hypersaline, few—if any—aquatic or benthic species were noted based on anecdotal observations.

More recently, invertebrates such as worms, mollusks, land crabs, and fiddler crabs have been observed along canal banks while anemones, tube worms, pistol shrimp, diving beetles, horseshoe crabs, and blue crabs have been observed within the canal itself. Increased numbers of fish species have also been observed, from a system primarily dominated by sheepshead minnows to a wider range of fish including mojarra, sailfin mollies, glass minnows, mummichogs, sea trout, toadfish, barracuda, snook, and tarpon. These initial observations of increased biological diversity within the canals are commensurate with salinity and nutrient management efforts which have resulted in consistently lower salinity, nitrogen and algae concentrations.

These management efforts appear to have increased the diversity of the food web within the CCS and have consequently increased habitat quality for higher trophic levels. For example, a record number of crocodile hatchlings (565) were recorded in 2021; in 2022, there was a record number of nests on-site (33) with 512 crocodile hatchlings tagged. This success is attributable to FPL's habitat improvement measures as part of its continued commitment to improving and protecting ideal crocodile habitat. In addition to crocodiles, the CCS supports a wide population of wading birds.

Continued implementation of the NMP, TEP, and salinity management initiatives within the CCS have resulted in water conditions that have trended towards and achieved targets identified in the NMP which are considered favorable for the reduction in the dominance of algae in the CCS, and are more conducive to seagrass re-establishment. However, the CCS is a large and complex system, and the biological responses are often driven by a number of interacting local, regional, and meteorological factors. FPL will continue to monitor CCS water quality and biologic responses resulting from the implementation of the cooling canal management plans and make necessary adjustments as needed to maintain a sustainable cooling system.

7   SUMMARY AND RECOMMENDATIONS

7.1 OVERALL SUMMARY

> FPL employs three types of data and associated analyses (monitoring, electromagnetic surveys, and modeling) to assess progress in meeting the objectives of the MDC CA and FDEP CO. Analyses of data through Year 4 of remediation demonstrate that the net westward migration of the hypersaline plume has been halted, and hypersaline groundwater from the CCS is being intercepted, captured, contained, and retracted by RWS operations. The CSEM data shows that the volume of hypersaline water in the compliance area has been reduced by 67% since remediation began in 2018. In addition, many of the groundwater monitoring wells are showing declining trends in salinity, and there are notable improvements in CCS water quality, reductions in algae, and continued improvements in thermal efficiency. Evaluations to better align groundwater monitoring data, AEM surveys, and groundwater modeling results will continue in preparation for the Year 5 Remedial Action Annual Status Report (RAASR).

FPL submits this Year 4 RAASR, which covers RWS operations and groundwater monitoring data from July 1, 2021, to June 30, 2022, in compliance with the monitoring and reporting objectives of the MDC CA and the FDEP CO. This report incorporates Year 4 RWS operational summary, groundwater monitoring well data and analysis, CSEM results based on the May 2022 survey, the updated and recalibrated regional groundwater model (Version 7) including remediation year 5 and 10 forecasts, and CCS management information. This report also includes a summary of CA and CO compliance activities undertaken and completed since the CA and CO were executed (Appendix A). The following is a summary of the major findings of this evaluation:

- After four years of remediation operations, the CA objectives to intercept, capture, contain and demonstrate statistically valid reductions in the salt mass and volumetric extent (retraction) of hypersaline groundwater from the CCS continue to be met. The CO requirement to halt the westward migration of hypersaline water from the CCS within 3 years was achieved and documented in the April 2021 Year 2 Part 2 RAASR; significant reductions continue to be demonstrated by analyses conducted in this report.

- The RWS operated 93.8% of the reporting period; there were 574 hours (22.8 days; 6.2%) when the entire system was shut off for testing, maintenance, system enhancements, and the CSEM survey.

- Approximately 6.18 billion gallons of hypersaline water and 2.37 billion pounds of salt were removed during this reporting period from the RWS and UICPW. Since inception of the remediation system, approximately 23.43 billion gallons of hypersaline

groundwater and 9.24 billion pounds of salt have been extracted from the Biscayne Aquifer.

- Water table drawdowns from RWS operations continue to be negligible at less than 0.10 ft.

- In total, 21 of 26 monitoring wells west and north of the CCS used in the remediation assessment showed a statistically significant declining trend in one or more parameters (i.e., quarterly chloride, quarterly tritium, and weekly average automated salinity) and multiple wells had at least one or more parameters that were the lowest value on record this reporting period.

- Greatest reductions in chloride levels are being measured in shallow monitoring wells next to the CCS where shallow fresher groundwater replaces hypersaline water along the top of the plume. The gradual reductions occurring in the middle and deep monitoring wells near the CCS are expected to increase as the continuing plume retraction reaches the narrow monitoring intervals of the deeper monitoring wells.

- There is only one shallow well, TPGW-17S, that remains hypersaline. The lowest chloride concentration this reporting period was 20,200 mg/L, only 1,200 mg/L above the threshold of 19,000 mg/L. Notable reductions in bulk conductivity were observed in the induction log just above the well screen indicating freshening is occurring vertically at this location. Three other shallow wells that were hypersaline at the start of RWS operations became saline in prior reporting periods and remain saline this reporting period with chloride concentrations well below 19,000 mg/L.

- All but three of the intermediate and deep monitor wells (TPGW-15D, TPGW-22M and TPGW-L3-58) showed a statistically significant decline in one or more parameters (e.g., salinity, chloride, tritium) since the inception of the RWS.

- The fact that the majority of the wells have a declining trend since the start of the RWS and a number of the wells, including intermediate and deep wells, continue to show lower chloride, salinity, and/or tritium concentrations each year indicates positive progress in meeting the objectives of the CA and CO.

- Chloride reductions in the compliance area in the middle well at TPGW-5, which is over 3 miles west of the RWS, is an indication of the lateral reach of the withdrawal system.

- Monitoring well data provide a localized assessment of change and must be used in conjunction with tools such as AEM and modeling that help provide greater spatial coverage and comprehensive insights into the progress of remediation.

- Year 4 AEM results, compared to the 2018 baseline survey results, indicate the volumetric extent of the hypersaline plume has been reduced by 67% after 4 years of RWS operation. The location of the leading edge of the CCS-sourced hypersaline plume

west and north of the Plant site is shown to have retracted back towards the CCS by as much as 1.25 miles.

- Based on AEM data, the greatest reduction in hypersalinity volume is occurring in the lower portion of the aquifer as the plume west of the L-31E canal is retracting eastward.

- Two sources of hypersaline groundwater, coastal naturally occurring evaporated seawater and the CCS, occur within the survey area. The spatial extent of hypersaline water in the upper 6.2 meters north of Palm Drive and east of the L-31E levee are reflective of non-CCS-sourced hypersaline water that formed from seawater encroachment into the coastal marsh areas during Hurricane Irma. In the groundwater model, coastal evaporative hypersalinity forms south of the CCS, sinks to lower layers where it comingles with CCS-sourced hypersalinity, and appears to be captured by the southern RWS wells. Additional evaluation of this modeled condition will be conducted during Year 5 to determine how or if it impacts CCS plume remediation.

- A number of updates to the groundwater model have reduced total model error (defined as the cumulative difference between model estimated value and actual measured values), produced a groundwater model concurrent with measured aquifer CCS sediment properties and hydraulic conductivities estimated from geological and geophysical logs, and improved model representations of plume reductions associated with 4 years of remediation.

- The Year 4 recalibrated V7 model forecast simulations for Years 5 and 10 of remediation show improved hypersaline retraction results. Complete retraction predominantly occurs in shallow and intermediate model layers (upper two thirds of the aquifer) by 2028. Partial retraction in the deepest model layers is shown to occur in the northern portion of the plume by 2028, while westward movement of hypersaline interface shown in previous model versions along the base of the aquifer is halted or reversed in the V7 model.

- Two sensitivity simulations were run using the V7 model that used AEM-derived western edge positions of the plume as initial conditions and modified how the L-31E canal interacts with groundwater. These runs showed mixed results with retraction generally consistent with the RWS capture zones in the bottom model layers but greater retraction than the original V7 predictive model. The sensitivity simulation presents a possible conceptual model for consideration in the V8 model for the Year 5 RAASR.

- In addition to the RWS operation and reduction in groundwater hypersalinity to the west and north of the CCS, FPL has successfully completed multiple restoration and remediation activities outlined in the CA and the CO which have resulted in tangible improvements within the CCS:

  - Reduction of the annual average salinity in the CCS to 36.1 PSU (June 1, 2021, to May 31, 2022) which is its lowest annual level since 1977. Reducing salinities

in the CCS reduces the formation of hypersaline water and reduces the driving head on hypersaline groundwater beneath the CCS aiding in the retraction of the hypersaline plume.

— CCS thermal efficiencies have exceeded the CO minimum value of 70% since 2016, with the annual average CCS thermal efficiency for the period from June 2021 through May 2022 being 86.2% (FPL 2022).

— There is a statistically significant declining trend in TN over the past 3 plus years, while the total phosphorus levels remain relatively low, ranging between 0.01 to 0.05 mg/L.

— Algae, which have dominated the CCS since 2014, show dramatic declines during the reporting period, reaching their lowest levels since 2016. Reductions in turbidity and increases in water clarity have been coincident with the algae reduction.

— Salinity, nutrient, and thermal management actions appear to be driving the CCS ecosystem towards a new equilibrium which is currently characterized by lower algal densities, lower particulate nutrient loads, improved water clarity, and coincident increases in biodiversity, including expanding seagrasses and increased crocodile utilization, all of which have been documented over the past 2 years.

7.2 REFINEMENTS

FPL has implemented actions, including the following, to enhance the ongoing remediation and to further the objectives of the CA and CO.

Hypersaline Groundwater Remediation

- Processes and procedures to improve resiliency of the RWS system and maximizing flow, specifically the following:

  — Ongoing systematic refurbishment of each of the extraction wells to maintain system performance and reduce downtime due to repairs.

  — Improvements in the electrical resilience of the system to storms via better grounding systems.

  — Optimization of the SCADA system programming to maintain extraction flows even when more than two wells are offline for repairs or maintenance.

  — Reconfiguration of the DIW piping, flow patterns, and flowmeter location to reduce interferences and obtain more accurate velocity and flow readings, which allows for maximizing injection volume.

Groundwater Monitoring Network Expansion

- After permits were issued by SFWMD and U.S. Army Corps of Engineers, the new monitoring well cluster TPGW-23, located along the L-31E canal road 0.5 mile north of Palm Drive, was completed; and data collection began mid-August 2022.

Cooling Canal System Salinity Reduction

- A modification to the site certification license PA 03-45F was issued to FPL (October 19, 2021), authorizing use of the new F-7 CCS freshening well and increasing the UFA allocation for wells F-1 through F-7 from 14 mgd (5,110 million gallons per year) to 30 mgd (10,950 million gallons per year), with a maximum monthly allocation of 34 mgd (1,033.6 million gallons per month). This additional allocation will offset evaporative losses of fresh water from the CCS that exceed the 14 mgd previously allocated, thereby limiting dry season salinity increases that occur under the previous allocation and achieving annual average CCS salinities of 34 PSU. FPL began increasing freshening inflows starting in November 2021.

7.3 RECOMMENDATIONS

Given the significant progress of remediation since initiation of the RWS, FPL does not propose any changes to the agencies' approved remediation plan at this time. However, based on review of Year 4 AEM survey data and the updated/recalibrated Year 4 (V7) forecast modeling, FPL plans to undertake the following recommended actions:

- Conduct the following evaluations of AEM results to better align monitoring well, modeling, and AEM results:

  - Conduct additional evaluation to verify the AEM documented changes along the western edge of the plume to verify the progress made in plume retraction and better inform the model calibration and resulting remediation forecast reliability.

  - Investigate the nature of isolated lenses of hypersalinity located in the southwest portion of the compliance area in layer nine.

  - Evaluate AEM-identified areas of lower salinity groundwater located along the base of the aquifer beneath AEM-identified hypersaline layers

  - Investigate areas where AEM-estimated chloride values significantly differ from adjacent monitoring well values

- Refine the technique for using inputs from the water and salt balance in the groundwater flow and saltwater transport model.

- Continue to explore alternative conceptual models of the near-RWS flow system to align the groundwater modeled hypersaline interface more closely with those characterized by CSEM and monitor well data.

- CCS salinities and climate conditions should continue to be monitored and the model updated and recalibrated with more data reflective of longer RWS operations. The longer period of RWS operation and consequent changes to salinities over a progressively larger area will help inform the model and increase its accuracy in simulating the effect of the RWS and forecasting longer-term performance.

- Additional analysis to understand the hypersaline plume development and retraction in the lower model layers.

- Evaluations conducted to verify the degree to which model-generated, non-CCS hypersaline groundwater impacts remediation objectives.

- Use the groundwater model to assist in the evaluation of potential CCS management and RWS operations.

It is important to note that the aquifer system is complex and subject to many external factors beyond the CCS and RWS; therefore, continued monitoring, model updates, and scientific data analyses are performed to improve our understanding of the impact of RWS operations in concert with these other factors. FPL will continue to monitor and evaluate progress in meeting the requirements of the CA and CO and make recommendations for modifications as needed.

8 REFERENCES

Arcadis 2020. Review of Aerial Electromagnetic Surveys at Turkey Point Power Plant, Southern Florida; prepared for Miami-Dade County Department of Environmental Resource Management.

DBHYDRO, 2022. South Florida Water Management District, www.sfwmd.gov/dbhydro. Accessed October 28.

ENERCON. 2016. PTN Cooling Canal System, Electromagnetic Conductance Geophysical Survey, Draft Final Report, Florida Power and Light Turkey Point Power Plant, 9700 SW 344th Street, Homestead, FL 33035.

Efron, Bradley. 1979. Bootstrap Methods: Another Look at the Jackknife. Annals of Statistics 7: 1–26.

Efron, Bradley, and Rob Tibshirani. 1986. Bootstrap Measures for Standard Errors, Confidence Intervals, and Other Measures of Statistical Accuracy. Statistical Science 1: 54–77.

Fish, J.E. and M. Stewart. 1991. Hydrogeology, aquifer characteristics, and ground-water flow of the surficial aquifer system, Dade County, Florida. U.S. Geological Survey, Water Resources Inv. 91-4000.

Fisher, R. A. 1935. Design of Experiments. Hafner: NY.

Fitterman, D.V. and S.T. Prinos. 2011. Results of time-domain electromagnetic soundings in Miami-Dade and Southern Broward Counties, Florida. U.S. Geological Society Open- File Report 2011-1299, ix, 42 p.

Fitterman, D.V., M. Deszcz-Pan, and T. Scott. 2012. Helicopter Electromagnetic Survey of the Model Land Area, Southeastern Miami-Dade County, Florida. U.S. Geological Society Open-File Report 2012–1176:77.

Florida Power & Light Company (FPL). 2012. Florida Power & Light Company Comprehensive Pre-Uprate Monitoring Report for the Turkey Point Monitoring Project. Prepared for Florida Power & Light Company by Ecology and Environment, Inc. October 31, 2012.

———. 2013. Florida Power & Light Company Quality Assurance Project Plan (QAPP) for the Turkey Point Monitoring Project. Prepared for Florida Power & Light Company by Ecology and Environment, Inc. June 2013.

———. 2016a. Florida Power & Light Company Comprehensive Post-Uprate Monitoring Report for the Turkey Point Monitoring Project. Prepared for Florida Power & Light Company by Ecology and Environment, Inc. March 2016.

———. 2016b. Turkey Point Cooling Canal System Nutrient Management Plan. September 2016.

———. 2016c. Turkey Point Cooling Canal Thermal Efficiency Plan. December 2016.

———. 2017. Florida Power & Light Company Annual Monitoring Report for the Turkey Point Monitoring Project. Prepared for Florida Power & Light Company by Ecology and Environment, Inc. September 2017.

———. 2018a. Florida Power & Light Company Recovery Well System Startup Report. Prepared for Florida Power & Light Company by Ecology and Environment, Inc. October 2018.

———. 2018b. Florida Power & Light Company Turkey Point Recovery Well System (RWS) Second Quarter Status Report. December 2018.

———. 2018c. Florida Power & Light Company Annual Monitoring Report for the Turkey Point Monitoring Project. Prepared for Florida Power & Light Company by Ecology and Environment, Inc. August 2018.

———. 2018d. Florida Power & Light Company 2018 Annual Turkey Point Power Plant Remediation/Restoration Report. December 2018.

———. 2019a. Florida Power & Light Company Turkey Point Recovery Well System (RWS) Third Quarter Status Report. March 2019.

———. 2019b. Florida Power & Light Company Turkey Point Recovery Well System (RWS) Fourth Quarter Status Report. June 2019.

———. 2019c. Florida Power & Light Company Turkey Point Remedial Action Annual Status Report. November 2019.

———. 2019d. Florida Power & Light Company Annual Monitoring Report for the Turkey Point Monitoring Project. Prepared for Florida Power & Light Company by Ecology and Environment, Inc. August 2019.

———. 2020a. Florida Power & Light Company Turkey Point Remedial Action Annual Status Report, Year 2, Part 1. Prepared for Florida Power & Light Company by WSP. November 2020.

———. 2020b. Florida Power & Light Company Annual Monitoring Report for the Turkey Point Monitoring Project. Prepared for Florida Power & Light Company by Ecology and Environment, Inc.

———. 2021a. Florida Power & Light Company Turkey Point Remedial Action Annual Status Report, Year 2, Part 2. Prepared for Florida Power & Light Company by Stantec. April 2021.

———. 2021b. Florida Power & Light Company Turkey Point Remedial Action Annual Status Report. Prepared for Florida Power & Light Company by Stantec. November 2021.

———. 2021c. Florida Power & Light Company Annual Monitoring Report for the Turkey Point Monitoring Project. Prepared for Florida Power & Light Company by Stantec. August 2021.

———. 2022. Florida Power & Light Company Annual Monitoring Report for the Turkey Point Monitoring Project. Prepared for Florida Power & Light Company by Stantec. August 2022.

GTI (Groundwater Tec, Inc.). 2022. Review of FPL's RAASR Year 3 and The Variable Density Groundwater Flow and Solute Transport Model (v6). Prepared for Miami-Dade County Division of Environmental and Resources Management. February 2022.

Hughes J.D. and White, J.T. 2014. Hydrologic Conditions in Urban Miami-Dade County, Florida, and the Effect of Groundwater Pumpage and Increased Sea Level on Canal Leakage and Regional Groundwater Flow. U.S. Geological Survey Scientific Investigations Report 2014–5162, 175 pp. https://doi.org/10.3133/sir20145162.

JLA Geoscience, Inc. 2010. Geology and Hydrogeology Report for FPL, Turkey Point Plant Groundwater, Surface Water, and Ecological Monitoring Plan, FPL, Turkey Point Plant, Homestead, Florida. Prepared for Florida Power & Light Company. October 2010.

JLA Geosciences, Inc. 2022. Core Permeability Estimation – TPGW and RWS Wells – Layer Subdivisions, Technical Memorandum. June 30, 2022.

Langevin, C.D., Thore, D.T., Dausman A.M., Sukop, M.C., and Guo, W., 2008. SEAWAT Version 4: A Computer Program for Simulation of Multi-Species Solute and Heat Transport: USGS Techniques and Methods Book 6, Chapter A22, 39 p.

Pitman, E. J. G. 1937. Significance Tests Which May Be Applied to Samples from Any Population. Royal Statistical Society Supplement 4: 119–30, 225–32.

Prinos, S.T., M.A. Wacker, K.J. Cunningham, and D.V. Fitterman. 2014. Origins and delineation of saltwater intrusion in the Biscayne aquifer and changes in the distribution of saltwater in Miami-Dade County, Florida. U.S. Geological Survey Scientific Investigations Report 2014–5025. 101 pp. http://dx.doi.org/10.3133/sir20145025.

SFNRC (South Florida Natural Resources Center). 2012. Hydrology and Salinity of Florida Bay. Status and trends: 1990-2009. Technical Series 2012:1.

Schamper, C., E. Auken, and K. Sorensen, 2014, Coil response inversion for very early time modelling of helicopter-borne time-domain electromagnetic data and mapping of near-surface geologic layers: European Association of Geoscientists & Engineers, Geophysical Prospecting, 62, No.3, p.658-674. https://doi.org/10.1111/1365-2478.12104.

SFWMD (South Florida Water Management District). 2015. Applicant's Handbook for Water Use Permit Applications within the South Florida Water Management District.

Stringer, C.E., M.C. Rains, S. Kruse, and D. Whigham. 2010. Controls on water levels and salinity in a barrier island mangrove, Indian River Lagoon, Florida. Wetlands. 30(4):725-734.

Tetra Tech, 2016. A Groundwater Flow and Salt Transport Model of the Biscayne Aquifer, Technical Memorandum provided to Florida Power & Light, June 10, 2016.

United States Environmental Protection Agency, 2009. Statistical Analysis of Groundwater Monitoring Data at RCRA Facilities Unified Guidance.

Zheng, C., and Wang, P., 1998. MT3DMS – Documentation and User's Guide, U.S. Army Corps of Engineers Waterways Experiment Station Technical Report, 214 p.

United States Department of the Interior

NATIONAL PARK SERVICE
Southeast Regional Office
Atlanta Federal Center
1924 Building
100 Alabama St., SW.
Atlanta, Georgia 30303

DEC 1 9 2016

Mr. Frank Akstulewicz
Director, New Reactor Licensing
Office of Administration, Mail Stop: OWFN 12 H8
U.S. Nuclear Regulatory Commission
Washington, DC 20555-0001

ORCA COMMENTS
EXHIBIT 2
MAY 2023

Colonel Jason Kirk
District Commander
U.S. Army Corps of Engineers
701 San Marco Boulevard
Jacksonville, Florida 32207

Dear Mr. Akstulewicz and Colonel Kirk:

The National Park Service (NPS) appreciates the opportunity to be a cooperating agency with the Nuclear Regulatory Commission (NRC) and the U.S. Army Corps of Engineers (USACE) for the development of the Final Environmental Impact Statement (FEIS) regarding Combined Licenses for Turkey Point Nuclear Plant Units 6 and 7 as proposed by Florida Power and Light (FPL). We appreciate the extensive work done by the NRC and the USACE staff and their willingness to meet extensively with the NPS. However, the NPS continues to have serious concerns regarding the adequacy and accuracy of the FEIS. The NPS is also taking this opportunity to comment on the NRC's Final Safety Evaluation Report (FSER) because it describes natural phenomena, including hurricanes and storm surge, which may negatively affect Units 6 and 7 and have both human and environmental consequences for Biscayne and Everglades National Parks (NP).

USACE is preparing a Least Environmentally Damaging Practicable Alternative (LEDPA) for Clean Water Act Section 404 wetland permits and a Public Interest Review (PIR) in accordance with Clean Water Act Sections 10 and 14 of the Rivers and Harbors Act. According to the FEIS, neither the LEDPA nor the PIR is addressed in this FEIS but will be part of USACE's Record of Decision (ROD). The NPS asserts that there is strong public interest regarding ongoing operational problems with the existing Turkey Point facility, which would be complicated by Units 6 and 7, affecting the success of the multi-billion dollar Comprehensive Everglades Restoration Plan (CERP) and its Biscayne Bay Coastal Wetlands (BBCW) project, as well as the ecological health of Biscayne and Everglades NP fragile resources. As such, the NPS formally

requests that USACE provide its LEDPA and PIR for public review before it issues its ROD. Public comment is not only warranted on the review of the LEDPA, but vital to ensuring that USACE decisions are not contrary to the public interest; are in agreement with the content of the FEIS; and ensure CERP and NPS resources are unnecessarily adversely impacted.

On June 20, 2009, FPL submitted a Combined Construction and Operating License (COL) application to the NRC to build two additional nuclear reactors at the Turkey Point power plant facility in Homestead, Florida. Other proposed infrastructure includes the construction of additional access roads, bridges, a reclaimed water treatment facility, reclaimed and potable water pipelines, Radial Collector Wells (RCW) and associated pipelines, expansion of an existing barge basin, and two separate electric transmission corridors. The Turkey Point power plant complex is located adjacent and contiguous to Biscayne NP and Biscayne Bay and two miles south of Biscayne NP's visitor center. Everglades NP's boundary is located seven miles west of the facility and, as will be articulated throughout this letter, its resources would also be impacted by construction and operation of the project. FPL has also proposed to construct the western powerline adjacent to Everglades NP and the eastern powerline corridor within a small portion of Biscayne NP where FPL has an existing powerline easement. Taken together, this project poses serious direct and cumulative impacts to NPS resources. As such, the NPS questions whether it is good public policy to further expand a nuclear power plant already experiencing environmental problems in a location between two national parks, experiencing an elevated rate of sea level rise, and is highly vulnerable to storm surge. Moreover, the NPS does not have confidence that mitigation can adequately compensate for adverse impacts.

As a cooperating agency, the NPS has continually shared its concerns regarding the accuracy and adequacy of the impacts analysis regarding NPS resources and the CERP. The NPS submitted comments on the Preliminary Draft FEIS on July 8, 2016; Draft Environmental Impact Statement (DEIS) on July 17 and 23, 2015; preliminary draft hydrology and ecology sections of the DEIS on October 8, 2014 and November 25, 2014; Draft Biological Assessments and Essential Fish Habitat Report on January 31, 2014; and scoping comments on August 16, 2010. We have enclosed these documents and incorporated them by reference into this letter.

I. Alternative Site Analysis

As the NPS has stressed throughout this process, it does not seem to be in the public interest to expand a power plant adjacent to Biscayne NP and near Everglades NP. Combined, these National Parks contributed approximately $135 million in 2015 to the local economy, and further provide a critical function of buffering inland areas that would otherwise be more vulnerable to hurricanes, storm surge, and sea level rise. Moreover, both parks contain numerous fragile threatened and endangered species, and are undergoing major multi-billion dollar ecological restoration activities. Nonetheless, the NRC and USACE have not fully considered alternative sites for the project aside from Turkey Point.

The analysis of environmental impacts for all of the energy generating alternatives is based on locating them solely at the Turkey Point location. As an example, the analysis for the natural gas alternative assumed building and operation of a natural-gas-fired plant at the Turkey Point site without analyzing siting the plant at a different location.

FPL applied different criteria to screening the non-Turkey Point sites than it used to screen the existing Turkey Point site. In the analysis of environmental impacts for siting locations at Glades, Martin, Okeechobee, and St. Lucie, these sites were only evaluated as to the environmental impacts of siting a new two-unit nuclear power plant. It is unlikely that the Turkey Point site would have ranked as high for FPL if there was not an existing, operating nuclear power plant at that site. FPL selectively applied its own screening criteria to the other candidate areas including, but not limited to, avoidance of high population areas, ecologically sensitive and special designations, and special dedicated land uses such as national parks. It is probable that the Turkey Point site would have been screened out utilizing the above criteria.

The siting analysis overlooks the impact of supporting infrastructure, such as the FPL's proposed Western Transmission Corridor nearly adjacent to Everglades NP. It also neglects to consider:

- the presence of major Federal investments including Biscayne and Everglades NPs and numerous other protected areas;
- the high concentration of sensitive Federal and State listed Threatened and Endangered species in South Florida, a biodiversity hotspot;
- Federal, state, and nonprofit investment in the multi-billion CERP BBCW Project;
- major problems relating to the Industrial Wastewater Facility (IWF), including violation of its National Pollution Discharge Elimination System (NPDES) permit, recent algae blooms, and a demonstrated hydrologic connection to Biscayne Bay and Biscayne NP;
- the subterranean hypersaline plume underlying the Turkey Point facility and Biscayne NP, which was created by (and remains hydrologically connected to) the IWF;
- radioactive tritium, a tracer for the IWF, is found well above background levels within Biscayne NP and Biscayne Bay;
- the IWF poses an acute risk to sensitive NPS resources from hurricane and storm surge events;
- sea level rise is occurring at an increased rate in South Florida;
- the site of Units 6 and 7 is important mud flat and wetland habitat for shorebirds and nearly adjacent to the NPS boundary;
- impacts to the experience of National Park visitors and recreationists, where park visitations brings an estimated $135 million (2015) to the local economy; and
- the presence of Metropolitan Miami, which is clearly within the 50 mile radius and is the eighth most populous urban area in the United States. Any evacuation would require a route going north toward the City of Miami and heavily populated areas which are downwind of prevailing winds during much of the year.

As such, cumulative impact levels for water and ecological resources at Turkey Point are grossly underrated in the FEIS.

The NPS contends the FEIS does not sufficiently support the NRC's conclusion that "from an environmental perspective, none of the viable alternatives is environmentally preferable to building a new baseload nuclear power generation plant at the Turkey Point site." It appears that the four inland alternative locations do not pose the same level of environmental concern.

Additionally, a number of pending legal actions exist that have an impact either directly or indirectly on this project. Among these is a now final order issued by the Third District Court of Appeal (3rd DCA) reversing and remanding the Final Order on Certification (Siting Order) rendered by Florida's State Siting Board; FPL's pending motions were denied on November 22, 2016. The Siting Order was reversed in its entirety (i.e. Units 6 and 7 and supporting infrastructure, including the Western Transmission Corridor), not in part, and remanded for further review consistent with local environmental regulations, comprehensive plans, and applicable environmental regulations.

As further evidence of the existing and potential future infeasibility of nuclear expansion at the Turkey Point site, FPL has stated earlier this year before the Florida Public Service Commission that they plan to take at least a four year "pause" before construction to analyze economic factors affecting the decision to proceed with an expanded nuclear facility at Turkey Point.

The NPS continues to assert that scientific uncertainty and numerous legal and regulatory issues, most of which relate to the IWF, and the uncertainty of when this project could be built should be considered and resolved before Units 6 and 7 are built because they may exacerbate current problems.

II. Units 6 and 7 Increases IWF Risk to Biscayne NP

[handwritten: SAME ARGUMENT APPLIES TO TPP Units 3 & 4 renewal to 2053]

A basic question neither the FEIS or FSER addresses is how the construction and operation of Units 6 and 7, which would be surrounded by IWF canals, would impact the surrounding area if a hurricane and major storm surge event were to occur. Because of its coastal location, experts have noted and it has been well publicized that reactors at Turkey Point are similarly susceptible as those in Fukushima, Japan to natural disasters. For example, how would the outer walls of the Units 6 and 7 block island affect the IWF, Biscayne NP and Biscayne Bay, if the eye of Hurricane Matthew, or a comparable storm, passed over Turkey Point? In October 2016, Hurricane Matthew passed very close to the Florida coast as a Category 3 to 4 storm and created more than 12 feet of storm surge in Lake Worth, located 90 miles north.

A concerning and reasonably foreseeable scenario is that a storm surge event would push Biscayne Bay water westward over the narrow eastern berm and across an IWF canal before contacting the outer wall of Units 6 and 7. Polluted IWF water could then be pulled back in part into Biscayne NP and Biscayne Bay either over the narrow eastern levee or through subsurface connectivity. There is also a high likelihood that such a storm surge event upon contact with the outer walls of Units 6 and 7 could be driven back toward the levee thereby causing a breach of the eastern levee and driving significant amounts of polluted IWF water into Biscayne NP and the Biscayne Bay. Breaches of the levee further south could also cause newly stored Units 6 and 7 dredge spoils to enter Biscayne NP and Biscayne Bay. These risks would likely increase when future sea level rise is combined with a storms anticipated storm surge. These reasonably foreseeable scenarios are not analyzed in either the FEIS or Safety Report. The enclosed map titled "Hurricane/Storm Surge Risk to Biscayne National Park" depicts this concern in detail.

[handwritten: This IWF was overtopp by Hurrica IRMA storm surge. Sep. 2017]

Even though much can be learned from prior storm events, models that analyze past storm forward speed, trajectory, and initial tide level show that a storm as small as a Category 3 could

lead to over wash of the IWF under the right conditions, and larger storms and sea level rise increase that likelihood. The NPS enclosed map titled "Modeled Storm Surge from Category 3 and Category 5 Hurricanes" further illustrates this concern.

The NPS raised these concerns previously and was advised by NRC that they would be considered in the FSER. However, upon review, it appears that the FSER solely analyzes safety issues within the Unit 6 and 7 block island. The NPS has routinely asserted that the IWF is unsustainable and that its presence adjacent to the National Park System's preeminent marine park poses a serious risk to sensitive NPS resources in the event of a major hurricane and storm surge event. Excessive IWF water entering Biscayne NP and Biscayne Bay would likely impair NPS resources for future generations to enjoy, which the NPS is required to prevent under the 1916 NPS Organic Act, as well as the "rare combination of terrestrial, marine, and amphibious life in a tropical setting" that Biscayne NP was established to preserve.

[handwritten margin note: Same concern applies to continued operation of TPP Units 3 & to 2053 w/ IWF]

III. Direct and Cumulative Impacts to Federal Investments
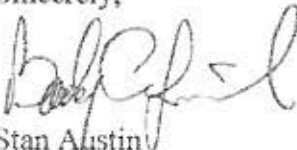
The FEIS neglects to recognize and accurately reflect past and existing environmental impacts from the Turkey Point facility and reasonably foreseeable future impacts that would occur through the construction and operation of Units 6 and 7 and supporting infrastructure.

- **Comprehensive Everglades Restoration Plan and Biscayne Bay Coastal Wetlands Project:** The NPS disagrees with the impact levels that USACE has assigned to the cumulative impacts for surface water use, groundwater use, surface water quality, and groundwater quality. While stating in one part of the FEIS that withdrawals of surface water from the L-31E Canal would only be allowed during periods of excess flow, consumptive use of surface water from L-31E would not alter the volume of water in Biscayne Bay. As such, the FEIS is inaccurate because the important issue is maintaining freshwater delivery to Biscayne Bay, not the volume of saltwater in the Bay. Elsewhere the FEIS states that the use of surface water from the L-31E Canal diverts it from and could result in less freshwater available for CERP BBCW Project. The NPS considers this a diversion and elimination of freshwater that will negatively impact Biscayne NP, Biscayne Bay, and the BBCW Project.
- **Industrial Wastewater Facility:** The FEIS understates the negative cumulative impacts of past, present, and future use of the IWF. Despite extensive monitoring over a period of years, a hypersaline plume also containing other pollutants such as phosphorus, nitrogen and ammonia has been allowed to migrate west toward Miami-Dade County's drinking water wellfield and east to Biscayne NP and Biscayne Bay. The presence of the tracer element tritium in Bay waters adjacent to the Turkey Point facility is evidence of connectivity and movement of the IWF water into the ecologically sensitive waters of Biscayne NP and Biscayne Bay in violation of FPL's strict liability NPDES permit as well as the Federal Court 1971 Final Judgment. At present there is no guarantee that any efforts to eliminate the plume and its movement will be successful.
- **Radial Collector Wells:** The NPS is concerned that the analysis in the FEIS is inaccurate because it relies on an assumption that the RCWs will be used as a water source only in an emergency and on a short-term basis. The FEIS does not analyze whether extended RCW operations could draw the subterranean hypersaline plume

- **Chemicals of Emerging Concern (CECs):** Given the large volume of reclaimed wastewater used for Units 6 and 7 (up to 120 Million Gallons per Day (MGD)), even a very low concentration of CECs that are released and fall within the NPS boundary or the Bay, will provide a loading over time that is physiologically and ecologically significant. These areas as Outstanding Florida Waters have and non-degradation standard under the state.
- **Roads:** The 3rd DCA found that filling land and constructing structures in the East Everglades would negatively impact sheet flow and the hydrologic resources of the area thereby adding more negative cumulative impacts to the proposed expansion project. The 3rd DCA further found that the effect on the area's hydrology would destroy the plant species that supplies the base for the food chain in the ecosystem and will adversely affect the endangered birds that nest and feed on the west side of the L-31N Canal; in addition, these adverse impacts would also affect the County's water supply. However, given the 3rd DCA decision, the location of roads is uncertain at present.

If you have any questions, or need additional information regarding our comments, please contact Energy and Environmental Protection Specialist Bryan Faehner at (202) 513-7256 or bryan_faehner@nps.gov.

Sincerely,

Stan Austin
Regional Director

Enclosures (2)
Map titled "Hurricane/Storm Surge Risk to Biscayne National Park"
Map titled "Modeled Storm Surge from Category 3 and Category 5 Hurricanes"

cc:
Chairman Stephen G. Burns, Commissioner, U.S. Nuclear Regulatory Commission
Kristine L. Svinicki, Commissioner, U.S. Nuclear Regulatory Commission
Jeff Baran, Commissioner, U.S. Nuclear Regulatory Commission
Vonna Ordaz, Office Director (Acting), Office of New Reactors, U.S. Nuclear Regulatory Commission
Anna Bradford, Deputy Division Director, Division of New Reactor Licensing, Office of New Reactors, U.S. Nuclear Regulatory Commission
Alicia Williamson, Project Manager, NRL, U.S. Nuclear Regulatory Commission
Manny Comar, Project Manager, NRL, U.S. Nuclear Regulatory Commission
Megan Clouser, Senior Project Manager, U.S. Army Corps of Engineers
Ashleigh Blackford, Supervisory Biologist, U.S. Fish and Wildlife Service
Chris Militscher, Chief of the NEPA Program Office, U.S. Environmental Protection Agency
Pedro Ramos, Superintendent, National Park Service
Margaret Goodro, Superintendent, National Park Service

ENVIRONMENT   APRIL 21, 2016 3:00 AM

Evidence of salt plume under Turkey Point nuclear plant goes back years

HIGHLIGHTS

Engineers warned decades ago of flaws in cooling canal design

Internal review by FPL engineers in 2010 said fixes could worsen plume

On Thursday, Florida environmental regulators approved controversial management plan

The cooling canals of Turkey Point 4:03

f   🐦   ✉   ❮

❮   1 of 12   ❯

Matt Raffenberg, FPL's environmental services director, talks about how FPL is working on ways to better control water temperature and salinity in the 39 cooling canals at the Turkey Point power plant. **Emily Michot** - emichot@miamiherald.com

BY JENNY STALETOVICH
jstaletovich@miamiherald.com

In the wake of revelations last month that its aging cooling canals at Turkey Point were leaking into Biscayne Bay, Florida Power & Light rushed to do damage control: company leadership went on the defensive, insisting they were acting responsibly and, in a full page ad, blaming "misinformation" for fanning unfounded fears.

"We're not punting on this at all," president and CEO Eric Silagy told the Miami Herald editorial board earlier this month as he laid out a list of on-going fixes.

"If this company has given that impression, that's my fault," he said. "What is frustrating a little bit is we've worked really hard over the decades to do the right thing."

But critics contend the powerful utility worked even harder at delay tactics in the face of mounting evidence that its compromised canal system had produced an underground plume of saltwater threatening nearby drinking supplies and contaminating Biscayne Bay.

How long have Turkey Point's cooling canals been leaking? Critics say decades | Miami Herald

1/24/17, 8:42

Records show FPL had been warned for years about problems and even conducted its own research in 2010 that concluded its key fix — adding millions of gallons of brackish water to freshen the super salty canals — would likely make the plume worse. After overheated canals forced the plant's two reactors to partially power down in 2014, the utility pushed state regulators and water managers repeatedly to add more water, solutions that would allow it to continue operating under Nuclear Regulatory Commission limits but potentially increase the extent and spee

At the time, the

system" not imp

The end result, say environmentalists and others who pushed FPL to move faster over the years, are patchwork fixes and shortsighted solutions they say have failed to deal with broader problems caused by the 44-year-old canals.

"They're band-aids," said Steve Torcise, whose family has operated a rock mine just west of the canals for 90 years and earlier this year won a legal fight demanding the state overhaul a management plan that allowed FPL to add more water without fully addressing the impact on the plume. An administrative judge in February faulted the Florida Department of Environmental Protection for being too weak and not citing FPL.

Despite the criticism, the DEP on Thursday approved the plan, dismissing many of the judge's findings. In a 28-page decision, DEP Secretary Jon Steverson wrote the judge "inappropriately invaded the exclusive province" of the state's ability to regulate the utility. The city of Miami, which had joined the lawsuit with Torcise, plans to appeal.

"We will be pursuing all available appellate remedies to challenge this ruling," said deputy city attorney Barnaby Min.

In the meantime, the salt plume continues to grow. According to the DEP's own 2014 management plan, it has advanced at a rate of 525 to 660 feet per year with up to 600,000 pounds of salt escaping daily from the canals. That's pure salt, not salty water.

66

"THEIR FIRST ORDER OF BUSINESS HAS TO BE TO DO NO HARM TO OUR COMMUNITY AND TO OUR ENVIRONMENT."

Miami-Dade County Commissioner Daniella Levine Cava

"FPL definitely should have shared that they were working on a solution, instead of fighting us in court," said Miami-Dade County Commissioner Daniella Levine Cava, who pressed for information from additional monitoring wells that this year confirmed the presence of tritium, a radioactive isotope used to trace cooling canal water, in Biscayne Bay.

"Their first order of business has to be to do no harm to our community and to our environment," she said. "They want to be known as being good stewards, so it's especially incumbent upon them to set the example."

How long have Turkey Point's cooling canals been leaking? Critics say decades | Miami Herald

1/24/17, 8:42

Turkey Point's leaky cooling canals

Using tritium, a radioactive isotope found in cooling canal water, Miami-Dade County officials detected canal water spreading through groundwater between 2011 and 2013. While tritium is not at dangerous levels, canal water could be causing elevated amounts of ammonia and phosphorus dangerous to marine life

Tritium concentration (pCi/L)

1.59 - 419.05	2,088.89 - 2,506.36
419.05 - 836.51	2,506.36 - 2,923.82
836.51 - 1,253.97	2,923.82 - 3,341.28
1,253.97 - 1,671.43	3,341.28 - 3,758.74
1,671.43 - 2,088.89	• Tritium sample sites

June 2011 quarterly sampling

March 2013 quarterly sampling

Source: Miami-Dade County Department of Environmental Resources Management

MARK O BUIZ mcruz@miamiherald.com
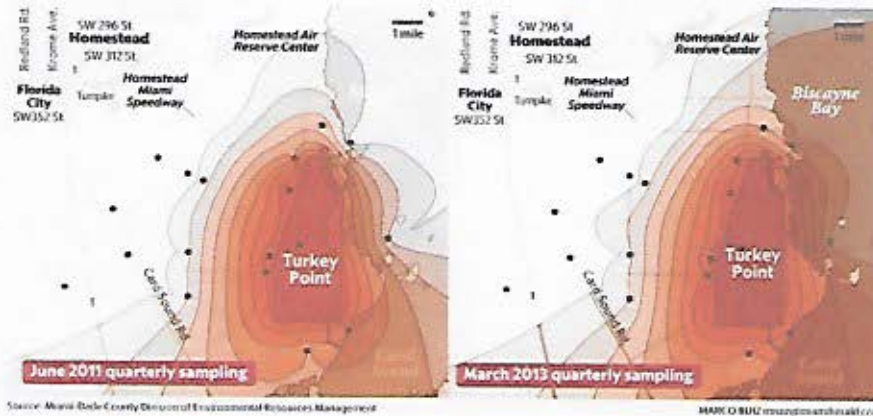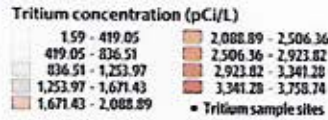
This month, County Commissioner Dennis Moss, whose district covers the canals, asked the Environmental Protection Agency to weigh in, joining Rep. Jose Javier Rodriguez, D-Miami, who in March requested an investigation. In a letter to Rodriguez this week, EPA regional administrator Heather McTeer Toney said the agency has been meeting with county, state and FPL officials to collect information. The agency has already made one visit to the canals, and plans to before the end of the month, a spokeswoman said.

Worsening conditions have also caught the attention of Monroe County, which operates its only wellfield west of the canals. The county, which this week passed a resolution raising concerns, is considering buying land further west to relocate its well field as well as build an additional reverse osmosis plant in Key West, an expensive option that can make salt water fit for human consumption.

"The cooling canals have been on our radar screen as long as I've been here," said Florida Keys Aqueduct Authority deputy director Tom Walker. "We literally have a line we watch."

How FPL got to this point is a complex path of regulatory decisions and company expansion, complicated by the singular design of the cooling canals. Turkey Point is the only nuclear power plant in the country that uses the radiator-like cooling system spanning 5,900 acres. It also sits atop the Biscayne aquifer, a pitted layer of coral rock that looks more like a hardened sponge than solid ground.

In 1972, when the canals were created — a compromise FPL says it was forced to accept after federal environmental regulators sued in court to stop the plant from dumping cooling water directly into the bay — it was understood canals in such porous geology would leak. So the design included a critical feature: a straight, deep canal, called an interceptor ditch, to stop saltwater piling up under the canals from migrating west.

▶

Turkey Point's leaky cooling canals

Using tritium, a radioactive isotope found in cooling canal water, Miami-Dade County officials detected canal water spreading through groundwater between 2011 and 2013. While tritium is not at dangerous levels, canal water could be causing elevated amounts of ammonia and phosphorus dangerous to marine life.

Tritium concentration (pCi/L)

- 1.59 - 419.05
- 419.05 - 836.51
- 836.51 - 1,253.97
- 1,253.97 - 1,671.43
- 1,671.43 - 2,088.89
- 2,088.89 - 2,506.36
- 2,506.36 - 2,923.82
- 2,923.82 - 3,341.28
- 3,341.28 - 3,758.74
- • Tritium sample sites

June 2011 quarterly sampling

March 2013 quarterly sampling

Source: Miami-Dade County Division of Environmental Resources Management

MARCO RUIZ mruiz@miamiherald.com

How long have Turkey Point's cooling canals been leaking? Critics say decades | Miami Herald

1/24/17, 8:4

f | y . | ✉ | <
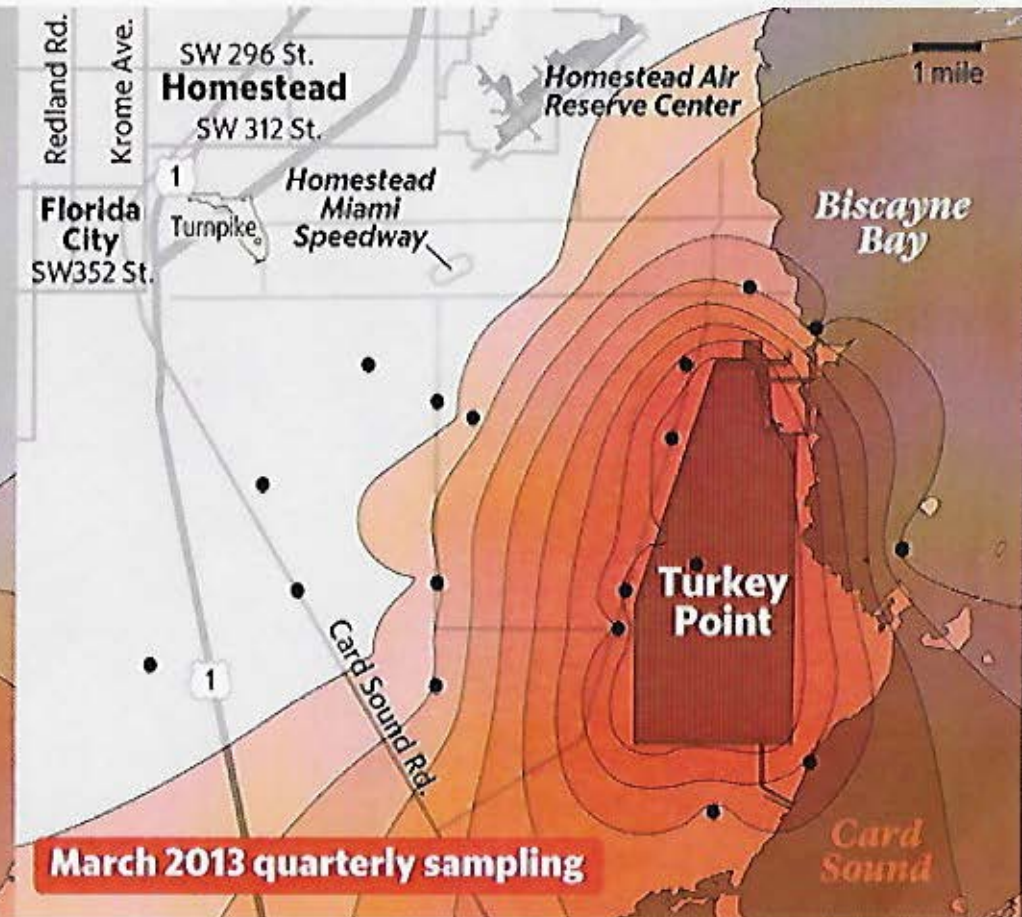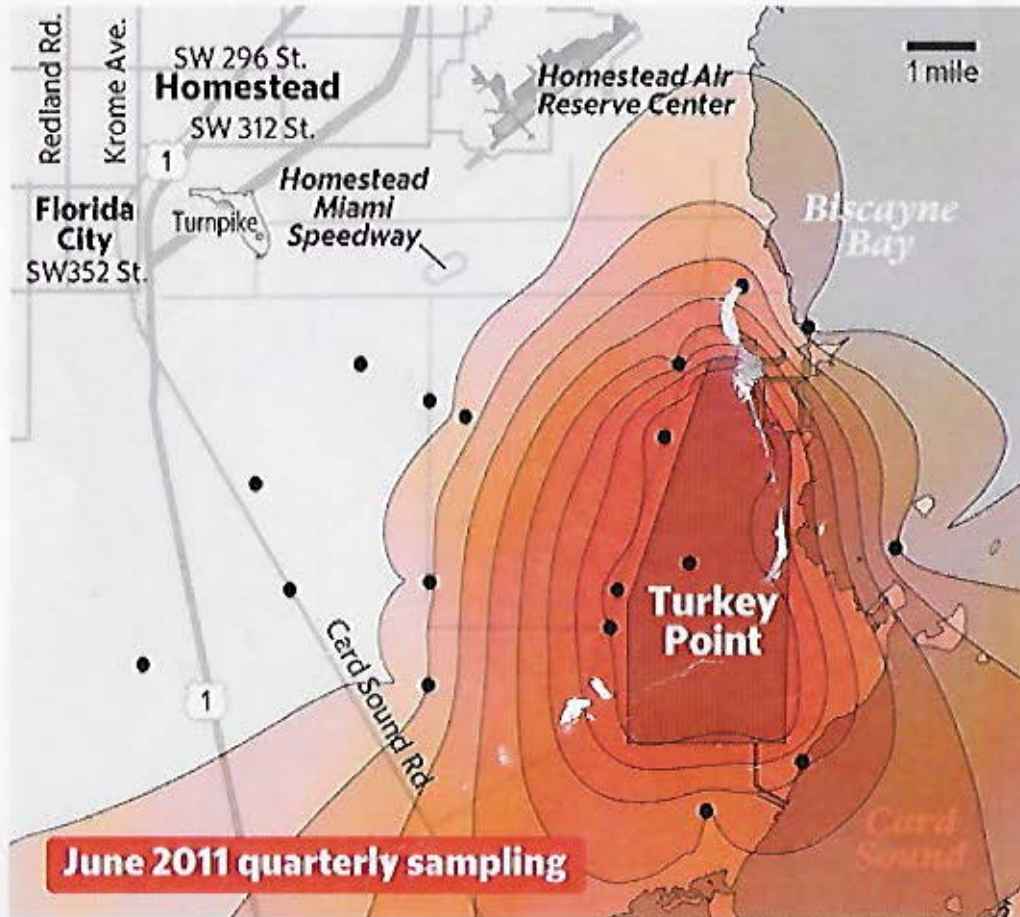
Turkey Point's salt problem explained

Engineer Ed Swakon created this video model of an expanding saltwater plume near Turkey Point using data collected from groundwater sampling. Swakon, who was hired by Atlantic Civil, a rock mining company that has sued FPL, depicted what the underground salt front looked like over time and expanded as conditions in the canals grew saltier.

The interceptor ditch was important because South Florida's drinking water supply also sits just below the surface in the Biscayne aquifer. Canals dredged in the 1940s to drain the Everglades had caused the salt front to migrate inland. But over the years water managers installed hundreds of gates and other controls to stop the migration — and in some cases, even reverse it.

But by the 1980s, there already was an indication that Turkey Point's ditch wasn't effective, with the underground salt front moving just west of what was suppose to act as a barrier.

Under all five management plans for Turkey Point drawn up by the Florida environmental regulators and water managers over the decades, FPL has been under orders to maintain the quality of surrounding groundwater. A network of monitoring wells was dug to keep watch.

Over the years, the number of wells dwindled, falling to just four by 1983. If state regulators were watching them, they weren't doing it very closely, said consulting engineer Ed SwakonTorcise hired him to investigate the plume after plans to expand a rock mine near Homestead were nearly derailed when environmental regulators wondered whether mining would pull the saltwater front inland.

In 2007, Swakon went to the South Florida Water Management District, the regulatory agency keeping tabs on salt water intrusion, and asked for old records. To his surprise, Swakon found salinity in groundwater spreading and spiking. By 2001 and 2002, readings showed the front — water with higher salt concentrations than in Biscayne Bay — had reached Southwest 137th Avenue about three miles to the west.

66

"THEY NEVER REALLY DID A LONG TERM HISTORY OF THE DATA. THEY ONLY [COMPARED] QUARTER TO QUARTER AND THERE WAS VERY LITTLE DIFFERENCE."

Ed Swakon, president EAS Engineering

"The way the reports were written, they never really did a long term history of the data. They only [compared] quarter to quarter and there was very little difference," he said. "But if you really plotted it, and somebody had taken the time, they would have seen each successive quarter got a little worse and a little worse."

Swakon said he and Torcise met with FPL officials to report their findings, but got no response. An FPL spokesman later called them "unfounded allegations." At the time, the utility was in the midst of hammering out a new administrative order required by a $3 billion uprating project of Turkey Point's two nuclear reactors that FPL said it needed to keep up with increasing demand: as much as 40 percent of the power the county needed was being imported, FPL officials said in a 2007 zoning meeting.

How long have Turkey Point's cooling canals been leaking? Critics say decades | Miami Herald

1/24/17, 8:4:

The uprate would increase power output by 15 percent but also raise temperatures in the cooling canals, with the effect of increasing evaporation and salt concentrations. FPL officials planned to offset additional heat going into the canals by shutting down the plant's two oldest fossil fuel burning units. The move was expected to cap the heat increase to only by 2.5 degrees — an impact FPL insisted would not effect the operation of the canals.

But modeling done by the U.S. Geological Survey in 2009 found that as the canals grew hotter and saltier, they could potentially shoot "saline fingers" to the bottom of the 98-foot thick aquifer —sometimes as fast as a few days. The extra salty water could then spread laterally, expanding the plume.

Water managers, whose approval was key to the uprating moving forward, wanted to know if the interceptor ditch was still an effective barrier. At the time, FPL officials assured them it was.

Engineers who designed the ditch weren't so confident. According to a report compiled this year by University of Miami hydrologist David Chin for Miami-Dade County, the engineers worried as early as 1971 that saltwater could migrate inland even if the ditch was properly operated. Chin also found the ditch only blocks shallow saltwater from spreading — and the canal system was pushing it deeper into the Biscayne aquifer.

Faced with increased scrutiny, FPL hired its own engineers to look for remedies, according to an in-house study Torcise obtained in his recent lawsuit. Completed in August 2011, the study found that canal water had moved 3.5 miles west of the plant and was spreading at a relatively brisk pace of 500 feet a year. In response to a question, an FPL spokesman this week revised that figure, saying the rate has since slowed to just over 120 feet a year.

FPL's engineers offered five alternatives, including building massive slurry walls underground to stop water from moving at a cost of $134.4 million. But the cheapest and preferable alternative, the engineers said, was adding fresher water from the Floridan aquifer.

"The alternative is attractive because it effectively removes the source of the hypersaline water," engineers wrote. But a "potentially negative aspect" of the remedy, they said, was it did nothing to stop the westward movement of saltwater. Nor did the other four.

Despite the findings, FPL officials in 2010 and 2011 continued to work with water managers on an elaborate monitoring plan that also for the first time included checking for tritium, a radioactive isotope found in canal water that could be used as a tracer. In 2011, as part of their effort to confirm tritium as the best tracer, district hydrologists John Janzen and Steven Krupa found that canal water was in wells at Southwest 137th Avenue. Tritium was also found in surface water just east of the canals and at the mouth of the Card Sound Canal. To get a better read, the hydrologists recommended installing a better network of wells.

But in its annual post-uprate report in October 2012, FPL continued to debate the 2009 USGS findings of the expanding plume, arguing that the wells used by the agency might not be connected or in the same zone because of the "complex geology of the area." Still, the utility agreed a plume existed and offered solutions.

FPL managers now say the location of the saltwater plume wasn't in dispute — just the exact cause of it.

66

"WE ALWAYS SAID WE WERE PART OF IT, BUT THERE'S OTHER FACTORS."

FPL senior director Steve Scroggs

"We always said we were part of it, but there's other factors," including lowering the water table seasonally for nearby farmers, senior project director Steve Scroggs said this week. "It's easy to say it's all FPL. It's not."

How long have Turkey Point's cooling canals been leaking? Critics say decades | Miami Herald

1/24/17, 8:42

Meanwhile, the boundaries of the tritium were growing clearer. A Miami-Dade County contour map of samples in 2011 and 2013 show tritium detected well beyond cooling canal borders. County officials had been keeping an eye on the wells, but had no authority without a water quality violation, said Lee Hefty, director of the Division of Environmental Resources Management. Instead, he said, they pushed for the district to act.

In April 2013, the Water Management District finally officially notified FPL that the canals were in violation. The utility responded by asking to add 14 million gallons of water a day from the Floridan aquifer, which it said would reverse the plume, a prediction that contradicts the earlier 2010 report. But district hydro-geologist Jeff Giddings found FPL used faulty modeling. While adding Floridan water reduced salinity in the canals, it did nothing to reduce the underground plume.

District consultant William Nuttle also concluded more water would just increase seepage and warned that FPL failed to account for local conditions including a major change on the horizon: sea rise. A foot rise, now predicted by the National Oceanic and Atmospheric Administration by 2030, would put the shoreline west of the canals.

As the agencies tried to hammer out a deal, temperatures in the canal spiked in the summer of 2014, prompting the utility to scramble for solutions, including getting operating limits raised to 104 degrees, the highest in the country, and an emergency permit to pump up to 100 million gallons of water a day from a nearby drainage canal. The utility also began pumping water from unregulated marine wells.

Over the next year, Miami-Dade County officials estimate that FPL pumped more than 12 billion gallons of water into the canals. Half that came from the marine wells with a quarter coming from the nearby L-31e canal. Rain supplied just 37 percent, even though company officials say rain remains the primary source of water to address increasing evaporation with higher temperatures.

What caused the spike remains in dispute. Chin, whose final report is due next month, concluded that the uprating project caused it. FPL blames a local drought. In July 2014, FPL environmental services director Matt Raffenberg said rainfall over the canals amounted to just 5.29 inches and only 20 inches in all of 2013.

> **66**
>
> **"IF IT'S SUCH AN IMPORTANT FACILITY, YOU WOULD EXPECT ITS DESIGN WOULD NOT BE BASED UPON THE WEATHER."**
>
> Lee Hefty, director of Miami-Dade County's Division of Environmental Resources Management

"If it's such an important facility, you would expect its design would not be based on the weather," Hefty said. "It sounds like a funny thing to say, but really it's a fairly significant facility. I would have expected their design engineers would have contemplated how that facility would operate without rain."

FPL's Scroggs also said that when the canals were briefly shut down, sediment built up in the northwest corner, which slowed flowed, turned the water browner and hotter, and caused an algae bloom to spread. Sediment had not been removed from the canals since 1990s, Scroggs said, because it is expensive.

When the state finally issued a new administrative order late in 2015, allowing FPL to pump more water into the canals to lower salinity and "abate" the plume without fully spelling out how, Torcise, environmentalists, neighboring cities and the county sued. Last month, a Tallahassee administrative judge ordered the state to redo the plan after it failed to cite FPL for a specific violation.

On Thursday, DEP chief Steverson wrote that the order in fact contained remedies which were not suitable for judicial review and that choosing to fix the problem, rather than penalize FPL, was up to the department.

How long have Turkey Point's cooling canals been leaking? Critics say decades | Miami Herald

1/24/17, 8:42

The state's decision, South Miami Mayor Phil Stoddard said, comes as no surprise given the utility's political connections.

"I suspect there's incentive enough for DEP to disrespect the administrative law judge and the public welfare to avoid holding FPL responsible for the environmental damage they've done."

On May 15, FPL is also due to submit a clean-up plan to the county, which pulled out of the suit and hammered out its own deal. The plan calls for FPL to install extraction wells to pump the extra salty water deep into the boulder zone, which environmentalists worry won't do enough to address the plume. To address high levels of ammonia and phosphorus leaking into the bay, FPL also dug a 30-foot deep well east of the canals, which it did without consulting the county environmental staff, prompting another letter from Hefty to better spell out plans.

FPL now says the cooling canals are back under control, that salinity is a third lower than last summer and, now that they've cleared sediment and have permission to add water from the deeper brackish Floridan aquifer, they expect the canals to work properly. Efforts to address the plume was delayed not by them, Scroggs said, but by a complicated bureaucratic system.

"For years people knew about this and everybody talked about what we would do. Well, we finally broke through that," he said. "I'm living everyday with the delays and the questions and the go back and do this and the back and forth. It's an incredibly complex process with multiple people and multiple interests. But at the end of the day, we've moved to a place where we're taking action."

Follow Jenny Staletovich on Twitter @jenstaletovich

RELATED CONTENT

· The cooling canals of Turkey Point

MORE ENVIRONMENT

SUGGESTED FOR YOU

| The Extended Family Of President Obama | 14 Reasons Why Trump Won The Election | 19 Things To Know About FOX News Anchor Megyn Kelly | Madonna Says Women To Blame For Trump's Win |
| PoliticsChatter | PoliticsChatter | PoliticsChatter | PoliticsChatter |

COMMENTS

Memorandum

MIAMI-DADE COUNTY

Date: March 7, 2016

To: Honorable Chairman Jean Monestime
and Members, Board of County Commissioners

From: Carlos A. Gimenez
Mayor

Subject: Report on Recent Biscayne Bay Water Quality Observations associated with Florida Power and Light Turkey Point Cooling Canal System Operations – Directive 152884

The following is provided to the Board of County Commissioners (Board) pursuant to a request by Commissioner Levine Cava at the December 15, 2015 Board meeting for a report regarding preliminary information on water quality impacts to Biscayne Bay associated with operations of the Florida Power and Light Turkey Point Power Plant Cooling Canal System

If you have any questions or concerns, please contact Lee N. Hefty, Assistant Director, Division of Environmental Resources Management, Department of Regulatory and Economic Resources, at (305)372-6754 or at heftyl@miamidade.gov

Attachment

c: Abigail Price-Williams, County Attorney
Office of the Mayor Senior Staff
Lourdes M Gomez, Deputy Director, Department of Regulatory and Economic Resources
Lee N. Hefty, Assistant Director, Environmental Resources Management, Department of
Regulatory and Economic Resources
Charles Anderson, Commission Auditor
Eugene Love, Agenda Coordinator

Background

FPL owns and operates a Cooling Canal System consisting of an approximately 5,900 acre network of unlined canals at the Turkey Point Power Plant. The Cooling Canal System was constructed in the early 1970s and serves as Turkey Point's Industrial Waste Water Treatment Facility. In that function, the Cooling Canal System serves as the heat sink for the power plant and it also receives industrial waste water discharges from plant operations. The Cooling Canal System water removes excess heat from power plant operations and is then returned to the Cooling Canal System where it cools by evaporation. As a result of the evaporation process, chemical constituents in cooling canal water such as dissolved salts become more concentrated. Historical data indicate that initial salinity (dissolved salts) levels in the Cooling Canal System in 1973 were less than 30 practical salinity units and were lower than levels typical of marine waters such as Biscayne Bay. However, long term monitoring data indicate that water quality within the Cooling Canal System has deteriorated over time. The Cooling Canal System is a "closed loop" system because it is not directly connected to adjoining surface waters. However, the porous geology of the underlying Biscayne Aquifer allows water from the Cooling Canal System to move freely through the ground beyond the limits of the Cooling Canal System and beyond the property boundaries of the Turkey Point Power Plant. This creates concerns with potential impacts of the poorer quality Cooling Canal System water reaching sensitive water resources beyond the boundaries of the Cooling Canal System.

History

In October 2008, FPL received approval from the State of Florida to modify the existing nuclear power plant units to increase their power generating capacity (referred to as an "Uprate" or the "Uprate project"). As a condition of that approval, FPL implemented an enhanced monitoring plan to evaluate the potential water quality impacts associated with implementation of the Uprate and the Cooling Canal System. Following commencement of construction on the power plant uprate work at Turkey Point in early 2012, water quality in the Cooling Canal System further deteriorated ultimately affecting the heat exchange capacity of the water in the Cooling Canal System. By the summer of 2014, salinity levels in the Cooling Canal System had reached a record high of more than 100 practical salinity units, which is approximately three (3) times the salinity levels typical for Biscayne Bay. In addition, intake water temperature in the Cooling Canal System had exceeded the federal operating license criteria of 100 degrees Fahrenheit, reaching nearly 102 degrees Fahrenheit and requiring FPL to seek and obtain approval from the Nuclear Regulatory Commission for a new intake operating temperature limit of 104 degrees Fahrenheit.

- In order to address emerging operational concerns with the Cooling Canal System, FPL proposed to improve water quality by pumping additional water into the Cooling Canal System. Under this approach, FPL sought approval for use of water from the L-31E Canal as a temporary source of freshwater to improve water quality in the Cooling Canal System. In August 2014, the South Florida Water Management District issued an Emergency Order to FPL authorizing the temporary installation of pipelines and associated equipment to transfer water from the L-31E Canal to the Cooling Canal System to moderate the unusually high temperatures and salinity in the Cooling Canal System. In September 2014, the Board of County Commissioners (Board) approved Class I permit application CLI-2014-0312 authorizing 0.24 acres of temporary impacts to halophytic (salt tolerant) wetlands for the temporary installation of two, 36-inch above ground pipelines to facilitate the transfer of water from the L-31E Canal to the Cooling Canal System in an attempt to address the higher salinity and higher

temperatures in the Cooling Canal System. As a condition of the approval and pursuant to the Class I permit, the temporary pumping activities ceased October 15, 2014, and the pipes were removed.

Monitoring data indicates that the Cooling Canal System salinity and temperature began to temporarily improve in late summer of 2014 with salinity decreasing to near 60 practical salinity units by October of that year. However, salinity and temperature began to increase over the winter months and early spring of 2015. FPL subsequently sought approval to reinstall the pipes to again convey water from the L31E into the Cooling Canal System. In April 2015, the South Florida Water Management District issued a Final Order to FPL, authorizing the temporary pump installation and water withdrawal from the L-31E Canal as a temporary measure to occur June 1 through November 30, 2015, and June 1 through November 30, 2016. The Final Order required that the state-mandated daily water reservation for Biscayne Bay (504 acre feet/day) be achieved prior to FPL's use of water from the L31E.

In May 2015, the Board approved a modification to the Class I permit to authorize reinstallation of the pipelines in wetlands to facilitate an additional period of water transfer from the L-31E to the Cooling Canal System, but the Board approval limited the authorized time period to one (1) season from May 26, 2015 through January 1, 2016. As a result, the Class I permit required that the pipelines be removed by January 1, 2016. In addition, the permit required that additional water quality monitoring stations be established to further evaluate any potential impact associated with pumping additional water into the Cooling Canal System, and the permit required that FPL develop a long term plan to address water quality issues associated with the Cooling Canal System. By December 2015, salinity levels in the Cooling Canal System decreased to 34 practical salinity units following the pumping of additional water from the L31E and unusually heavy rain. FPL requested a second modification to the Class I permit in November 2015 to allow the pipes to remain in wetlands through May 2016, but not allow use of the pipes for pumping water from the L31E during that timeframe. The request would allow the pipelines to remain in wetlands over the winter months while FPL evaluated emerging water quality data and considered the need for use of the pipelines for pumping additional water during the summer of 2016. The Board approved the modification request allowing the pipes to remain until May 31, 2016, during such time when pumping of water from the L31E is not authorized. It should be noted that FPL will need further approval from the Board for the pipelines to remain beyond the May 31, 2016 date and for use of the pipelines to pump any additional water from the L31E Canal into the Cooling Canal System.

Impact on Biscayne Bay
As noted above, long term monitoring data indicate that water quality within the Cooling Canal System has deteriorated over time (Attachment A). Due to the porous nature of the Biscayne Aquifer underlying the Cooling Canal System, a hyper saline plume of Cooling Canal System water has migrated outside the boundaries of the Cooling Canal System through the groundwater and has moved beyond the boundaries of the Turkey Point facility property. Pursuant to Florida law, the siting and permitting of power plants are reviewed and approved by the State under the Power Plant Siting Act. In its role as an affected agency, Miami-Dade County participated in the State's Power Plant Siting Act process and provided comments to the state on conditions of certification for the Uprate Project at Turkey Point. The Power Plant Siting Act certification for the Uprate Project includes a condition that requires FPL to take additional measures if the State concludes the project is causing harm to waters of the State or exceeding State or County water quality standards. Following review of monitoring data from the uprate monitoring program, County staff advised the State of concerns with water quality impacts associated with the Cooling Canal System and of impacts to water resources of the County and the State. On December 23, 2014, the State of Florida Department of Environmental Protection issued an Administrative Order to FPL regarding water quality issues

associated with the Cooling Canal System. However, County staff did not agree that the Administrative Order adequately addressed concerns related to these impacts. Therefore, on February 9, 2015, Miami-Dade County filed an objection to the Administrative Order and requested an administrative hearing on the matter. In addition, County staff advised FPL of the County's intention to pursue corrective action under Miami-Dade County's own regulatory authority.

On October 2, 2015, the Division of Environmental Resources Management (DERM) within the Department of Regulatory and Economic Resources issued FPL a Notice of Violation and Notice for Corrective Action for violations of the County's water quality standards for chloride in groundwater outside of the Cooling Canal System and beyond the boundaries of the property (Attachment B). FPL expressed a willingness to address the County's concerns by implementing corrective actions, and DERM and FPL met to discuss required actions. On October 7, 2015, FPL entered into a Consent Agreement with Miami-Dade County (Attachment C). The Consent Agreement includes components of a long term plan for FPL to address water quality issues associated with the Cooling Canal System. The Consent Agreement requires FPL to implement actions to abate water quality within the Cooling Canal System to reduce the threat the system poses to adjoining water resources. To address this issue, FPL proposes to use water from wells constructed into the Florida Aquifer to supply water to the Cooling Canal System to control salinity that would otherwise continue to increase due to evaporation. In addition, the Consent Agreement requires FPL to remediate water quality impacts of the hyper-saline plume that has migrated landward outside the boundaries of the property. To address this issue, FPL is obligated under the Consent Agreement to design and construct a network of groundwater extraction wells along the landward boundary of the facility to capture, contain, and retract the hyper-saline plume. The wells will extract hyper-saline water from the surficial Biscayne Aquifer and dispose of it via deep well injection into the boulder zone of the Floridan Aquifer. Other components of the Consent Agreement require FPL to: a) evaluate other sources of water to control salinity in the Cooling Canal System including the use of reuse water from the County's South District Waste Water Treatment Plant; b) evaluate existing operations of the Cooling Canal System Interceptor Ditch originally implemented to control the westward migration of saline water from the Cooling Canal System to identify improvements or alternatives; c) modify water management operations at their neighboring FPL-owned Everglades Mitigation Bank to minimize overdrainage of the basin, which is under existing pressure of salt intrusion exacerbated by the westward migration of the hyper-saline Cooling Canal System groundwater plume; d) provide flowage easements to the South Florida Water Management District if required, and e) agree to work cooperatively with agencies involved in regional restoration efforts related to the Comprehensive Everglades Restoration Plan Biscayne Bay Coastal Wetlands Project and other hydrologic improvement projects. FPL is presently implementing the requirements of the Consent Agreement.

As previously stated, monitoring data indicate that a hyper-saline groundwater plume originating from the Cooling Canal System has migrated landward and is impacting water quality. Factors that affect movement of Cooling Canal System water and the groundwater plume include water elevation (or stage) in the areas surrounding the Cooling Canal System, the stage of the water in the Cooling Canal System, and the density of the various water segments. In addition to the existing water quality monitoring network associated with previous State and County approvals (and due to concerns with potential offsite migration of Cooling Canal System water as a result of pumping additional water from the L31E Canal and other sources into the Cooling Canal System), the modified Class I permit required that additional monitoring stations be established. In particular, the permit required that FPL establish water quality monitoring stations immediately adjacent to the Cooling Canal System in surface waters tidally connected to Biscayne Bay. Additional surface water stations were established in June 2015.

Monitoring data from these stations has documented changes in water quality over several months since the sampling began. In particular, the data indicate that concentrations of nutrients such as phosphorous and ammonia began to increase in September 2015 and continued to increase over the next few months. For example, data results for ammonia at station TPBBSW-7B were below the County's water quality standard of 0.5 milligrams per liter during initial sampling from early June through late August 2015, but these values increased to as much as 3.29 milligrams per liter by December 2015. Elevated levels of phosphorous were also detected in excess of the state numeric nutrient criteria of seven (7) parts per billion with results typically ranging from three (3) to 230 parts per billion with one (1) result as high as 893 parts per billion. Other sample results included higher than normal salinities and temperatures, as well as higher than expected levels for chlorophyll, which can be an indication of algal blooms. The data indicate that the observed increases coincide with increases in the water stage within the Cooling Canal System (Attachment D). It should be noted that unusually heavy localized rain in the fall of 2015, combined with FPL's pumping of additional water from the L-31E Canal, as well as additional water associated with operation of the Cooling Canal System Interceptor Ditch pumping lead to record high water stage in the Cooling Canal System in December 2015 (Attachment E). This record high water stage in the Cooling Canal System would be expected to result in increased seepage of water from the Cooling Canal System into surrounding ground waters and perhaps surface waters.

In late December 2015/early January 2016, DERM staff conducted a special sampling event jointly with FPL to further evaluate and confirm these earlier findings. Because the existing stations are sampled at the bottom of the water column, additional water samples were also collected at multiple depths at each station to better evaluate the potential influence of groundwater on surface water at these sites. In addition to resampling the existing stations, additional locations with similar site characteristics were also sampled in the vicinity of the Cooling Canal System. These stations are characterized by being deeper dredged areas located near the Cooling Canal System. Water depths at these sites are as much as 24 feet deep in some areas. It is likely that the groundwater plume associated with the Cooling Canal System is intersecting these deeper areas. As part of this sampling effort, DERM also collected surface water samples for tritium analysis. Tritium is an isotope of hydrogen that is frequently associated with the operation of nuclear power plants. Water in the Cooling Canal System has higher levels of tritium than levels found naturally in the environment and tritium is therefore being used as a tracer to track the movement of Cooling Canal System water in this area. Over the past five-year period, tritium levels in the Cooling Canal System typically ranged between 1,200 and 16,500 picocuries (measurement of radioactive elements) per liter (pCi/L), while levels for tritium in the surface waters of Biscayne Bay were typically less than 20 pCi/L.

Data results from the special sampling event confirmed earlier results showing elevated levels of nutrients at these stations as well as at other similar deeper areas located in the vicinity of the Cooling Canal System. Data results indicate that surface water quality at these sites is stratified with better water quality at the surface and decreasing water quality with increasing depth. Although most stations met County water quality standards for ammonia at the surface, nearly all of these stations exceeded the County's water quality standard for ammonia at the bottom with results typically ranging between 1.3 to 2.6 milligrams per liter with one (1) sample result as high as 9.5 milligrams per liter. Results for tritium were also stratified through the water column based on sample depth, however all samples were higher than background levels typical for Biscayne Bay. Most notably, tritium results for bottom samples at locations nearest to the Cooling Canal System ranged from 2,652 to 4,317 pCi/L. The results for tritium provide the most compelling evidence that water originating from the Cooling Canal System is reaching these tidal surface waters connected to Biscayne Bay.

In summary, water from the Cooling Canal System is migrating outside the boundaries of the Cooling Canal System away from the Turkey Point facility property with impacts measured in both surface and groundwater. FPL is required to implement provisions of the Consent Agreement to address the landward migration of the hyper-saline plume. However, further evaluation and action is needed to address the recent discovery of impacts to surface waters tidally connected to Biscayne Bay. This includes further evaluation of the relationship between the Cooling Canal System and its associated groundwater plume and impacts to tidally connected surface waters. In response to the recent data, FPL is performing additional modeling to further review the Cooling Canal System and groundwater flux under various water stage scenarios. The outcome of this effort will be needed to inform and refine FPL's long term plan for managing water quality in the Cooling Canal System through the addition of other water sources. DERM will continue to pursue resolution of these issues through provisions of the existing Consent Agreement or through a subsequent enforcement action.

Attachments   Attachment A   Graph Historical Data for CCS
               Attachment B   Notice of Violation
               Attachment C   Consent Agreement
               Attachment D   Graph Increasing Ammonia in Tidal Surface Water
               Attachment E   Cooling Canal System Water Level and Water Inputs

ABOUT (HTTPS://WWW.NFLT.ORG/ABOUT/)

(https://www.nflt.org/)

TAKE ACTION
(HTTPS://WWW.NFLT.ORG/TAKE-ACTION/)

(https://www.nflt.org/)

CONNECT
(HTTPS://WWW.NFLT.ORG/CONNECT/)

MEMBERSHIP
(HTTPS://WWW.NFLT.ORG/MEMBERSHIP/)

ORCA COMMENTS
EXHIBIT 5
MAY 2023

Recharging the Floridan Aquifer: Threats to the Floridan Aquifer

August 22, 2022

Master Naturalist Spotlight Series

Recharging the Floridan Aquifer: Threats to the Floridan Aquifer

Jon Heggie with National Geographic states, "Florida's booming population is writing a water check its aquifers can't cash…" Some of the threats to the Floridan aquifer include the following:

Figure 1: FDOT 2020 Population Growth

Population Growth

Florida's population has grown from about two million in the 1940s to around 21 million today, with a projection of over 26 million within the next 20 years.

At the heart of the problem is over-extraction: there are simply too many people taking too much water from the aquifer (about:blank). In the early, to mid-1900s developers began to capitalize on Florida's natural beauty and warm climate, draining wetlands to build homes and fueling development that turned Florida into one of the fastest growing states: an **estimated 900 people a day move here**, adding another 300,000 people a year.

The population growth also diminishes recharge as lands that recharge the aquifer are drained and covered with concrete.

Contamination:

Groundwater quality is also impaired not only by point contamination sources such as industrial or municipal waste repositories but also by nonpoint contamination events such as the widespread application of **fertilizers** and a wide range of chemicals for increased agricultural production.

Over Extraction (from other than population growth):

Of the seven billion gallons of freshwater used daily across Florida's agriculture, industry, power plants, and public water

Figure 2: Construction site drainage in Flagler County, photo by Stephanie Hezel

sectors, most are taken from the Floridan aquifer. **Half of all the water taken from the public supply ends up watering private lawns.** Indoors, around 24 percent of a household's water goes to toilets, 20 percent is used for showers and nearly 19 percent for running faucets for everything from brushing teeth to rinsing plates.

Saltwater Intrusion:

Over-extraction and diminishing recharge areas cause salt water to be drawn toward the freshwater zones of the aquifer and seep into the aquifer at levels that make its water undrinkable.

If water is pumped out at a rate faster than the aquifer is replenished, the pressure of freshwater over saltwater in the land mass is decreased.

Figure 4: Source US Geological Survey (USGS.gov)

This decrease may cause the level of saltwater to rise in the aquifer, degrading water quality. This problem can be controlled by careful attention to well location and pumping rates.

The Effects of Climate Change:

Did you know since 1880, the global sea level has risen about eight inches? **Scientists expect the global sea level to rise another one to four feet by 2100.**

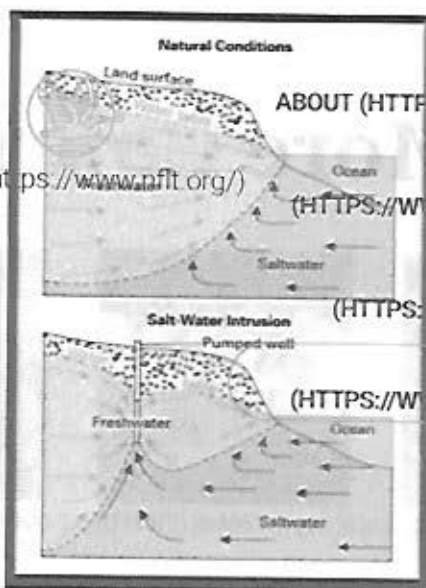A changing climate impacts the quantity and quality of

groundwater through increased risks of drought (about:blank), changes in precipitation (about:blank) and temperature (about:blank), decreases in snowmelt (about:blank), and rising sea levels (about:blank). As the sea level rises, the amount of saltwater infiltrating the groundwater aquifer will increase, which can make the water too salty for human consumption.

Protect and Preserve viable Recharge Areas:

With all of the threats to the Floridan aquifer, it's important to **protect and preserve** those areas of NE Florida where, when it rains, the water will filter through the soil and replenish the aquifer to help ensure adequate and high-quality water resources in the future.

More Connections

(https://www.nflt.org/category/annual-reports/) (https://www.nflt.org/category/blog/) (https://www.nflt.org/category/events/) (https://www.nflt.org/category/news/

(https://www.nflt.org/category/newsletter/) (https://www.nflt.org/category/job-openings/)

NATIONAL GEOGRAPHIC | **CREATIVE WORKS**

VIDEO

Floridan aquifer: Why one of our rainiest sta... water

ooming population is writing a water check its aquifers can't cash; from lawn sprinklers nd use less water.

In a little over 50 years, half of the freshwater basins in the US may not be able to meet our usage demands. National Geograpic photographer Erika Larsen is in her home state of Florida looking for ways to prevent a looming water crisis.
NATIONAL GEOGRAPHIC

BY **JON HEGGIE**

> **This is Paid Content. The editorial staff of National Geographic was not involved in the preparation or production of this content.**

Millions of years ago, in the ocean above what is now Florida, a small crustacean dies. It sinks to the seafloor where, in time, it is covered by the skeletons of other fish, shellfish, and coral until it forms part of a thousand-foot layer of limestone rock. Around 30 million years ago, sea levels fall, and Florida emerges from the ocean to form dry land. But Florida never really dries out, and water gradually erodes the porous limestone to form cracks, passages, and vast underground spaces that fill with rain. This is the Floridan aquifer, the natural freshwater reservoir that underpins life in the Sunshine State.

Florida's famous springs are so large that they support entire river ecosystems, such as the Suwannee and Santa Fe, and the underlying aquifer feeding these springs provides most of the 100 to 150 gallons of water Florida residents use every day. Indoors, around 24 percent of a household's water goes to toilets, 20 percent is used for showers, and nearly 19 percent for running faucets for everything from brushing teeth to rinsing plates. Half of all the water taken

from the public supply ends up watering private lawns—some 900 million gallons a day. Of the seven billion gallons of freshwater used daily across Florida's agriculture, industry, power plants, and public water sectors, most is taken from the Floridan aquifer. ·

Many residences in Florida boast lush gardens and are never very far from green recreational areas. Almost 50 percent of domestic water usage goes on maintaining these manicured lawns— all of which comes from the increasingly stressed aquifers.
PHOTOGRAPH BY SHUTTERSTOCK
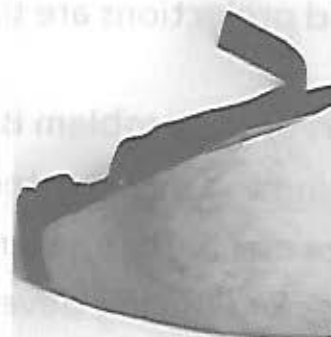
Stretching beneath most of Florida the Floridan aquifer is the largest and deepest in the state, and reaches into parts of Georgia, Alabama, Mississippi, and South Carolina. It is an 82,000-square-mile reservoir that holds billions of gallons of freshwater—some of it perhaps 26,000 years old. Across the state, wells have been drilled to tap into this seemingly endless water supply. But serious challenges to the Floridan aquifer are forcing residents to realize their water supply may be limited. Over-extraction, sea level rise, and an increasing risk of saltwater intrusion are all straining the aquifer's resources.

For thousands of years the Floridan aquifer has been capturing and storing rainwater in a complex hydrological system. Florida is the fifth rainiest state in the U.S., and, on average, receives 51 inches of rain a year. About 70 percent of all rainfall returns to the atmosphere through evaporation or transpiration by plants, but Florida's loose sandy soils and porous limestone bedrock allow around 13 inches of the rain that reaches the ground to soak into the earth. This recharges the Floridan aquifer and keeps the water flowing from the state's

springs.

Every decade has seen at least one severe and widespread drought. And the Floridan aquifer has always been able to recover, but the freshwater flowing into some springs has dropped significantly. A 2018 study revealed a 32 percent reduction in average spring flows between 1950 and 2010; divers now walk through caves that they previously had to swim through. The aquifer is in trouble, and projections are that Florida's freshwater basins may get even drier.

At the heart of the problem is over-extraction: there are simply too many people taking too much water from the aquifer. In the 1900s developers began to capitalize on Florida's natural beauty and warm climate, draining wetlands to build homes and fueling development that turned Florida into one of the fastest growing states: an estimated 900 people a day move here, adding another 300,000 people a year making more demands on an already stressed water supply. And most of that water is drawn from the Floridan aquifer, dangerously depleting its water levels.

When an aquifer's water levels drop, the pressure that keeps water flowing through it also drops and the system breaks down. In Florida, the health of the aquifer is visible in its springs: with insufficient water to create high pressure, the flows stop, algae forms, and the springs' clear waters become stagnant and brackish, and may even ultimately run dry. Research shows that a 10- to 20-foot drop in water levels can stop a spring flowing; some urbanized areas of Florida have recorded 90-foot drops. Silver Springs, one of the Floridan aquifer's largest springs, has seen its prodigious output fall from 500 million gallons to around 200 million gallons per day—an alarming 60 percent decline.
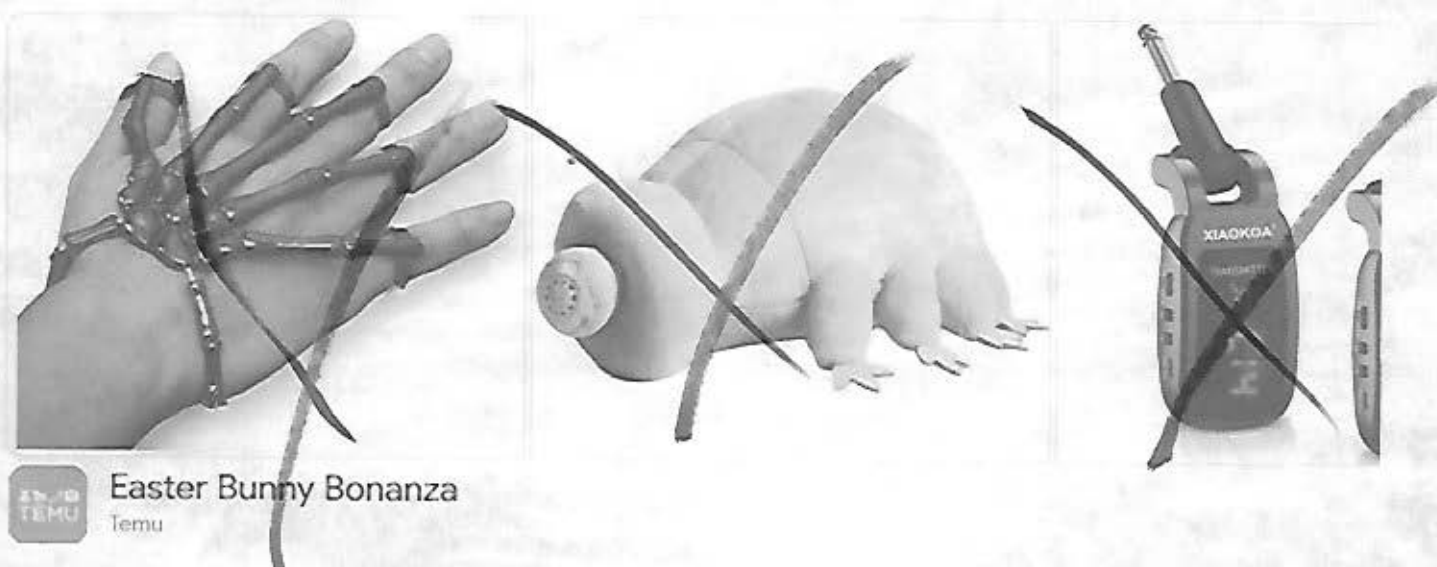
Such a depletion of the aquifer's water levels brings the danger of saltwater intrusion. Beneath the Floridan aquifer is an ancient saltwater sea pushing upward, but held in check by the freshwater above it. Over-extraction and diminishing recharge are weakening the freshwater lens and allowing saltwater to rise and seep into the aquifer at levels that make its water undrinkable. Rising sea levels driven by climate change are speeding up this process around Florida's extensive coastline. If freshwater levels in the Floridan aquifer continue to fall, the main source of usable water in Florida could be contaminated—and the consequences would be devastating.

But saltwater intrusion can be reversed and there is still time to save the Floridan aquifer. In 2017 the Department of Environmental Protection proposed 747 projects to conserve water around the state. Efforts are being made to restore wetlands, including the Everglades, make development and construction more sustainable, and create more reservoirs. There are also calls for reform to curb the agricultural sector's daily water consumption of 1.5 billion gallons. In some locations, desalination plants turn brackish and saltwater into freshwater, but costs are twice as expensive. With household water use one of the fastest growing drains on the Floridan aquifer, this is a problem that everyone can help solve. Florida residents are being encouraged to irrigate or water lawns less, take shorter showers, minimize toilet flushing, and turn off faucets whenever possible. This includes making the most of water-efficient washing machines and dishwashers and not pre-rinsing dishes, which wastes as much as 20 gallons of water per load. A dishwasher and detergent can do the work in a closed cycle that uses only five gallons of water. If everyone altered a few of their water-wasting habits, it could make a big difference to the health of the Floridan aquifer, and help in maintaining levels of freshwater there that will reduce the risk of saltwater intrusion.

Silver springs State Park is Florida's first tourist attraction, and the state's popularity as a tourist destination is only increasing; as is the stress this puts on the water supply. Developments of everything from golf courses, to residential areas, to holiday resorts are rapidly dep...**Read More**
PHOTOGRAPH BY SHUTTERSTOCK

But the water crisis is not restricted to Florida alone—or even California, Texas, and Arizona. It is part of a wider national water crisis across that United States. A government-backed study predicts serious water shortages in nearly half of America's water basins in around 50 years—sooner in some places. As the nation's population grows and climate change brings a hotter and drier normal to many parts of the country, people are starting to recognize that it's time to turn off the free-running faucet and build a more sustainable relationship with the water we need to survive.

SHARE　　　　　**TWEET**　　　　　**EMAIL**

READ THIS NEXT

The Nature Conservancy

RENEW

DONATE

STORIES IN FLORIDA

Protecting Fresh Water

We're working to ensure clean water for Florida's people and nature.

July 14, 2020 | *Last updated July 28, 2022*

SHARE   f   🐦   in   ✉   🖨

ORCA COMMENTS
EXHIBIT 7
MAY 2023

Our long-term vision for freshwater conservation in Florida is simple but ambitious: Florida must have enough clean water for both people and nature.

The Florida Everglades, one of the only great grasslands in the world, is marked by a silent, slow sheet of fresh water moving above and below ground. This vast wetland provides water to nearly 8 million people living in the southern stretches of the state. The Everglades recharges the aquifer as it slowly soaks up and releases waters southward. As a result of past wetland drainage, Florida has lost large supplies of fresh water for both people and wildlife. But that loss does not have to be permanent.

We're working to protect, restore and connect lands and wetlands critical to the replenishment of the state's aquifers. These lands provide critical habitat for wide-ranging species, like the Florida panther and black bear, as well as other species such as the red-cockaded woodpecker and sandhill crane. We completed restoration of the wetlands on our Disney Wilderness Preserve, perfecting the process of wetlands restoration over the last 20 years and applying lessons learned to help restore other conservation land. We work with ranchers in the northern Everglades to reduce agricultural water use and nutrient run-off and to protect lands for water recharge. This has provided a foundation for meaningful change in the Everglades.

GREAT BLUE HERON   A mother and young nest in Florida's Everglades National Park. © Kent Mason

We helped preserve 350,000 acres and facilitated expenditure of $280 million dollars through federal programs to protect and restore wetlands that help replenish the aquifer. Today, these wetlands are returning at least 500 million gallons of water from seasonal rains to the aquifer. And, as part of these efforts, we helped secure The Everglades Headwaters National Wildlife Refuge and Conservation Area, the first refuge established in two decades and the first of its kind in Florida. It links public and private lands with 150,000 acres for recreation while helping restore the natural flow of water to the greater Everglades. These efforts are essential for improving water quality and preserving wildlife habitat.
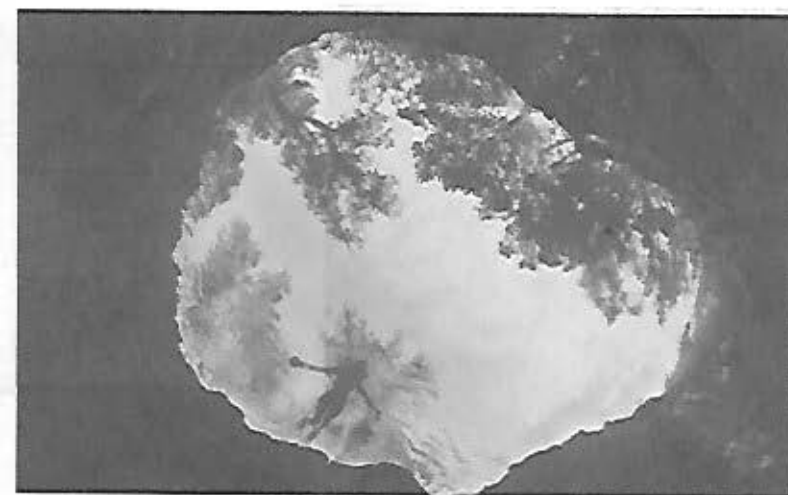
FLORIDA SPRINGS Swimmer in a deep spring at Ichetucknee Springs State Park in Fort White, Florida. © Jennifer Adler

MANATEES IN FRESHWATER SPRINGS Two adult manatees share a special moment together while aggregating in a freshwater spring in North-central Florida. © Joseph Ricketts/TNC Photo Contest 2021

Because large-scale water storage and treatment is key to restoring the health of the Everglades, we support the completion of the regional storage and water-quality projects that are part of state and federal programs for restoring the Everglades. We helped to secure $200 million in funding to support the multibillion dollar State and Federal Everglades restoration effort, including funding for completion of two large reservoirs, both of which capture excess discharges from Lake Okeechobee to protect the Caloosahatchee and St. Lucie estuaries from harmful algal blooms caused by excess nutrients and pollution. These projects are critical to improving the health of the estuaries, which are damaged by high water releases from Lake Okeechobee. We also support completion of the Herbert Hoover dike to protect both people and nature from the damaging effects of flooding.

FLORIDA'S ESSENTIAL SOUTH DADE WETLANDS (1:40) 55,000 acres of freshwater wetlands span across south Florida, linking two national treasures: Everglades National Park and Biscayne National Park. TNC FL Field Rep. Roberto Torres describes how this critical land helps to recharge Florida's aquifer, preserving our precious freshwater resources.

Recovering Natural Springs

Florida's springs provide critical groundwater to rivers and estuaries while offering unique opportunities for swimming, fishing and other recreational pursuits. Visitors contribute hundreds of millions of dollars to Florida's economy each year.

Florida's springs are struggling, though. The Floridan aquifer, the source of groundwater for most of Florida's springs and 90% of the state's drinking water, is being depleted as water demand from urban areas and unsustainable agricultural practices continually increase. Pollution, including fertilizer and sewage runoff, invasive species, excessive nutrients and erosion are also damaging the health of our springs.

MANATEES AT PLAY   Manatees enjoy the waters at Three Sisters Spring, Crystal River, Florida. © Carol Grant

We are here to help. Our springs initiative focuses on collaborative approaches to placing freshwater springs into sustainable management and lasting protection. We're taking a multifaceted approach in key springs and springsheds by developing restoration initiatives like pilot projects, studies, springshed planning, land protection and outreach. We're using science to back us, examining water flows needed to make springs healthy. We're demonstrating how industries can minimize their footprint in the springshed. We're supporting education and outreach to further the springs legacy. Protecting Florida's iconic springs is essential for wildlife, such as the Florida manatee.

Help Us

Support Our Work in Florida

DONATE NOW
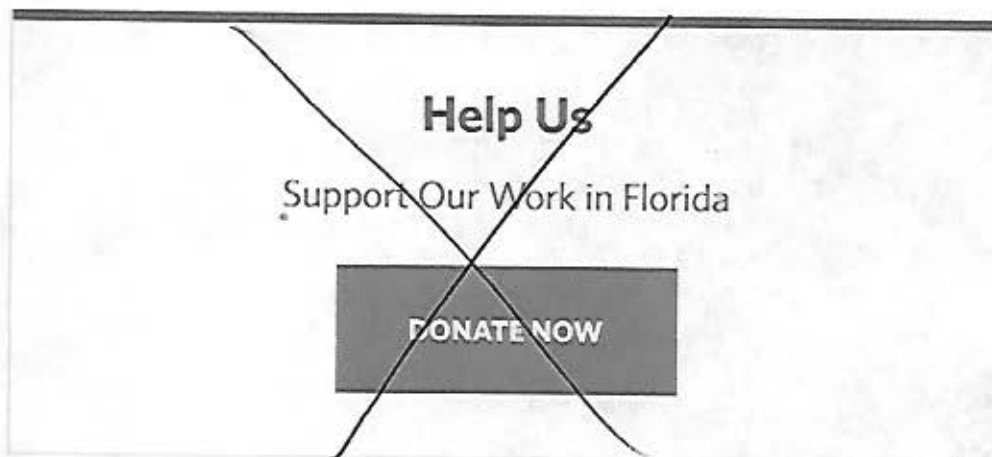
Despite recent declines in the quantity and quality of water, we believe vibrant communities with sustainable economies and healthy springs systems can coexist, but changes in people's behavior and actions will be necessary. TNC is hard at work on the ground, in the water, and with local, state and federal governments, universities, other environmental organizations, businesses and individuals to ensure our freshwater future.

Our World/Our Florida
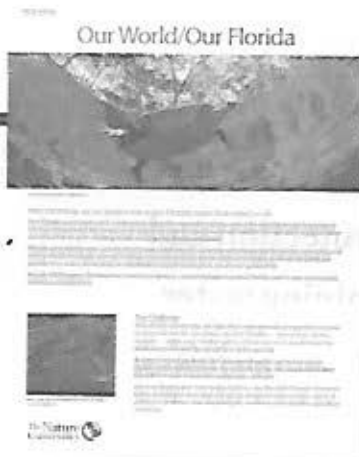
Freshwater Fact Sheet

DOWNLOAD

The Washington Post

Seas have drastically risen along southern U.S. coast in past decade

Multiple new studies highlight a rate of sea level rise that is 'unprecedented in at least 120 years' along the Gulf of Mexico and southeastern U.S. coast

By Chris Mooney and Brady Dennis

April 10, 2023 at 5:00 a.m. EDT

Scientists have documented an abnormal and dramatic surge in sea levels along the U.S. gulf and southeastern coastlines since about 2010, raising new questions about whether New Orleans, Miami, Houston and other coastal communities might be even more at risk from rising seas than once predicted.

The acceleration, while relatively short-lived so far, could have far-reaching consequences in an area of the United States that has seen massive development as the wetlands, mangroves and shorelines that once protected it are shrinking. An already vulnerable landscape that is home to millions of people is growing more vulnerable, more quickl potentially putting a large swath of America at greater risk from severe storms and flooding.

The increase has already had major effects, researchers found. One study suggests that recent devastating hurricanes, including Michael in 2018 and Ian last year, were made considerably worse by a faster-rising ocean. Federal tide gaug data from the National Oceanic and Atmospheric Administration suggest that the sea level, as measured by tide gauge Lake Pontchartrain in New Orleans, is eight inches higher than it was in 2006, just after Hurricane Katrina.

"The entire Southeast coast and the Gulf Coast is feeling the impact of the sea level rise acceleration," said Jianjun Yir climate scientist at the University of Arizona and the author of one of two academic studies published in recent weeks that describe the changes.

Yin's study, published in the Journal of Climate, calculates the rate of sea-level rise since 2010 at more than 10 millimeters — or one centimeter — per year in the region, or nearly 5 inches in total through 2022. That is more than double the global average rate of about 4.5 millimeters per year since 2010, based on satellite observations of sea leve from experts at the University of Colorado at Boulder.

While the annual totals might sound minor, even small changes in sea levels over time can have destructive consequences. Yin's study suggested that Hurricanes Michael and Ian, two of the strongest storms ever to hit the Uni States, were made considerably worse in part from additional sea level rise.

"It turns out that the water level associated with Hurricane Ian was the highest on record due to the combined effect of sea-level rise and storm surge," Yin said.

A second study by a long list of sea-level experts, led by Sönke Dangendorf of Tulane University and published in Nat Communications, finds the same trend since 2010 across the U.S. Gulf Coast and southeastern coastlines, calling the rise "unprecedented in at least 120 years."

"It's a window into the future," said Dangendorf, who collaborated with experts at multiple U.S. institutions and Britain's National Oceanography Center. The rates are so high in recent years, Dangendorf said, that they're similar to what would be expected at the end of the century in a very high greenhouse gas emissions scenario.

An additional two studies on rapid sea-level rise and how it is affecting the region have been released by scientists in preprint form but have not yet passed through peer review, suggesting a swell of scientific attention on the subject.

The new findings are striking in part because the rapid rise appears to be caused by profound changes in the ocean. In parts of Texas and Louisiana, sinking land has long been a factor that contributes to sea levels growing relatively high over time. But in the latest studies, scientists show a rapid rise of sea levels in places such as Pensacola and Cedar Key Fla., where the land is not sinking as rapidly as it is in places such as Grand Isle, La., or Galveston, Tex.

In general, higher seas in the Gulf of Mexico and around Florida mean that hurricane risks in some of the most expos and storm-prone parts of the United States are growing only more acute.

In addition, as seas rise and people continue to move to high-risk areas along the coasts, scientists say that millions o acres of U.S. land and hundreds of thousands of homes and offices could slip below swelling tide lines. Experts from t nonprofit First Street Foundation also projected recently that properties in many coastal areas could lose value as flooding intensifies, a shift that could harm homeowners and erode local tax bases.

Scientists are not entirely on the same page about the causes driving the phenomenon, or whether the recent acceleration in rising seas will continue at such a rapid clip. Researchers typically prefer to rely on decades of data to more certain of trends in the climate system, and their causes. In that context, the recent sea-level rise has happened over a relatively short time period. That makes the trend as ambiguous as it is worrying.

Still, this much seems clear: The rapid sea-level rise appears to start in the Gulf of Mexico, which has been warming f faster than the global ocean. Warm water naturally expands, causing sea levels to rise. That warm water also gets carr by currents out of the gulf and along the East Coast, affecting places such as Georgia and the Carolinas.

Will this trend continue? That remains less clear, scientists say.

The waters that have helped drive up sea levels in Gulf of Mexico are very warm even at deep levels, based on a prepr study by Jacob Steinberg and colleagues at the Woods Hole Oceanographic Institution, NASA's Jet Propulsion Laboratory, the University of Hawaii at Manoa and the National Center for Atmospheric Research.

Steinberg and colleagues suggest that the trend implicates a warm current called the Loop Current, which enters the ; from the Caribbean Sea and in turn is part of a broader pattern of circulation in the Atlantic Ocean.

The warm Loop Current is "bringing water in, not just at the surface but with depth," Steinberg said. The current ofte extends hundreds of yards beneath the sea surface, Steinberg added, and will spin off warm water blobs, which scientists call "eddies," which move across the gulf.

Yin also ties the change to the Loop Current and in his study goes further, describing it as an aftereffect of a major slowdown event in the overall circulation of the Atlantic Ocean that occurred in 2009-2010. If true, this would sugges that these sea level changes may be tied to a broader pattern that reflects how climate change is altering the circulatic of the oceans.

Dangendorf, lead author of the Nature Communications study, isn't convinced. While noting the same rapid sea level rise in recent years as the other works, his study determines the cause is a combination of factors, some of them natur

"We have this forced acceleration, but then on top we have that natural variability, and over the last couple of years w were unlucky, having that acceleration superimposed on natural variability," Dangendorf said.

Nevertheless, Dangendorf said that the rapid sea-level changes are troubling, are having immediate effects, and are more like what scientists once would have expected only if the world kept pumping massive amounts of planet-heatin gases into the atmosphere.

He's not alone.

Data from NOAA show that "high tide flooding," even on sunny days, has more than doubled throughout the Gulf Coa and Southeast coastal regions since 2000.

"It messes up your daily life. It interrupts your daily life," said Thomas Wahl, a professor of coastal risks and engineering at the University of Central Florida, and a co-author of the paper in Nature Communications. "It corrodes infrastructure. It corrodes cars that are driving through saltwater on a daily basis. You can't open your business or get work."

Then there is the fact that in low-lying regions with little elevation, even small amounts of sea-level rise can make storms that much more calamitous. Waves push closer to shore, worsening erosion. Surges push farther inland. Wetlands can erode rapidly.
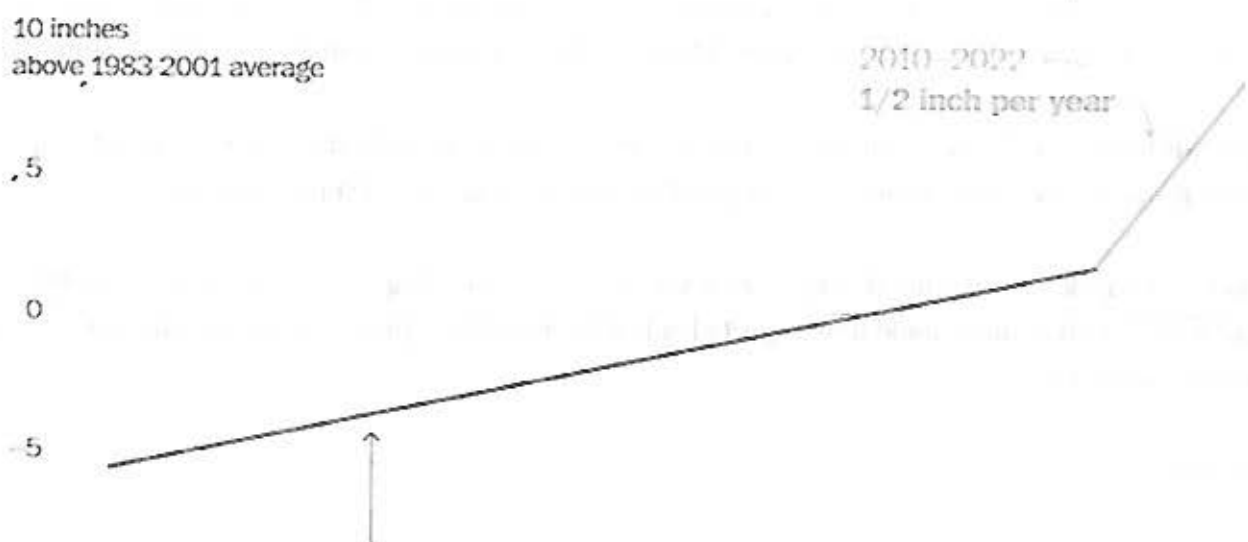
"Now you have a higher base water level," Wahl said. "If you have a hurricane now as opposed to the same hurricane 1 years ago, the impacts would be different."

A fourth study in preprint form, by scientists with the University of Miami, NOAA, NASA and multiple institutions in the United States and Australia, finds that the major rise in sea level in the Southeast since 2010 accounts for "30-50% of flood days in 2015-2020."

"In low-lying coastal regions, an increase of even a few centimeters in the background sea level can break the regional flooding thresholds and lead to coastal inundation," the study notes.

The critical question, of course, is whether the current rates of change documented by researchers will continue — leading, potentially, to well over a foot of additional sea-level rise in coming decades — or if they will return to levels more in line with global averages.

Rapid sea level rise at Pensacola, Fla.

10 inches
above 1983-2001 average

2010-2022
1/2 inch per year

.5

0

-5

−10

1923–2009
1/12 inch per year

−15

1925   1950·   1975   2000
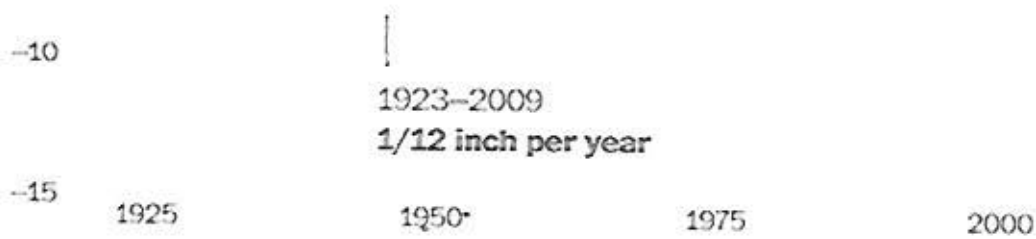
Source: NOAA

Based on sea-level records from Pensacola and Galveston, which date back a century or longer, the Gulf Coast also saw rapid rise in sea level in the 1940s, a trend that had subsided by the 1950s. But it is not yet clear if this event will prove similar.

Overall, the pace of sea-level rise is accelerating globally, and scientists have been unequivocal that seas will continue to rise well into the future, even if humans manage to drastically cut greenhouse gas emissions.

In a report last year, NOAA and other federal agencies found U.S. coastlines on average are projected to face an additional foot of rising seas over the next three decades. The report gave particularly high projections for the Gulf Coast, in significant part because of recent trends. Earlier this year, new research documented how the amount of excess heat buried in the planet's oceans, a strong marker of climate change, had again reached a record high in 2022.

In the same report, NOAA found that if sea-level rise along the eastern part of the Gulf Coast continues on its recent trajectory, it would rival a high-end sea level forecast for the year 2050. NASA recently released a sea-level tool that includes similar findings, showing seas rising at a rate that exceeds even the high-end forecasts at sites such as Pensacola, Fla., and Dauphin Island, Ala.

Despite the ongoing scientific debate regarding the cause of the current sea-level surge in the Gulf of Mexico and in the U.S. Southeast, the tangible effects it imposes on communities are likely to mount.

"It's very difficult for me to say what's going to happen in the near term," said Ben Hamlington, a NASA sea-level expert and a co-author on Steinberg's study. "It's not like these rates are immediately going to turn around."
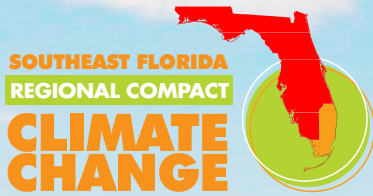
Unified Sea Level Rise Projection Southeast Florida

Prepared by the

**Southeast Florida Regional Climate Change Compact's
Sea Level Rise Ad Hoc Work Group**

Table of Contents

Recommended Citation

Southeast Florida Regional Climate Change Compact Sea Level Rise Work Group (Compact). February 2020. A document prepared for the Southeast Florida Regional Climate Change Compact Climate Leadership Committee. 36p.

Sea Level Rise Ad Hoc Work Group

The Southeast Florida Regional Climate Change Compact wishes to acknowledge the Work Group participants for contributing to the development of the projection and guidance document:

- Ricardo Domingues, University of Miami/National Oceanic and Atmospheric Administration*
- David Enfield, Ph.D., National Oceanic and Atmospheric Administration (retired)
- Nancy J. Gassman, Ph.D., City of Ft. Lauderdale
- Laura Geselbracht, The Nature Conservancy
- Katherine Hagemann, C.F.M., Miami-Dade County
- Jake Leech, Ph.D., Palm Beach County
- Jayantha Obeysekera, Ph.D., P.E., Florida International University (Chair)
- Akintunde Owosina, P.E., South Florida Water Management District
- Joseph Park, Ph.D., P.E., U.S. Department of Interior*
- Michael Sukop, Ph.D., PG, CHg, Florida International University
- Tiffany Troxler, Ph.D., Florida International University
- John Van Leer, Sc.D., University of Miami
- Shimon Wdowinski, Ph.D., Florida International University
- Staff Liaison: Samantha Danchuk, Ph.D., P.E., Broward County
- Compact Staff Support: Lauren Ordway, Institute for Sustainable Communities

* Staff participation from federal agencies does not necessarily imply official review or opinions of their agencies.

The Compact also wishes to express its appreciation to those whom provided technical guidance in the early phase of the process to support the recommendations of the Work Group:

- Andrea Dutton, Ph.D., University of Wisconsin
- John Hall, Ph.D., Bureau of Land Management
- Robert E. Kopp, Ph.D., Rutgers University
- Glenn Landers, P.E., U.S. Army Corps of Engineers*
- Mark Merrifield, Ph.D., Scripps Institution of Oceanography at the University of California San Diego
- Gary Mitchum, Ph.D., University of South Florida
- William Sweet, Ph.D., National Oceanic and Atmospheric Administration
- Philip R. Thompson, Ph.D., University of Hawaii
- Chris Weaver, Ph.D., Environmental Protection Agency

*Participants contributed information, engaged in group meetings and/or online discussions, and helped develop or review portions of the group report. Participation by these individuals does not necessarily imply personal or agency agreement with the complete findings and recommendations of this report.

Executive Summary

Early in the Southeast Florida Regional Climate Change Compact's ("the Compact") work together, Broward, Miami-Dade, Monroe, and Palm Beach counties recognized the need to unify a diversity of local sea level rise projections to create a single, regionally unified projection, ensuring consistency in adaptation planning and policy, and infrastructure siting and design in the Southeast Florida four-county region. The Compact published the first Regionally Unified Sea Level Rise Projection for Southeast Florida in 2011, and updated the projection in 2015. This document, the Compact's third Regionally Unified Sea Level Rise Projection, provides an update to the amount of anticipated sea level rise in Southeast Florida through 2120. These projections represent a consensus from a technical Work Group consisting of members from the academic community and federal agencies, with support from local government staff, and incorporates the most up-to-date, peer-reviewed literature, and climate modeling data. The Projection supports local government, regional entities, and other partners in understanding vulnerabilities associated with sea level rise and informs the development of science-based adaptation strategies, policies, and infrastructure design.

The 2019 Projection is based on projections of sea level rise developed by the Intergovernmental Panel on Climate Change (IPCC) Fifth Assessment Report (IPCC, 2014), as well as projections from the National Oceanic and Atmospheric Administration (NOAA) (Sweet et al., 2017), and accounts for regional effects, such as gravitational effects of ice melt, changes in ocean dynamics, vertical land movement, and thermal expansion from warming of the Florida Current that produce regional differences in Southeast Florida's rate of sea level rise compared to global projections.

Based on past and current emissions, all projection curves assume a growing greenhouse gas emission concentration scenario, in which emissions continue to increase until the end of the century, consistent with the IPCC Fifth Assessment Report's (AR5) Representative Concentration Pathways (RCP 8.5). Estimates of sea level rise are provided from a baseline year of 2000, and the planning horizon has been extended to 2120, in response to the release of climate scenarios extending beyond the year 2100 by federal agencies (NOAA and the U.S. Army Corps of Engineers) and the need for planning for infrastructure with design lives greater than 50 years.

In the short term, sea level rise is projected to be 10 to 17 inches by 2040 and 21 to 54 inches by 2070 (above the 2000 mean sea level in Key West, Florida). In the long term, sea level rise is projected to be 40 to 136 inches by 2120. Projected sea level rise, especially beyond 2070, has a significant range of variation as a result of uncertainty in future greenhouse gas emissions reduction efforts and resulting geophysical effects.

The 2019 Unified Sea Level Rise Projection includes three curves for application, in descending order, the NOAA High Curve, the NOAA Intermediate High Curve, and the curve corresponding to the median of the Intergovernmental Panel on Climate Change (IPCC) AR5 RCP 8.5 scenario. A fourth curve, the NOAA Extreme curve, is included for informational purposes, not for application, illustrating the possible upper limit of sea level rise in response to potential massive ice sheet collapse in the latter part of the century. This curve underscores that without imminent and substantial reductions in greenhouse gas emissions, much greater sea level rise is possible more than 100 years from now.

This guidance document describes the recommended application of the projection as it relates to both high- and low-risk projects and short- and long-term planning efforts. The Work Group recommends that this guidance be updated, at a minimum every five years to reflect the ongoing advances in scientific knowledge related to global climate change and potential impacts.

Introduction

IMPACTS ASSOCIATED WITH SEA LEVEL RISE FOR SOUTHEAST FLORIDA

The climate is changing, manifesting in significant impacts for the Southeast Florida region, including increasing average temperatures, more intense storm events, and rising sea levels. Sea level rise, caused by the thermal expansion of warming ocean water and melting land ice as the earth warms, is one of the most evident impacts in our region given Southeast Florida's low-lying elevation and porous geology.

The consequences associated with sea level rise are already apparent in Southeast Florida and pose an immediate and real threat to lives, livelihoods, economies, and the environment. Consequences include physical impacts such as coastal inundation and erosion, increased frequency of flooding in vulnerable coastal areas as well as inland areas due to impairment of the region's largely gravity-driven stormwater infrastructure system, reduced soil infiltration capacity, and saltwater intrusion of drinking-water supply. Moreover, the impacts of surge from tropical storms or hurricanes are exacerbated as a result of sea level rise. Increased pollution and contamination as a result of flooding degrades natural resources critical to the region's economy. Consequences also include cascading socio-economic impacts such as displacement, decrease in property values and tax base, increases in insurance costs, loss of services and impairment of infrastructure such as roads and septic systems. ***Appendix A: State of the Science***, describes the interconnected processes and resulting impacts of sea level rise in additional detail.

The extent of these impacts into the future is dependent upon the factors influencing the rate of sea level rise such as thermal expansion of oceans and increased rate of melting of land-based ice sheets due to global warming, the degree to which society limits greenhouse gas emissions in the near-term, and the decisions and investments made by communities to increase their climate resilience. One of the values of the Unified Sea Level Rise Projection is its application for scenario testing to better understand the potential impacts and timeline of sea level rise within the Southeast Florida community.

OBSERVED SEA LEVEL RISE IN SOUTHEAST FLORIDA

Global mean sea level (GMSL) during 2018 was the highest annual average in the satellite altimetry record (1993–2018), rising approximately 3 inches above the 1993 average (Thompson et al., 2019). Projections anticipate an increase in the acceleration of sea level rise regionally based on recent observations in response to changes in the speed and thermodynamics of the Florida Currents and Gulf Stream (Domingues et al., 2018; Sweet et al., 2017; Volkov et al., 2019). Based on the 5-year moving average, the observed sea level rise at the Key West tide gauge from 2000 to 2017 is 3.9 inches. Whether this rapid rise will be persistent into the future is unclear at this time.

HOW ARE GREENHOUSE GAS EMISSIONS AND SEA LEVEL RISE RELATED?

Since the beginning of the Industrial Revolution, human activities have caused significant increases in emissions of greenhouse gases in the atmosphere, such as carbon dioxide, methane, and nitrous oxides in addition to natural emissions of these gases due to the biome carbon and nitrogen cycles. Major sources of carbon dioxide are the burning of fossil fuels such as coal, petroleum-based liquid fuels, and natural gas for electric

power generation, transportation, and industrial processes. These greenhouse gases trap heat from the sun in a natural process called the "greenhouse effect," which would otherwise be radiated back to space. Problematically, as the concentrations of these gases accumulate in the earth's atmosphere as a result of human activities, the earth's average temperature continues to rise. This process is called "global warming."

More than 90% of the warming that has happened on Earth over the past 50 years has been transferred to the ocean. Sea level rise is a result of both the expansion of seawater as the ocean temperature increases, as well as the melting of glaciers and ice sheets. As a result of continuing global warming, the rate of sea level rise accelerates with passing time.

FUTURE PROJECTIONS IF EMISSIONS ARE REDUCED

The rate of sea level rise projected, particularly in the latter half of the century, is dependent upon the amount of greenhouse gas emissions generated in the next decade and sustained in the coming decades. Rapid and immediate global, federal, state, local, and individual action will be necessary to limit the amount of sea level rise adaptation required. The four greenhouse gas concentration scenarios, known as the Representative Concentration Pathways (RCPs) are sets of scenarios for greenhouse gas emissions dependent upon reduction commitments, economic activity, energy sources, population, and land use trajectories, and other socio-economic factors. RCPs are input into climate models which yield sea level rise scenarios. The lowest concentration scenario, RCP 2.6, is viewed as the scenario necessary to keep global temperature increases below 2°C and slow the rate of sea level rise (van Vuuren et al 2011a). This scenario would require that greenhouse gas emissions peak around 2020 and decrease at 4% annually (van Vuuren et al., 2011a). Future global mean sea level would be significantly lower for RCP 2.6 compared to that of RCP 8.5 (IPCC, 2019). The types of reduction strategies necessary to reduce regional emissions can be found in the Compact's Regional Climate Action Plan (www.rcap2.org).

WHAT ARE RCPS?

The future impacts of climate depend not only on the response of our Earth system, but also on how global society responds through changes in technology, economy, policy, and lifestyle. These responses are uncertain, so future scenarios are used to explore the consequences of different options. Representative Concentration Pathways (RCPs) are possible future scenarios for greenhouse gas emissions, or concentration pathways, used within the IPCC AR5 and other complex climate modeling activities that simulate how the climate might change in the future. There are generally four of these scenarios used in climate modeling: RCP 8.5, RCP 6, RCP 4.5, and RCP 2.6. The numbers in each RCP refers to the amount of radiative forcing produced by greenhouse gases in 2100, which is a measure of the energy absorbed and retained by the lower atmosphere. For example, in RCP 8.5 the radiative forcing is 8.5 watts per meter squared (W/m^2) in 2100.

RCPs start with atmospheric concentrations of greenhouse gases rather than socioeconomic processes (van Vuuren et al., 2011b). This is important because every modelling step from a socioeconomic scenario to climate change impacts adds uncertainty. That said, these concentration pathways are dependent upon reduction commitments, economic activity, energy sources, population, land use trajectories, and other socio-economic factors that could lead to a particular concentration pathway and magnitude of climate change.

SCENARIO COMPONENT	RCP 2.6	RCP 4.5	RCP 6	RCP 8.5
Greenhouse gas emissions	Very low	Medium-low mitigation Very low baseline	Medium baseline; high mitigation	High baseline
Agricultural area	Medium for cropland and pasture	Very low for both cropland and pasture	Medium for cropland but very low for pasture (total low)	Medium for both cropland and pasture
Air pollution	Medium-Low	Medium	Medium	Medium-high

Main characteristics of each Representative Concentration Pathway (RCP). *Vuuren et.al., 2011*

RCP PRIMARY CHARACTERISTICS

>> RCP 2.6 is representative of scenarios in the literature that lead to very low greenhouse gas concentration levels. It is a "peak-and-decline" scenario; its radiative forcing level first reaches a value of around 3.1 W/m^2 by mid-century, and returns to 2.6 W/m^2 by 2100. In order to reach such radiative forcing levels, greenhouse gas emissions (and indirectly emissions of air pollutants) are reduced substantially, over time (Van Vuuren et al. 2007a).

>> RCP 4.5 is a stabilization scenario in which total radiative forcing is stabilized shortly after 2100, without overshooting the long-run radiative forcing target level (Clarke et al. 2007; Smith and Wigley 2006; Wise et al. 2009).

>> RCP 6 is a stabilization scenario in which total radiative forcing is stabilized shortly after 2100, without overshoot, by the application of a range of technologies and strategies for reducing greenhouse gas emissions (Fujino et al. 2006; Hijioka et al. 2008).

>> RCP 8.5 is characterized by increasing greenhouse gas emissions over time, representative of scenarios in the literature that lead to high greenhouse gas concentration levels (Riahi et al. 2007).

(Characteristics quoted from van Vuuren et.al., 2011)

Purpose and Intended Use

WHO SHOULD USE THIS PROJECTION AND GUIDANCE DOCUMENT?

The Unified Sea Level Rise Projection for Southeast Florida and this guidance document are intended to assist decision-makers at both the local and regional levels in Southeast Florida to plan for and make decisions about sea level rise and associated vulnerabilities based on best-available science. The projection (Unified Sea Level Rise Projection for Southeast Florida) contains a graph and table describing the anticipated rise in sea level from 2000 through 2120. The projection can be used to estimate future potential sea level elevations in Southeast Florida and the relative change in sea level from today to a point in the future. The section, *Guidance for Application*, contains directions and specific examples of how the projection can be used by local governments, planners, designers, engineers, and developers. This regional projection is offered to ensure that all major infrastructure projects throughout the Southeast Florida region have the same basis for design and construction relative to future sea level.

WHO DEVELOPED THE UNIFIED SEA LEVEL RISE PROJECTION FOR SOUTHEAST FLORIDA?

In 2010, the Southeast Florida Regional Climate Change Compact first convened the Sea Level Rise Ad Hoc Work Group (Work Group) for the purpose of developing a Unified Sea Level Rise Projection for the region. The Work Group reviewed existing projections and scientific literature and developed a unified regional projection for the period from 2010 to 2060 (Compact, 2012), and recommended a review of the projection four years after its release in 2011.

In September 2014, the Sea Level Rise Work Group was reconvened to develop the second update of the Unified Sea Level Rise Projection, based on projections and scientific literature released since 2011, which was published by the Compact in October 2015 (Compact, 2015).

Based on guidance from the Work Group, and in response to emergent research since the publication of the 2015 report, the Compact reconvened the Work Group in 2019 to produce the third update. In particular, new research has indicated the potential for faster rates of melting of the Antarctic Ice Sheet, triggering the likelihood of higher rates of rise in the future. In addition, the Work Group opted to include the regional sea level rise rates as reported in the Fourth National Climate Assessment (Sweet et al., 2017).

The Ad Hoc Sea Level Rise Work Group consists of experts within the academic community and federal agencies, and is supported by individuals from local government and staff support to the Compact. Most of the 2019 Work Group members contributed to the previous Compact projections.

FREQUENCY OF FUTURE UPDATES

The Southeast Florida Regional Climate Change Compact is committed to updating the Unified Sea Level Rise Projection periodically, and at a minimum every five years, to incorporate the latest scientific understanding of climate change and sea level rise for Southeast Florida. Scientific understanding of sea level rise is rapidly advancing, generating new, peer-reviewed literature and modeling from a variety of key sources, including the Intergovernmental Panel on Climate Change (IPCC), the National Oceanic and Atmospheric Administration (NOAA), and the U.S. Army Corps of Engineers (USACE), among other recognized sources. By updating this document and the Unified Sea Level Rise Projection at least every five years, the Compact seeks to provide ongoing and current guidance for regionally consistent sea level rise planning and decision-making.

Unified Sea Level Rise Projection for Southeast Florida

2019 PROJECTION AND SUMMARY

This Unified Sea Level Rise Projection for Southeast Florida updated in 2019 projects the anticipated range of sea level rise for the region from 2000 to 2120 (Figure 1). The projection highlights three planning horizons:

1. **short term:** by 2040, sea level is projected to rise 10 to 17 inches above 2000 mean sea level.
2. **medium term:** by 2070, sea level is projected to rise 21 to 54 inches above 2000 mean sea level.
3. **long term:** by 2120, sea level is projected to rise 40 to 136 inches above 2000 mean sea level.

Details of the projection development methodology appear in the next section.

The Projection is recommended to be applied in the following manner:

- The blue shaded zone between the IPCC median curve and the NOAA Intermediate-High curve is recommended to be generally applied to most projects within a short-term planning horizon (up to 2070). The IPCC median curve represents the most likely average sea level before 2070, but is not representative of the realistic interannual and interdecadal variations that will occur with sea level rise values within the blue shaded zone. The IPCC median curve can be used for non-critical, low risk projects with short design lives (<50 years) that are adaptable, and have limited interdependencies with other infrastructure or services. All other projects with design lives that end before 2070 should consider values within the blue zone or along the NOAA Intermediate-High curve based on risk tolerance.

- For non-critical infrastructure in service during or after 2070, the NOAA Intermediate-High Curve is recommended. Sea level rise is unlikely to exceed the NOAA Intermediate-High Curve by 2100.

- The NOAA High curve of the projection, above the shaded zone, should be utilized for planning of critical, high risk projects in service after 2070 or for projects which are not easily replaceable or removable or are critically interdependent with other infrastructure or services. Examples are: major roads and bridges, water and wastewater utilities, power plants including nuclear, major urban developments, etc. Sea level rise is very unlikely to be higher than the NOAA High curve before 2100.

- The NOAA Extreme curve is displayed on the Unified Sea Level Rise Projection for informational purposes but is not recommended for design.

TABLE 1: Sea Level Rise Projection data by decadal intervals

DATUM: FEET 2000 MSL				DATUM: FEET NAVD			
YEAR	IPCC MED 50%	NOAA2017 INT-HIGH	NOAA2017 HIGH	YEAR	IPCC MED 50%	NOAA2017 INT-HIGH	NOAA2017 HIGH
2000	0.00	0	0	2000	-0.80	-0.78	-0.78
2010	0.19	0.3	0.33	2010	-0.61	-0.49	-0.45
2020	0.39	0.56	0.69	2020	-0.42	-0.22	-0.09
2030	0.63	0.98	1.18	2030	-0.17	0.2	0.4
2040	0.84	1.38	1.74	2040	0.04	0.6	0.96
2050	1.13	1.94	2.46	2050	0.33	1.15	1.68
2060	1.40	2.56	3.38	2060	0.60	1.78	2.6
2070	1.72	3.31	4.49	2070	0.91	2.53	3.71
2080	2.03	4.17	5.74	2080	1.23	3.38	4.96
2090	2.40	5.12	7.09	2090	1.59	4.34	6.3
2100	2.72	6.14	8.56	2100	1.92	5.35	7.78
2120	3.29	7.64	11.32	2120	2.49	6.86	10.54
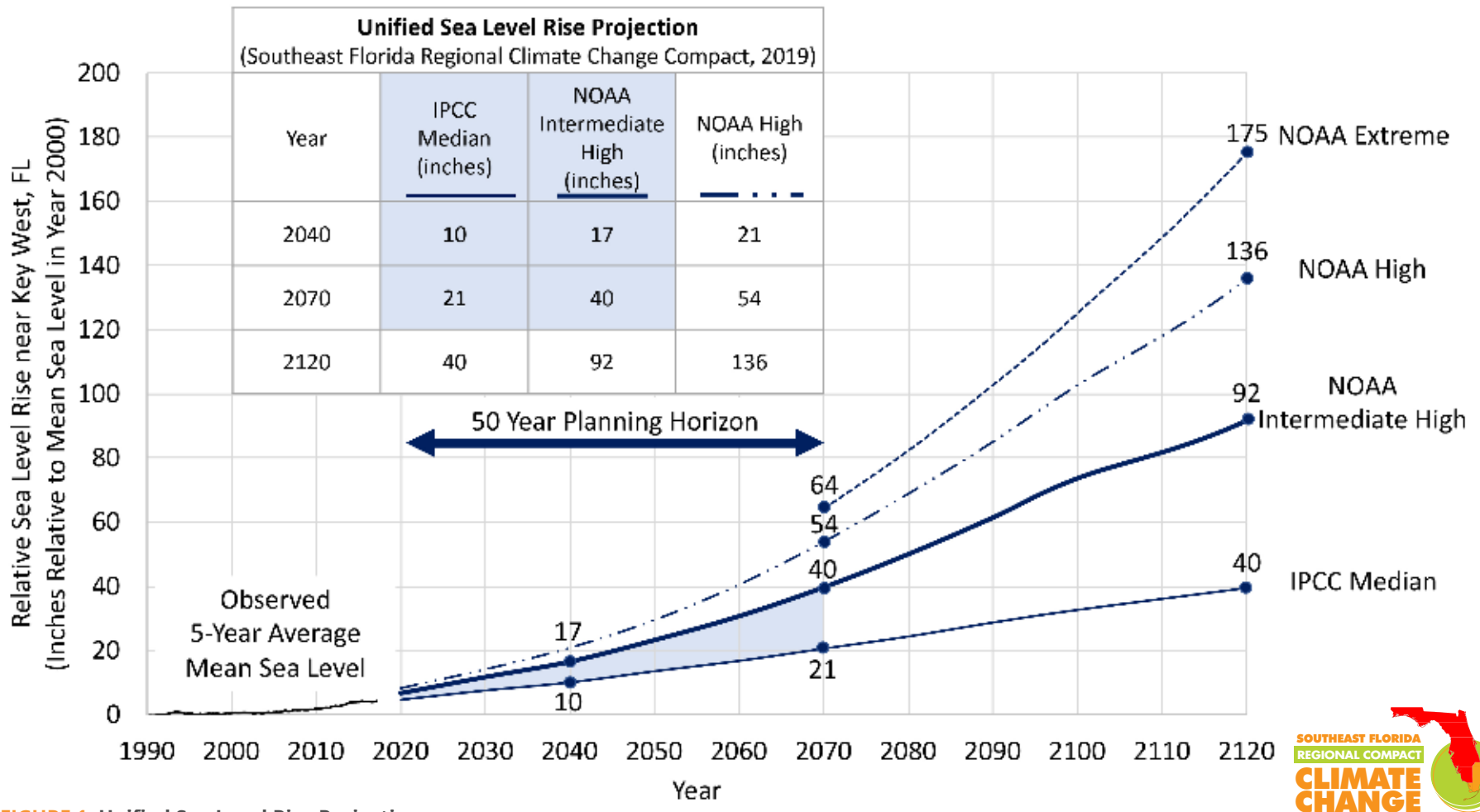
FIGURE 1: Unified Sea Level Rise Projection

These projections start from zero in year 2000 and are referenced to mean sea level at the Key West tide gauge. Based on the 5-year average of mean sea level, approximately 3.9 inches of sea level rise has occurred from 2000 to 2017 (see historic sea level section of guidance document). The projection includes global curves adapted for regional application: the median of the IPCC AR5 RCP 8.5 scenario (Growing Emissions Scenario) as the lowest boundary (solid thin curve), the NOAA Intermediate High curve as the upper boundary for short-term use until 2070 (solid thick line), the NOAA High curve as the upper boundary for medium and long-term use (dash dot curve). The shaded zone between the IPCC AR5 RCP 8.5 median curve and the NOAA Intermediate High is recommended to be generally applied to most projects within a short-term planning horizon. Beyond 2070, the adaptability, interdependencies, and costs of the infrastructure should be weighed to select a projection value between the IPCC Median and the NOAA High curves. The NOAA Extreme curve (dash curve) brackets the published upper range of possible sea level rise under an accelerated ice melt scenario. Emissions reductions could reduce the rate of sea level rise significantly.

Projection Development Methodology

PROJECTION UPDATE

The key components of the methodology used to develop the Unified Sea Level Rise Projection are as follows:

Starting in 2000: The year 2000 has been selected as the initial year of the projection because of its use as the reference year for the latest regional sea level projections published by NOAA (Sweet et al., 2017), which is the primary source of the data used in this report. The previous projection started in 1992, based on the midpoint of the tidal epoch from 1983 to 2001 which defined the previous elevation of mean sea level. Defining mean sea level by a timeframe is necessary because sea level is constantly changing. A fixed elevation is necessary to serve as a baseline for which to add sea level rise projections and to convert to elevations in other datums. NOAA has determined a new mean sea level for 2000, the midpoint of the tidal epoch from 1991 to 2009. A comparison of the 2015 and 2019 Unified Sea Level Rise Projection is presented in the next section.

Updated Planning Horizons: To align with a 20-year planning horizon for land use and a 50-year planning horizon for infrastructure, the sea level rise values displayed were moved to 2040 and 2070, respectively.

Planning Horizon of 2120: In response to the release of climate scenarios extending beyond 2100 by federal agencies including the US Army Corps of Engineers (USACE) and the National Oceanographic and Atmospheric Administration (NOAA) and the need for planning for infrastructure with design lives greater than 50 years, the Unified Sea Level Rise Projection time scale has been extended to 2120.

Tide Gauge Selection: The Key West gauge (NOAA Station ID 8724580) was maintained as the reference gauge for calculation of the regional projection, consistent with all previous projections. In addition, appropriate conversion calculations are provided in Section 4: Guidance for Application, in order to reference the projection to the Miami Beach gauge (NOAA Station ID 8723170), the South Port Everglades gauge (NOAA Station ID 8722956) or the Lake Worth Pier gauge (NOAA Station ID 8722670). The Key West gauge has recorded tidal elevations since 1913. Tidal records from Miami Beach, South Port Everglades and Lake Worth Pier are available since 2003, 2018 and 1996, respectively.

Updated Historic Data: Observed data from the Key West tide gauge was plotted from 1992 to 2017 based on the mean sea level, averaged over 5-year intervals. These data were obtained from the USACE Sea Level Tracker, https://climate.sec.usace.army.mil/slr_app/.

Selection of NOAA (2017) Regional Projections and Update of IPCC Median Curve: The regional sea level projections available from NOAA (Sweet et al., 2017) replaced two of the three previously used curves. The selected curves are regional projections rather than previously used global projections. The NOAA Intermediate High regional projection was selected as the upper short term boundary for typical infrastructure because of its IPCC determination to be very likely under the RCP 8.5 emissions pathway, which aligns with current global emissions trends. The NOAA Intermediate High regional projection also approximates the previously used USACE High curve. The NOAA High curve was updated with its regional projection. The third curve, the IPCC Median, was reprojected for the region (Key West) rather than global scale, using the NOAA (Sweet et al., 2017) methodology.

Reference to NOAA Extreme Curve: The NOAA Extreme curve is displayed on the Unified Sea Level Rise Projection for informational purposes but is not recommended for design.

COMPARISON WITH PREVIOUS PROJECTIONS

Table 2 compares values from the 2015 and 2019 Unified Sea Level Rise Projections at the planning horizons referenced in the 2015 projection. The numeric values have been rounded for simplicity. The difference in the reference elevation for the two projections is less than 1 inch (1992 mean sea level compared to 2000 mean sea level) and was considered to be included in the rounding error to allow this comparison. The lowest curve, the IPCC median, increased by 2 to 3 inches in the 2019 projection. The upper boundary of the short term projection increased by 2 to 5 inches (for planning horizons before 2060). The NOAA High curve used for critical infrastructure or planning horizons after 2060 increased 7 to 22 inches, the most significant change between projections.

TABLE 2: **Comparison of Unified Projection in 2015 and 2019 at Key West**

UNIFIED SEA LEVEL RISE PROJECTION COMPARISON						
Year	**High Adaptability**	←	→		**Low Adaptability**	
	2015	**2019**	**2015**	**2019**	**2015**	**2019**
	IPCC Median Global (inches)	IPCC Median Regional (inches)	USACE High (inches)	NOAA Inermediate High (inches)	NOAA High (inches)	NOAA High (inches)
2030	6	8	10	12	12	14
2060	14	17	26	31	34	41
2100	31	33	61	74	81	103

Note: The NOAA Extreme curve values are not included in the table because there was not a comparable curve in the 2015 projection.

Guidance for Application

GUIDANCE IN APPLYING THE PROJECTIONS

Audiences

The Unified Sea Level Rise Projection for Southeast Florida is intended to be used for planning purposes by a variety of audiences and disciplines when considering sea level rise in reference to both short- and long-term planning horizons as well as infrastructure siting and design in the Southeast Florida area. Potential audiences for the projections include, but are not limited to, elected officials, urban planners, architects, engineers, developers, resource managers, and public works professionals.

One of the key values of the projection is the ability to associate specific sea level rise scenarios with timelines. When used in conjunction with vulnerability assessments, these projections inform the user of the potential magnitude and extent of sea level rise impact at a general timeframe in the future. The blue shaded portion of the projection provides a likely range for sea level rise values at specific planning horizons. Providing a range instead of a single value may present a challenge to users such as engineers who are looking to provide a design with precise specifications. Public works professionals and urban planners need to work with the engineers and with policymakers to apply the projection to each project based on the nature, value, interconnectedness, and life cycle of the infrastructure proposed.

Finally, elected officials should use the projections to inform decision-making regarding adaptation policies, budget impacts associated with design features that address future sea level rise, capital improvement projects associated with drainage and shoreline protection, and land use decisions.

Applying Projection Curves to Infrastructure Siting And Design

When determining how to apply the projection curves, the user needs to consider the nature, value, interconnectedness, and lifespan of the existing or proposed infrastructure. An understanding of the risks that critical infrastructure will be exposed to throughout its life cycle such as sea level rise inundation, storm surge, and nuisance flooding and a plan for adaptation must be established early in the conceptual phase. A determination must be made on whether or not threats can be addressed mid-life cycle via incremental adaptation measures, such as raising the height of a sluice gate on a drainage canal. If incremental adaptation is not possible for the infrastructure proposed and inundation is likely, designing to accommodate the projected sea level rise at conception or selection of an alternate site should be considered. Forward thinking risk management is critical to avoiding loss of service, loss of asset value, and most importantly loss of life or irrecoverable resources. The guidance in the following paragraphs can be considered for selection of curves from the projection for project applications.

>> Application of the IPCC Median Curve

The IPCC Median or lower blue shaded portion of the projection can be applied to most infrastructure projects before 2070 or projects whose failure would result in limited consequences to others. An example low risk projects may be a small culvert in an isolated area. The designer of a type of infrastructure that is easily replaced, has a short lifespan, is adaptable, and has limited interdependencies with other infrastructure or services must weigh the potential benefit of designing for higher sea level rise with the additional costs. Should the designer opt for specifying the lower curve, she/he must consider the consequences of under-designing for the potential likely sea level condition. Such consequences may include premature infrastructure failure.

>> Application of the NOAA Intermediate High Curve

Projects in need of a greater factor of safety related to potential inundation should consider designing for the NOAA Intermediate High Curve. Examples of such projects may include evacuation routes planned for reconstruction, communications and energy infrastructure, and critical government and financial facilities or infrastructure that may stay in place beyond a design life of 50 years.

>> Application of the NOAA High Curve

Due to the community's fundamental reliance on major infrastructure, existing and proposed critical infrastructure should be evaluated using the NOAA High curve. Critical projects include those projects which are not easily replaceable or removable, have a long design life (more than 50 years), and are interdependent with other infrastructure or services. If failure of the critical infrastructure would have catastrophic impacts, it is considered to be high risk. Due to the community's critical reliance on major infrastructure, existing and proposed high risk infrastructure should be evaluated using the NOAA High curve. Examples of high risk critical infrastructure include nuclear power plants, wastewater treatment facilities, levees or impoundments, bridges along major evacuation routes, airports, seaports, railroads, and major highways.

Projection Referenced to the North American Vertical Datum

The Unified Sea Level Rise Projection referenced to the North American Vertical Datum (NAVD) is shown in Figure 2 and summarized in Table 3. Each NOAA tide gauge in the region has published datums that can be used for conversions between elevations (https://tidesandcurrents.noaa.gov/datums.html?id=8724580).

FIGURE 2: Unified Sea Level Rise Referenced to NAVD
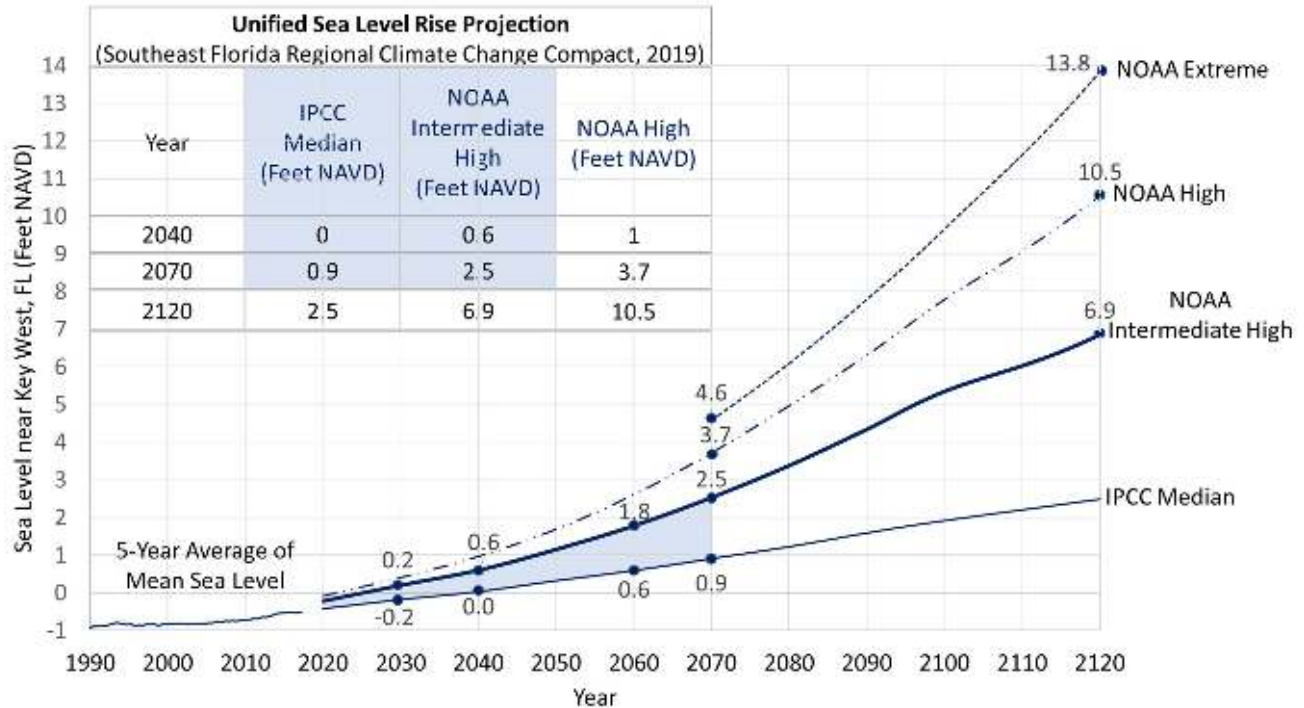
TABLE 3: Unified Sea Level Rise Projection Referenced to NAVD

UNIFIED SEA LEVEL RISE PROJECTION (Southeast Florida Regional Climate Change Compact, 2019)		
Year	IPCC Median (Feet NAVD)	NOAA Intermediate High (Feet NAVD)	NOAA High (Feet NAVD)
2040	0	0.6	1
2070	0.9	2.5	3.7
2120	2.5	6.9	10.5

Referencing to Today's Sea Levels

Based on the 5-year average of mean sea level at Key West, sea level rose approximately 3.9 inches from 2000 to 2017 (NOAA, 2020). This value of 3.9 inches can be subtracted from the rise projected in Table 1 to obtain an estimate of how much sea level will rise from the 2017 mean sea level. Note the availability of computed values for the 5-year average of mean sea level will always be delayed as a function of needing to have 2.5 years data past the date in order to compute the average.

To compute the rise expected from any future date relative to the existing sea level, the linear trend should be computed and its slope should be multiplied by the number of years that have passed since 2000. Based on a linear trend analysis of the historic record at Key West, sea level has risen at a rate of approximately 0.1 inches

per year. Note this linear trend will change as more data are collected by the tide gauge. Also, when the slope of the linear trendline changes, the computed amount of rise will change. Care should be taken to consider the computation methodology before comparing statements of relative sea level rise for a distinct time period.

TOOLS AVAILABLE TO VISUALIZE SEA LEVEL RISE

The observed data and NOAA curves included in the projection can be reproduced using the USACE Sea Level Rise calculator http://corpsmapu.usace.army.mil/rccinfo/slc/slcc_calc.html and USACE Sea Level Tracker https://climate.sec.usace.army.mil/slr_app/. Inundation from sea level rise can be visualized by using the Florida Sea Level Sketch Planning Tool https://sls.geoplan.ufl.edu/beta/viewer/.

Summary

The Work Group recommends the use of the NOAA High curve, the NOAA Intermediate High curve, and the median of the IPCC AR5 RCP 8.5 scenario (IPCC, 2013) as the basis for a Southeast Florida sea level rise projection for the 2040, 2070 and 2120 planning horizons. In the short term, mean sea level rise is projected to be 10 to 17 inches by 2040, and 21 to 54 inches by 2070 (above the 2000 mean sea level).

Both mean and annual average of sea level exhibit significant variability over time and that should be considered when using the projections. Annual average of sea level at the Key West gauge has risen approximately 3.9 inches from 2000 to 2017 (which is much larger than the linear trend-derived rate of rise reported by NOAA). Whether this rapid rise will be persistent into the future is unclear at this time.

In the long term, sea level rise is projected to be 40 to 136 inches by 2120. The IPCC Median or lower blue shaded portion of the projection can be applied to most infrastructure projects before 2070 or projects whose failure would result in limited consequences to others. Projects in need of a greater factor of safety related to potential inundation should consider designing for the NOAA Intermediate High Curve. For critical infrastructure projects with design lives in excess of 50 years, use of the NOAA High curve is recommended with planning values of 54 inches in 2070 and 136 inches in 2120. Sea level will continue to rise even if global mitigation efforts to reduce greenhouse gas emissions are successful at stabilizing or reducing atmospheric CO_2 concentrations; however, emissions mitigation is essential to moderate the severity of potential impacts in the future. A substantial increase in sea level rise within this century is likely and may occur in rapid pulses rather than gradually.

The recommended projection provides guidance for the Compact Counties and their partners to initiate planning to address the potential impacts of sea level rise in the region. The shorter-term planning horizons (through 2070) are critical to implementation of the Southeast Florida Regional Climate Change Action Plan, to optimize the remaining economic life of existing infrastructure, and to begin to consider adaptation strategies. As scientists develop a better understanding of the factors and reinforcing feedback mechanisms impacting sea level rise, the Southeast Florida community will need to adjust the projections accordingly and adapt to the changing conditions. To ensure public safety and economic viability in the long run, strategic policy decisions will be needed to develop guidelines to direct future public and private investments to areas less vulnerable to future sea level rise impacts.

Literature Cited

Arns, A., Wahl, T., Dangendorf, S., & Jensen, J. (2015). The impact of sea level rise on storm surge water levels in the northern part of the German Bight. *Coastal Engineering, 96*, 118–131. doi: 10.1016/j.coastaleng.2014.12.002

Chen, C., Liu, W., & Wang, G. (2019). Understanding the Uncertainty in the 21st Century Dynamic Sea Level Projections: The Role of the AMOC. *Geophysical Research Letters, 46*(1), 210–217. doi: 10.1029/2018gl080676

Chen, X., Zhang, X., Church, J. A., Watson, C. S., King, M. A., Monselesan, D., ... Harig, C. (2017). The increasing rate of global mean sea-level rise during 1993–2014. *Nature Climate Change, 7*(7), 492–495. doi: 10.1038/nclimate3325

Church, J. A., & White, N. J. (2011). Sea-Level Rise from the Late 19th to the Early 21st Century. *Surveys in Geophysics, 32*(4-5), 585–602. doi: 10.1007/s10712-011-9119-1

Southeast Florida Regional Climate Change Compact Technical Ad hoc Work Group (Compact). 2011. A Unified Sea Level Rise Projection for Southeast Florida. A document prepared for the Southeast Florida Regional Climate Change Compact Steering Committee. 27 p. Retrieved from: https://southeastfloridaclimatecompact.org//wp-content/uploads/2014/09/sea-level-rise.pdf

Southeast Florida Regional Climate Change Compact (Compact). 2012. Analysis of the Vulnerability of Southeast Florida to Sea Level Rise. 181 p. Retrieved from: http://www.southeastfloridaclimatecompact.org//wp-content/uploads/2014/09/vulnerability-assessment.pdf

Southeast Florida Regional Climate Change Compact Technical Ad hoc Work Group (Compact). 2015. A Unified Sea Level Rise Projection for Southeast Florida. A document prepared for the Southeast Florida Regional Climate Change Compact Steering Committee. 35 p. Retrieved from: https://southeastfloridaclimatecompact.org/wp-content/uploads/2015/10/2015-Compact-Unified-Sea-Level-Rise-Projection.pdf

Dangendorf, S., Marcos, M., Wöppelmann, G., Conrad, C., Frederikse, T., Riva, R. 2017. Reassessment of 20th century global mean sea level rise. PNAS June 6, 2017 114 (23) 5946-5951.

Decker, J. D., Hughes, J. D., & Swain, E. D. (2019). Potential for increased inundation in flood-prone regions of southeast Florida in response to climate and sea-level changes in Broward County, Florida, 2060–69. *Scientific Investigations Report*. doi: 10.3133/sir20185125

Domingues, R., Goni, G., Baringer, M., & Volkov, D. (2018). What Caused the Accelerated Sea Level Changes Along the U.S. East Coast During 2010–2015? *Geophysical Research Letters, 45*(24). doi: 10.1029/2018gl081183

Ezer, T., Atkinson, L. P., Corlett, W. B., & Blanco, J. L. (2013). Gulf Streams induced sea level rise and variability along the U.S. mid-Atlantic coast. *Journal of Geophysical Research: Oceans, 118*(2), 685–697. doi: 10.1002/jgrc.20091

Ezer, T., & Atkinson, L. P. (2014). Accelerated flooding along the U.S. East Coast: On the impact of sea-level rise, tides, storms, the Gulf Stream, and the North Atlantic Oscillations. *Earths Future, 2*(8), 362–382. doi: 10.1002/2014ef000252

Ezer, T., & Atkinson, L. P. (2017). On the predictability of high water level along the US East Coast: can the Florida Current measurement be an indicator for flooding caused by remote forcing? *Ocean Dynamics*, 67(6), 751–766. doi: 10.1007/s10236-017-1057-0

Ezer, T., Atkinson, L. P., & Tuleya, R. (2017). Observations and operational model simulations reveal the impact of Hurricane Matthew (2016) on the Gulf Stream and coastal sea level. *Dynamics of Atmospheres and Oceans, 80*, 124–138. doi: 10.1016/j.dynatmoce.2017.10.006

Florida Oceans and Coastal Council. 2010. Climate Change and Sea-Level Rise in Florida: An Update of "The Effects of Climate Change on Florida's Ocean and Coastal Resources." [2009 Report] Tallahassee, Florida. vi + 26 p. www.floridaoceanscouncil.org.

Glick, P. (2006). *An unfavorable tide: global warming, coastal habitats and sportfishing in Florida*. Washington, DC: National Wildlife Federation.

Gornitz, V., M. Oppenheimer, R. Kopp, P. Orton, M. Buchanan, N. Lin, R. Horton, & D. Bader. (2019). New York City Panel on Climate Change 2019 Report Chapter 3: Sea level rise. Ann. New York Acad. Sci., 1439, 71-94. doi:10.1111/nyas.14006

Hall, J.A., S. Gill, J. Obeysekera, W. Sweet, K. Knuuti, & J. Marburger. (2016). Regional Sea Level Scenarios for Coastal Risk Management: Managing the Uncertainty of Future Sea Level Change and Extreme Water Levels for Department of Defense Coastal Sites Worldwide. U.S. Department of Defense, Strategic Environmental Research and Development Program. 224 pp.

Hansen, J., Sato, M., Hearty, P., Ruedy, R., Kelley, M., Masson-Delmotte, V., … Lo, K.-W. (2015). Ice melt, sea level rise and superstorms: evidence from paleoclimate data, climate modeling, and modern observations that 2 °C global warming is highly dangerous. *Atmospheric Chemistry and Physics Discussions, 15*(14), 20059–20179. doi: 10.5194/acpd-15-20059-2015

Hay, C., Mitrovica, J. X., Gomez, N., Creveling, J. R., Austermann, J., & Kopp, R. E. (2014). The sea-level fingerprints of ice-sheet collapse during interglacial periods. Quaternary Science Reviews, 87, 60–69. doi: 10.1016/j.quascirev.2013.12.022

IMBIE Team. 2019. Mass balance of the Greenland Ice Sheet from 1992 to 2018. Nature. doi: 10.1038/s41586-019-1855-2.

IPCC, 2013: *Climate Change 2013: The Physical Science Basis. Contribution of Working Group I to the Fifth Assessment Report of the Intergovernmental Panel on Climate Change* [Stocker, T.F., D. Qin, G.-K. Plattner, M. Tignor, S.K. Allen, J. Boschung, A. Nauels, Y. Xia, V. Bex and P.M. Midgley (eds.)]. Cambridge University Press, Cambridge, United Kingdom and New York, NY, USA, 1535 pp.

IPCC, 2014: *Climate Change 2014: Impacts, Adaptation, and Vulnerability. Part A: Global and Sectoral Aspects. Contribution of Working Group II to the Fifth Assessment Report of the Intergovernmental Panel on Climate Change* [Field, C.B., V.R. Barros, D.J. Dokken, K.J. Mach, M.D. Mastrandrea, T.E. Bilir, M. Chatterjee, K.L. Ebi, Y.O. Estrada, R.C. Genova, B. Girma, E.S. Kissel, A.N. Levy, S. MacCracken, P.R. Mastrandrea, and L.L. White (eds.)]. Cambridge University Press, Cambridge, United Kingdom and New York, NY, USA, 1132 pp.

IPCC, 2014: *Climate Change 2014: Synthesis Report. Contribution of Working Groups I, II and III to the Fifth Assessment Report of the Intergovernmental Panel on Climate Change* [Core Writing Team, R.K. Pachauri and L.A. Meyer (eds.)]. IPCC, Geneva, Switzerland, 151 pp.

IPCC, 2018: *Summary for Policymakers. In: Global Warming of 1.5°C. An IPCC Special Report on the impacts of global warming of 1.5°C above pre-industrial levels and related global greenhouse gas emission pathways, in the context of strengthening the global response to the threat of climate change, sustainable development, and efforts to eradicate poverty* [Masson-Delmotte, V., P. Zhai, H.-O. Pörtner, D. Roberts, J. Skea, P.R. Shukla, A. Pirani, W. Moufouma-Okia, C. Péan, R. Pidcock, S. Connors, J.B.R. Matthews, Y. Chen, X. Zhou, M.I. Gomis, E. Lonnoy, T. Maycock, M. Tignor, and T. Waterfield (eds.)]. World Meteorological Organization, Geneva, Switzerland, 32 pp.

IPCC, 2019: Summary for Policymakers. In: *IPCC Special Report on the Ocean and Cryosphere in a Changing Climate* [H.-O. Pörtner, D.C. Roberts, V. Masson-Delmotte, P. Zhai, M. Tignor, E. Poloczanska, K. Mintenbeck, A. Alegría, M. Nicolai, A. Okem, J. Petzold, B. Rama, N.M. Weyer (eds.)]. In press.

Kirshen, P., Knee, K., & Ruth, M. (2008). Climate change and coastal flooding in Metro Boston: impacts and adaptation strategies. *Climatic Change*, 90(4), 453–473. doi: 10.1007/s10584-008-9398-9

Kleinosky, L. R., Yarnal, B., & Fisher, A. (2006). Vulnerability of Hampton Roads, Virginia to Storm-Surge Flooding and Sea-Level Rise. *Natural Hazards*, 40(1), 43–70. doi: 10.1007/s11069-006-0004-z

Knutson, T. R., Sirutis, J. J., Zhao, M., Tuleya, R. E., Bender, M., Vecchi, G. A., … Chavas, D. (2015). Global Projections of Intense Tropical Cyclone Activity for the Late Twenty-First Century from Dynamical Downscaling of CMIP5/RCP4.5 Scenarios. *Journal of Climate*, 28(18), 7203–7224. doi: 10.1175/jcli-d-15-0129.1

Kopp, R. E., Horton, R. M., Little, C. M., Mitrovica, J. X., Oppenheimer, M., Rasmussen, D. J., ... Tebaldi, C. (2014). Probabilistic 21st and 22nd century sea-level projections at a global network of tide-gauge sites. *Earths Future*, 2(8), 383–406. doi: 10.1002/2014ef000239

Masui, T., Matsumoto, K., Hijioka, Y., Kinoshita, T., Nozawa, T., Ishiwatari, S., ... Kainuma, M. (2011). An emission pathway for stabilization at 6 Wm−2 radiative forcing. *Climatic Change*, 109(1-2), 59–76. doi: 10.1007/s10584-011-0150-5

Melet, A., Meyssignac, B., Almar, R., & Cozannet, G. L. (2018). Under-estimated wave contribution to coastal sea-level rise. *Nature Climate Change*, 8(3), 234–239. doi: 10.1038/s41558-018-0088-y

Mitrovica, J. X., Gomez, N., Morrow, E., Hay, C., Latychev, K., & Tamisiea, M. E. (2011). On the robustness of predictions of sea level fingerprints. *Geophysical Journal International, 187*(2), 729–742. doi: 10.1111/j.1365-246x.2011.05090.x

Mitrovica, J.X., N. Gomez, & P.U. Clark. (2009). The Sea-Level Fingerprint of West Antarctic Collapse. *Science* 323:753. doi:10.1126/science.1166510.

NOAA, 2014.Sea Level Rise and Nuisance Flood Frequency Changes around the United States. Technical Report NOS CO-OPS 073.Sweet W. V., Park J., Marra J., Zervas C., Gill S.http://tidesandcurrents.noaa.gov/publications/NOAA_Technical_Report_NOS_COOPS_073.pdf

NOAA, 2020. "Relative Sea Level Trend, 8724580 Key West, Florida. https://tidesandcurrents.noaa.gov/sltrends/sltrends_station.shtml?id=8724580

NOAA, 2020b. "U.S. Average Seasonal Cycle in Meters +/-95% Confidence Interval." https://tidesandcurrents.noaa.gov/sltrends/calc_avg_seasonal_us.html

Obeysekera, J., M. Irizarry, J. Park, J. Barnes, & T. Dessalegne. (2011), "Climate Change and Its Implication for Water Resources Management in South Florida," *Journal of Stochastic Environmental Research & Risk Assessment*, 25(4), 495.

Obeysekera, J., Sukop, M., Tiffany, T., Irizarry, M., & Rogers, M. (2019). Potential Implications of Sea-Level Rise and Changing Rainfall for Communities in Florida using Miami-Dade County as a Case Study. Miami FL: Sea Level Solutions Center, Florida International University. Retrieved from https://slsc.fiu.edu/_assets/pdfs/fbc_fiu_finalreport_22aug2019.pdf

Oppenheimer, M., B.C. Glavovic , J. Hinkel, R. van de Wal, A.K. Magnan, A. Abd-Elgawad, R. Cai, M. Cifuentes-Jara, R.M. DeConto, T. Ghosh, J. Hay, F. Isla, B. Marzeion, B. Meyssignac, and Z. Sebesvari, 2019: Sea Level Rise and Implications for Low-Lying Islands, Coasts and Communities. In: *IPCC Special Report on the Ocean and Cryosphere in a Changing Climate* [H.-O. Pörtner, D.C. Roberts, V. Masson-Delmotte, P. Zhai, M. Tignor, E. Poloczanska, K. Mintenbeck, A. Alegría, M. Nicolai, A. Okem, J. Petzold, B. Rama, N.M. Weyer (eds.)]. In press.

Park, J., & Sweet, W. (2015). Accelerated sea level rise and Florida Current transport. *Ocean Science, 11*(4), 607–615. doi: 10.5194/os-11-607-2015

Piecuch, C. G., Huybers, P., Hay, C. C., Kemp, A. C., Little, C. M., Mitrovica, J. X., ... Tingley, M. P. (2018). Origin of spatial variation in US East Coast sea-level trends during 1900–2017. *Nature, 564*(7736), 400–404. doi: 10.1038/s41586-018-0787-6

Rahmstorf, S., Box, J. E., Feulner, G., Mann, M. E., Robinson, A., Rutherford, S., & Schaffernicht, E. J. (2015). Exceptional twentieth-century slowdown in Atlantic Ocean overturning circulation. *Nature Climate Change, 5*(5), 475–480. doi: 10.1038/nclimate2554

Rasmussen, D. et al., 2018. Extreme sea level implications of 1.5° C, 2.0° C, and 2.5° C temperature stabilization targets in the 21st and 22nd centuries. Environmental Research Letters, 13 (3), 034040.

Riahi, K., Rao, S., Krey, V., Cho, C., Chirkov, V., Fischer, G., ... Rafaj, P. (2011). RCP 8.5—A scenario of comparatively high greenhouse gas emissions. *Climatic Change, 109*(1-2), 33–57. doi: 10.1007/s10584-011-0149-y

Scoccimarro, E. et al., 2017. Tropical Cyclone Rainfall Changes in a Warmer Climate. In: Hurricanes and Climate Change [Collins, J. M. and K. Walsh (eds.)]. Springer International Publishing, Cham, 3, 243-255.

Shakhova, N., Semiletov, I., & Chuvilin, E. (2019). Understanding the Permafrost–Hydrate System and Associated Methane Releases in the East Siberian Arctic Shelf. *Geosciences, 9*(6), 251. doi: 10.3390/geosciences9060251

Smeed, D. A., Mccarthy, G. D., Cunningham, S. A., Frajka-Williams, E., Rayner, D., Johns, W. E., ... Bryden, H. L. (2014). Observed decline of the Atlantic meridional overturning circulation 2004–2012. *Ocean Science, 10*(1), 29–38. doi: 10.5194/os-10-29-2014

Sukop, M. C., Rogers, M., Gaunel, G., Infanti, J., & Hagemann, K. (2017). High Temporal Resolution Modeling Of The Impact Of Rain, Tides, And Sea Level Rise On Water Table Flooding In The Arch Creek Basin, Miami-Dade County Florida Usa. doi: 10.1130/abs/2017am-302263

Sweet, W.V., Dusek, G., Obeysekera, J. T. B., & Marra, J. J. (2018). Patterns and projections of high tide flooding along the US coastline using a common impact threshold. NOAA Technical Report NOS CO-OPS 086

Sweet, W.V., Kopp, R.E., Weaver, C.P., Obeysekera, J., Horton, R.M., Thieler, E.R., & Zervas, C. (2017b). Global and Regional Sea Level Rise Scenarios for the United States.*NOAA Technical report NOS CO-OPS 083*, Silver Spring, Md., 75 p.

Thompson, P. R., Widlansky, M.J., Leuliette, E., Sweet, W., Chambers, D.P., Hamlington, B.D., Jevrejeva, S., Marra, J.J., Merrifield, M.A., Mitchum, G.T, & Nerem, N.S. (2019). Sea level variability and change [in "State of the Climate in 2018"]. Bull. Amer. Meteor. Soc., 100 (9), S181–S185, doi:10.1175/2019BAMSStateoftheClimate.1.

USACE. 2015. USACE Sea Level Change Curve Calculator (2015.46) http://www.corpsclimate.us/ccaceslcurves.cfm

Valle-Levinson, A., Dutton, A., & Martin, J. B. (2017). Spatial and temporal variability of sea level rise hot spots over the eastern United States. *Geophysical Research Letters, 44*(15), 7876–7882. doi: 10.1002/2017gl073926

van Vuuren, D. P., Edmonds, J., Kainuma, M., Riahi, K., Thomson, A., Hibbard, K., Hurtt, G. C., Kram, T., Krey, V., Lamarque, J-. F., Masui, T., Meinshausen, M., Nakicenovic, N., Smith, S. J., & Rose, S. K. (2011). The representative concentration pathways: an overview. *Climatic Change* 109, 5-31. https://doi.org/10.1007/s10584-011-0148-z

van Vuuren, D. P. V., Stehfest, E., Elzen, M. G. J. D., Kram, T., Vliet, J. V., Deetman, S., ... Ruijven, B. V. (2011a). RCP2.6: exploring the possibility to keep global mean temperature increase below 2°C. *Climatic Change, 109*(1-2), 95–116. doi: 10.1007/s10584-011-0152-3

Volkov, D. L., Lee, S. K., Domingues, R., Zhang, H., & Goes, M. (2019). Interannual Sea Level Variability Along the Southeastern Seaboard of the United States in Relation to the Gyre-Scale Heat Divergence in the North Atlantic. *Geophysical Research Letters, 46*(13), 7481–7490. doi: 10.1029/2019gl083596

Wdowinski, S., Bray, R., Kirtman, B. P., & Wu, Z. (2016). Increasing flooding hazard in coastal communities due to rising sea level: Case study of Miami Beach, Florida. *Ocean & Coastal Management, 126*, 1–8. doi: 10.1016/j.ocecoaman.2016.03.002

Wdowinski, S. (2019). Coherent spatio-temporal variations in the rate of sea level rise along the US Atlantic and Gulf coasts, Abstract T23A-0341, to be presented at 2019 Fall Meeting, AGU, 2019.

WMO 2019: Global Climate in 2015-2019: Climate change accelerates. World Meteorological Organization.

Yamada, Y. et al., 2017. Response of Tropical Cyclone Activity and Structure to Global Warming in a High-Resolution Global Nonhydrostatic Model. Journal of Climate, 30 (23), 9703-9724, doi:10.1175/jcli-d-17-0068.1.

Yin, J., Schlesinger, M. E., & Stouffer, R. J. (2009). Model projections of rapid sea-level rise on the northeast coast of the United States. *Nature Geoscience, 2*(4), 262–266. doi: 10.1038/ngeo462

Appendix A: State of Science Update

REGIONAL AND GLOBAL SEA LEVEL RISE OBSERVATIONS

Historic Sea Level Rise in Southeast Florida

Based on the 5-year average of mean sea level, approximately 3.9 inches of sea level rise has occurred from 2000 to 2017. Figure A-1 shows the rise of sea level as observed in Key West for the time period from 1913 to 2020 and includes the monthly mean sea level data, the 5-year average of mean sea level and a linear trendline through the monthly mean sea level. The linear trend does not match the monthly mean sea level data well. The linear trend suggests sea level rose only 2 inches from 2000 to 2019, which is less than the 5-year average trend analysis from 2000 to 2017 shown (NOAA, 2020). The 5-year average of the monthly mean sea level illustrates the variability in sea level throughout the time period and highlights the continued increase in sea level above the linear trend in the last decade.
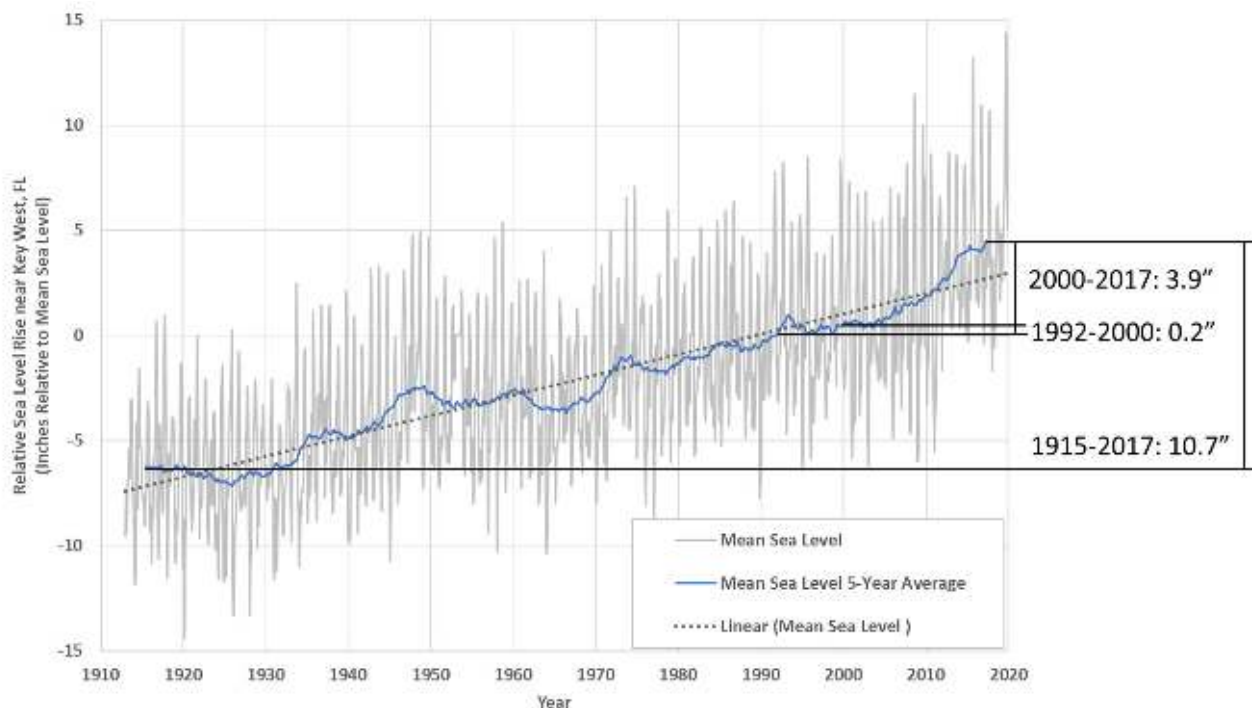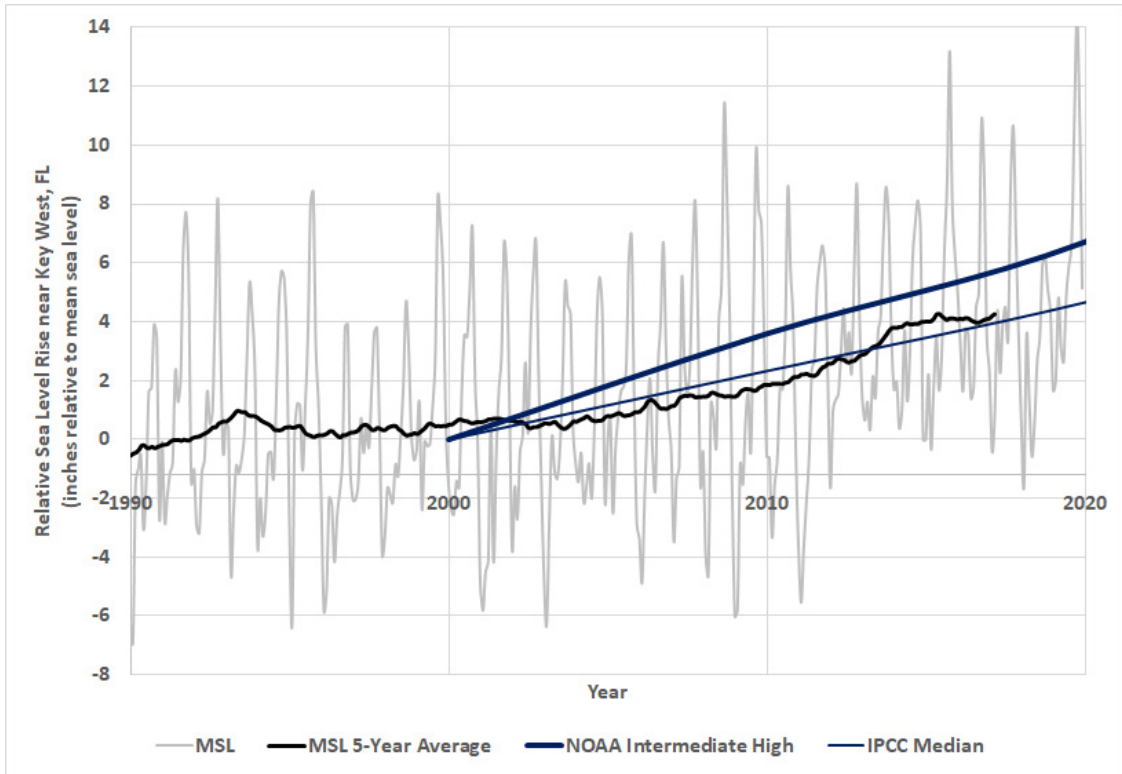

FIGURE A-1. Relative Sea Level Rise in Key West, Florida (NOAA Station ID 8724580) presented as monthly mean sea level, 5-year average of monthly mean sea level and linear trend of monthly mean sea level. Annotated measurements on right of figure are computed by subtracting the 5-year average mean sea levels for the years listed. Sea level rise computed based on the linear trend will differ from the 5-year mean sea level trend shown.

As discussed in the following sections describing the factors influencing sea level rise, the changing climate will drive new nonlinear trends in sea level that deviate from historic trends, hence the need for the Unified Projection. Although significant changes in sea level trends are anticipated over the coming decades, a preliminary comparison of the Unified Projection and the available measured data is presented in Figure A-2. The 5-year average mean sea level was observed to track between the IPCC Median and NOAA Intermediate High curves from 2013 to 2017 (2017 was the last year of computable 5-year average at the time of publication).

Monthly mean sea level was observed to exceed the NOAA Intermediate High curve in almost every tidal cycle since 2000. For additional context, the linear trend based on historic data included in Figure A-1 remains below the IPCC Median curve from 2007 onward and below the 5-year average of mean sea level from 2010 onward.

FIGURE A-2. **Comparison of the Unified Sea Level Rise Projection from 2000 to 2020 and Relative Sea Level Rise in Key West, Florida from 1990 to 2020.** Monthly mean sea level and the 5-year average of monthly mean sea level are based on measurements from NOAA Station ID 8724580.

ACCELERATION OF SEA LEVEL RISE

Dangendorf et al., (2017) produced a global mean sea level reconstruction for the 21st century incorporating up-to-date observations of vertical land motion and corrections for local gravitational changes resulting from ice melting and terrestrial freshwater storage. Their results provided a global sea level rise rate of 1.1 ± 0.3 millimeter per year before 1990 that is below previous estimates, and a rate of 3.1 ± 1.4 millimeter per year from 1993 to 2012 that is consistent with independent estimates from satellite altimetry.
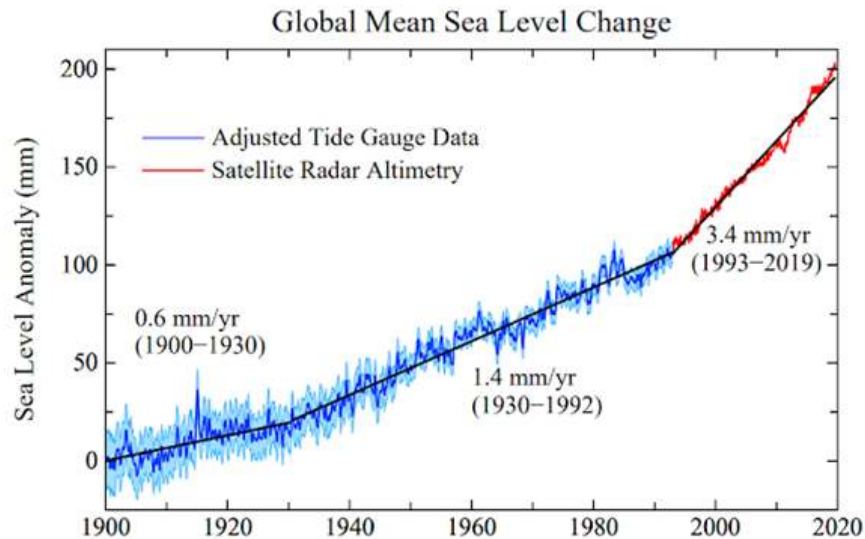
FIGURE A-3. **Global mean sea level change from 1900 to 2019 and increasing acceleration rates** (modified by Hansen et al., (2015) from Church and White (2011) and Hay et al., (2014). 1993 to 2019 data distributed by AVISO+ (https://www.aviso.altimetry.fr) with support from CNES.

Recent analyses of tide gauge records acquired along the United States Atlantic coast indicate year-to-year acceleration in the rate of sea level rise (Sweet et al., 2017). During 2010-2015, accelerated sea level rise at rates five times the global average was observed between Key West and Cape Hatteras (Valle-Levinson, 2017), and is attributed to the warming of the Florida Current (Domingues et al., 2018). Locally, Wdowinski et al. (2016) analyzed the Virginia Key tide gauge record (near Miami) and found a significant acceleration in the rate of sea level rise since 2006. The average rate of regional sea level rise since 2006 was 9±4 millimeters per year, significantly higher than the global average rate, which has been estimated to be in the range of 4-5 millimeters per year for the post-2006 period (WMO, 2019). The global and regional processes driving sea level rise and its acceleration are discussed in the following sections.

NOAA Sea Level Rise Scenarios

For the Compact 2019 projections, the workgroup referenced the technical information provided in the NOAA report (Sweet et al., 2017) which was also used as input to the sea level rise chapter of the National Climate Assessment (NCA) (https://science2017.globalchange.gov/chapter/12/). The sea level projections in the NOAA report were developed by a Federal Interagency Sea Level Rise Task Force and they included six scenarios (Table A-1 below) using a risk-based framing approach to deal with uncertainties. The scenario approach is similar to the regional sea level rise scenarios produced by Hall et al. (2016) and they are linked to the greenhouse gas emission scenarios, RCP 2.6, 4.5, and 8.5 as shown in Table A-1. The NOAA 2017 report includes the best available research since the production of the Compact 2015 report and is considered to be a reliable source of data from the national effort on sea level rise projections. More importantly, the projections are

available regionally and that allowed the work group to customize 2019 projections using the Key West gauge as was done for the 2015 projections.

TABLE A-1: Interpretations of the Interagency Global Mean Sea Level (GMSL) rise scenarios (National Climate Assessment (NCA), Chapter 12)

SCENARIO	INTERPRETATION
Low	Continuing current rate of GMSL rise, as calculated since 1993
	Low end of *very likely* range under RCP 2.6
Intermediate-Low	Modest increase in rate
	Middle of *likely* range under RCP 2.6
	Low end of *likely* range under RCP 4.5
	Low end of *very likely* range under RCP 8.5
Intermediate	High end of *very likely* range under RCP 4.5
	High end of *likely* range under RCP 8.5
	Middle of *likely* range under RCP 4.5 when accounting for possible ice cliff instabilities
Intermediate-High	Slightly above high end of *very likely* range under RCP 8.5
	Middle of *likely* range under RCP 8.5 when accounting for possible ice cliff instabilities
High	High end of *very likely* range under RCP 8.5 when accounting for possible ice cliff instabilities
Extreme	Consistent with estimates of physically possible "worst case"

In general, the global sea level rise pathways for different emission scenarios are not very different until about the mid-century after which they deviate significantly (e.g. Figure 4.2, IPCC 2019). The broad range of sea level rise projection during the latter part of the century reflects the significant uncertainty in predicting the contributions of individual sea level rise components, attributable primarily to ice cliff instability. Driven by the desire to capture the potential for larger sea level rise resulting from rapid melting from the ice sheets towards the latter part of the century, the work group made a decision to select higher scenarios that are also consistent with the growing emission scenario, RCP 8.5. Recent sea level rise guidance from the Tampa Bay Region recommended the use of RCP 8.5 "*…until the private and public sectors make meaningful efforts to reduce greenhouse gas emissions.*" Consequently, the Intermediate High, and High scenarios (Table A-1) were included in the 2019 scenarios set. Consistent with the 2015 projections, IPCC Median scenario for RCP 8.5 was added to define the lower boundary of the range. The IPCC Median (with a Global Mean Sea Level, GMSL, rise of 0.73 meters) lies between Intermediate Low (0.5 meter of GMSL) and Intermediate (1 meter GMSL) scenarios in the NOAA 2017 set (Table A-1). The Work Group also included the NOAA 2017 Extreme Scenario as an estimate of the upper bound of what could happen as a result of a catastrophic ice sheet collapse and the primary intent of this inclusion was to emphasize what could happen to GMSL if the emissions were allowed to continue without mitigation.Inclusion of such an extreme scenario is not unprecedented. For instance, New York City (Gornitz et al., 2019) included a new, physically plausible, upper-end scenario dubbed ARIM (Antarctic Rapid Ice Melt) scenario for this purpose. The California guidance also includes a similar scenario, called H++ which reflects extreme sea level but with unknown probability.

FACTORS INFLUENCING FUTURE SEA LEVEL RISE

Global Processes

Thermal expansion

Warming of oceans leads to a lower density and as a consequence volume per unit mass increases. The ocean has absorbed more than 90% of the heat that is generated by heat trapping greenhouse gasses making the thermal expansion a significant component of the observed sea level rise. Thermal expansion is expected to increase, but its contribution to the global sea level rise may be exceeded by the increased contributions from melting land-based ice sheets.

Acceleration of Ice Melt

Accelerated melting of glaciers and ice sheets of Greenland and Antarctica has become the predominant factor affecting sea level rise acceleration (Oppenheimer et al., 2019). Melting is caused by anthropogenic forcing leading to increasing temperatures and warming of the atmosphere, warm currents moving along the coast of Greenland, and warm ocean water moving under and up into ice sheets through deep outlet glacial fjords in Greenland and Antarctica in response to meteorologic changes. The rate of melt of the Greenland Ice Sheet was relatively stable in the 1990s and has increased since then to a rate seven times greater than in 1992 (IMBIE, 2019; Chen et al., 2017). The rate of acceleration peaked in 2011, slowed in response to cooler conditions until 2016, but has begun increasing again. Although all of the ice melt processes are not fully represented in the climate projection models, studies suggest contributions from ice melt are likely to match the estimates of melt from the IPCC AR5 RCP 8.5 scenario (Oppenheimer et al., 2019).

Based on geologic records from the last two pre-historical periods that the Greenland and Antarctica ice sheets melted, global mean sea level likely rose 18 to 27 feet in response, but potentially as much as 75 feet. Models and analyses cannot yet confirm if similar rates of pre-historic rise will occur in response to melt in the future (Oppenheimer et al., 2019). The possibility of such extreme rise in response to ice melt prompted the inclusion of the NOAA Extreme curve for reference in the Unified Sea Level Rise Projection and to highlight the importance of greenhouse gas mitigation. Although unlikely and not appropriate for infrastructure planning, the Work Group wanted to acknowledge the evolving science in projecting accelerating ice melt and bracket the uncertainty in rise at the end of the century based on the most recent observations and models.

Thawing Permafrost

Frozen soils are both a major source of emissions today, and a major sink for carbon during past ice ages. Permafrost is permanently frozen soil, which holds vast amounts of organic material in a suspended state of decay. It is found in vast, remote and inaccessible places: under tundra's covered active layer (seasonally melted mud), underwater, and under sea ice and/or snow. It is the least understood, but potentially one of the most important climate change drivers. Satellite remote sensing is less useful in its direct observation of permafrost, compared to other phenomena important to sea level rise. But the high atmospheric methane concentration in the atmosphere above the northern polar region stands out above other regions on earth. Russian, Alaskan and other scientists from around the world are actively investigating the potential for significant additional emissions of carbon dioxide and methane from thawing permafrost (Shakova et al., 2019). Prior to the last three decades, heavy multi-year sea ice protected solid frozen permafrost, and the methane sequestered within it as massive subaqueous methane hydrate deposits. Release of this methane could constitute a powerful tipping point for atmospheric warming, and the glacial melting to follow. It is unknown when such a tipping point is likely to occur, but the continued acceleration of global warming with business as usual, RCP 8.5, puts us on a dangerous trajectory.

Regional/ Local Processes

Distinct rates of sea level rise recorded along the U.S. East Coast are currently largely modulated by the effect of various regional and local processes (Piecuch et al., 2018). The long-term regional sea level rise projections employed in this report are primarily based on the recent scenarios convened by the Sea Level Rise and Coastal Flood Hazard Interagency Task Force (Sweet et al., 2017), which explicitly consider these effects from regional drivers. As an example, regional drivers may account for an additional 37 centimeters of sea level rise by 2100 in Key West under the assumptions linked with the NOAA Intermediate-High scenario, totaling 1.87 meters of sea level rise compared with 1.5 meters globally. The following section describes the most important regional drivers that can affect rates of sea level rise in Southeast Florida.

Vertical Land Movement

Vertical earth movements (subsidence or uplift), which regionally and locally modify the averaged rate of sea level change, result in a relative rate of change that varies from one location to another. These land movements are inferred from historical tide data and geodesic measurements. When added to projected rates of mean sea level rise, the vertical land movement results in a perceived rates of sea level rise change ranging from increased rise in regions of subsidence (e.g., New Orleans) to falling sea levels where the land is being uplifted (e.g., along the northern border of the Gulf of Alaska). Sea level rise in geologically stable regions have only small differences with respect to the global rate of rise. Some of the processes leading to vertical land movement include the post-glacial rebound (known as Glacial Isostatic Adjustment — GIA), sediment compaction, dam retention, and groundwater and oil withdrawal.

A robust method for estimating vertical land movements is based on continuous GPS measurements conducted at selected locations. Over the past two decades, more than 60 continuous GPS stations were constructed and operated in Florida by federal and state institutes, including the Continuously Operating Reference (COR) network, US Coast Guard, Florida Department of Transportation, and others. The length of record in these stations vary from one to fourteen years, reflecting the difficulties in maintaining smooth operation of a continuous GPS station. The continuous GPS measurements indicate that vertical land movements in Florida are fairly small; they vary in the range of ±4 millimeters/year. In South Florida, in general, coastal land elevations are considered relatively stable—meaning that the land is not experiencing significant uplift or subsidence. Therefore, the processes listed above are likely not playing a major role on the current sea level rise rates observed in Southeast Florida. It is important to note, however, that the vertical land movement that is occurring is non-uniform across South Florida, and movement measured at specific monitoring stations sites may not reflect vertical land movement in adjacent areas.

Ocean Dynamics, Gulfstream/ Circulation

Regional patterns of sea level change are partly due to trends in ocean currents, redistribution of temperature and salinity, and atmospheric pressure. The reasons for changes in "Ocean Dynamics" are well known (Hall et al., 2016). Thermal expansion changes the elevation of the sea surface non-uniformly and to balance the resulting pressure gradient, ocean mass will flow from areas of large water depths into shallower continental shelf areas (Hall et al. 2016; Yin et al. 2009). Long-term changes in ocean dynamics still represent one of the largest sources of uncertainty for long-term projections of sea level rise (Kopp et al., 2014; Chen et al., 2019), and current observations show only a modest decline in the strength of the Florida Current flow.

Ocean circulation has changed little during the current period of scientific observation, but in the future it may considerably alter the relative rate of sea level rise in some regions, including Southeast Florida. The potential slowing of the Florida Current and Gulf Stream could result in a more rapid sea level rise along the east coast of North America. By 2100, these circulation changes could contribute an extra eight inches of sea level rise in

New York and three inches in Miami according to Yin et al. (2009). Most of the global climate models used by the IPCC (IPCC, 1913 project a 20-30% weakening of the Atlantic Meridional Overturning Circulation (AMOC), of which the Gulf Stream and Florida Current are a part, a response to warming caused by increasing greenhouse gases. Measurements of the AMOC have yet to conclusively detect the beginning of this change, however there has been a report of a recent decline in AMOC strength by Smeed et al. (2014) that coincides with the mid-Atlantic hotspot of sea level rise reported by Ezer et al. (2013) and Rahmstorf et al. (2015). Recent analysis of the Florida Current transport has detected only a slight decrease in circulation over the last decades. Assuming the long-term slowdown of the AMOC does occur, sea level rise along the Florida east coast could conceivably be as much as twenty centimeters (eight inches) greater than the global value by 2100. Given that changes in ocean dynamics, such as these changes projected for the AMOC, are still one of the main sources of uncertainty for long-term regional sea level rise scenarios (e.g. Kopp et al., 2014; Piecuch et al., 2018), longer records of the Florida Current and Gulf Stream transport are required to confirm if the long-term decline in the strength of the flow persists, or if it is associated with interannual/decadal natural variations. Recent regional sea level rise scenarios for the U.S. coasts have been made available by the Sea Level Rise and Coastal Flood Hazard Interagency Task Force (Sweet et al., 2017), and explicitly consider regional effects of changes in ocean dynamics and other local contributors, as described above.

Regional Ocean Heat Content Changes
Recent studies revealed accelerated rates of year-to-year changes in regional sea level variability along the U.S. East Coast (Valle-Levinson et al., 2017). Even though these variations are not necessarily linked with long-term sea level rise trends, these accelerated changes currently contribute to flooding conditions often observed at Southeast Florida communities. Analysis showed that accelerated sea level rise recently observed for Southeast Florida from 2010 to 2015 were in fact associated with thermal expansion from warming of the Florida Current during the same time period, as reported in Domingues et al., (2018). Further analysis (Volkov et al., 2019) revealed that such warming was linked to large-scale heat convergence within the North Atlantic subtropical gyre caused by changes in the Atlantic Meridional Overturning Circulation (AMOC). While current findings indicate that these effects occur mostly on year-to-year timescales, under a long-term scenario that includes the decline in the AMOC circulation (as suggested by IPCC 2013), it is likely that amplified sea level rise rates may be observed along Southeast Florida through similar mechanisms.

Sea level fingerprinting (Gravitational Effects)
Melting ice sheets in polar regions is one of the main processes contributing to sea level rise, but not in a spatially uniform manner, because of gravitational forces. Melting ice sheets reduces the mass of water stored in polar regions and, consequently, reduce the gravitational attraction of continental ice sheets. As a result, the volume of ocean water near the melting ice sheet decreases, leading to reduction in sea level height near the polar regions, and an increase in sea level further away. This process is termed sea level fingerprinting (Mitrovica et al., 2011, 2009). It suggests a counterintuitive change in regional patterns of sea level changes, in which sea level height decreases near the source of fresh water supply to the ocean.

A sea level fingerprinting study by Hay et al. (2014) suggest that melting of the Greenland Ice Sheet results in a slightly lower rate of sea level rise along the Florida shorelines with respect to the global mean rate. The calculated change is 20% of the total contribution of the Greenland Ice Sheet to the global mean rate, which is currently estimated as 1-1.5 millimeters/year. According to Hay et al. (2014), melting of the West Antarctic Ice Sheet increases the rate of sea level rise along the Florida coast by 20% with respect to the total contribution of the West Antarctic Ice Sheet to the global mean rate, which is so far about 0.75-1 millimeters/year. Thus far, the contribution of sea level fingerprinting in southeast Florida had been fairly small, about 0.2-0.3 millimeters/year.

However, in the future with increasing rate of polar ice melt, the effect of sea level fingerprinting can increase, especially if the Antarctic Ice Sheet will melt significantly faster than the Greenland Ice Sheet. It should be noted that the NOAA (2017) scenarios used for the current projections explicitly account for regional fingerprinting.

EFFECTS OF GREENHOUSE GAS EMISSIONS

The Intergovernmental Panel on Climate Change based the climate projections of their Fifth Assessment Report on four greenhouse gas concentration scenarios, known as the Representative Concentration Pathways (RCPs) (IPCC, 2014). These RCPs are sets of scenarios for greenhouse gas emission, greenhouse gas concentration, and land use trajectories; their primary product is greenhouse gas concentration scenarios for use as inputs into climate models (van Vuuren et al., 2011a). The number in the name of each RCP is the end-of-century radiative forcing in W/m^{-2} caused by the greenhouse gas concentrations in 2100.

The lowest concentration scenario, RCP 2.6, is viewed as the scenario necessary to keep global temperature increases below 2°C (van Vuuren et al 2011a). This scenario would require that greenhouse gas emissions peak around 2020 and decrease at 4% annually (van Vuuren et al. 2011a). The highest concentration scenario, RCP 8.5, assumes a greatly increased population with low economic and efficiency gains by 2100, along with a strong dependence on fossil fuels, including a ten-fold increase in coal use by the end of the century (Riahi et al., 2011).

RCP 4.5 and RCP 6.0 are concentration scenarios sitting between these two extremes. In the RCP 4.5 scenario, emissions valuation policies, reaching $85 per ton of carbon dioxide by 2100, drive alternatives in energy production and land use changes to reduce emissions. It assumes use of bioenergy production coupled with carbon capture and storage to produce energy with net-negative carbon emissions. RCP 6.0 assumes cost-effective reduction of emissions through a global emissions permit market, and includes a shift from coal-fired to gas-fired energy production and more than 30% non-fossil fuel energy production by 2100 (Masui et al., 2011).

Beyond these four concentration pathways, the IPCC recently released a report outlining the emissions scenarios required to limit global warming to 1.5°C (IPCC, 2018). In this model pathway, global net anthropogenic carbon dioxide emissions decline by about 45% from 2010 levels by 2030, reaching net zero around 2050. The report also contains an emissions projection to limit global warming to 2.0°C; in this scenario, carbon dioxide emissions decline by about 25% by 2030, and reach net zero around 2070.

Prior to 2050, different emission scenarios produce minor differences in sea level rise projections, however, they diverge significantly past mid century. After 2050, the sea level rise projections increasingly depend on the trajectory of greenhouse gas emissions, underscoring the critical need for urgent and ambitious decarbonization policies and efforts.
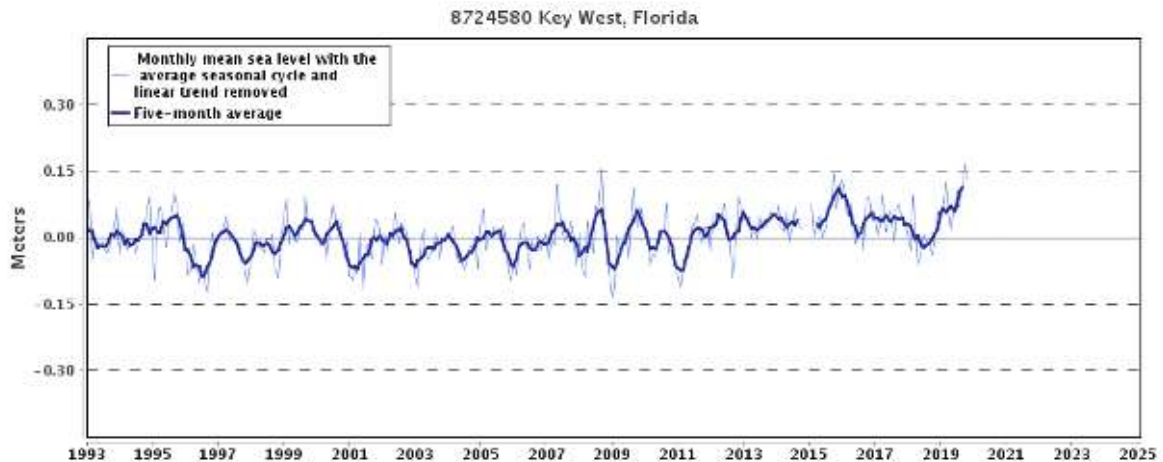
Seasonal Cycle of Sea Level and Interannual Variability

There is a strong seasonality to average sea level variation with any given year. This is primarily driven by seasonal oceanographic and atmospheric processes such as fluctuations in coastal ocean temperature, salinity, winds, atmospheric pressure, and ocean currents. In Southeast Florida, the sea level driven by astronomical tides exhibits a strong seasonality with higher than average values during the months of September to November with a peak during the month of October (Figure A-4). The seasonal high in October may be as much as 5-6 inches above the average. The high values during September to November, superimposed on the mean sea level curve and diurnal and semidiurnal tides further exacerbates the recurrent flooding that has been increasing in recent years.

In addition to the seasonal fluctuations, sea level may also exhibit interannual variability due to fluctuations in oceanographic and atmospheric processes (Figure A-4). Such fluctuations may further increase the mean annual sea level above the average seasonal cycle shown in Figure A-4 and they may persist at a higher or lower level for several years. For example, Figure A-5 shows that the annual fluctuation since about 2012 has been largely positive until 2019, a pattern that is not characteristic of annual variability since 1990. It is possible that such a persistence may be due to a systematic trend in ocean currents and/or other atmospheric-oceanographic process but it is too early to make such an attribution.
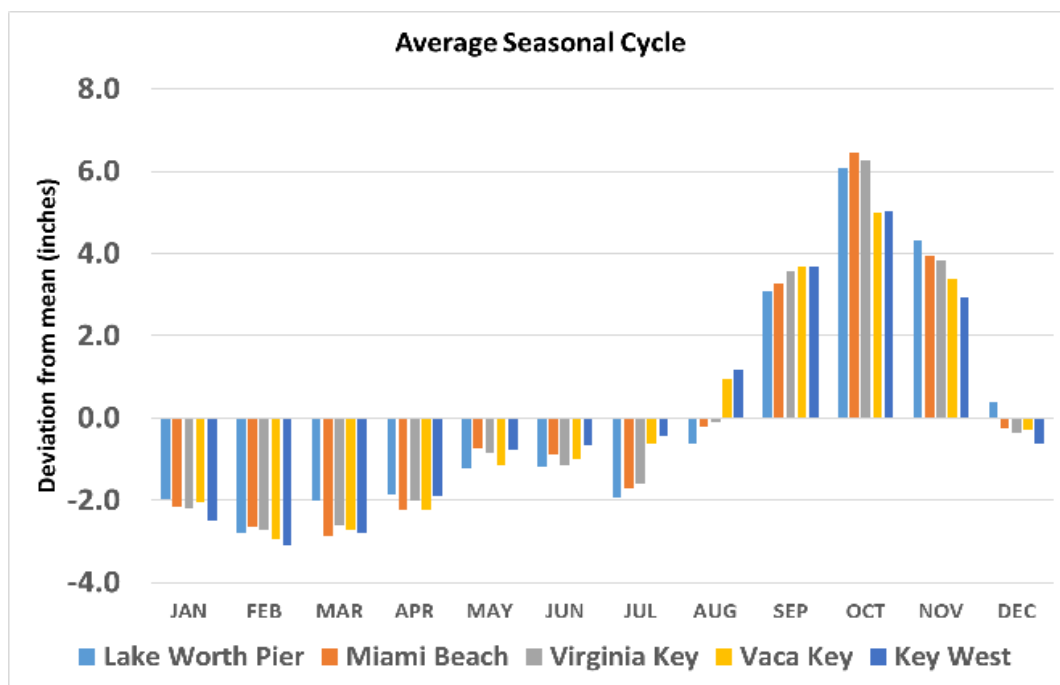
FIGURE A-4: **Tidal water elevations in the Southeast Florida area average 5 to 6 inches higher at the end of the summer** (NOAA, 2020b). This increases the risk of recurrent high tide street flooding and more severe storm surge impacts, particularly during periods of astronomical high tides (i.e. king tides). Ongoing and accelerating local sea level rise will just make this problem worse.

FIGURE A-5: The plot shows the interannual variation of monthly mean sea level and the 5-month running average. The average seasonal cycle and linear sea level trend have been removed (Retrieved from NOAA Tides and Currents website (https://tidesandcurrents.noaa.gov/)

Increase in Recurrent Tidal Flooding

Accelerating rates of sea level rise, due to both global and regional processes, have resulted in increased flooding frequency in several coastal communities along the US Atlantic coast, including the Southeast Florida region (Ezer et al., 2013; Ezer and Atkinson, 2014; Kirshen et al., 2008; Kleinosky et al., 2006; Sweet et al., 2018; Wdowinski et al., 2016; 2019; Valle-Levinson et al., 2017). These recurrent flood events, often termed "nuisance flooding," occur during high tide conditions, with or without heavy inland rainfall. When flooding events occur due to high tide flooding alone, they are also termed "king tides", or "sunny-day flooding." Recurrent tidal flooding results in inundation, impedes access, impairs stormwater drainage infrastructure, and damages vulnerable systems. With sea level rise, the frequency of tidal flooding will increase, leading to chronic flooding approaching permanent inundation.

An analysis of flooding frequency from 1998 to 2013 in Miami Beach revealed that recurrent tidal flooding events quadrupled, from two events during the eight years from 1998-2005, to 8 to 16 total events in the following eight years from 2006-2013 (Wdowinski et al., 2016). In 2005, 2015, 2016, and 2017, compound flooding induced by hurricanes led to the highest observed numbers of annual flood days on record (Ezer and Atkinson, 2017; Ezer et al., 2017; Wdowinski, 2019). From 2006 to 2012, recurrent tidal flooding occurred approximately every other year, typically during the fall (September through November). Since 2010, higher than normal tides have also been observed in the winter and spring seasons (Figure A-6, Wdowinski et al., 2019). In 2019, unprecedented flooding occurred in Key Largo, where a neighborhood was flooded continuously for more than four months.

How will flooding frequency evolve over time?

On the national scale, NOAA (2014) published an assessment of nuisance flooding finding that the duration and frequency of these events are intensifying around the United States. Subsequently, Park and Sweet (2015) demonstrated that coastal areas are experiencing an increased frequency of flood events (an acceleration) over the last few decades, and that this acceleration in flood occurrence will continue regardless of the specific rate of sea level rise. The recent assessment published by NOAA (Sweet et al., 2018) in fact shows that the number of high-tide flooding days has been increasing at a nonlinear rate for locations along the U.S. East Coast, including Southeast Florida. Results from this assessment indicate that under the NOAA Intermediate scenario, Miami

will likely experience approximately 60 days of high-tide flooding per year by 2050, while under the NOAA Intermediate-High scenario this number may exceed 150 days per year (Figure A-7, personal communication, Sweet et al., 2018).
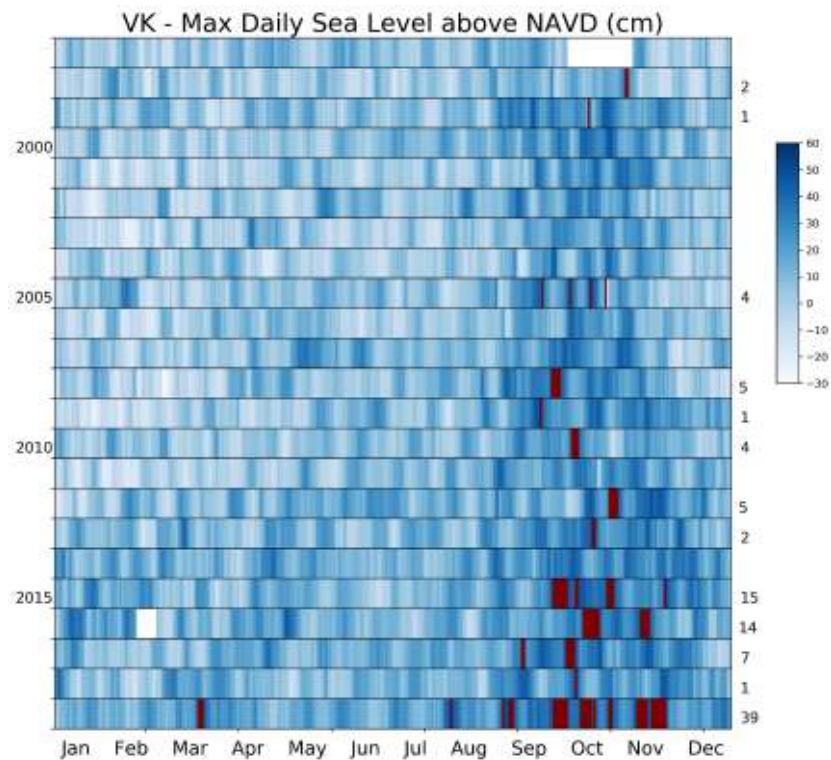
FIGURE A-6. Frequency of tidal flooding in Miami Beach, based on Virginia Key tide gauge. Higher than normal tides shown as red bars in figure. Number of events in a given year listed in right margin of graphic (Wdowinski, 2019).
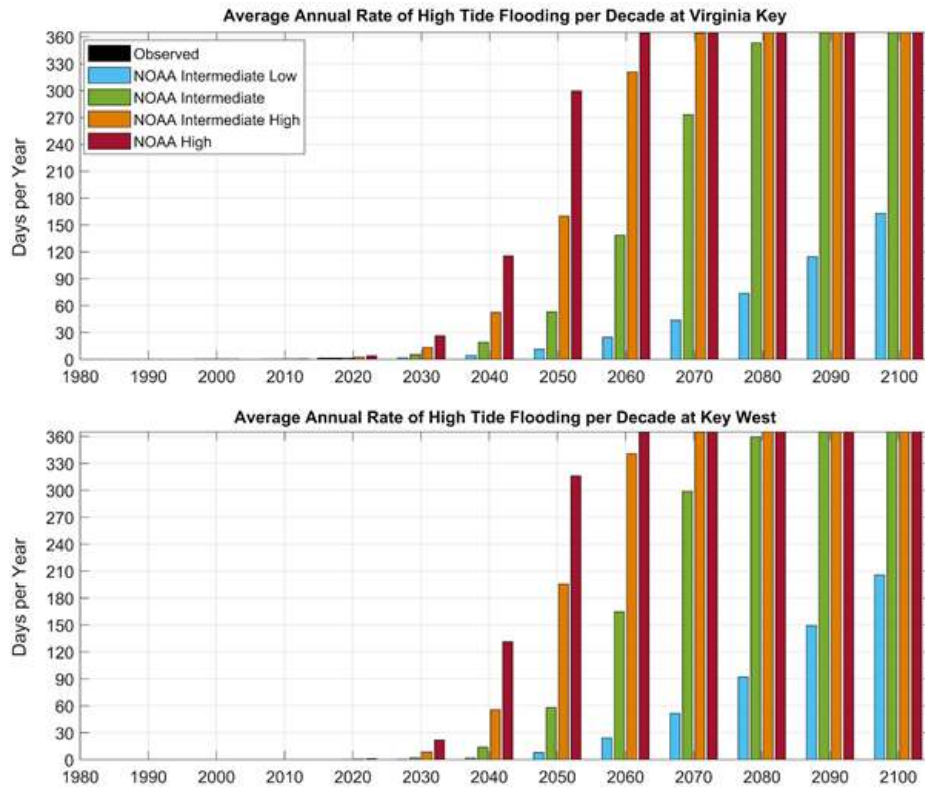
FIGURE A-7: Projected annual frequencies of high tide flooding associated with the NOAA sea level rise (Sweet et al., 2017) estimated at NOAA tide gauges in Virginia Key and Key West. High tide flooding threshold values levels above MHHW are 0.52 meters for Virginia Key, and 0.53 meter for Key West (Courtesy of William Sweet - NOAA National Ocean Service).

Groundwater Rise and Reduced Drainage Capacity

Sea level rise may also affect flooding by raising the water table and reducing the ability of rainfall to infiltrate and be stored in the soil. In coastal areas of Southeast Florida, groundwater levels were observed to rise at the same rate as sea level rise over the long term (Decker et al., 2019; Sukop et al., 2018). Flooding as a consequence of groundwater rise and reduced soil storage is anticipated to double or triple in flood frequency over the next 40 years (Sukop et al., 2018; Obeysekera et al., 2019). By 2070, certain coastal areas of South Florida are projected to lose all wet season storage capacity (Obeysekera et al., 2019).

In one example, Sukop et al. (2018) examined the long-term record of water levels in a well (G-852, in the North Miami/Arch Creek area) approximately one mile from tide water at Biscayne Bay. The water levels in the well have been increasing at approximately 2.8 millimeters/year since at least 1974. This rate is consistent with the rate of sea level rise at Key West of 2.42 millimeters/year over the same time period. (https://tidesandcurrents. noaa.gov/sltrends/sltrends_station.shtml?id=8724580).

As part of an assessment for the Florida Building Commission, Obeysekera et al. (2019) used projections of sea level rise from previous versions of this report in groundwater models to estimate the change in water table elevation in Miami-Dade County by 2069. Between 2010 and 2069, drainage capacity is estimated to decrease by four to ten inches of water in most of the county (Figure A-8) under the high sea level rise scenario.
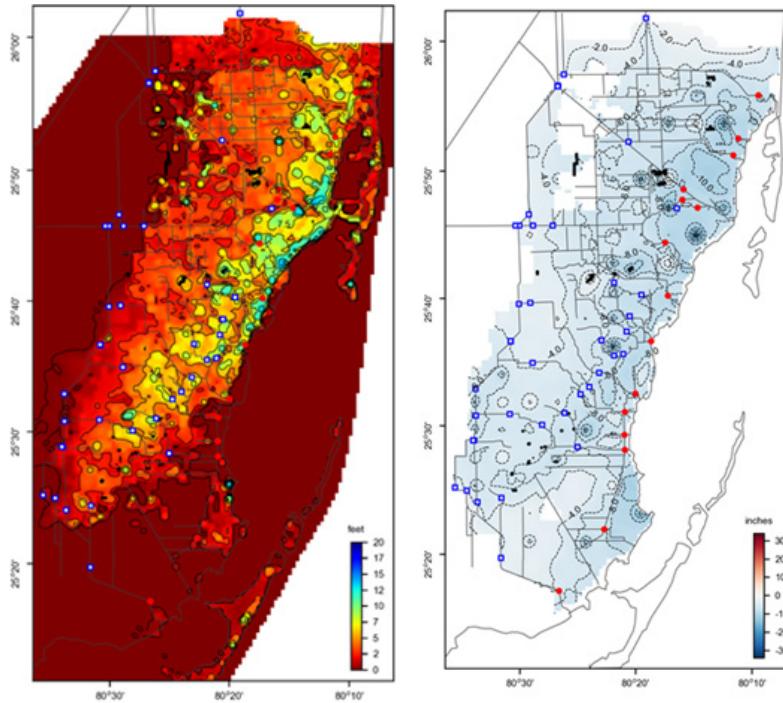
FIGURE A-8: Miami-Dade County depth to water in 2069 (left) and loss of wet season soil storage capacity from 2015 through 2069 (right) (Obeysekera et al., 2019).

Increasing sea levels also have the potential to compromise the capacity of coastal water control structures (also known as salinity barriers). As the ocean-side water levels increase, the water control gates of these gravity structures cannot be opened due to the threat of saltwater entering into the canals they serve and potentially contributing to saltwater intrusion (Obeysekera et al. 2011).

Storm Surge, Waves, and Sea Level Rise

Storm surge and sea level rise are independent coastal processes that, when occurring simultaneously, lead to compounded impacts. Sea level rise has the potential to increase the inland areal extent inundated by surges, the depth of flooding, power of the surge, and the extent and intensity of damage associated with storm surge and waves. As a result, severe storms of the future may cause significantly more damage than storms of equal intensity occurring at today's sea level. The frequency of extreme sea levels that cause severe flooding will also increase as a consequence of sea level rise (Rasmussen, 2018). To avoid impacts from surge, coastal infrastructure design elevations and reinforcement will need to consider the relationship between future sea level rise and surge.

The effects of sea level rise on storm tides or surge is nonlinear and location specific. Analyses that superimpose sea level rise projections on top of surge depths are likely not capturing the nonlinearity of the processes, and may possibly underestimate depths and forces. Reduction of sea bottom stress and tidal wave energy dissipation in waters deepened by sea level rise can result in higher surge heights in shallow nearshore waters (Arns et al., 2015). Similarly, changes in deep water wave heights and wave periods can increase wave setup and swash zone activity (Melet et al., 2018). Location- specific projections of future waves and the interactions between sea level, tides and surges are not yet available (Oppenheimer et al., 2019), but site-specific modeling of the impacts of future severe storms on infrastructure has occurred for projects across the Compact four-county region by increasing water levels to represent future conditions.

Rare, extreme water levels that typically occured once every 100 years in the past are projected to occur annually or more frequently by 2065 in response to sea level rise (Oppenheimer et al., 2019). The Intergovernmental Panel on Climate Change has concluded high confidence in this projected frequency and suggested adaptation planning occur before extreme events become regular in the latter half of the 21st century. Moreover, the duration, precipitation, landfalls, and intensity of future hurricanes is predicted to increase with global warming (IPCC, 2014; Knutson et al., 2015; Scoccimarro et al., 2017; Yamada et al., 2017).

Natural Resource Degradation

As sea level rise increasingly inundates coastal areas, natural resources in the ecologically diverse and important transition zone—including mangrove forests, tidal flats, and beaches—will be degraded unless focused effort is devoted to: 1) accommodating the inland migration of coastal habitats, and 2) implementing coastal management practices that maintain coastal elevation at pace with sea level rise rates (Glick 2006, Florida Oceans and Coastal Council 2010). In Southeast Florida, existing urban development in the form of seawalls, roads, and other infrastructure currently blocks much of the ability of coastal habitats to migrate as sea level rises. Reduced freshwater delivery and conversion of coastal areas to non-vegetated lands limit or eliminate plant growth, diminish the capacity for coastal areas to maintain natural system functions, and result in natural system decline. Intrusion of saltwater inland, into inland water bodies, and within the aquifer is already negatively impacting freshwater resources. With further sea level rise, these impacts will worsen or accelerate without adaptation that includes coastal management. Inundation of shorelines will also increase the extent and severity of beach erosion in previously stable coastal areas. In combination, these impacts will cascade throughout the region's ecosystems even if they are not immediately adjacent to open water areas.

These ecosystems (natural infrastructure) and the natural resources they support, are critical to the resilience of people and the urban environment. Natural systems provide many important benefits. These include providing nesting, spawning, and feeding habitat for numerous species including sea turtles, shorebirds, fish, and invertebrates; contributing to climate change mitigation via sequestration of carbon dioxide from the atmosphere; enhancing storm protection, water and air purification; moderating urban heat effects; and supporting livelihoods and economic activity throughout South Florida that depend on tourism and recreational and commercial fisheries. The region can manage for natural resource benefits by providing space for habitat transitions, implementing practices that help adapt coastlines to sea level rise, and reducing anthropogenic pressures (e.g., nutrient and solid waste pollution, recreational activities that can damage natural resources, development practices) that would compound the degrading effects of sea level rise.
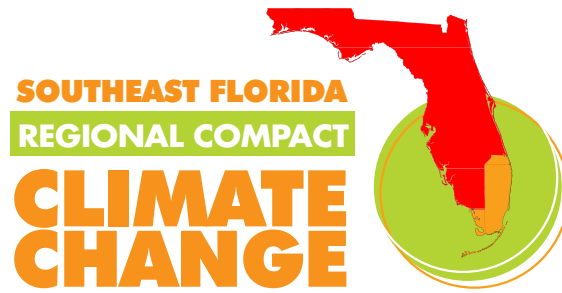
For more information, visit:
www.climatecompact.org

World is on brink of catastrophic warming, U.N. climate change report says

A dangerous climate threshold is near, but 'it does not mean we are doomed' if swift action is taken, scientists say

By Sarah Kaplan

Updated March 20, 2023 at 5:33 p.m. EDT | Published March 20, 2023 at 9:01 a.m. EDT

The world is likely to pass a dangerous temperature threshold within the next 10 years, pushing the planet past the p[oint] of catastrophic warming — unless nations drastically transform their economies and immediately transition away fro[m] fossil fuels, according to one of the most definitive reports ever published about climate change.

The report released Monday by the U.N. Intergovernmental Panel on Climate Change (IPCC) found that the world is likely to surpass its most ambitious climate target — limiting warming to 1.5 degrees Celsius (2.7 degrees Fahrenheit) above preindustrial temperatures — by the early 2030s.

Beyond that threshold, scientists have found, climate disasters will become so extreme that people will not be able to adapt. Basic components of the Earth system will be fundamentally, irrevocably altered. Heat waves, famines and infectious diseases could claim millions of additional lives by century's end.

l warming

Human activities have already transformed the planet at a pace and scale unmatched in recorded history, the IPCC said, causing irreversible damage t[o] communities and ecosystems. Yet global emissions continue to rise, and curr[ent] carbon-cutting efforts are wildly insufficient to ward off climate catastrophe.

current global pace of
emissions, the world will
ough its remaining "carbon
by 2030. Doing so would put
ig-term goal of keeping
warming to 1.5 degrees
s (2.7 degrees Fahrenheit)
ably out of reach.

Monday's assessment synthesizes years of studies on the causes and consequences of rising temperatures, leading U.N. Secretary General Antóni Guterres to demand that developed countries such as the United States eliminate carbon emissions by 2040 — a decade earlier than the rest of the world.

With few nations on track to fulfill their climate commitments and with the developing world already suffering disproportionately from climate disasters, said, rich countries have a responsibility to act faster than their low-income counterparts.

The IPCC report shows humanity has reached a "critical moment in history," IPCC Chair Hoesung Lee said. The worl has all the knowledge, tools and financial resources needed to achieve its climate goals, but after decades of disregard scientific warnings and delaying climate efforts, the window for action is rapidly closing.

Calling the report a "how-to guide to defuse the climate time-bomb," Guterres announced on Monday an "acceleratio agenda" that would speed up global actions on climate.

Emerging economies including China and India — which plan to reach net zero in 2060 and 2070, respectively — mu hasten their emissions-cutting efforts alongside developed nations, Guterres said.

Both the U.N. chief and the IPCC also called for the world to phase out coal, oil and gas, which are responsible for mc than three-quarters of global greenhouse gas emissions.

"This report offers hope, and it provides a warning," Lee told reporters Monday. "The choices we make now and in th next few years will reverberate around the world for hundreds, even thousands, of years."

A stark scientific outlook

Already, the IPCC's synthesis report shows, humanity has fundamentally and irreversibly transformed the Earth syst Emissions from burning fossil fuels and other planet-warming activities have increased global average temperatures at least 1.1 degrees Celsius (2 degrees Fahrenheit) since the start of the industrial era. The amount of carbon dioxide the atmosphere hasn't been this high since archaic humans carved the first stone tools.

Though much of the synthesis report echoes warnings scientists have issued for decades, the assessment is notable for the blunt certainty of its rhetoric. The phrase "high confidence" appears nearly 200 times in the 36-page summary chapter. Humanity's responsibility for all of the warming of the global climate system is described as an unassailable "fact."

Yet the report also details how public officials, private investors and other powerful groups have repeatedly failed to heed those warnings. More than 40 percent of cumulative carbon emissions have occurred since 1990 — when the IPCC published its first study on the dangerous consequences of unchecked warming. Governments continue to subsidize fossil fuel use; banks and businesses invest far more in polluting industries than they do in climate solutions. The consumption habits of the wealthiest 10 percent of people generate three times as much pollution as those of the poorest 50 percent, the report said.

Decades of delay have denied the world any hope of an easy and gradual transition to a more sustainable economy, the panel says. Now, only "deep, rapid and ... immediate" efforts across all aspects of society — combined with still-unproven technologies to pull carbon from the atmosphere — will be able to stave off catastrophe.

"It's not just the way we produce and use energy," said Christopher Trisos, director of the Climate Risk Lab in the African Climate and Development Initiative at the University of Cape Town and a member of the core writing team for the synthesis report. "It's the way we consume food, the way we protect nature. It's kind of like everything, everywhere all at once."

But few institutions are acting fast enough, the report said. November's U.N. climate conference in Egypt ended without a resolution to phase down oil, gas and coal — a baseline requirement for curbing climate change. Last year, China approved its largest expansion of coal-fired power plants since 2015. Amid soaring profits, major oil companies are dialing back their clean-energy initiatives and deepening investments in fossil fuels.

Humanity is rapidly burning through our "carbon budget" — the amount of pollution the world can afford to emit and still meet its warming targets, the IPCC said, and it projected that emissions from existing fossil fuel infrastructure will make it impossible to avoid the 1.5-degree threshold.

Yet even as environmental ministers met in Switzerland last week to finalize the text of the IPCC report, the U.S. government approved a new Arctic drilling project that is expected to produce oil for the next 30 years, noted Hans-Ott Pörtner, a climatologist at Germany's Alfred Wegener Institute and a co-author of a dozen IPCC reports, including the latest one.

"These decisions don't match reality," he said. "There is no more room for compromises."

Failure to act now won't only condemn humanity to a hotter planet, the IPCC says. It will also make it impossible for future generations to cope with their changed environment.

These changes have caused irrevocable damage to communities and ecosystems, evidence shows: Fish populations are dwindling, farms are less productive, infectious diseases have multiplied, and weather disasters are escalating to unheard-of extremes. The risks from this relatively low level of warming are turning out to be greater than scientists anticipated — not because of any flaw in their research, but because human-built infrastructure, social networks and economic systems have proved exceptionally vulnerable to even small amounts of climate change, the report said.

The suffering is worst in the world's poorest countries and low-lying island nations, which are home to roughly 1 billion people yet account for less than 1 percent of humanity's total planet-warming pollution, the report says. But as climate disruption increases with rising temperatures, not even the wealthiest and most well-protected places will be immune.

In 2018, the IPCC found that a 1.5C world would be overwhelmingly safer than one that is 2 degrees Celsius (3.6 degrees Fahrenheit) warmer than the preindustrial era. At the time, scientists said humanity would have to zero out carbon emissions by 2050 to meet the 1.5-degree target and by 2070 to avoid warming beyond 2 degrees.

Five years later, humanity isn't anywhere close to reaching either goal. Unless nations adopt new environmental policies — and follow through on the ones already in place — global average temperatures could warm by 3.2 degrees Celsius (5.8 degrees Fahrenheit) by the end of the century, the synthesis report says. In that scenario, a child born today would live to see several feet of sea level rise, the extinction of hundreds of species and the migration of millions of people from places where they can no longer survive.

"We are not doing enough, and the poor and vulnerable are bearing the brunt of our collective failure to act," said Madeleine Diouf Sarr, Senegal's top climate official and the chair for a group of least-developed countries that negotiate together at the United Nations.

She pointed to the damage wrought by Cyclone Freddy, the longest-lasting and most energetic tropical storm on record, which has killed hundreds of people and displaced thousands more after bombarding southern Africa and Madagascar for more than a month. The report shows that higher temperatures make storms more powerful and sea level rise makes flooding from these storms more intense. Meanwhile, the report says, the death toll from these kinds of disasters is 15 times as high in vulnerable nations as it is in wealthier parts of the world.

If the world stays on its current warming track, the IPCC says, global flood damage will be as much as four times as high as it will be if people limit temperature rise to 1.5 degrees.

"The world cannot ignore the human cost of inaction," Sarr said.

The price of delay

The report reveals thresholds in how much warming people and ecosystems can adapt to. Some are "soft" limits — determined by shortcomings in political and social systems. For example, a low-income community that can't afford build flood controls faces soft limits to dealing with sea level rise.

But beyond 1.5 degrees of warming, the IPCC says, humanity will run up against "hard limits" to adaptation. Temperatures will get too high to grow many staple crops. Droughts will become so severe that even the strongest wa conservation measures can't compensate. In a world that has warmed roughly 3 degrees Celsius (5.4 degrees Fahrenheit) — where humanity appears to be headed — the harsh physical realities of climate change will be deadly fc countless plants, animals and people.

"It's as if we're traveling on a carbon-intensive superhighway and we're in the fast lane," Trisos said. Unless people immediately pump the brakes on carbon emissions, we will zoom past the off exit for 1.5 degrees of warming — and there will be no turning back.

Yet just like drivers who have missed their exit, humanity must strive to stay as close as possible to the 1.5-degree targe Trisos said. "We can still take the 1.6 exit, which will be better than 1.7."

"With every increment of global warming, the danger will increase," he added. "As we leave it later and take hotter and hotter exits, the fewer options we have to thrive."

'It does not mean we are doomed'

Despite its stark language and dire warnings, the IPCC report sends a message of possibility, said Friederike Otto, a climate scientist at Imperial College London and a member of the core writing team for the report.

"It's not that we are depending on something that still needs to be invented," she said. "We actually have all the knowledge we need. All the tools we need. We just need to implement it."

In many regions, the report says, electricity from renewable sources such as solar and wind is now cheaper than power rom fossil fuels. Several countries have significantly reduced their emissions in the past decade, even as their economies grew. New analyses show how efforts to fight climate change can benefit society in countless other ways, rom improving air quality to enhancing ecosystems to boosting public health. These "co-benefits" well outweigh the osts of near-term emissions reductions, even without accounting for the long-term advantages of avoiding dangerous varming.

he IPCC also underscored that tackling climate change can help address global inequities — and vice versa. Stronger afety nets and policies that aid the poor can help foster support for the massive changes needed to help curb carbon missions, the report says. Helping developing nations build renewable energy infrastructure will both avert emissions nd alleviate the energy poverty that afflicts more than 700 million people worldwide, it said.

"It gives a goal to work toward, to a world that looks different," Otto said of the report. "It does not mean we are doomed."

Report authors say the IPCC's assessment comes at a pivotal moment. Beginning this year, nations are required to sta[rt] updating the emissions-cutting pledges they made in Paris in 2015. Diplomats are also hashing out the details of a "lo[ss] and damage" fund established at least year's climate talks, which would provide compensation to vulnerable countrie[s] suffering irreversible climate harms.

By the end of the COP28 climate conference in Dubai in December, Guterres said, the world's leading economies shou[ld] adopt climate plans in line with the IPCC's findings.

The steep political stakes of the IPCC's findings were evident during the report's marathon approval session, with representatives from nearly 200 countries haggling over the document's discussion of climate justice.

The science is indisputable, Lee said Monday: The world will not avoid catastrophic warming unless rich nations spee[d] up their own carbon cuts and help poorer countries do the same.

What's not yet clear is whether world leaders will follow through. When asked about Guterres's call for developed countries to move faster toward net-zero emissions, a State Department spokesperson instead directed attention towa[rd] China, which is now the world's largest annual producer of greenhouse gases.

But the planet can't afford further delays or finger-pointing, the U.N. chief said.

"Demanding others move first only ensures humanity comes last," he said. "We don't have a moment to lose."

Science   Politics & Policy   Justice   Fossil Fuels   Clean Energy   ≡

# Inside Climate News   Donate

Science

US Emissions of the World's Most Potent Greenhouse Gas Are 56 Percent Higher Than EPA Estimates, a New Study Shows

Electric utilities are likely responsible for the nation's higher than expected emissions of sulfur hexafluoride, a greenhouse gas 25,000 times worse for the climate than carbon dioxide.

By Phil McKenna 🐦
January 31, 2023

[handwritten box:] ORCA COMMENTS EXHIBIT 11 MAY 2023
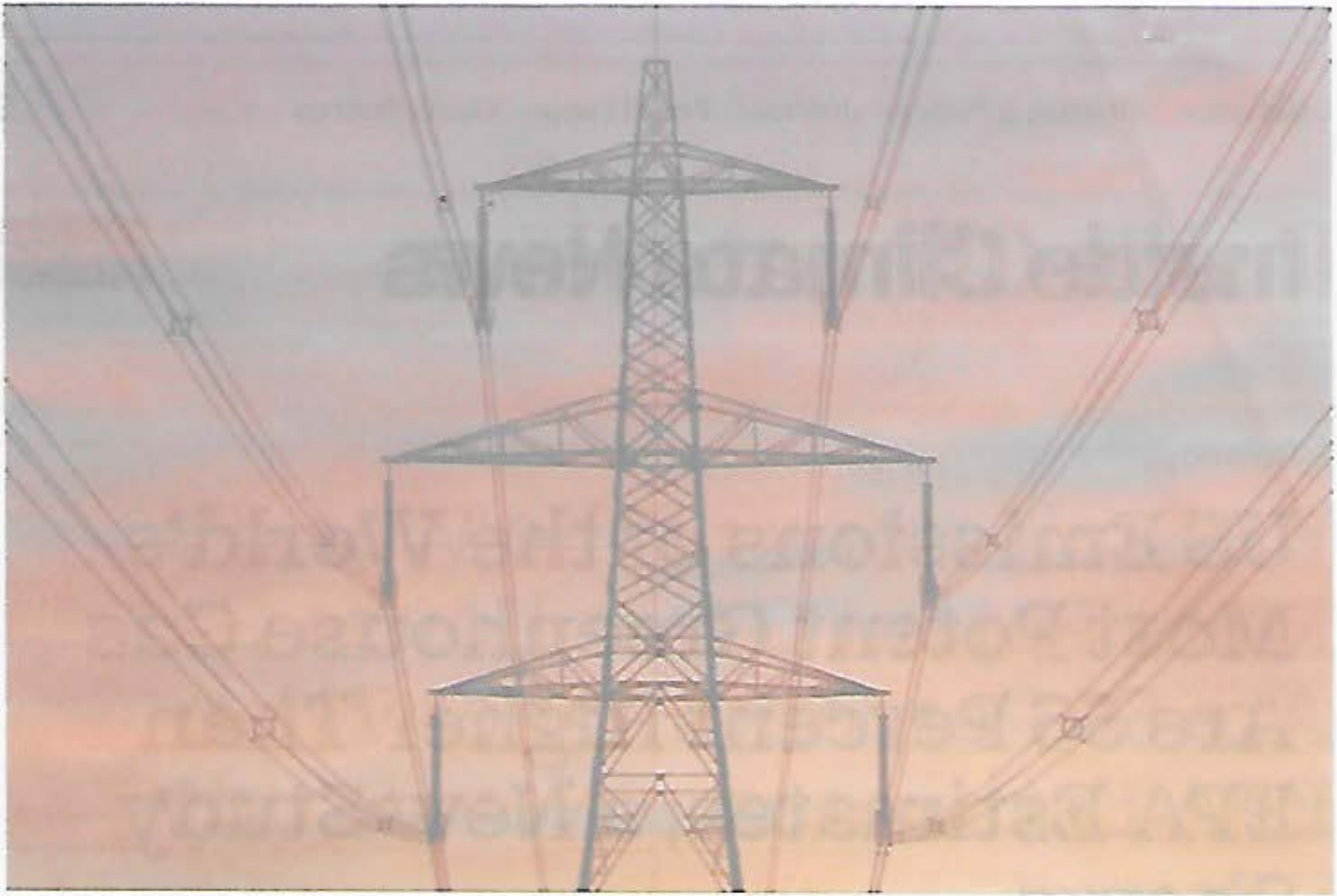
Electricity pylon and power cables. Credit: Tim Graham/Getty Images

While emissions of sulfur hexafluoride (SF6), the world's most potent greenhouse gas, have fallen sharply in the U.S. in recent decades, actual emissions are significantly higher than the official government estimates, a new study concludes.

Across the United States, 390 metric tons of SF6 were emitted into the atmosphere in 2018, the most recent year for which data are available, according to a new study resulting from a joint initiative between the National Oceanic and Atmospheric Administration and the Environmental Protection Agency. The study, designed to better quantify SF6 emissions in the U.S., was published in the journal Atmospheric Chemistry and Physics.

SF6, a man-made gas used by electric utilities to quickly interrupt the flow of electricity in high voltage circuit breakers, is also the most potent greenhouse gas ever studied by the Intergovernmental Panel on Climate Change. The gas is 25,200 times more effective at warming the planet than carbon dioxide, making even small releases of SF6 cause for concern.

Newsletters

We deliver climate news to your inbox like nobody else. Every day or once a week, our original stories and digest of the web's top headlines deliver the full story, for free.

ICN Weekly
Saturdays

Our #1 newsletter delivers the week's climate and energy news — our original stories and top headlines from around the web.

Get ICN Weekly

Inside Clean Energy
Thursdays

Dan Gearino's habit forming weekly take on how to understand the energy transformation reshaping our world.

Get Inside Clean Energy

Today's Climate
Twice-a-week

A digest of the most pressing climate-related news, released every Tuesday and Friday.
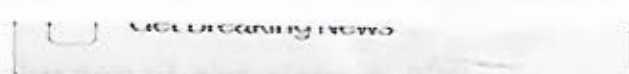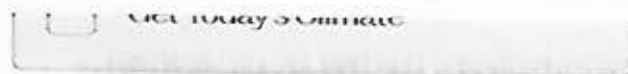
Get Today's Climate

Breaking News
Daily

Don't miss a beat. Get a daily email of our original, groundbreaking stories written by our national network of award-winning reporters.

Get Breaking News

The volume of SF6 released in 2018 is less than half of what it was a decade prior, but still equaled the annual greenhouse gas emissions of 2.1 million automobiles, according to the Environmental Protection Agency's greenhouse gas equivalency calculator.

The vast majority of SF6 emissions come from the electric power sector and occur either during routine servicing of electrical equipment or through ongoing leaks in aging or poorly sealed storage tanks and other electrical equipment.

"Substantial additional emission reductions can be achieved if more efforts were put into minimizing emissions during servicing or through improving sealing materials in the electrical distribution systems," said Lei Hu, a researcher with the National Oceanic and Atmospheric Administration and the study's lead author.

The Electric Power Systems Partnership, a voluntary program run by the EPA, has helped electric utilities reduce emissions of SF6 by approximately 80 percent since 1990, according to the agency. Emissions reductions have come through the use of newer, less leak-prone equipment and better servicing practices that prioritize capturing and reusing SF6 gas. SF6-free circuit breakers are also increasingly being deployed by some electric utilities as alternative technologies become available.

However, not all electric utility companies participate in the EPA's emission reduction program. Duke Energy, one of the largest electric power corporations in the U.S. based on

revenue, does not participate and Duke Energy Carolinas, the company's subsidiaries in North and South Carolina, had the highest SF6 leak rate of any electric utility that reported emissions to the EPA in 2021.

Duke Energy spokesman Jeff Brooks told Inside Climate News in November that the company was "working to learn more about" the EPA-industry partnership to reduce SF6 emissions, a program that has been operating since 1999. The company declined to comment on Tuesday as did the Edison Electric Institute, a trade association that represents all U.S. investor-owned electric companies.

In its annual U.S. greenhouse gas inventory published in April, the EPA mentioned preliminary data from NOAA and EPA scientists, which suggested higher-than-expected U.S. emissions of SF6.

"The preliminary results of research conducted by the National Oceanic Atmospheric Administration indicate that U.S. emissions of SF6 are significantly higher than what is being estimated in the current inventory for emissions of SF6 from all sources," the report said.

The report suggested that the EPA may need to improve its estimates of SF6 emissions from electric utilities that are believed to have relatively low SF6 emissions and are therefore not required to report their emissions to the agency. The report also flagged "end-of-life" emissions from old electrical equipment at the time of disposal as a potential source of higher-than-expected emissions.

Now, the agency is moving forward with some of the changes.

"The EPA has revised its method for estimating emissions of

SF6 from these non-reporting facilities," Melissa Sullivan, a spokeswoman for the agency, said. "Specifically, rather than assuming that the average SF6 emission rate of non-reporting facilities has declined at the same rate as that of reporting facilities, the EPA is now assuming that the average SF6 emission rate of non-reporting facilities has declined much more slowly than the average emission rate of reporting facilities."

Sullivan said the change will bring the agency's estimate for SF6 emissions into better agreement with emissions inferred from atmospheric observations, starting with the next annual U.S. greenhouse gas inventory, a draft of which will be published in February.

Hu said the current study could serve as a guide for other countries as they try to get a better handle on their annual SF6 emissions. Current national inventories like that of the U.S. only account for half of all global SF6 emissions based on estimates derived from global atmospheric concentrations of the pollutant.

"There is a huge gap in the global reporting of SF6," Hu said. "Maybe other countries can consider a similar approach so